KONINKLIJKE AKADEMIE VAN WETENSCHAPPEN
TE AMSTERDAM

PROCEEDINGS

VOLUME XXXV

No. 6

CONTENTS

Palæontology. — *The distinct organization of Pithecanthropus of which the femur bears evidence, now confirmed from other individuals of the described species.* By EUG. DUBOIS.

(Communicated at the meeting of June 25, 1932).

Forty years ago the two principal skeletal remains, the skullcap and the femur, of *Pithecanthropus erectus* were excavated at Trinil, Java. It was then supposed by the author of the species, that both were remains of the same organism, species or even individual. The skullcap indeed so closely resembles that part of the body in the Anthropoid Apes, especially the Gibbons, on one hand, and in Man, on the other, that the name *Pithecanthropus*, for the genus, is fully appropriate. The name *erectus* was given to the species on account of the strikingly human-like essential features of the femur, which imply erect attitude and gait. Together with those features, however, the Trinil femur, in the opinion of the author of the species, presented important differentiating characters, so that he found it possible, at least, to regard the skull and the femur as having been

parts of one organism. Nearly conclusive indirect evidence for the belonging together of the two fossils, possibly once organically associated in virtue of their morphological aspect, was seen in that they were found in exactly the same layer of the fluvial deposit of volcanic ashes, the one from the other at only about 12 m distance.

The principal differentiating character in the Trinil femur: "the popliteal space less developed, very convex in its middle, so that at this height the shaft is almost round instead of flattened", was not acknowledged as such by the eminently competent anatomists MANOUVRIER (1896) and HEPBURN (1897). They tried to show, that this striking character is not exclusively seen in the Trinil femur but is found, although seldom to the same amount, on human femora. They and many others regarded the Trinil femur as human. They disregarded other characteristic features and did not give much attention to the general aspect of the femur, which, however, induced RUDOLF VIRCHOW (1895) to the pronouncement that the femur, notwithstanding its resemblance to the human one, "shows in its straightness, as in the rounding of its diaphysis, particularly in its lower part, so many agreements with the femur of a gibbon, that I find no difficulty in attributing it to a giant gibbon." Again BUMÜLLER (1899). comparing the human femur with femora of Apes and that of *Pithecanthropus*, resolved to designate, for the time being, the pithecanthropus as *Hylobates giganteus*. Up to the present, the opinion of MARCELLIN BOULE ("Les Hommes fossiles. Deuxième Edition". 1923) is, that the resemblance of the remains of the Pithecanthrope to the same skeletal parts of the Gibbons favours the view that the discussed form "may have been a large species either of the Gibbon genus, or rather of a closely allied genus related to the same group. This form might have been superior to its congeners, not only in the size but also in other morphological characters, and particularly in cerebral capacity, a character of the first importance in which *Pithecanthropus* truly approaches the human stock."

The prevailing view on the Trinil femur, however, at present as well as in the past, is to consider it absolutely ("durchaus", "vollständig") human. This, assuming the two skeletal remains were organically associated, implies the supposition that in the anthropogenesis the acquisition of the human, exclusively upright gait preceded the evolution of the brain and the skull, "that the frame of man reached its perfection for pedal progression long before his brain attained its present complex structure." Now modern biology does not admit as possible the existence of any unfinished, imperfect species i.e. full-grown organism. Nevertheless, those well-founded biological conceptions are still entirely neglected in many researches concerning *Pithecanthropus* and fossil man, up to the present time. Thus HANS WEINERT, in a recent elaborate morphological study ("Pithecanthropus erectus". Zeitschrift für Anatomie und Entwicklungsgeschichte. Band 87, Heft 3 und 4. 1928) treating the different remains, concurs with MANOUVRIER in that the particular features

of the Trinil femur cannot be utilized to characterize a form deviating from the human. He says that he expects that by further comparisons, at least a smooth transition between recent human femora and the femur of the Pithecanthropus can be found and, at the end of his treatise, states: "Der *Pithecanthropus erectus* war ein *Homo*, dessen bis heute noch einsame Stellung und dessen unbestrittene Bedeutung den Gattungsnamen "Affenmensch" rechtfertigen." — For all that an unfinished organism!

It thus appears clearly that we have to regard the femur of the *Pithecanthropus* species as the true key bone of his frame, a key admitting us to the knowledge of its organization. Now, as to know a species well, one single individual is insufficient, what we have wanted, for forty years, are thigh bones of other individuals of the described species, to ascertain if the particular features seen in the femur of 1892 are essential characters of the species, and belong to a distinct, although more or less human-like organization, or mere individual differences, which are also proper to man. Will another femur present the same differentiating characters? Or was MANOUVRIER right in saying: "il est très possible et même, je crois, probable que si l'on trouve un second fémur de même race, il sera très différent de celui qu'on possède"?

The answer to these questions has been long in coming, for at present, as in 1859, DARWIN's plaintive words are true: "our palaeontological collections are very imperfect". In these forty years no remains of another pithecanthrope came to light ..... till the first day of this month eight overlooked pieces appeared of three thigh bones of the described species.

On that day, at Leyden, in my Java collection, from a lot of inconsiderable fragments of ribs from different Trinil mammals, which I was minutely examining, were separated some dissimilar fragments, not belonging to ribs. Amongst them a bone a foot long, still partially covered with rock, which my diligent assistant in the arranging of the Collection, Dr. BERNSEN, whose loss we now deplore, had put aside for my inspection, because he regarded it as a dubitable piece of a deers horn. To my great joy I soon recognized it as the shaft of another *Pithecanthropus* thigh bone: It presented some of the same characteristics which differentiate the Trinil femur of 1892 from a human femur. Then, searching further between the ribfragments for similar pieces, that might possibly fit, I found the defective upper extremity to that thigh bone shaft, which was broken off beneath the small trochanter, and 6 other pieces of different sizes, which enabled me to compose two more shafts of *Pithecanthropus* thigh bones.

None of the three is by far comparable with the splendidly conserved femur of 1892, but they all unquestionably belong to the described species.

From the first and least incomplete bone I have now removed nearly the whole of the hard strongly adhering rock, a pyritous impregnation of andesite. The two other bones were nearly bare of rock but more broken.

For convenience, I will now designate the femur of 1892 by I, that with

the superior extremity by II, the one composed of four fragments by III, and that composed of two pieces with a filled up gap in the middle by IV.

The surface of the three new femora is more or less strongly corroded, evidently by sulphuric acid originated from weathering pyrite, most so III and IV, the least II, probably because this fossil was still, to a great extent, covered with unweathered pyrite, whereas the pyrite formerly extant too on III and IV weathered away in the rock, and at the same time corroded the surface of those fossils.

The specimens, as said above are very incomplete. From the head of II only a core, from both its trochanters only the bases remained, the fore-upper side of the neck is wanting. Thus the spongiosa, at the upper end of the femur, is, to a large extent, laid open, so that its human-like architecture is clearly apparent. Comparing this and the two other defective bones with the complete femur I, I estimate that from II the lower end is broken off to higher than 4 cm above the condyles on the backside, and that the length of the bone in the complete state was at least 4 cm more than that of I. The total length of the fragment is about 40 cm.

From III are wanting the upper and the lower end, from the level of the middle of the small trochanter, above, to higher than 2 cm above the backside of the condyles, below. This shaft measures in total length 32½ cm, and the complete bone was about 1½ cm longer than I.

From IV also both ends are wanting, the upper one broken off at about the same level as III, the lower more than 2½ cm above the patellar surface. The full length of this shaft is 31½ cm. The complete bone was of about equal length with I.

The four thigh bones are from four different individuals, as shown by their individual features (especially differences in platymery and the crista and fossa glutaea). The bones II and IV are from the right side, I and III from the left side. Judging from the relatively great length of the neck, II belonged to a male, and I, with a much (about 13 mm) shorter neck, to a female. This is in accordance with the fact that the skullcap of 1891, to which this femur was probably individually associated, presents female characters, admitting that in this respect of sexual dimorphism *Pithecanthropus* resembled Man and the Anthropoid Apes.

The new femora of *Pithecanthropus erectus* were found in a collection of fossil bones acquired from excavations executed at Trinil in 1900, conducted under my direction by my former assistant in Java, the late sergeant-engineer KRIELE. The collection was sent to Leyden in the same year, for completion of that which I brought to Holland in 1895. In the year 1900 (the last of Dutch collecting work at Trinil) a very large excavation, 75 m long and 6 to 14 m broad, was effectuated, which enclosed the excavations, on the same, left, bank of the Soloriver, of all the former years, from 1891. The exact site of these fossil remains in the excavation is not known, because they were not remarked as uncommonly important and mixed

up with fragments of different ribs and some other fossils of small value. It is, however, possible to ascertain that the distance of the three new thigh bones from the site of the skullcap of 1891 was between 16 and 48 m. Now considering that the skullcap and femur I were found at only about 12 m the one from the other (perhaps only 10 m, certainly not 15 m, as appears from my notes of that time), in a part of the excavations where corrosion of the bones was generally less [1]), whereas the surface of the three new thigh bones is intensively corroded, considering, further, that very likely the skullcap and the femur I are both feminine, it appears as very probable that none of the three new thigh bones was individually associated with this skull.

Aside from unessential individual differences, the three new femora are, evidently, characterized by the same features which distinguish the Trinil femur of 1892 from any common human femur. This was manifest at a glance, as soon as, on the day of the discovery, the general form and the surface of the bones were completely laid bare.

There is no doubt any longer now, that those particular features which struck me, in 1892, and struck RUDOLF VIRCHOW, in 1895, as differentiating the femur of the *Pithecanthropus erectus* from that bone in Man, are characteristic and distinguish the genus.

Indeed, in all four of the thigh bones, we find quite essential human characteristics in combination with the same important different features. Again and again we now see, in a human-like femur, the peculiar rounding of the lower part of the diaphysis, and the popliteal surface transversally convex in the middle, a rounding and a convexity beginning at and descending from the point of divergence of the external supracondylar line, the continued labium laterale cristae femoris.

On femur II, the one with the preserved upper end part, we find the posterior surface of the collum, like in femur I, nearly flat and vertical, not rounded to the front as in the human femur, showing, together with what is preserved of the trochanter major, that, the same as in femur I, the posterior border of the trochanter was perpendicular, and itself, seen from the outside, had a perpendicular direction, in the upward prolongation of the diaphysis, which implies a more pronounced concavity of the crista intertrochanterica above the trochanter minor. Thus in femur II we find again, like in femur I, the trochanter major directed perpendicularly, not incline forward as it does in Man.

As at first ROUX instructed us, the form of a bone is merely the expression of its function. This must especially be true for a human-like femur, which performs a so pregnant function in the organization. The urgent question thus arises: Which is the functional significance of the morphological characteristics, distinguishing the femur of *Pithecanthropus* from that bone in Man?

[1]) Femur I is quite unaffected by corrosion, the skullcap yet less than the new femora.

Obviously the special features of the first should be attributed to static and mechanic differences in the animal organization. Such differences imply differences in the musculature and the attachments of the muscles.

Now it seems that the attachment of the adductor magnus muscle, so important a muscle in the human posture and gait, was in some respects different in *Pithecanthropus*. Probably the roundness of the lower part of the diaphysis and the median swelling of the popliteal surface favoured an extension of the fleshy median attachment of the muscle, here descending as far as in that surface, a similar extension to that occurring in the great Anthropoid Apes.

Such a condition of the adductor magnus muscle implies an important difference from the human locomotor functions.

The other strikingly specific character of the femur in *Pithecanthropus*, the vertical direction of the trochanter major, seems to have been related to a difference in the surface of origin of the glutaeus medius and minimus muscles. Probably the origin of those powerful muscles did not extend so much to the front on the narrower ilium as it does in Man on account of his anteriorly expanded ilium. For this can explain a more vertical direction of the insertion tendons of those muscles bringing about the perpendicularity of the trochanter major in *Pithecanthropus*. We find, indeed, a similar combination of a narrow ilium with a vertical trochanter major in *Hylobates agilis* (and the other little Gibbon species), and of an anteriorly expanded ilium with a frontwards inclining trochanter in *Hylobates (Symphalangus) syndactylus*.

In this way, again, we may assume important differences from the human locomotion.

In the ordinary locomotion of Man each leg supports alternately the body, in such a way that with the transversal knee axis placed as much as possible horizontally, chiefly the external condyle of the femur is loaded. For this reason (generally admitted) the diaphysis is thicker above this than above the internal condyle — and also as a rule than between the two condyles. The crista femoris, which may be strengthened to a "pilastre", is continued in the diverging external supracondylar line along with the transferring of the greatest thickness of the diaphysis from the middle of the backside of the bone to the external tuberosity or epicondylus lateralis.

In the femur of *Pithecanthropus*, on the contrary, the diaphysis maintains its greatest median thickness below the bifurcation of the labia, up to close above the knee-joint. Evidently the line of pressure from the trunk lay here on the inner side of the external condyle, because in the habitual locomotion the supporting leg was not placed near the line of gravity of the body, but further outward. Consequently the transverse axis of the knee-joint did not remain horizontal, as it was in the human-like locomotion, but inclined inwards, and the pressure weighed on the inner border of the foot. The leg then remained in abduced

position, and at the same time in outward rotation on account of the particular condition of origin and insertion of the powerful glutaeus medius and minimus muscles. On adduction by the no less powerful adductor magnus muscle, the leg, on account of the probably peculiar attachment of that muscle, remained in outward rotation. This was a necessary condition if the most habitual locomotion consisted in climbing — properly walking — aloft big trees, with alternately extended legs. Hence also when the glutaei muscles mentioned were bringing the trunk above the extended and in adduction fixed leg, they together with the adductor magnus muscle rotated the trunk at the same time with the front to the other side. Thus the femur of *Pithecanthropus erectus*, although well fit for a locomotion on the ground resembling the human gait, was most likely by no means so exclusively adapted for it as in Man, but more appropriate to a habitual treegoer, a dendrobates.

Of course, these more or less exactly described functions are only probabilities. However this be, the morphological evidence acquired proves beyond a doubt that the skull and the femur which were excavated in 1891—1892, can have been associated in one and the same organism, a distinct species, which as such had a complete and finished, not an imperfect organisation.

I still believe, now more firmly than ever, that the *Pithecanthropus* of Trinil is the real "missing link". In a sense, for I have learned to see the evident continuity of the organic world in another light than before, and to conceive that no continuity can be found in the links, the distinct species, themselves. Continuity only existed in the invisible germ thread running through them. Evolution, as evidenced in the central organ of animal life, is phyloblastesis, by geometrical, not arithmetical progression.

Physics. — *Optische Untersuchung des Zusammenstosses von Gasatomen mit einer Wand.* Von L. S. ORNSTEIN und W. R. VAN WIJK. Mitteilung aus dem Physikalischen Institut der Universität Utrecht.

(Communicated at the meeting of June 25, 1932).

Der Zusammenstoss von Gasatomen oder Molekülen mit einer Wand ist gewöhnlich in der Weise untersucht worden, dass irgendeine mittlere Grösse, wie etwa die Aenderung der mittleren Energie der Moleküle beim Auftreffen auf die Wand, gemessen wurde.

An Versuche, welche tiefer in die Natur der Vorgänge eindringen, liegen

nur die Molekularstrahlexperimente [1]) vor sowie auch eine in diesem Institut ausgeführte Arbeit, wobei längs optischem Weg die Verteilungsfunktion der Rotationsenergie bestimmt wurde [2]). Die analoge Untersuchung der Verteilungsfunktion der Translationsenergie, welche eine genaue Analyse der Form der Spektrallinien fordert, ist jetzt von uns an Helium vorgenommen worden, und obwohl definitive Resultate bisher noch ausstehen, hat sich doch herausgestellt dass eine Entscheidung mit den heutigen Hilfsmitteln der Spektroskopie möglich ist. Die schematische Aufstellung zeigt die Figur 1.

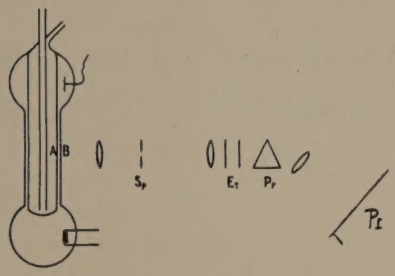

Fig. 1

Das Spektralrohr *Sp.* bestand aus zwei koaxialen Zylindern, von denen die Innere *A* wassergekühlt und die Aeussere *B* elektrisch geheizt wurde, auf ungef. 320° C. Der Abstand der beiden Zylinderwände betrug 0.1 cm. Das Helium hatte einen Druck von etwa 0.01 cm, sodass die freie Weglänge der Atome von derselben Grössenordnung wie der Abstand der Wände war. Das Rohr wurde auf einem Induktorium mit 500 Periodenstrom betrieben. In der Heizwicklung der Wand *B* war ein schmales Rechteck ausgespart, das auf dem Kollimatorspalt *Sp.* abgebildet wurde, wonach das Licht das Fabry-Pérot Interferometer *Et* und das Zerlegungsprisma *Pr* durchlief, um schliesslich auf der photographischen Platte *Pl* zu einem scharfen Bilde des Kollimatorspaltes fokussiert zu werden. Die Beobachtung geschah also senkrecht auf der Wand, was zur Folge hat, dass die auf die Wand *B* zufliegenden Atome eine violettverschobene Frequenz ausstrahlen und die von *B* weglaufenden eine nach Rot verschobene.

Sieht man vorläufig von den Zusammenstössen der Atome untereinander völlig ab, dann würde man die folgende Struktur der Spektrallinie erwarten. Weil die Wand *A* rauh war, (sie war mit Kupferoxyd geschwärzt), verlassen die Atome dieselbe mit einer Maxwellschen Geschwindigkeitsverteilung, sodass der violettverschobene Teil der Spektrallinie die Form einer Fehlerkurve hat. Der rotverschobene Teil gibt die Verteilung, wie dieselbe durch den Zusammenstoss abgeändert worden ist. Nehmen wir an dass diese Letztere aus zwei Maxwellschen Verteilungen aufgebaut ist, von welchen die eine von den elastisch reflektierten Atomen herrührt und die Temperatur der Wand *A* besitzt, während die andere die kondensierte und wieder abgedampfte Atome enthält und somit die Temperatur von *B* hat, dann bekommen wir Linienformen, wie sie in der Figur 2 gezeichnet sind. Die beigeschriebenen Zahlenwerte stellen den Akkommodationskoeffizient vor auf welchen die Kurven sich beziehen. Bei einem Akkommo-

[1]) I. Estermann u. O. Stern. Zt. f. Phys. **61**. 95. 1930.
[2]) W. R. v. Wijk, Zt. f. Phys. **75**. 584, 1932.

dationskoeffizienten a ist die Maximalhöhe der Verteilungskurve der elastisch reflektierten Molekülen 1—a, wenn die Höhe der Einfallsverteilung 1 ist, und die der abgedampften aT_k/T_w wo T_k/T_w das Verhältnis der Wandtemperaturen (T_k = Temperatur der kalten Wand A) vorstellt. Denn es gilt die Stetigkeitsbedingung $N_k V_k = N_w V_w$, worin N die Molekularen Dichten und V die mittleren Geschwindigkeiten sind, sodass das N_k in dem Verhältnis $\sqrt{\frac{T_w}{T_k}}$ zu dem N_w steht. Weil die Maximalhöhe der Maxwellschen Verteilung proportional dem Produkte von N und $\frac{1}{\sqrt{T}}$ ist, kommen wir zu dem obigen Wert der Maximalhöhe für die zweite Verteilungsfunktion. Die Kurven in der Figur 2 sind alle für das Verhältnis $T_k/T_w = \frac{1}{2}$ berechnet.

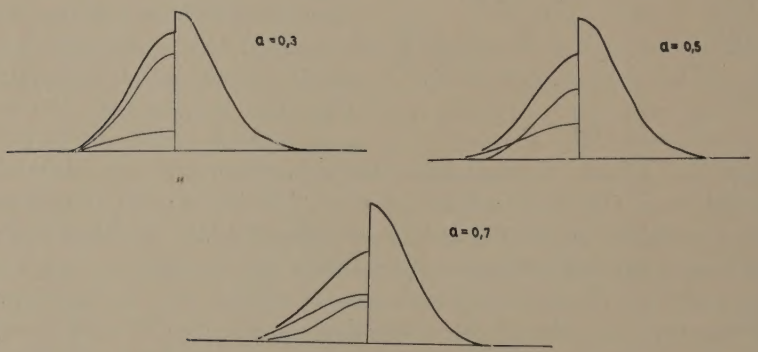

Fig. 2

Diese wirkliche Linienform wird aber noch durch den Apparat verzerrt, worauf schon P. P. KOCH hingewiesen hat [1]), was aber erst vor kurzem von H. C. BURGER und P. H. VAN CITTERT eingehend untersucht worden ist [2]). Dieselben haben auch eine noch unveröffentlichte Apparatur konstruiert, womit es möglich ist die wahre Linienform zu bestimmen, wenn die Intensitätsverteilung, welche der Spektralapparat für eine streng monochromatische Spektrallinie liefert, bekannt ist, und sie waren so liebenswürdig das Verfahren für uns auszuführen. Die vom Apparat gelieferten scheinbaren Intensitätsverteilungen sind in der Figur 3 dargestellt, wobei als vierte Kurve die experimentell gefundene Intensitätsverteilung der Singulettlinie 5016 Å gezeichnet ist, wie diese sich aus der photographischen Aufnahme nach Reduktion der Abstandsunterschiede im Bild der Linie auf Wellenlängenskala und nach Umrechnung der photographischen Schwär-

[1]) P. P. KOCH. Ann. d. Phys. (4) **42**. 1. 1913.
[2]) H. C. BURGER u. P. H. v. CITTERT. Zt. f. Phys. **44**. 58. 1927; **51**. 638. 1928.

zung auf Intensitäten mittels des üblichen Utrechter Verfahrens als Mittelkurve aus vier Ordnungen ergeben hat.

Man sieht, dass die experimentelle Kurve mit keiner der theoretischen ganz übereinstimmt, dass sie aber am meisten der Kurve für $a = 0.3$ ähnlich

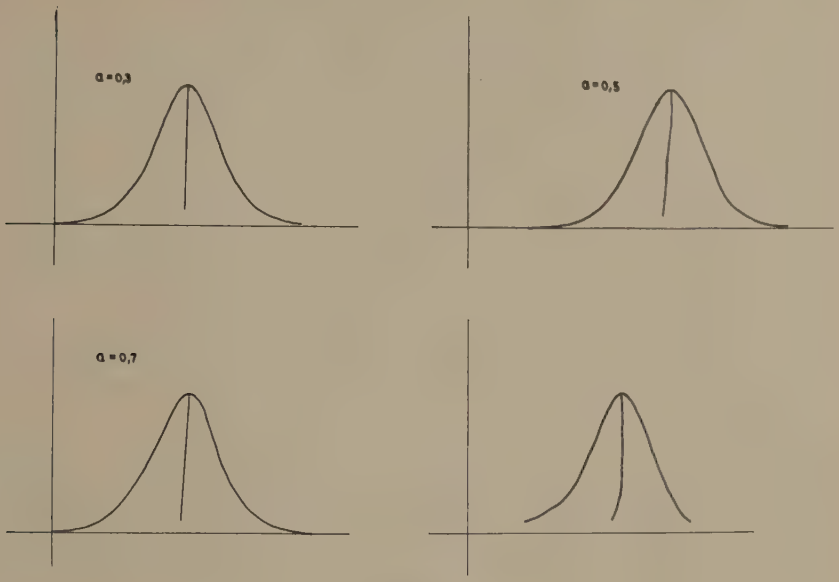

Fig. 3

ist. Die erwarteten Asymmetrieen in den Intensitätsverteilungen sind am leichtesten aus der Neigung der Mittellinie, die in jeder der Kurven gezogen ist, ersichtlich. Die Asymmetrieen in den obigen Kurven sind nur ganz gering, weil wir vorläufig nur mit einer schwachen Versilberung gearbeitet haben, um erst die Methode und die richtige Form des Spektrallrohres auszuarbeiten. Weil die gefundene Asymmetrie in Richtung und Grössenordnung mit der theoretischen übereinstimmt, meinen wir aber, dass mit einem grösseren Auflösungsvermögen, womit jetzt gearbeitet wird, das Problem zur Lösung gebracht werden kann.

Wir möchten zum Schluss noch eine Bemerkung machen über eine wichtige Anwendungsmöglichkeit des beschriebenen Spektrallrohres für die Untersuchung der (Hyper) Feinstruktur.

Bei dem heutigen Stand der Feinstrukturspektroskopie wird die Grenze der Auflösbarkeit von nahe zu einander liegenden Spektralllinien bis zum Element Cadmium hinauf mehr von der Eigenbreite der Spektralllinien als vom beschränkten Auflösungsvermögen des Apparates gestellt. Verringerung der Eigenbreite, welche hauptsächlich vom Dopplereffekt verursacht wird, durch intensive Kühlung ist wohl nur beim Helium in effektiver Weise anzuwenden, sodass hier eine wesentliche Grenze vorliegt, solange

die Dopplerverteilung der Spektralllinie beibehalten bleibt. Sobald aber die Linienform durch äussere Eingriffe derartig beeinflusst wird, dass eine etwaige Feinstruktur zutage treten kann, ist die Grenze wieder ganz auf die technische Frage der Konstruktion von Spektrallapparaten mit höchster Auflösungskraft zurückgeführt. Eine solche Beeinflussung der Linienform findet in unsrem oben beschriebenen Rohr statt, wenn der Akkommodationskoeffizient des Gases nicht allzusehr von der Einheit abweicht, was nur beim Wasserstoff und Helium der Fall ist. In der Figur 4 sind die Linienformen gezeichnet worden, einerseits für eine Doppler-

Fig. 4

verteilung der einzelnen Komponenten eines engen Dubletts mit einem Abstand vom halben Betrag der Halbwertsbreite und ein Intensitätsverhältnis 1 : 2 der Komponenten, und andererseits für dasselbe Dublett, aufgenommen zwischen Wänden von der die eine die Temperatur der ursprünglichen Dopplerverteilung besitzt während die andere eine doppelt so hohe Temperatur hat. Dabei ist Sorge getragen worden dass eben die richtige Wand geheizt ist, damit die Seite der starken Komponente, welche die Schwächere überdeckt hat, herabgedrückt worden ist. Der grosse Vorteil der vorgeschlagenen Methode ist an diesem Beispiel wohl ohne weiteres ersichtlich ; sie wird erst recht die grossen Fortschritte in der Auflösungskraft der Interferenzapparate (Multiplexspectroscope!) der letzten Zeit zur Geltung kommen lassen.

Physics. — *Measurements about the Velocity of Sound in Nitrogen Gas.* By W. H. KEESOM and J. A. v. LAMMEREN. (Communication N°. 221*c* from the KAMERLINGH ONNES-Laboratory at Leiden).

(Communicated at the meeting of June 25, 1932).

§ 1. *Introduction.* In Comm. Nos. 209*a* and *c* and 213*b* [1]) W. H. KEESOM and A. v. ITTERBEEK reported on an apparatus suitable for the determination of the velocity of sound in gases at low temperatures. This apparatus we now used to make measurements in nitrogen gas at temperatures extending from 0° C. down to the liquid nitrogen range. As shown by the authors mentioned it is possible, by measuring the velocity of sound in dependence on the pressure, to calculate the ratio c_p/c_v and the second virial coefficient B as a function of the temperature.

In these experiments we considered more closely the influence of the resonator, this influence being of high importance when extrapolating the velocity of sound to a pressure $p = 0$.

§ 2. *Experimental methods.* For the methods we refer to Comm. N°. 213*b*. The temperature was determined by means of two platinum resistance thermometers. We used four resonators indicated by R_I, R_{II}, R_{III} (brass tube) and R_{IV} (copper tube), the dimensions of which are given in table I.

TABLE I.

Resonator	Diameter mm	Length mm 0° C.
R_I brass	62	297.7
R_{II} „	36	804.8
R_{III} „	35	299 0
R_{IV} copper	35	801.4

R_{IV} was made of copper in order to obtain a more uniform temperature in the long cryostat needed.

In view of the influence of the end-openings in the resonator we have always given these openings exactly the same diameter (1 mm). The nitrogen was obtained by heating sodium azide NaN_3, spread out in a horizontal glass tube. The gas was liquefied in a condenser cooled with liquid air boiling under reduced pressure. After fractional evaporation it was led into the resonator. This method guarantees a sufficient degree of purity.

[1]) W. H. KEESOM and A. VAN ITTERBEEK. These Proceedings **33**, 440, 1930; **34**, 204, 1931; Comm. Leiden Nos. 209*a* and 213*b*. A. VAN ITTERBEEK and W. H. KEESOM, Wisen Natuurk. Tijdschrift **5**, 69, 1930; Comm. Leiden No. 209*c*.

§ 3. *Experimental results.* *a.* Measurements at 0° C., summarized in table II.

TABLE II.

Velocity of sound in nitrogen at 0° C.			
Resonator	Pressure at	$W_{obs.}$ m/sec	W m/sec
R_I	0.9844	336.5_5	337.0_6
R_{II}	0.9937	336.3	337.1
R_{III}	0.9842	336.7	337.5

In this and following tables $W_{obs.}$ means the average value obtained from several observations and W the velocity of sound corrected for the influence of the wall. To calculate this correction we used the formula of KIRCHHOFF-HELMHOLTZ [1]).

From table II it appears that the influence of the end-openings of the resonator R_{III} is considerably greater than is the case for R_I and R_{II}, for which this influence is much diminished by the large diameter resp. length. Furtheron the correction in these resonators will prove to be very small.

The agreement between the results in R_I and R_{II}, when the formula of KIRCHHOFF-HELMHOLTZ is applied, is very satisfactory. Our value of the velocity of sound at 0° C. agrees rather well with that found by other observers [2]).

b. Measurements at temperatures of liquid ethylene. The results are communicated in table III.

TABLE III. Resonator R_I.

Velocity of sound in nitrogen at liquid ethylene temperatures.			
T °K.	Pressure at	$W_{obs.}$ m/sec	W m/sec
166.03	1.0090	262.0	262.2
161.14	0.9925	257.9	258.1
156.53	0.9786	254.1	254.3
146.04	0.9506	245.8	246.0

[1]) Compare Comm. No. 209*a*.

[2]) G. SCHWEIKERT, Ann. d. Phys. (4) **48**, 593, 1915.
H. B. DIXON, C. CAMPBELL and A. PARKER, Proc. Roy. Soc. London (A) **100**, 1, 1921.

c. Temperatures of liquid oxygen and nitrogen, tables IV, V and VI.

TABLE IV. Resonator R_I.

Velocity of sound in nitrogen gas.			
T °K.	Pressure at	$W_{obs.}$ m/sec	W m/sec
90.37	0.9299	190.9_8	191.0_8
	0.7293	191.6_7	191.7_8
	0.5541	192.1_1	192.2_3
	0.4380	192.5_3	192.6_7
	0.3207	192.7_7	192.9_4
	0.1973	193.1_1	193.3_2
	0.1176	193.0_9	193.3_7
82.95	1.0146	181.7_9	181.8_7
	0.7957	182.7_2	182.8_1
	0.5953	183.3_2	183.4_2
	0.4179	183.9_7	184.0_9
	0.2923	184.4_8	184.6_3
	0.1921	184.8_2	185.0_8
	0.1022	185.2_8	185.5_3
77.95	0.9026	175.9_8	176.0_6
	0.7122	176.8_8	176.9_6
	0.5789	177.4_9	177.5_8
	0.4380	177.9_4	178.0_5
	0.3029	178.6_5	178.7_8
	0.2025	179.0_8	179.2_4
	0.1183	179.5_5	179.7_6
71.92	0.3879	170.8_1	170.9_1
	0.3382	171.0_2	171.1_3
	0.2627	171.5_1	171.6_3
	0.1931	171.9_2	172.0_6
	0.1188	172.4_4	172.6_3

TABLE V. Resonator R_{III}.

T °K.	Pressure at	$W_{obs.}$ m/sec	W m/sec
79.17	0.9633	177.2_8	177.4_0
	0.6410	178.7_1	178.8_7
	0.4515	179.4_2	179.6_1
	0.2921	180.0_6	180.3_0
	0.1560	180.8_9	181.2_2

TABLE VI. Resonator R_{IV}.

T °K.	Pressure at	$W_{obs.}$ m/sec	W m/sec
78.36	0.9088	176.4_4	176.5_8
	0.7083	177.3_4	177.5_0
"	0.5270	178.0_8	178.2_6
	0.3692	178.7_0	178.9_2

The results of the tables IV, V and VI are compared in § 4c.

§ 4. *Calculations* [1]).

a. 0° C and temperatures of liquid ethylene.

With the formulas deduced in Comm. N°. 209c [2]) we calculated c_p/c_v, $(c_p/c_v)_{p=0}$, c_v and c_p from W (tables II and III). For that purpose through three values of B, derived by NIJHOFF [3]) from the measurements of KAMERLINGH ONNES and VAN URK [4]) in the corresponding temperature range, we laid a curve of the second degree in $1/T$, with which we could calculate the values of B, dB/dT and d^2B/dT^2.

The results of these calculations are given in tables VII and VIII.

TABLE VII. Resonator R_I, 0° C.

Presssure at	c_p cal/mole	c_v cal/mole	c_p/c_v	$(c_p/c_v)_{p=0}$
0.9844	6.97	4.97	1.402	1.400

From the value of $(c_p/c_v)_{p=0}$ it appears that the influence of the end-openings in Resonator R_I may be supposed to be negligible. Our value 1.402 for c_p/c_v agrees with 1.4018 found by BRINKWORTH [5]) at 17° C.

[1]) Mol. weight M = 28.016.
[2]) loc. cit.
[3]) G. P. NIJHOFF, Diss. Leiden 1928. Comm. Leiden Suppl. No. 64*f*.
[4]) H. KAMERLINGH ONNES and A. TH. VAN URK. Comm. Leiden No. 169*d*.
[5]) J. H. BRINKWORTH, Proc. Roy. Soc. London (A) **111**, 124, 1926.

TABLE VIII. Resonator R_I.

Temperatures of liquid ethylene.					
T °K.	Pressure at	c_p cal/mole	c_v cal/mole	c_p/c_v	$(c_p/c_v)_{p=0}$
166.03	1.0090	7.00	4.97	1.407	1.400
161.14	0.9925	7.01	4.98	1.407	1.400
156.53	0.9786	7.03	5.00	1.406	1.398
146.04	0.9506	6.97	4.93	1.413	1.403

The small deviations of $(c_p/c_v)_{p=0}$ from the value 1.400 may be due to the fact that the temperature has not been very constant during the measurements.

b. Temperatures of liquid oxygen and nitrogen.

1. *Resonator R_I*. In Fig. 1 we plotted W as a function of the pressure.

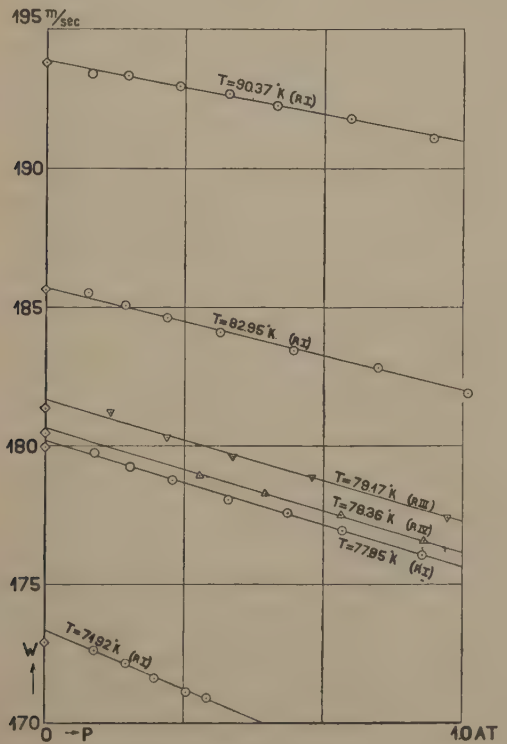

Fig. 1

It follows from Comm. N⁰. 209c § 2 that it is possible to calculate a formula representing the change of the second virial coefficient B with T from the dependence of $\left(\frac{\partial W^2}{\partial p}\right)_{p=0}$ on the temperature.

We have tried to determine this function by representing the dependence of W^2 on the pressure by a quadratic formula in p with three coefficients. These coefficients were calculated by the method of least squares. We observe, however, that it is not possible to obtain certainty about the coefficient of p^2, on account of the comparatively small range of pressures. We therefore then determined only two coefficients by representing the dependence of W on the pressure by a linear formula. Thus we still obtain a quadratic dependence of W^2 on p.

So we postulated finally:

$$W = W_0 (1 + sp).$$

The coefficients W_0 and s were calculated from the data in table IV by means of the method of least squares.

From the coefficient W_0 the value $(c_p/c_v)_{p=0}$ can be derived by the relation:

$$\left(\frac{c_p}{c_v}\right)_{p=0} = \frac{M W_0^2}{RT} \quad . \quad . \quad . \quad . \quad . \quad . \quad . \quad . \quad (1)$$

S is calculated from:

$$S = \frac{RT}{2 W_0^2}\left(\frac{\partial W^2}{\partial p}\right)_{p=0} = RT \,.\, s = B + \frac{T}{\lambda}\cdot\frac{dB}{dT} + \frac{T^2}{2\lambda(\lambda+1)}\cdot\frac{d^2B}{dT^2}, \quad . \quad (2)$$

where $\lambda = \frac{(c_v)_{p=0}}{R}$.

The results of these calculations are shown in table IX and plotted in Fig. 2 (indicated by ⊙).

TABLE IX.

T °K.	W_0 m/sec	s at^{-1}	$S \,.\, 10^3$	$(c_p/c_v)_{p=0}$
90.37	193.8_4	—0.01486	—4.919	1.400_7
82.95	185.7_0	—0.01979	—6.013	1.400_5
77.95	180.2_0	—0.02554	—7.291	1.403_4
71.92	173.3_4	—0.03705	—9.757	1.407_5

2. *Resonators R_{III} and R_{IV}.*

In view of the correction on the velocity of sound due to the

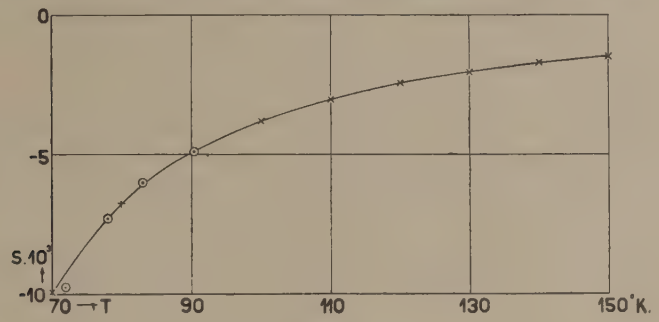

Fig. 2

resonator, we have controlled the measurements, mentioned in 1, using the resonators R_{III} and R_{IV} (table V and VI, indicated in Fig. 1 by ▽ resp. △). To be able to compare the results with those found in R_I we have also extrapolated to a pressure zero, but now with a coefficient s derived from the first measurements. See § 5.

The coefficient W_0 has been calculated by the method of least squares.

TABLE X.

Resonator	T °K.	s at^{-1}	W_0 m/sec	$(c_p/c_v)_{p=0}$
R_{III}	79.17	−0.02505	181.67	1.404_4
R_{IV}	78.36	−0.02409	180.66	1.403_2

At these temperatures the influence of the end-openings proves to be perceptible in resonator R_{III}, although this influence is much smaller than at 0° C.

Here also we obtain a good agreement by applying the formula of KIRCHHOFF-HELMHOLTZ.

3. We observe (tables IX and X), that $(c_p/c)_{p=0}$ slightly exceeds the value 1.400, the more so as the temperature is lower. If, however, we calculate [1]) theoretically the part of c_v corresponding to the rotational movement of the molecules, deriving the moment of inertia of the nitrogen molecule from RASETTI [2]), we find that the rotational energy must have already reached the classical value.

At 90.37 and 82.95° K. the agreement with the theoretical value is very satisfactory. For the temperatures 77.95 and 71.92° K. there is a

[1]) S. DÄUMICHEN, Zs. f. Phys. **62**, 414, 1930.

[2]) F. RASETTI, Proc. Nat. Acad. Amer. **15**, 515, 1929.

discrepancy of which we cannot find, what experimental error could have caused it. We observe that for oxygen a similar discrepancy was found [1]).

In Fig. 1 we also plotted the velocity of sound in the ideal gas, with $(c_p/c_v)_{p=0} = 1.400$ (indicated by ⊙).

§ 5. *Calculation of the dependence of the second virial coefficient B on the temperature.*

We calculated a curve $B = f(1/T)$ of the fourth degree in $1/T$ from the following data on B and S (comp. equation (2)):

$$\left.\begin{array}{ll} T = 77.95\ ^\circ\text{K}. & 10^3 . S = -7.291 \\ T = 90.37 & 10^3 . S = -4.919 \\ T = 126.77 & 10^3 . B = -4.542 \\ T = 140.00 & 10^3 . S = -1.726 \\ T = 151.90 & 10^3 . B = -3.117 \end{array}\right\}\ ^2)$$

We found:

$$10^3 B = -4.090 + \frac{24.627}{T} 10^2 - \frac{57.319}{T^2} 10^4 + \frac{41.159}{T^3} 10^6 - \frac{11.403}{T^4} 10^8 . \quad (3)$$

We took $\lambda = 5/2$ also at the lowest temperatures. From this formula we calculated values of S and B (table XI). The first have been plotted in Fig. 2 (indicated by ×).

TABLE XI.

T °K.	$10^3 . S$	$10^3 . B$
70	−9.961	−13.382
80	−6.787	−10.319
90	−4.971	− 8.411
100	−3.813	− 7.026
110	−3.022	− 5.937
120	−2.455	− 5.052
130	−2.038	− 4.322
140	−1.727	− 3 711
150	−1.492	− 3.204

[1]) W. H. KEESOM, A. VAN ITTERBEEK and J. A. VAN LAMMEREN. These Proceedings **34**, 1001, 1931. Comm. Leiden No. 216*d*.

[2]) The values of B were derived from measurements of KAMERLINGH ONNES and VAN URK. loc. cit. We calculated the value of S at $T = 140^\circ$ K. from B-values in this temperature range.

In Fig. 3 the B-points following from our formula are indicated by △.

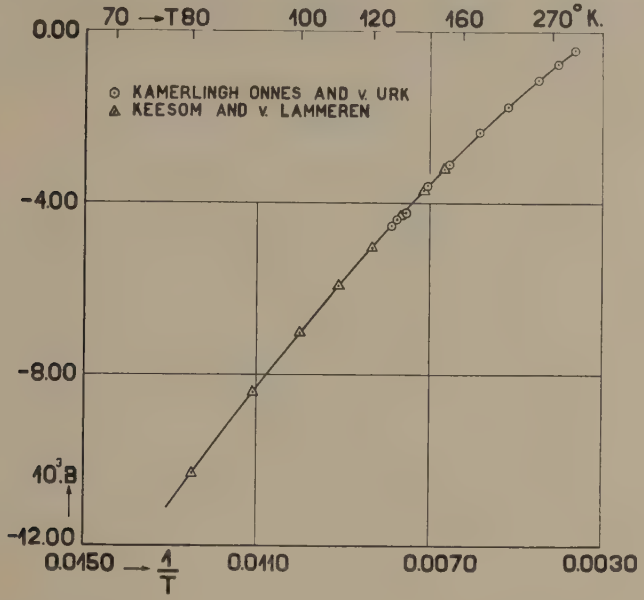

Fig. 3

§ 6. *Calculation of the ratio c_p/c_v and the specific heats themselves.* Deriving B and dB/dT from the formula (3) mentioned above and the third virial coefficient C by means of "the average empirical reduced equation of state" [1]) we calculated c_p/c_v, c_p and c_v at the temperatures 90.37 and 82.95° K. W was calculated from the coefficients W_0 and s (§ 4). The formulas used have been published by A. VAN ITTERBEEK [2]). The results are shown in table XII.

TABLE XII.

T °K.	Pressure at	c_p cal/mole	c_v cal/mole	c_p / c_v
90.37	0.0	6.94	4.96	1.400_7
	0.3	7.01	4.97	1.409_7
	0.6	7.08	4.99	1.419_1
	0.9	7.15	5.00	1.428_9
82.95	0.0	6.94	4.96	1.400_5
	0.3	7.05	5.00	1.411_0
	0.6	7.15	5.03	1.422_1
	0.9	7.25	5.08	1.433_9

[1]) H. KAMERLINGH ONNES and W. H. KEESOM, Encycl. d. Math. Wiss. V **10**, 615, 1912. Comm. Leiden Suppl. No. **23**, 117, 1908.

[2]) A. VAN ITTERBEEK, Wis- en Nat. Tijdschr. **5**, 192, 1932. Comm. Leiden Suppl. N°. 70*b*.

For comparison we refer to the value of c_p found by SCHEEL and HEUSE [1]) being 7.162 at the temperature 92° K. and a pressure of about one atmosphere.

We gladly record our thanks to Mr. W. BEVELANDER, phil. nat. cand., for his assistance in this investigation.

Summary.

The velocity of sound in nitrogen gas has been measured in the temperature range extending from 0° C. down to liquid nitrogen temperatures, in dependence on the pressure. Four resonators are used to get an idea of the validity of the formula of KIRCHHOFF-HELMHOLTZ. This formula proves to give good results. A curve $B = f(1/T)$ (B being the second virial coefficient) has been calculated holding from 150 down to 80° K. Also the ratio c_p/c_v and the specific heats c_p and c_v were calculated.

[1]) K. SCHEEL and W. HEUSE, Ann. d. Phys. (4) **40**, 473, 1913.

Physics. — *On the Anomaly in the Specific Heat of Liquid Helium.* By W. H. KEESOM and Miss A. P. KEESOM. Communication N°. 221*d* from the KAMERLINGH ONNES Laboratory at Leiden.

(Communicated at the meeting of June 25, 1932).

§ 1. *Introduction.* The investigation on the specific heat of liquid helium made by one of us with Dr. CLUSIUS [1]) gave rise to some questions which made a nearer investigation of the anomaly of the specific heat of that substance, revealed by the investigation mentioned, desirable.

So it seemed important to see whether the curve of the specific heats obtained should undergo some change if a better heat conduction in the liquid was provided for. In this connection the course of the curve of the specific heats above 2.19° K attracted special attention. Although we have not yet been able to make experiments in which the conditions of heat supply and heat conduction were the most ideal ones, we could make some measurements with improved heat conduction in the liquid in such a way that we can draw at least a preliminary conclusion concerning this question.

[1]) W. H. KEESOM and K. CLUSIUS. These Proceedings, **35**, 306. 1932; Comm. Leiden No. 219e.

Furthermore an examination of the course of the specific heat in the vicinity of the top of the specific heat curve by measurements with a very small temperature rise was interesting.

This paper contains the results of some series of experiments on these lines.

§ 2. *Method.* We followed the method and used the same apparatus as described by one of us and Dr. CLUSIUS in Comm. N°. 219*e*, with the following alterations:

a. A better heat conduction in the liquid helium was ensured by means of a copper cross about 1 mm thick soldered to the cover of the copper container of the liquid helium. This cross reached as far as quite near to the bottom and to the side wall of the container.

b. The temperature rise in the specific heat measurements was chosen of the order of magnitude of 0.01 degree in the vicinity of 2.19° K[1]).

c. The change of temperature during the experiment was observed by reading the galvanometer deflection [2]). Moreover by properly switching in a shunt in the galvanometer circuit, the temperature of the core during the heating period was followed.

The temperatures were always measured with the phosphorbronze thermometer. On April 28th we used a measuring current of 1.34 mA, with which CLUSIUS calibrated the wire. On April 21st we used a measuring current of 0.406 mA and derived our calibration curve from measurements made with this measuring current by one of us and VAN DEN ENDE on another part of the same phosphorbronze wire. For this purpose we took two cooling curves, on which the point 2.19° K very clearly distinguished itself. We estimate the accuracy reached to be 0.01° K. The accuracy of our measurements of temperature differences is much higher.

In order to derive the temperature increase $\triangle T$ from the increase of the resistance of the phosphorbronze wire $\triangle W$, we made a curve of dT/dW as a function of T.

§ 3. *Results.* Tables I and II contain the results obtained.

In Fig. 1 the galvanometer readings during the measurements I*f*—I*i* of April 28 are represented. The readings during the heating periods (scale 42—46) were made while the galvanometer was shunted.

From the regularity of the readings it is seen that measurements of the specific heat with a temperature increase of about 0.01 degree are quite

---

[1]) KEESOM and CLUSIUS (These Proceedings **35**, 317, 1932, note 1) had already made a successive series of such small heatings in this temperature region, and so reached the important conclusion concerning the absence of any transformation heat, without however making exact measurements in that experiment.

[2]) KEESOM and CLUSIUS continually adjusted the compensation bank and made their readings on the bank.

TABLE I.

Specific heat of liquid helium.
Measurements of April 21st. 1932.

No.	Current mA	Time seconds	Tension Volts	Heat supplied cal.	Temperature °K	Temp. increase °K	Heat capacity cal/°K	Spec. heat cal/°K.g.
Ia	16.75	48	1.017	0.1836	1.315	0.117_8	1.559	0.138
b	22.48	28	1.366	0.1931	1.330	0.118_6	1.628	0.144
c	23.80	44	1.448	0.3406	1.593	0.069_3	4.915	0.434
d	28.24	68	1.725	0.7439	1.918	0.069_7	10.673	0.968
IIa	19.75	46	1.199	0.2447	2.126	0.011_8	20.734	1.828
b	16.74	42	1.021	0.1612	2.089	0.009_1	17.697	1.559
c	16.74	48	1.021	0.1842	2.113	0.009_9	18.610	1.642
d	16.74	36	1.021	0.1382	2.125	0.007_1	19.467	1.717
e	16.76	34	1.022	0.1308	2.134	0.006_4	20.408	1.800
f	16.74	62	1.020	0.2377	2.147	0.011_5	20.651	1.821
g	16.74	72	1.020	0.2761	2.160	0.011_8	23.943	2.065
h	16.72	68	1.019	0.2602	2.172	0.010_2	25.508	2.251
i	16.72	78	1.019	0.2984	2.184	0.009_4	31.749	2.802
j	24.11	66	1.470	0.5253	2.205	0.030_2	17.394	1.535
k	16.41	64	1.003	0.2366	2.230	0.025_1	9.425	0.832
l	16.41	64	1.003	0.2366	2.257	0.030_1	7.859	0.694
m	16.41	44	1.003	0.1626	2.282	0.024_4	6.666	0.588
n	16.43	50	1.003	0.1850	2.305	0.027_4	6.753	0.596
o	16.43	52	1.003	0.1924	2.330	0.029_5	6.523	0.576
p	16.43	44	1.003	0.1628	2.356	0.026_4	6.168	0.544
q	29.6_3	80	1.801	0.9587	2.451	0.153_4	6.250	0.551
r	30.6_3	78	1.873	1.0049	2.613	0.164_5	6.109	0.539
s	30.6_3	78	1.875	1.0060	2.784	0.160_7	6.260	0.552
t	30.6_3	80	1.873	1.0307	2.949	0.149_9	6.876	0.607

The resistance in the Voltmeter circuit was 1000 Ohm. The calorimeter was for series I filled at 2.734 °K and contained 11.314 g. helium. For series II it was filled at 2.706 °K and contained 11.332 g helium. Measuring current 0.406 mA.

TABLE II.

Specific heat of liquid helium.
Measurements of April 28th, 1932.

No.	Current mA	Time seconds	Tension Volts	Heat supplied cal.	Temperature °K	Temp. increase °K	Heat capacity cal/°K	Specific heat cal/°Kg.
Ia	15.98	60	0.967	0.2083	2.120	0.0105_8	19.688	1.740
b	16.00	62	0.969	0.2164	2.137	0.0103_2	20.969	1.854
c	16.00	60	0.969	0.2089	2.150	0.0094_3	22.153	1.958
d	16.00	60	0.969	0.2089	2.160	0.0088_9	23.498	2.077
e	15.96	60	0.967	0.2080	2.170	0.0082_0	25.366	2.242
f	15.96	60	0.967	0.2080	2.179	0.0075_3	27.623	2.442
g	15.92	60	0.967	0.2075	2.186	0.0066_9	31.016	2.742
h	15.94	60	0.967	0.2077	2.196	0.0118_5	17.527	1.549
i	15.92	60	0.967	0.2075	2.210	0.0182_8	11.351	1.003
j	15.92	58	0.967	0.2008	2.231	0.0196_9	10.198	0.901
k	15.90	60	0.965	0.2068	2.253	0.0241_9	8.549	0.756
l	15.90	60	0.965	0.2068	2.279	0.0263_6	7.845	0.693

The resistance in the voltmeter circuit was 1000 Ohm. The calorimeter was filled at 2.730 °K and contained 11.313 g helium. Measuring current 1.34 mA.

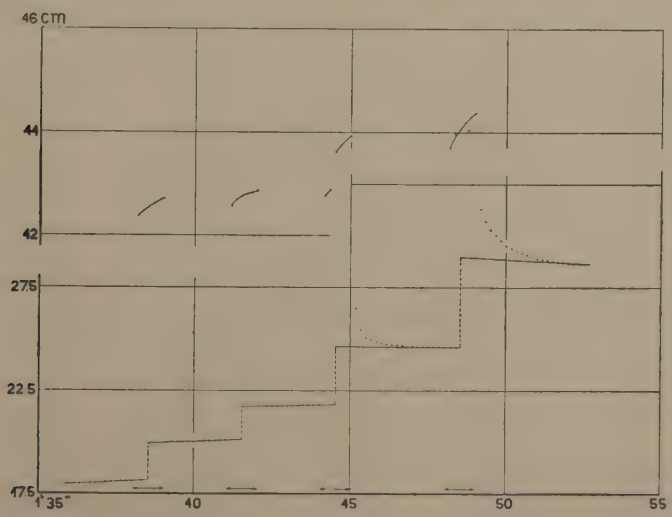

Fig. 1

feasible also in this region of temperatures. There are represented two heatings below (experiments I *f* and *g*) and one heating (I *i*) above the point 2.19° K, while from the jump in the heating period of experiment I *h* we derive that in this experiment that point was passed.

As the quantity of heat applied in these experiments was practically the same, the much larger temperature increase of I *i* compared with I *f* and I *g* immediately indicates the fall of the specific heat.

The attention is further drawn to the fact that the afterperiods above 2.19° K have quite another character than those below that point. It is evident that the distribution of the applied heat in the liquid is much faster below 2.19° K than above. One should be inclined to consider the facts that the heat supply is from above and that helium at 2.19° K has a maximum density, so that below that temperature convection currents are liable to occur, whereas this will not be the case at temperatures above 2.19° K, as an explanation of this difference. From certain thermodynamical reasoning it is however doubtful whether the density maximum really coincides with the jump in the specific heat, and it is therefore perhaps reasonable to look for another explanation. As such a change in the heat conductivity or in the viscosity of liquid helium present themselves. In this connection it is interesting that from other phenomena also the probability of a change in viscosity of liquid helium was deduced. It must be left to further experimental research to decide these questions.

The jump in the heating-period of experiment I *h* points to the same phenomenon: decrease of the heat transport through the liquid, possibly

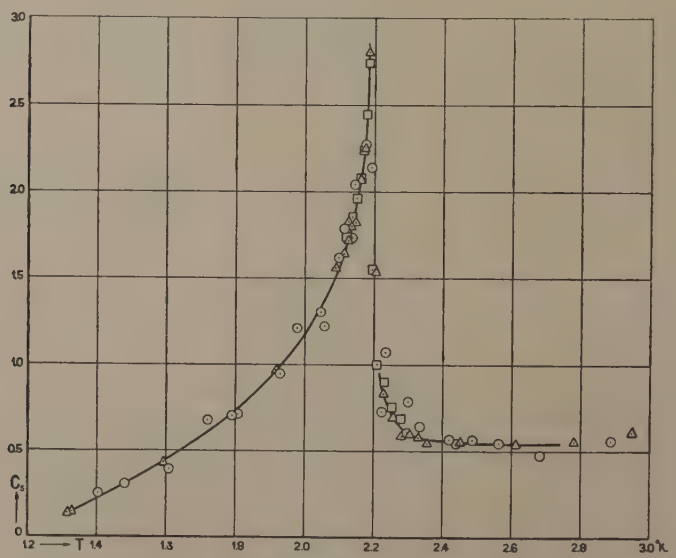

Fig. 2

△ April 21st. ⊡ April 28th. ⊙ KEESOM and CLUSIUS.

in consequence of a decrease in intensity of the convection currents by an increase of viscosity.

In Fig. 2 the results of the series of measurements of April 21st and 28th are compared with those obtained by KEESOM and CLUSIUS. It is clear that a good agreement exists. From this follows that the fact that heat is not immediately conducted through the liquid has not had an appreciable influence on the results of the measurements.

It is evident as well from Fig. 2 as from the data given in Table I and II that the points at temperatures 2.205 and 2.196 (experiments II *j* of April 21st and I *h* of April 28th) belong to measurements in which the jump in the specific heat is passed, so that the specific heat of these points is a certain average between the large and the small specific heats.

In Fig. 3 the results of the measurements of April 28th are represented separately.

§ 4. *Conclusions.* *a.* Each value of the specific heat measured is an average value over the temperature interval of the heating period. Con-

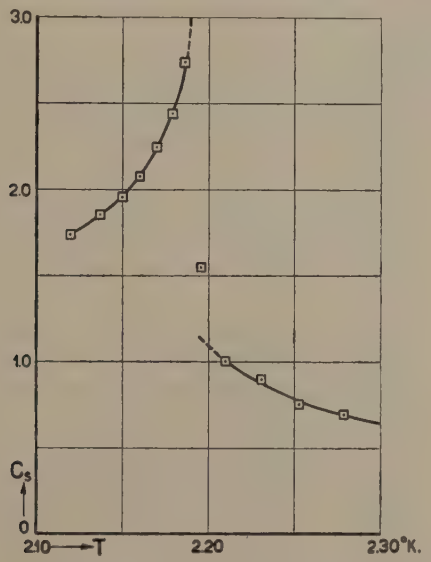

Fig. 3

sidering this one can safely conclude from the experiments II *i* of April 21st and I *g* of April 28th that the true specific heat at the higher limit of the temperature intervals involved was at least 3.0. This value corresponds to the temperature 2.189° K.

The highest specific heat measured above the point 2.19° K is 1.003 at 2.210° K (I *i* April 28th). This is the average specific heat between 2.201 and 2.219° K. Considering also the results of the following experiments

one may conclude that the true specific heat at 2.201° K probably surpasses 1.1 very little, if at all. The same conclusion is arrived at by an analysis of experiment I *h* of the same day. To explain the average specific heat found in this experiment one must moreover assume that the jump in the specific heat must have occurred very shortly after the reading of 44 m 20 sec (cf. Fig. 1), and must have been completed within some thousandths of a degree.

So our conclusion is that the specific heat of liquid helium at about 2.19° K falls from a value of 3.0 to a value of about 1.1 certainly within 0.02 degree, very probably even within a couple of thousandths of a degree.

b. Leaving open the question whether the fall of the specific heat really occurs discontinuously in the strict sense of the word, or in a very small temperature interval, it will be appropriate from an experimental point of view to consider the fall to occur abruptly. For convenience sake it is desirable to introduce a name for the point at which this jump occurs. According to a suggestion made by Prof. EHRENFEST we propose to call that point, considering the resemblance of the specific heat curve with the Greek letter λ, the *lambda-point.*

The curve that shows how the lambda-point depends on the pressure will be called the *lambda-curve* [1]).

As in several cases it is also convenient to distinguish between the two conditions of the liquid helium with such different values of the specific heat, we will continue to call liquid helium I the liquid helium above the lambda-temperature (for the pressure considered) and liquid helium II the liquid helium below that temperature.

We gladly express our thanks to J. A. KOK, phil. nat. cand., for his help with these measurements.

Summary.

The specific heat of liquid helium under its saturated vapour pressure was measured in the vicinity of 2.19° K with temperature increases of 0.01 to 0.02 degree. The specific heat has a maximum value of about 3.0 at 2.19° K and falls down to 1.1 certainly within 0.02° K, probably within a couple of thousandths of a degree.

---

[1]) Cf. W. H. KEESOM and K. CLUSIUS. These Proceedings **34**, 605, 1931. Comm. Leiden. N°. 216*b*.

Physics. — *On the change of the specific heat of tin when becoming supraconductive.* By W. H. KEESOM and J. A. KOK. (Communication N°. 221e from the KAMERLINGH ONNES-Laboratory at Leiden).

(Communicated at the meeting of June 25, 1932).

§ 1. *Introduction.* In Comm. N°. 219*b* [1]) one of us with VAN DEN ENDE reported on measurements of the specific heat of tin, and concluded that the atomic heat of tin at or near 3.7° K. suffers a rapid change or a jump, so that just below 3.7° K. the atomic heat is larger than just above. The authors remarked further that the coincidence (or nearly so) with the transition point suggests that this rapid change or jump is connected with supraconductivity.

When in measurements, made by one of us and Miss KEESOM [2]) on the specific heat of liquid helium, it had appeared that it was quite feasible to make rather accurate measurements for that substance with heatings of the order of 0.01 of a degree, we resolved to try whether it should be possible to do so too for the much smaller heat capacity of a tin block such as the above-mentioned authors used in their investigation. We hoped thus to be able to discover whether the change in the specific heat of tin has really the character of a jump, and if so, whether this jump coincides with the transition point to supraconductivity.

This paper deals with the results of a series of measurements made with this object in view.

In this series of measurements we did not intend to investigate the influence of a magnetic field, reserving this for a special examination. By chance, however, in a couple of measurements the tin was in such a magnetic field that it disturbed supraconductivity, so that we were able to draw already a preliminary conclusion about the influence of disturbing supraconductivity on the value of the specific heat.

§ 2. *Method.* For the details of the method we refer to Comm. N°. 221*d*. The measuring and heating core was the same as that which we used in our measurements on silver [3]). For the calibration of the phosphorbronze thermometer we refer to Comm. N°. 219*b*. We used for these measurements a ZERNIKE galvanometer *Zc*, measuring current 0.4 mA. A temperature

---

[1]) W. H. KEESOM and J. N. VAN DEN ENDE. Proceedings **35**. 143. 1932. Comm. Leiden No. 219*b*.

[2]) W. H. KEESOM and Miss. A. P. KEESOM. These Proc. **35**. 736. 1932. Comm. Leiden No. 221*d*.

[3]) W. H. KEESOM and J. A. KOK. These Proc. **35**. 301. 1932. Comm. Leiden No. 219*d*.

increase of 0.01 degree corresponded with a deflection of 6.6 cm on the galvanometer scale.

We made for these measurements a new block of tin, of the same degree of purity as that of Comm. N°. 219*d*, weight 742.4 g.

In consequence of a very slight untightness of the box [1]) surrounding the tin block the vacuum was not so high as we might have wished. Nevertheless we could derive specific heats with a reasonable degree of accuracy.

§ 3. *Results.* We obtained the results recorded in table I. They are represented in Fig. 1.

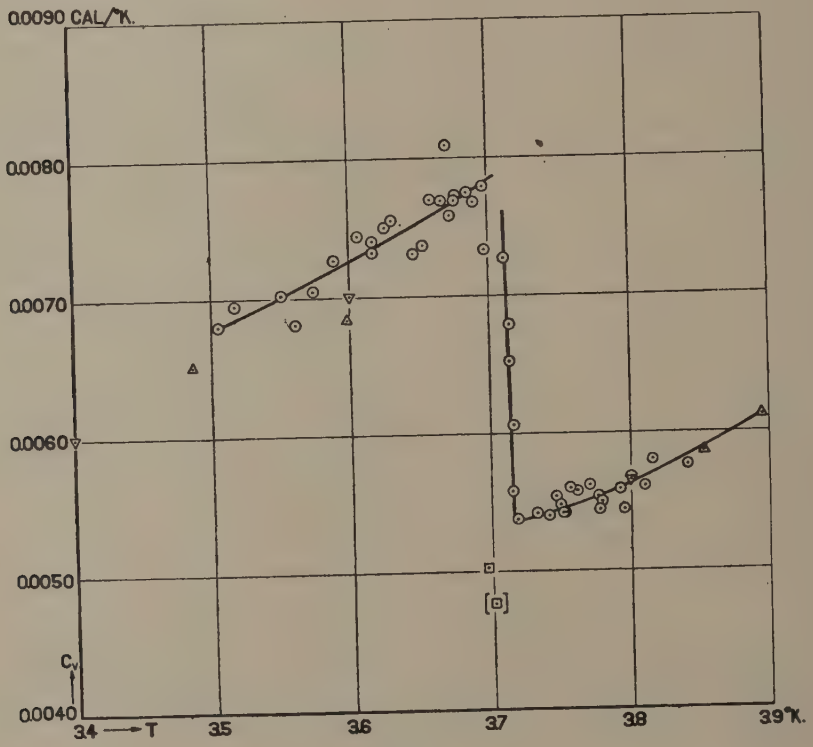

Fig 1

In Fig. 1 4 points measured by KEESOM and VAN DEN ENDE, indicated by △ have been plotted, as well as 3 other points, indicated by ▽ resulting from the smoothed curve they derived from their measurements. It appears that the agreement of our results with theirs is quite satisfactory.

The experiments II *p* and *q*, indicated by ⊡ in Fig. 1, deserve special attention because during them a magnetic field was applied for measurements in a neighbouring cryostat. With regard to the measurements to be made in this neighbour cryostat, our cryostat was partly surrounded by a

[1]) Comp. Comm. No. 219*b*. Fig. 3.

TABLE I.

ATOMIC HEATS OF TIN.
Measurements of May 26th, 1932.

No.	Heat supplied cal	Temperature °K.	Temperature increase °K.	Total heat capacity cal/°K.	Heat capacity core cal/°K.	Atomic heat cal/°K.	Θ
Ia	0.000306_3	3.505	0.0069_0	0.0443_9	0.0018_3	0.0068_0	143.3
b	0.000296_8	3.517	0.0065_5	0.0453_2	0.0018_4	0.0069_5	142.7
c	0.000282_4	3.551	0.0061_7	0.0457_7	0.0018_6	0.0070_2	143.6
d	0.000228_6	3.561	0.0051_4	0.0444_7	0.0018_7	0.0068_1	145.6
e	0.000309_3	3.574	0.0067_3	0.0459_6	0.0018_8	0.0070_5	144.4
f	0.000282_4	3.589	0.0059_6	0.0473_8	0.0018_9	0.0072_7	143.5
k	0.000376_6	3.617	0.0079_0	0.0476_7	0.0019_1	0.0073_2	144.2
l	0.000416_9	3.631	0.0084_8	0.0491_6	0.0019_2	0.0075_5	143.3
m	0.000470_7	3.646	0.0098_8	0.0476_4	0.0019_3	0.0073_1	145.5
n	0.000215_2	3.653	0.0044_8	0.0480_4	0.0019_4	0.0073_7	145.4
o	0.000390_0	3.677	0.0077_5	0.0503_2	0.0019_6	0.0077_3	144.0
p	0.000336_2	3.690	0.0067_2	0.0500_3	0.0019_7	0.0076_8	144.8
q	0.000511_0	3.718	0.0143_5	0.0356_1	0.0019_9	0.0053_8	164.4
r	0.000363_1	3.756	0.0098_0	0.0370_5	0.0020_3	0.0056_0	163.8
t	0.000322_8	3.777	0.0089_5	0.0360_7	0.0020_5	0.0054_4	166.4
u	0.000255_5	3.795	0.0070_8	0.0360_9	0.0020_6	0.0054_4	167.2
v	0.000443_8	3.841	0.0116_3	0.0381_6	0.0021_1	0.0057_6	165.9
IIa	0.000376_6	3.589	0.0079_5	0.0473_7	0.0018_9	0.0072_7	143.5
b	0.000376_6	3.606	0.0077_8	0.0484_1	0.0019_0	0.0074_4	143.1
c	0.000376_6	3.617	0.0078_1	0.0482_2	0.0019_1	0.0074_0	143.7
d	0.000295_9	3.626	0.0060_6	0.0488_3	0.0019_2	0.0075_0	143.4
e	0.000390_0	3.659	0.0077_0	0.0501_3	0.0019_4	0.0077_0	143.4
f	0.000322_7	3.667	0.0064_5	0.0500_3	0.0019_5	0.0076_9	143.9
g	0.000349_7	3.671	0.0073_0	0.0525_2	0.0019_5	0.0080_9	145.3
h	0.000416_9	3.673	0.0084_5	0.0493_4	0.0019_6	0.0075_8	144 8
i	0.000376_6	3.676	0.0075_2	0.0500_8	0.0019_6	0.0076_9	144.2
j	0.000430_3	3.685	0.0085_3	0.0504_5	0.0019_7	0.0077_5	144 1
k	0.000228_6	3.695	0.0045_1	0.0506_9	0.0019_8	0.0077_9	144.3

TABLE I. *(Continued).*

ATOMIC HEATS OF TIN.
Measurements of May 26th. 1932.

No.	Heat supplied cal	Temperature °K.	Temperature increase °K.	Total heat capacity cal/°K.	Heat capacity core cal/°K.	Atomic heat cal/°K.	Θ
m	0.000255_5	3.714	0.0059_7	0.0428_0	0.0019_9	0.0065_2	154.0
n	0.000255_5	3.714	0.0057_5	0.0444_3	0.0019_9	0.0067_9	151.9
o	0.000416_9	3.716	0.0106_7	0.0398_7	0.0019_9	0.0060_6	157.8
p[1])	0.000349_7	3.696	0.0104_6	0.0334_3	0.0019_7	0.0050_3	167.0
[q[1])	0.000309_3	3.701	0.0097_3	0.0317_9	0.0019_8	0.0047_7	170.2]
r	0.000430_3	3.698	0.0089_8	0.0479_2	0.0019_9	0.0073_4	147.8
s	0.000430_3	3.711	0.0090_6	0.0474_9	0.0019_9	0.0072_7	148.4
t	0.000416_9	3.732	0.0116_1	0.0359_1	0.0020_1	0.0054_2	164.6
u	0.000390_0	3.746	0.0106_4	0.0366_5	0.0020_2	0.0055_4	164.0
v	0.000443_8	3.751	0.0123_5	0.0359_4	0.0020_2	0.0054_2	165.4
w	0.000416_9	3.749	0.0114_8	0.0363_2	0.0020_2	0.0054_8	164.7
x	0.000376_6	3.752	0.0104_9	0.0359_1	0.0020_2	0.0054_2	165.5
y	0.000416_9	3.761	0.0112_9	0.0369_3	0.0020_3	0.0055_8	164.2
z	0.000403_5	3.770	0.0108_4	0.0372_2	0.0020_4	0.0056_2	164.1
α	0.000430_3	3.776	0.0117_3	0.0366_8	0.0020_5	0.0055_4	165.3
β	0.000322_8	3.779	0.0088_5	0.0364_7	0.0020_5	0.0055_0	165.8
γ	0.000349_7	3.792	0.0094_4	0.0370_4	0.0020_6	0.0055_9	165.4
δ	0.000430_3	3.800	0.0114_7	0.0375_2	0.0020_7	0.0056_7	165.0
ε	0.000376_6	3.810	0.0101_4	0.0371_4	0.0020_8	0.0056_1	166.1
ζ	0.000390_0	3.816	0.0101_7	0.0383_5	0.0020_8	0.0058_0	164.4
η	0.000282_4	3.715	0.0076_6	0.0368_7	0.0019_9	0.0055_8	162.2
ϑ	0.000349_7	3.741	0.0097_8	0.0357_6	0.0020_1	0.0054_0	165.1

magnetic shield. This caused, however, a constant magnetic field which we estimate on account of later measurements to have been about 2 gauss. During the measurements II p and q the total magnetic field was about 7 gauss. By this the transition point will have been lowered[2]) by an

[1]) Magnetic field on.

[2]) Comp. J. VOOGD. Thesis for the Doctorate, p. 27. Rapports et Communications 6^{me} Congr. Int. du Froid, Buenos Aires 1932. No. 29 § 6.

amount of 0.04 degree, so that the tin in these two experiments was not supraconductive.

A transformation heat at the transition point was not observed.

§ 4. *Conclusions.*

a. It follows from the results plotted in Fig. 1 that between 3.70 and 3.72° K. the atomic heat decreases from a value of 0.0078 to a value of 0.0054.

The temperature interval within which this change of the specific heat occurs can be more closely limited by considering the points II*k* and I*q*. As a matter of fact the final temperature in II*k* was 3.699° K., the initial temperature in I*q* 3.711° K. Considering the fact that we may conclude from the results of these experiments that the change in the specific heat must occur between these temperatures, the temperature interval mentioned must be smaller than 0.012 degree.

b. Comparing the temperatures mentioned under *a* with those at which the metal passes into the supraconductive state [1]), we conclude that the change of the specific heat observed coincides with an accuracy of about 0.01 degree with the transition to the supraconductive state.

In drawing this conclusion we have considered that our tin block was in a constant magnetic field of about 2 gauss (cf. § 3). This would have lowered the supraconductive transition point by about 0.015 degree. This may, however, have been approximately compensated by the effect of mechanical tensions that have arisen in the polycrystalline block during cooling. For these reasons a greater accuracy than 0.01 degree cannot be warranted.

c. The conclusion that the change of the specific heat is connected with the phenomenon of supraconductivity is corroborated by the fact, as shown by the measurements II*p* and *q*, that the larger value of the specific heat is not found if supraconductivity is impeded by the presence of a magnetic field.

d. Whether the change of the specific heat occurs abruptly at a definite temperature or in a small temperature interval will, no doubt, depend on the question whether the transition to supraconductivity occurs at a definite temperature or in a small temperature interval. Though we must leave the final conclusion on this point to further experimental investigation, we think it probable that in the case of a single crystal of pure metal the specific heat undergoes a jump at the supraconductive transition point.

e. Transition to the supraconductive state is not connected with a transformation heat.

We gladly record our thanks to Miss A. P. KEESOM, phil. nat. cand., for her help with the measurements.

[1]) Comp. J. VOOGD. Thesis for the Doctorate Leiden. 1931. p. 24. Fig. 4.

Summary.

Specific heats of tin were measured between 3.5 and 3.9° K., with heatings of the order of 0.01 degree. Between 3.70 and 3.72° K. the atomic heat decreases from a value of 0.0078 to a value of 0.0054. This change coincides with the transition of the supraconductive to the non-supraconductive state. A magnetic field that impedes the occurrence of supraconductivity prevents also the change in specific heat. Transition to the supraconductive state is not connected with a transformation heat.

Physics. — *The supraconductivity of gold-bismuth.* By W. J. DE HAAS and T. JURRIAANSE. (Communication N°. 220e from the KAMERLINGH ONNES Laboratory Leiden.)

(Communicated at the meeting of June 25, 1932).

W. J. DE HAAS, E. VAN AUBEL and J. VOOGD found, that the eutectic of the two non-supraconductive metals, gold and bismuth, becomes supraconducting at 1.84° K.

As is evident from the melting diagram of VOGEL [1]), this system consists of two phases viz. a solid solution with the gold lattice in which maximally 4 % Bi is solved and the pure bismuth; fig. 1.

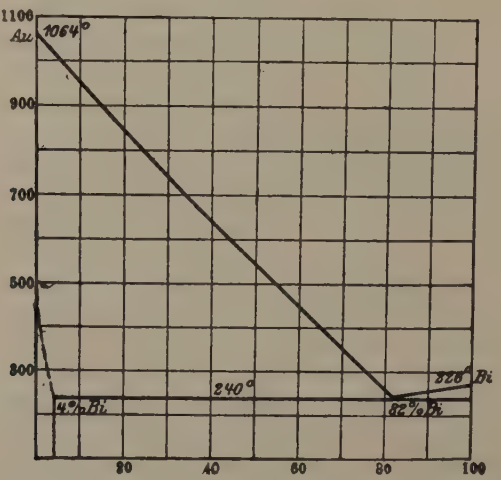

From these measurements the conclusion was drawn, that the supraconductivity was due to the gold phase [2]). To explain this behaviour of the gold-phase we may start from three hypotheses:

[1]) Zs. f. Anorg. u. allgem. Chem. **50**, 147, 1906.

[2]) Comm. Leiden No. 197c. These Proc. XXXII, p. 724.

1. Pure gold becomes supraconducting below the lowest temperature at which gold has been investigated. This implies an elevation of the transition point of more than 0°.8. This is rather improbable.

2. The melting diagram is wrong or a second crystal lattice exists.

3. The supraconductivity is purely due to the combination of these two non-supraconductors.

In this paper the investigations on this question will be discussed.

To test the first hypothesis we tried to find out by the Röntgenmethod of DEBIJE—SCHERRER, whether, in carefully tempered solid solutions, the lattice is strained to such a degree by the substitution of its atoms by the bismuth atoms that this might cause the great elevation of the transition point by 0.8 degree.

No change however was observed in the distances between the lines of the interference figure of the pure gold and of the solid solutions with a Bi concentration below 1 $^0/_{00}$.

At higher percentages of Bi e.g. 10 %, 20% and 40 % other lines occur than those of the gold lattice. According to the diagram of VOGEL these should be lines of the bismuth lattice. A comparison between photos of a solution 40 % Bi in gold and of pure bismuth showed that the new lines did *not* belong to the bismuth.

Evidently a third phase exists with a different crystal lattice.

A Röntgen photo of what VOGEL indicates as the eutectic gold-bismuth shows that this does not contain lines of the gold lattice and only bismuth lines and new lines.

The new phase can be separated from its eutectic with bismuth by washing away the bismuth with nitric acid.

Having done this we retain a fine powder and rather large crystals.

The chemical analysis by Dr. C. GROENEVELD gave a very constant composition with the formula Au_2Bi. Also the distance of the lines in the Röntgendiagram of the washed Au_2Bi powder and of the 10, 20, and 40 % solutions agreed within 1 $^0/_{00}$, so that we may assume that neither of the two components is soluble in the Au_2Bi. The structure analysis, too, gave the same result.

The Au_2Bi powder becomes supraconducting in liquid helium at just the same temperature as the eutectics and the solid solutions measured by DE HAAS, VAN AUBEL and VOOGD. Thus the new Au_2Bi-phase is the supraconductor in the system gold bismuth.

Angular measurements at the crystals taught that they were octahedral or crystal forms near these.

Rotation diagrams, after POLANYI—SCHIEBOLD, of some crystals round three mutually perpendicular axes gave the same interference figure, so that in fact the crystal is cubic. The edge is 7.94 Å.

The pycnometrically determined density is 15.46, so that we have 24 atoms per elementary cell. The röntgenographically determined density is 15.70.

A rotation diagram with a face diagram as axis (110) gave a zone distance $\sqrt{2}$ times as large as that of a (100) diagram.

This is an indication of a face-centred-translation-lattice. Also the extinctions in the DEBIJE—SCHERRER diagram are in agreement with this. We have therefore a face-centred-cube lattice. A calculation of the intensities shows that only the space-group O^4 is possible with the following point-arrangement.

$$Au \begin{cases} {}^1/_8\ {}^1/_8\ {}^1/_8,\ {}^5/_8\ {}^5/_8\ {}^1/_8,\ {}^5/_8\ {}^1/_8\ {}^5/_8,\ {}^1/_8\ {}^5/_8\ {}^5/_8,\ {}^1/_8\ {}^7/_8\ {}^7/_8,\ {}^5/_8\ {}^3/_8\ {}^7/_8, \\ {}^5/_8\ {}^7/_8\ {}^3/_8,\ {}^1/_8\ {}^3/_8\ {}^3/_8,\ {}^7/_8\ {}^1/_8\ {}^7/_8,\ {}^3/_8\ {}^5/_8\ {}^7/_8,\ {}^3/_8\ {}^1/_8\ {}^3/_8,\ {}^7/_8\ {}^5/_8\ {}^3/_8 \\ {}^7/_8\ {}^7/_8\ {}^1/_8,\ {}^3/_8\ {}^3/_8\ {}^3/_8,\ {}^3/_8\ {}^7/_8\ {}^5/_8,\ {}^7/_8\ {}^3/_8\ {}^5/_8 \end{cases}$$

$$Bi \begin{cases} {}^1/_2\ 0\ 0,\ {}^1/_2\ {}^1/_2\ {}^1/_2,\ 0\ 0\ {}^1/_2,\ 0\ {}^1/_2\ 0, \\ {}^3/_4\ {}^1/_4\ {}^1/_4,\ {}^3/_4\ {}^3/_4\ {}^3/_4,\ {}^1/_4\ {}^1/_4\ {}^3/_4,\ {}^1/_4\ {}^3/_4\ {}^1/_4 \end{cases}$$

The second possible point-arrangement is the above one displaced over half an identity period. Thus the gold and bismuth atoms are situated at points non-equivalent for the structure and therefore not statistically distributed, so that we can speak of Au_2Bi combination in which neither gold nor bismuth is soluble. We have, therefore, to do with a singular kind of crystal, which is in good agreement with the very low magnetic threshold value[1]) of the gold-bismuth. This is of the same order of magnitude as that of the pure supraconductors[2]). Until now always high magnetic threshold values have been given for solid solutions.

The results of the measurements and a complete discussion of the structure will appear in the next communication.

---

[1]) Comm. Leiden No. 214*b*. These Proc. XXXIV, p. 56.

[2]) Comm. Leiden No. 191*b*. These Proc. XXXI, p. 687.

Chemistry. — *Oxidation of phenol with peracetic acid. (Contribution to the knowledge of the substitution of benzene).* By Prof. J. BÖESEKEN.

(Communicated at the meeting of June 25, 1932).

Some years ago G. SLOOFF and one of us (B.) discovered that at the oxidation of naphtalene with peracetic acid a very considerable quantity of o-carboxy-cis-cinnamic acid is produced. So one of the benzene-rings of the naphtalene is opened, by which probably the naphtalene o-chinone as intermediate product is formed, because this is quantitatively oxidized by peracetic acid to o-carboxy-cis-cinnamic acid. (By the way we remark that this does not prove that in naphtalene there are one ring of benzene and one unsaturated ringsystem). They found that benzene was not attacked by 10 % peracetic acid, which statement we can confirm.

By introducing a hydroxyl-group in benzene, the ring becomes much more sensitive towards peracetic acid.

Some preliminary experiments with 10, 20, and 75 % peracetic acid showed that with more diluted solutions the oxidation proceeded regularly:

when oxidized with 75 % peracetic acid, the solution had to be cooled; next to relatively little cis-cis-muconic acid, fumaric acid was formed.

As by these preliminary experiments in all cases muconic acid m. p. 187° was obtained — to which because of its formation out of ortho-chinone we gave the cis-cis configuration [1]) — and as this requires for its formation out of phenol three molecules of peracetic acid, we added this amount.

As to these preliminary experiments the following details may be given:

For instance 10 gr. phenol were dissolved in 74.2 gr. 20 % peracetic acid; after 10 days the titre of the peracetic acid remained constant.

At first there is no colouring; after that a more and more intense red colour appears; after five days a white precipitate is formed, which after 10 days does not increase any more.

This white precipitate is filtered and has been recrystallized twice.

M. P. = 187°

0.1424 g 9.3 cc 0.218 n KOH
0.2821 g 18.10 „ „ „ „ } aeq. weight = 71 (Mol. weight = 142)

Elementar analyses; found 50.0 % C and 3.9 % H,

Calc for $C_6H_6O_4$ = 50.7 % C and 4.2 % H, aeq. weight 71 (mol. weight 142).

The filtrate is distilled in vacuo; after the distillation of the main quantity of the acid, long red needles begin to crystallize in the distilling flask. If we wash out the flask with ether, which is then vaporised, a syrup remains in which we find red needles and a colourless substance; these are put on a porous plate; the solid substance is extracted again with ether; a little muconic acid remains; after evaporation of the ether the red needles are this time left behind in pure condition. This appeared to be pheno-chinone m.p. 71°.

The syrup, which had penetrated into the porous plate was gathered in the following experiment; it had great reducing power and gave a precipitate with 2.4-di-nitro phenylhydrazine, which indicates the formation of a substance with aldehydic properties.

At the oxidation of 5 gr. phenol with 50 gr. 70.5 % peracetic acid the following phenomena were observed: the solution reddens at once, evolving large quantities of heat, which necessitates cooling. After some days the colour begins to diminish and is at last pale yellow, while a white precipitate is formed. This precipitate is cis-cis-muconic acid; the filtrate is vaporized at a pressure of 20 mm.; a pale yellow substance remains, which is soluble in water, has an acid reaction, discolours $KMnO_4$, gives the silver-mirror reaction and with 2.4 dinitrophenylhydrazine produces a little of a red precipitate.

---

[1]) This has in the meantime been confirmed by oxidising the acid with $KMnO_4$ which produces besides oxalic acid exclusively anti-tartaric acid (see next proceedings).

The melting point 194° is wrong, this ought to be 187°—188°.

When recrystallized out of aethylacetate it appears to be principally a white crystallized substance, m.p. 284°, acid, aeq. weight 61 ; on heating water is evolved besides a sublimate m.p. 51° ; i.e. *fumaric acid*.

Evidently the pheno-chinone is oxidized further by the very strong oxidizing agent and at last fumaric acid is formed.

During the final experiment 10 gr. phenol were oxidised with 210 gr. 10 % peracetic acid until the precipitate of muconic acid did not increase any more : the amount of this acid was 4.3 gr. An iodometric titration of the peracetic acid gives no good results, because pheno-chinone also liberates iodine from *KI*.

The filtrate is vaporized in vacuo, while the distillate, after decomposing the per acid by finely powdered platinum, is titrated with *KI* to determine the pheno-chinone.

Total of distillate : 212 gr. : 15.86 gr. requires 8.1 cc. 0.097 n thio
31. 75 gr. requires 16.15 cc. n thio
Average 0.233 gr. phenochinone
Altogether formed **1.6 gr.** phenochinone.

The rest of the distillate was extracted with a little dry ether : 1.1 gr. muconic acid remains. Altogether there was formed 5.4 gr. cis-cis muconic acid. The etheric solution gives, after distillation of the ether, a dark red syrup : this contains besides substances with reducing power chiefly pheno-chinone. As this cannot be titrated iodometrically, the whole was reduced with SO_2 ; then a small part of it is oxidized with $FeCl_3$, after that extracted with low-boiling petrol-ether ; after this the pheno-chinone crystallized in long red needles. When titrated iodometrically this amount distributed on the total quantity of residue comes to 3.1 gr.

Total amount $1.6 + 3.1 = $ **4.7 gr. phenochinone.**

So 10 gr. phenol have produced

5.4 gr. muconic acid aeq. to 3.6 phenol
4.7 gr. pheno-chinone aeq. to 4.4 phenol.

Consequently 80 % of the phenol is recovered. We tried to isolate other products from a part of the reduced liquid, which thus contains hydrochinol and phenol, after eliminating the excess of SO_2 by boiling the liquid. This was therefore treated with bromine ; only some tribromophenol (m.p. 92°) and distributed on the whole quantity, 6.5 gr. (equiv. to 2.92 gr. phenol) and a little monobromohydrochinol could be isolated.

From the results of this experiment of oxidation the following conclusion can be drawn : As in 4.7 gr. phenochinone 3.1 gr. of phenol are bound, 10.3—3.1 gr. = 6.9 gr. phenol are oxidized, of which 3.6 gr. in the direction of muconic acid and 4.7—1.3 = 1.6 gr. in the direction of *p*-chinone. Of 1.7 gr. of phenol the destiny is undefined. In view of the results of the experiment with very strong peracetic acid these are probably destroyed into substances which are resinified for the main part.

Hence we may conclude that the oxidation of the phenol is directed for almost equal parts to ortho and para. In view of the result of an oxidation

of phenol with H_2O_2 in presence of ferric salts whose green colour proves that pyrocatichol is produced. we should be inclined to admit that the oxidation into muconic acid and phenochinone goes via pyrocatichol and hydrochinol.

The following experiment proves that this conception does not hold true.

We have submitted these substances to the action of peracetic acid: 10 gr. of pyrocatechol were dissolved while cooling in 86 gr. of 10.2 % peracetic acid; a very strong colour appears. After some days a solid substance is deposed, which appeared to be muconic acid m.p. 187°: the amount was no more than 1 gr. After the evaporation in vacuo of the peracitic acid a black amorphous residue remained.

By dissolving 5 gr. of pyrocatechol with great precaution (cooling with ice) in 40 gr. of 78 % peracetic acid at first under development of carbonic acid a strong red colour appears, then the liquid is discoloured, while muconic acid is deposed m.p. 187° (1.3 gr.).

The filtrate of the muconic acid is liberated from the acetic and peracetic acid by distilling the latter substances in vacuo; there remains a pale yellow substance which dissolves in ether. When the ether is vaporized, a substance crystallizes, which is gathered, m.p. 286°, not readily dissolving in water, when heated above the meltingpoint it sublimates in long needles m.p. 51°. Aeq. weight (titration) = 60 hence the substance is **fumaric acid.**

In the ether a little of the substance with reducing power remains, which with dinitrophenylhydrazine produces a red precipitate that dissolves in sodium carbonate; when heated it is carbonized.

Analyses	*N*	22.4	and	23.2	mean	22.8 %
	C	45.0	,,	45.5	,,	45.3 %
	H	3.6	,,	3.5	,,	3.55 %.

These analyses of an impure substance do not tell us much more than the presence of 9 *C*-atoms to 4 *N*-atoms; consequently it is a hydrazone of a substance with 4 *C*-atoms. However it cannot possibly be a hydrazine of an aldehydic acid, because the necessary oxygen is lacking. The reactions to oxalic and glyoxylic acid were negative.

In a following experiment the proportion of the amount of muconic acid to the formed carbonic acid was determined, as the first indicates the amount of pyrocatechol, which alone has been opened and as the second is a measure of the destructive reaction. 15 gr. of pyrocatechol were added to 80 gr. of 70 % peracetic acid; the CO_2 was absorbed in potassium hydroxide until the development of CO_2 has ceased and the solution has been discoloured. Thus we obtained 4 gr. of muconic acid and 6.36 gr. CO_2. As 4 gr. of muconic acid is aequivalent to 3.1 gr. pyrocatechol, nearly 12 gr. of pyrocatechol have been decomposed in another direction. If we suppose that out of one molecule of pyrocatechol 2 molecules of CO_2 are formed (next to fumaric acid) then 8 gr. of pyrocatechol would have been used for this.

This result proves that the oxidation of pyrocatechol passes only for a small part via the ortho-chinol (20 %) and that consequently the oxidation of phenol can hardly pass over the pyrocatechol, because the first is converted for 36 % into muconic acid. *So phenol is a much better starting-point than pyrocatechol for the preparation of muconic acid.*

Consequently the formation of muconic acid out of phenol must take place as follows: An oxidation takes place at the C-atom which carries the phenolic hydroxylgroup and at the ortho C-atom. Probably the first product of oxidation passes via ortho-chinone into muconic acid.

Then the oxidation of hydrochinol was examined. 10 gr. of hydrochinol were dissolved in 86 gr. 10.2 % peracetic, acid; very soon chinhydron is deposed, totally 7.8 gr. Thus for about 40 % an oxidation of the hydrochinol to chinone takes place, which combines with the equivalent amount of unchanged hydrochinol and in this condition remains inert towards the diluted peracetic acid.

As phenol in phenochinon is protected against oxidation, this is also the case of the still more easily attackable hydrochinol in the chinhydron.

However, chinhydron is not proof against very concentrated peracetic acid. 5 gr. of hydrochinol added to 50 gr. 35 % peracetic acid produces at first a precipitate of chinhydron that redissolves very slowly. After 10 days the solution is discouloured; no cooling was needed. 1.5 gr. of a white substance is deposed. m.p. 286° aeq. weight 60. When heated above the meltingpoint a sublimate is formed: **fumaric acid.**

From the filtrate the acetic acid is vaporized in vacuo: A mixture remains which is easily soluble in water, has an acid reaction and an equivalent acid number of 64, probably essentially maleïnic acid. It produces a precipitate with $CaCl_2$, soluble in acetic acid. By distillation of a part an abundant sublimate of maleïnic acid-andhydride is obtained, which consequently proves the presence of maleïnic acid. Another part produces with dinitrophenyl-hydrazine in hydrochloric acid solution a precipitate which carbonizes at 162°—165°.

The analysis of this substance gave an average of $C = 45.5\ \%$, $H = 4.5\ \%$, $N = 18.5\ \%$, $O = 32.5\ \%$; the proportion between C and N 11: 4 proves that it is a hydrazone of a substance with 6 C-atoms, the amount of O-atoms is equal to 6, from which 4 belong to the two nitro-groups. Probably this substance is a hydrazone of an aldo- or keto-carbonic acid, as a phase of oxidation before the formation of maleïnic acid and fumaric acid.

Thus the oxidation of the hydrochinol gives in the beginning essentially *p*-chinone, which combines with unattacked hydrochinol, forming the much less easily oxidable chinhydron. Then this is slowly further oxidized, whereby one of the *CH* groups, which are all in ortho-position to the *CO* group is attacked. The molecule is broken up, which moreover causes the production of maleïnic acid by the side of fumaric acid.

It throws a light upon the oxidation of phenol in as much as here no hydrochinol can be formed; since in that case we should find it in the form of chinhydron.

So the oxidation of phenol directed to para produces (perhaps via a possible additionproduct) as first tangible product, parachinon, which is separated in the form of relatively stable phenochinone.

With this the course of the oxidation of phenol with peracetic acid is explained in great lines. It can be compared with the substitutionreactions of phenol, e.g. the nitration .... here too the same ortho and para directive action of the hydroxyl group can be observed.

Whereas however with the substitutionreaction after the first phase, which I should like to call the addition-phase, the benzene-ring redresses itself, this is not the case with the oxidation-reaction.

The oxidation carries through — instead of a orthosubstitutionproduct we get cis-cis-muconic acid, instead of the para-isomer the parachinone (resp. phenochinone).

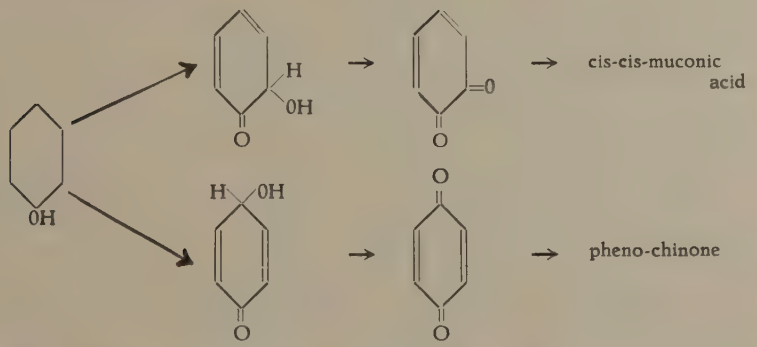

There remains to consider how the fumaric acid can be formed as destructionproduct of the benzene-ring, while one can exclusively expect maleïnic acid. We have proved that maleïnic acid is inert towards peracetic acid. When one dissolves maleïnic acid in 10 % peracetic acid and lets the solution at rest for about ten days, no reaction is produced and after vaporizing the reagent, there remains pure maleïnic acid m.p. 130°.

Neither is muconic acid (m.p. 187°) changed by peracetic acid; moreover one would expect one of the tartaric acids by the side of oxalic acid.

As oxalic acid has never been found, the once found muconic acid is not further destroyed. So one must state that the fumaric acid is formed at the moment that the benzene-ring — resp. chinoidic oxidation-products formed thereof — are attacked. The maleïnic acid can be produced by simple splitting of the para-chinone.

Laboratory of organic chemistry of the
May 1932. *University of Delft.*

Chemistry. — *The Structure of Tetra- and Tri-Phosphonitrile-Chloride.* By F. M. JAEGER and J. BEINTEMA.

(Communicated at the meeting of June 25, 1932).

§ 1. *Tetra-Phosphonitrile-Chloride*[1]: $(PNCl_2)_4$ crystallizes from benzene in beautiful colourless crystals which, in most cases, are tabular parallel to opposite faces of {110}. They are very lustrous, yielding sharp reflections.

Tetragonal-bipyramidal; apparently holohedral.

$$a : c = 1 : 1.5492 \text{ to } 1.5508.$$

Forms observed: $m = \{110\}$, predominant, yielding splendid reflections; $a = \{100\}$, narrower than m, but also very well reflecting; $r = \{101\}$, rather well developed and lustrous. The habitus of the crystals is prismatic along the c-axis. (Fig. 1).

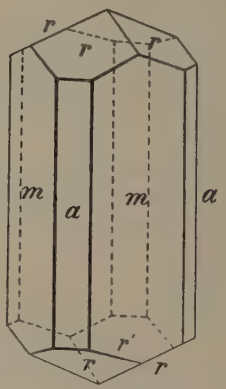

Fig. 1. *Tetraphosphonitrile-chloride.*

Angular Values:	*Observed:*		*Calculated:*	
$m : r = (110) : (101) =$	* 70°	6′	—	
$r : r = (101) : (011) =$	39	48	39°	48′
$a : r = (100) : (101) =$	61	9	61	13½
$r : r = (101) : (\bar{1}01) =$	57	42	57	33
$m : m = (110) : (1\bar{1}0) =$	90	1	90	0
$m : a = (110) : (100) =$	44	59	45	0

No distinct cleavability was observed.


Fig. 2. LAUE-*Pattern on (001) of Tetraphosphonitrile-Chloride. (Stereographical Projection.)*

Although the aspect of the crystals is quite holohedral, the hemihedral symmetry is clearly proved by a LAUE-pattern (tungsten: 40 *K.V.*) on (001): no vertical symmetry-planes are present, the image only showing a tetrad axis. As all faces of r are equally well developed, the presence of a horizontal plane of symmetry, however, is most probable; the tetragonal-bipyramidal symmetry C_{4h}, attributed to this compound, proves to be in perfect agreement with the other results of the spectrographical analysis.

[1]) R. SCHENCK and G. RÖMER, Ber. d.d. chem. Ges., **57**, (1924), 1351. W. GRIMME, Inaug. Dissert. Münster, (1926).

§ 2. Some rotation-spectrograms round [001] and [110] as axes of rotation were prepared. copper-x-radiation being used as luminous source.

1. *Rotation-spectrograms round* [001]. The crystal was oscillated through different angles (about 30°), the incident X-ray-pencil including different angles with the direction of the a-axis. The well developed spectrogram showed a principal spectrum and two or three accessory spectra. The most intensive spots were:

In the principal spectrum: (620) (**10**); (220) (**9**); (510) (**7**); (310) (**7**); (040) (**8**); (750) (**6**); (530) (**5**); (420) (**4**); (110) (**4**); (640) (**4**).

In the first acc. spectrum: (101) (**10**); (310) (**7**); (311) and (411) (**7**); (511) (**7**); (201) (**6**); (211) (**6**); (441) (**6**); (541) (**6**); (611) (**6**); (651) (**6**); (211) and (411) (**5**); (321) (**5**); (221), (331), (431) and (811) (**4**).

In the second acc. spectrum: (102) (**10**); (212) (**6**); (522) (**5**); (222) (**5**); (212), (302), (312), (322), (412), (432) and (512) (**4**).

In the third acc. spectrum: (313) (**7**); (443) (**6**); (223) (**5**).

2. *Rotationspectrograms round* [110].

A principal spectrum and six or seven accessory spectra ordinarily were observed. The following indices-triplets corresponded to the most intensive spots [1]).

In the principal spectrum: (111), (221), (333) and (443) (**3**); (002) (**2**); (114), (221), (223), (441), (550) and (770) (**2**).

In the first acc. spectrum: (101) (**6**); (102) (**4**); (212) (**4**); (321) (**4**); (541) (**4**); (542) and (762) (**3**); (761), (651) (**4**); (103), (651) (**3**).

In the second acc. spectrum: (311) (**5**); (201) (**3**); (313), (752), (642) (**3**); (312) (**2**); (1$\bar{1}$2) and (1$\bar{1}$1) (**2**); (750) (**5**); (640) (**4**).

In the third acc. spectrum: (301) (**6**); (2$\bar{1}$2), (522), (411) (**4**); (741) (**3**); (632), (851) (**4**); (302), (2$\bar{1}$3) and (304) (**3**).

In the fourth acc. spectrum: (221) (**6**); (311) (**6**); (223) (3$\bar{1}$3) (**4**); (401) (402) and (621) (**3**); (620) (**6**); (3$\bar{1}$0) (**7**); (511), (730) and (840) (**3**).

In the fifth acc. spectrum: (321) (**8**); (4$\bar{1}$1) (**6**); (6$\bar{1}$1) (**6**); (832) (**4**); (613), (3$\bar{2}$2), (3$\bar{2}$3) and (3$\bar{2}$4) (**3**); (942), (721), (**4**); (4$\bar{1}$2) (**3**).

In the sixth acc. spectrum: (5$\bar{1}$0) (**7**); (420) (**8**); (3$\bar{3}$1) (**5**); (5$\bar{1}$1) (**4**); (333), (5$\bar{1}$2) and (930) (**3**).

In the seventh acc. spectrum: (6$\bar{1}$1) (**10**); (522) (**4**); (811), (812), (921), (4$\bar{3}$4), (5$\bar{2}$3) (**3**); (432) (**3**); (701), (702) and (703) (**2**); (5$\bar{2}$4) (**2**).

---

[1]) The indices-triplets are indicated without the special algebraic signs of the spots observed, because only the total triplet $\{hkl\}$ is of interest.

From these spectograms, the identity-distances were determined to be:

$$I_{[001]} = 5.9 \text{ Å.}; \quad I_{[110]} = 15.4 \text{ Å.}$$

The sum of the indices $(h + k)$, as found with respect to these axes, proved to be always even. The real dimensions of the elementary cell, therefore, are: $a_0 = 10.9$ Å; $c_0 = 5.9$ Å.

These values were corrected by means of a BRAGG-spectrogram on (110), — *calcite* being used as a standard-material. From the distances of the lines observed, $d_{(110)}$ proved to be: 15.26 Å.; so that the true values of a_0 and c_0 become:

$$a_0 = 10.79 \text{ Å}; \quad c_0 = 5.93 \text{ Å}.$$

As the density of the crystals is: 2.18, the weight of the mass present within the elementary cell is: $1506 \cdot 10^{-24}$ grammes; as $(PNCl_2)_4$ weighs $765 \cdot 10^{-24}$ grammes, the mass indicated corresponds to: $P_8N_8Cl_{16}$.

The indices-triplets of the spots observed in the rotation-spectrograms were determined according to BERNAL's graphical method. It was proved that all triplets $(k\,k\,0)$, for which $(h + k)$ was odd, as well as all triplets $(0\,0\,l)$ for which l was odd, were absent. The space-group corresponding to the extinctions just mentioned is C^4_{4H}. As the positions in the elementary cell of the other symmetry-classes to be taken into account here are, at the highest, *four*fold positions, while 8 *P*- 8 *N*- and 16 *Cl*-atoms must be placed within the cell, the phosphorus- and nitrogen-atoms were to be distributed over *two* non-equivalent, the chlorine-atoms even over *four* non-equivalent positions. This is most improbable and, therefore, it is safe to exclude all symmetry-classes without the horizontal plane of symmetry.

The space-group C^4_{4H} is characterized by the presence of tetragonal screw-axes in $[001]_{00}$ and $[001]_{1/2\,1/2}$, dyad axes of rotation in $[001]_{1/2\,0}$ and $[001[_{0\,1/2}$, glidingplanes in $(001)_0$ and $(001)_{1/2}$ and 8 inversion-centra: $[1/4\ 1/4\ 0]$, $[1/4\ 3/4\ 1/2]$; etc.

§ 3. From the properties of the compound $(P\,N\,Cl_2)_4$, more especially from its high stability on evaporation and in many reactions in which no depolymerisation appears to occur, it may safely be concluded that the molecules $P_4\,N_4\,Cl_8$ as such are really present within the structure of the crystalline compound. Now only two *two*fold positions are present here, — they having the parameters:

$$[0\ 1/2\ 1/4],\ [1/2\ 0\ 3/4] \quad \text{and} \quad [0\ 1/2\ 3/4],\ [1/2\ 0\ 1/4].$$

It is in one of these places, which properly are equivalent, that the centres of gravity of both molecules $P_4\,N_4\,Cl_8$ must be situated, the symmetry of each molecule, therefore, being S_4. The *phosphorus*-atoms

then occupy, as well as the *N*-atoms, an eightfold position, while the *Cl*-atoms are distributed over two eightfold positions. As all atoms in the structure have three degrees of freedom, 12 parameters must be determined, so as to completely fix their positions. Tentatives will be made for the eventual calculation of these parameters.

§ 4. *Tri-Phosphonitrile-Chloride:* $(PNCl_2)_3$ crystallizes from ligroine in big, very lustrous, colourless crystals, which are perfectly developed. Their symmetry is rhombic-bipyramidal; the axial ratio is: $a:b:c = 0.9238:1:0.4397$.

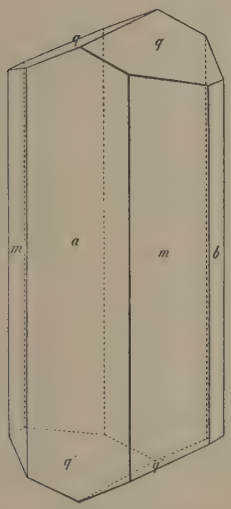

Fig. 3. *Tri-Phosphonitrile-Chloride.*

Forms observed: $a = \{100\}$, predominant, yielding very sharp reflections; $m = \{120\}$ [1]), often equally well developed as *a*, but sometimes narrower, very well reflecting, just as $q = \{011\}$; $b = \{010\}$, narrower than *m*, more feebly reflecting, but very well measurable. The habitus of the crystals is prismatic, with elongation in the direction of the *c*-axis; commonly they are thick tabular plates parallel to *a*. (Fig. 3).

Angular Values:	*Observed*:		*Calculated*:	
$a:m = (100):(120) =$	* 61°	$34\frac{1}{2}'$	—	
$q:q = (011):(011) =$	* 47	28	—	
$b:m = (010):(120) =$	28	$25\frac{1}{2}$	28°	$25\frac{1}{2}'$
$b:q = (010):(011) =$	66	16	66	16
$m:q = (120):(011) =$	69	21	69	16
$a:q = (100):(011) =$	90	0	90	0

No distinct cleavability was observed; perhaps an imperfect cleavability parallel to (011) may be present.

On $\{100\}$ and $\{010\}$ the extinction is parallel and perpendicular to the *c*-axis. The crystals are optically-biaxial, the plane of the axes being $\{100\}$, with the *c*-axis as the first bisectrix. The optical axes seem to emerge almost perpendiculary to the faces of $\{011\}$. The dispersion is weak, of rhombic character, with: $\varrho < v$. The double refraction is strong and positive.

§ 5. A series of rotation-spectrograms round [100], [010] and [001] were prepared, *copper-α*-radiation being used. The angle φ of oscillation was in all cases 30°.

1. *Rotation-spectrogram round* [100].

A principal spectrum and six accessory spectra were observed. The most intensive images observed were the following:

In the principal spectrum: (040) and (080) (**6**); (083), (051), (041), (020), (081) and (092) (**4**); (060), (061), (074) and (093) (**3**).

[1]) The true indices $\{120\}$, in stead of $\{110\}$, follow from the spectrographical measurements.

In the first acc. spectrum: (160) (**5**); (171) (**4**); (120), (131) and (180) (**3**).
In the second acc. spectrum: (220) (**5**); (260), (242), (272), (253), (2.11.2) (**2**).
In the third acc. spectrum: (320) (**10**); (361) (**7**); (361) (**6**); (363) (**5**); (331), (340) and (360) (**4**); (341) (**3**).
In the fourth acc. spectrum: (451) (**5**); (431) (**4**); (441), (452), (462), (443), (472), (441) and (492) (**2**).
In the fifth acc. spectrum: (531) (**8**); (542), (552), (543), (553), (563), (551), (571) and (581) (**3**).
In the sixth acc. spectrum: (651) (**7**); (621) and (641) (**6**); (631) (**5**); (632) and (643) (**3**).

The third and sixth spectra are somewhat stronger than the others. $I_{[100]} = 12.8$ Å.

2. *Rotation-spectrogram round* [010].

A principal spectrum and six accessory spectra were observed. The most intensive spots were:

In the principal spectrum: (802) (**8**); (301) (**4**).
In the first acc. spectrum: (10.1.1) (**5**); (211), (313) and (811) (**4**); (611), (711) and (911) (**3**).
In the second acc. spectrum: (321) (**5**); (221), (621) and (721) (**3**).
In the third acc. spectrum: (931) (**5**); (531) (**4**); (331) and (431) (**3**).
In the fourth acc. spectrum: (10.4.1) (**6**); (641) (**4**); (10.4.0) (3).
In the fifth acc. spectrum: (651) (**5**); (451) (**3**).
In the sixth acc. spectrum: (360) (**4**); (361), (760), (761) and (960) (**3**).

From this spectrogram follows: $I_{[010]} = 14.0$ Å.

3. *Rotation-spectrogram round* [001].

A principal spectrum and three accessory spectra were observed. The most intensive spots were:

In the principal spectrum: (040) (**8**); (080) (**5**); (360), (440) and (020) (**4**); (460), (060) and (160) (**3**).
In the first acc. spectrum: (041) and (361) (**8**); (021) and (051) (**6**); (101) and (031) (**5**); (451) (**4**); (131), (011) and (071) (**3**).
In the second acc. spectrum: (332) (**6**); (662) (**4**); (552), (542), (232), (122), (132) and (152) (**3**).
In the third acc. spectrum: (363) (**5**); (323) and (253) (**3**).

From the distances between the principal and the successive accessory spectra follows: $I_{[001]} = 6.3$ Å. These values of $I_{[100]}$, $I_{[010]}$ and $I_{[001]}$ were now corrected by means of BRAGG-spectrograms, *calcite* being used as standard-material. On (100) a 4th and a 6th order, on (010) only a 4th order spectrum were observed, from which the spacings: $d_{(100)} = 12.94$ Å. and $d_{(010)} = 14.00$ Å. were calculated; so that: $I_{[100]} = 12.94$ Å.; $I_{[010]} = 14.00$ Å. and $I_{[001]} = 6.16$ Å. These values lead to the axial ratio: $a : b : c = 0.9243 : 1 : 0.4397$, which is, for $a : b$, in perfect agreement

with the ratio found by the goniometrical measurements. As the volume of the rhombic cell is: 1116.10^{-24} cm^3 and its weight, according to STOKES' value: 1.98 for the density, is, therefore, 2210.10^{-24} grammes, the elementary cell contains a mass, corresponding to: $P_{12}\,N_{12}\,Cl_{24}$.

The fundamental cell is the *simple rhombic* one. Moreover, as extinction occurs for all triplets $\{h\,k\,0\}$, in which k is *odd* and for all triplets $\{h\,0\,l\}$ in which $(h+l)$ is odd, the space-group of the structure considered can easily be determined. If an interchange of the crystallographical axes be made in such a way [1]), that: $a_0 = 14.00$ Å.; $b_0 = 6.16$ Å. and $c_0 = 12.94$ Å., the old index h now becomes l', the old index k now becomes h' and the old index l now becomes k'. Therefore, intensities equal to *zero*, occur for all triplets $\{h'\,0\,l'\}$, if h' is *odd* and for all triplets $\{0\,k'\,l'\}$, if $(k'+l')$ is odd; as no other extinctions occur [2]), the space-group must be V_H^{16}.

§ 6. Also in the present case it is feasible to suppose, that the complex molecule: $(PNCl_2)_3$ is preserved in the crystal-structure; then its centre of gravity must occupy a *four*fold position in the cell.

In the group V_H^{16} there are two fourfold positions without a degree of freedom; the molecule occupying them, in that case has the proper symmetry: C_i; moreover, there is one fourfold position available with two degrees of freedom, the corresponding symmetry of the occupying molecule now being C_s. A molecule $(PNCl_2)_3$, however, cannot be centrically symmetrical; so that only the other alternative remains. The co-ordinates of the centres of gravity of the four molecules then are [3]):

$$[0,\,u,\,v];\ [{}^1/_2,\,{}^1/_2-u,\,\bar{v}];\ [0,\,{}^1/_2+u,\,{}^1/_2-v];\ [{}^1/_2,\,\bar{u},\,{}^1/_2+v].$$

§ 7. As to the structure of the molecules $(PNCl_2)_4$ and $(PNCl_2)_3$ we can finally make the following remarks. SCHENCK and RÖMER have, for both compounds, proposed *a cyclic* structure of the kind:

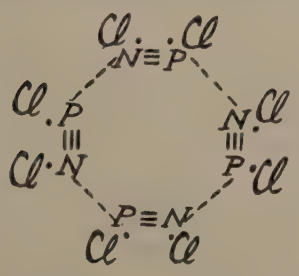

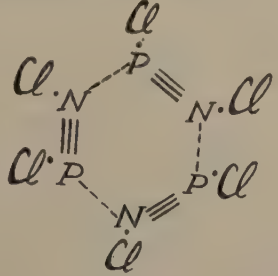

[1]) This corresponds to a rotation of the crystals through 90° round the c-axis, followed by the same rotation round the previous b-axis. The symbols of the faces thus become: $a = \{001\}$, $b = \{100\}$, $q = \{110\}$ and $m = \{201\}$, with: $a' : b' : c' = 2.2727 : 1 : 2.1006$.

[2]) H. MARK, *Die Verwendung der Röntgenstrahlen*, etc., (1926), p. 389.

[3]) R. W. G. WYCKOFF, *The Analytical Expression*, etc., Washington, (1922), p. 64.

In so far as the different indication of the bonds between the *P*- and *N*-atoms is really supposed simultaneously to express *a* difference in the way of linkage between these atoms, we here can state that, at least with respect to the second formula, the experience gained in this investigation cannot be reconciled with that formula. For the proper symmetry C_s of the molecule involves the presence of *a* symmetry-plane, and the latter makes it necessary that at least one of the phosphorus-atoms be linked to the two adjacent nitrogen-atoms in *a* quite *identical* way. Only if *all* these atoms were situated *in* this plane of symmetry, its presence would not interfere with the linkages mentioned; but this is impossible in connection with the dimensions of the elementary cell. Perhaps an electronic linkage of the following kind:

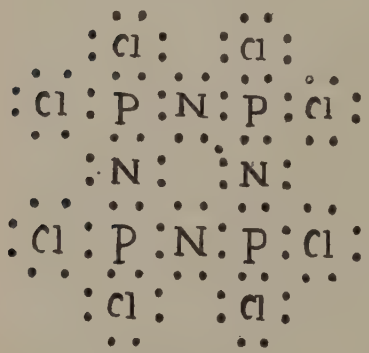

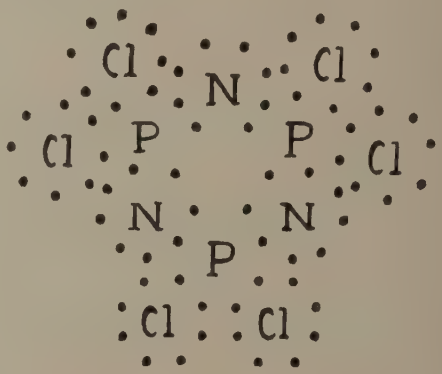

could be considered as in better agreement with the facts observed and our modern views. As soon as the right parameters of the atoms in this arrangement shall be calculated, we hope to return to this interesting problem about the constitution of these remarkable compounds.

Groningen, Laboratory for Inorganic and Physical Chemistry of the University.

Chemistry. — *The Exact Measurement of the Specific Heats of solid Substances at High Temperatures:* VI. *Metals in Stabilized and Non-stabilized Condition: Platinum and Silver.* By F. M. JAEGER, E. ROSENBOHM and J. A. BOTTEMA.

(Communicated at the meeting of June 25, 1932).

§ 1. In the course of our measurements of the specific heats of pure metals at high temperatures, we already had an opportunity to draw attention to the remarkable fact that many of those metals, as, for instance, *osmium, iridium, silver, gold,* etc., — even if *no* allotropic changes occur in them, — often yield too low and, moreover, irreproducible values of their mean specific heats, as long as they have not yet been subjected to a particular, preliminary thermal treatment [1]). A prolonged heating at temperatures in the vicinity of the meltingpoint or somewhat lower, followed by a slow cooling, appears, — thus, for instance, with *osmium* and *iridium,* — to bring them in most cases into a stable condition, in which, within the limits of experimental error (0.1—0.2 %), definite values of $\bar{c}_p$ at each temperature can be determined. If the metal has once been brought into this stable condition, it remains so in successive experiments, yielding values of $\bar{c}_p$, which now prove to be perfectly reproducible within the limits of error mentioned.

In the present paper we wish to communicate some of the results hitherto obtained in the systematical study of these phenomena. Their importance for the whole technique of specific heat measurements will be clear: many of the numerous discrepancies in the values of c_p for the same metal, as are met with in the literature, certainly must, for a good deal, be attributed to the fact that these numbers are not only obtained without taking the necessary painstaking precautions during the measurements themselves, but also with metals in a still *un*stabilized and, therefore, *in*definite inner condition. As small errors in the determination of the integral function: $Q_0 = F.(t)$ can already imply rather considerable divergences in the differential function: $c_p = \frac{\partial Q}{\partial t} = F'(t)$, it must be clear that a sufficient inambiguity about the true dependence of c_p on t, can possibly only be ascertained, if the calorimetric method used is able to furnish data of the very highest precision and reliability. In this laboratory two calorimeters of the most recent type of development, provided with all the improvements necessary to render them into the desired condition [2]), are now used for the

[1]) F. M. JAEGER and E. ROSENBOHM, these Proceed., **34**, (1931), 809; conf. also the Note at the bottom of the page.

[2]) F. M. JAEGER, E. ROSENBOHM and J. A. BOTTEMA, these Proceed., **35**, (1932).

measurements of the mean specific heats by two different and independently working observers, whose results at each moment can be compared and mutually controlled.

The observations here described were made with *platinum* and *silver*. both these metals being of the purest quality.

§ 2. *Platinum*. Because the values of $\bar{c}_p$ obtained in this laboratory [1]) for purest *platinum* happened to agree within about 0.15 % with those obtained by WHITE [2]) by means of his liquid-calorimeter, — in the first place comparisons of these values by means of two different calorimeters of the type described were made between 400° and 1600° C.

A vacuum-crucible of the shape mentioned before [3]) was filled with *platinum*-spheres of pea-size, obtained by suddenly quenching droplets of molten *platinum* of HERAEUS' purest quality (for resistance-thermometers) in a vacuum. The total weight of the *platinum* used was 75.598 grammes, of which 30.1 grammes represented the weight of the crucible itself, made of the metal hammered at 800°—900° C. and having been previously heated to the meltingpoint only at its upper rim, during the process of electrical soldering its cover, while the remaining part of the crucible was kept at a low temperature.

The values of the mean specific heats thus obtained (see Table I and the dotted lines *B'* in Fig. 1) proved to be *considerably lower*, — about 1.5 to 2 %, — than the values obtained before. Moreover, on starting the experi-

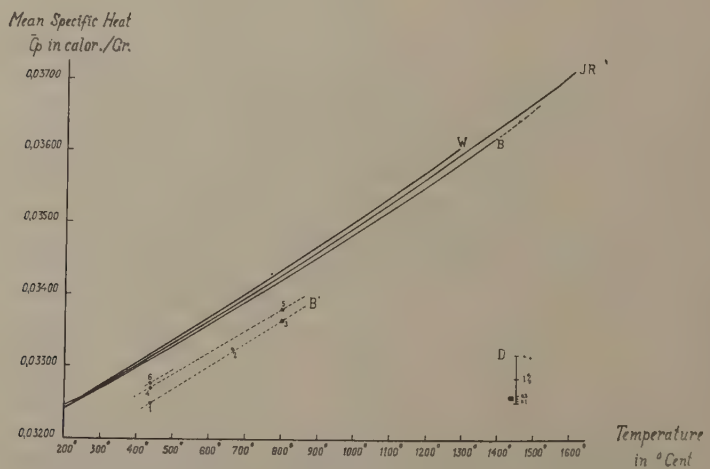

Fig. 1. Mean Specific Heats of Platinum in various Conditions.

[1]) F. M. JAEGER and E. ROSENBOHM, Receuil d. Trav. d. Chim. d. Pays-Bas, **47**, (1928), 534.

[2]) W. P. WHITE, Phys. Review, (2), **12**, (1918), 436.

[3]) F. M. JAECER and E. ROSENBOHM, Receuil d. Trav. d. Chim, d. Pays-Bas, **51**, (1932), 2.

TABLE I.

Mean Specific Heats $\bar{c}_p$ of Platinum in Different Conditions.

Temperature in ° C.:	Platinum (molten and suddenly quenched): (*B'*)	The same Metal (after heating at 1600° C. and slowly cooling): (*B*)	Platinum (hammered and plated at 800°—900° C.):	Normal Platinum	
				JAEGER and ROSENBOHM: (*JR*)	WHITE: (*W*)
404.5°	—	—	0.03301	0.03298	0.03304
407.8	—	0.03305	—	0.03299	0.03305
418.2	0.03270	—	—	0.03301	0.03307
419.0	0.03244 Irr.	—	—	0.03301	0.03308
419.7	0.03264	—	—	0.03302	0.03309
429.3	0.03241	—	—	0.03306	0.03312
443.5	—	—	0.03308	0 03310	0.03317
629.3	—	0.03362	—	0.03369	0.03377
630.2	0.03309	—	—	0.03370	0.03378
631.3	—	—	0.03365	0.03371	0.03379
733.0	—	—	0.03406	0.03402	0.03404
799.9	0.03375 Irr.	—	—	0.03421	0.03430
801.6	0.03360	—	—	0.03422	0.03431
801.9	—	0.03414	—	0.03423	0.03431
803.0	—	0.03423	—	0.03424	0.03432
1061.1	—	—	0.03505	0.03504	0.03512
1062.7	—	0.03505	—	0.03504	0.03513
1064.4	—	0.03507	—	0.03505	0.03514
1066.2	—	—	0.03518	0.03507	0.03516
1200.3	—	0.03538	—	0.03552	0.03563
1391.3	—	0.03604	—	0.03616	0.03619

ments at low temperatures, these values appeared to be quite *ir*reproducible, gradually increasing after each successive heating. If the crucible and its contents was, however, at once heated at 1600° C. for several hours and then slowly cooled, the values of $\bar{c}_p$ now proved to be identical within 0.15 % with those obtained by JAEGER and ROSENBOHM (curve *B* in Fig. 1).

These numbers remained constant in all later experiments.

The question, therefore, arises: are these discrepancies caused by the

contents of the crucible or by the hammered *platinum* of the crucible itself?

Experiments made with the empty crucible did not yield reliable results, as a consequence of the uncontrolable loss of heat of the shapeless and thin sheet of *platinum* during its introduction into the calorimeter and of the retarded heat-interchange with the calorimeter-block. Therefore, a vacuum-crucible was completely filled with the same hammered material, cut into small pieces, its total weight being 61.9075 grammes. The values of c_p measured (Table I) proved to be *practically identical* with those obtained by JAEGER and ROSENBOHM. From this result it must be concluded that the lower values of $\bar{c}_p$ of the curves *B'*, which deviate about 2 % from the normal ones, are characteristic of the *platinum*-spheres, i.e. of the metal in the quenched condition. If the quenched *platinum* be heated at 1600° C. for five hours and then slowly cooled, its internal structure evidently returns to the normal, stable condition; then the values of $_p$ re-assume their normal magnitude. In this connection we once more wish to emphasize, that the phenomenon just described has nothing at all to do with any occurring allotropic change: no such transformation does occur in the metal. Attention must also be drawn to the fact that, in this special case, the hammering of the metal at 800°—900° C. has evidently *no* appreciable effect on the values of $\bar{c}_p$ of normal *platinum*.

As we shall soon see, this is by no means generally the case.

The values obtained by MAGNUS [1]) are, at 600° C. already about 1 %, at 850° C. about 1.5 % lower than those of WHITE and ours; probably they correspond to one of the curves *B'* in Fig. 1 and then refer to an unstabilized material.

The curve *B* in Fig. 1 only differs slightly from our previously determined one; between 0° and 1400° C. it corresponds to the equation:

$$Q'_0 = 0{,}031678 \,.\, t + 0{,}315287 \,.\, 10^{-5} \,.\, t^2 - 0{,}541626 \,.\, 10^{-10}\, t^3;$$

so that the true specific heat c_p between these limits of temperature can be calculated from:

$$c_p = 0{,}031678 + 0{,}630574 \,.\, 10^{-5} \,.\, t - 0{,}1624878 \,.\, 10^{-9} \,.\, t^2.$$

Although the agreement between these four series of measurements, — including WHITE's results, — is a very satisfactory one, yet the divergences of the calculated *differential* values c_p are *appreciably greater* than those of the *mean* specific heats $\bar{c}_p$. This fact, as seen from the data in Table II and the curves of Fig. 2, once more illustrates, that even if the values of $\bar{c}_p$ agree within 0.1 or 0.2 %, the slope of the corresponding c_p-t-curves can still differ by 1 % or more; properly speaking, the method must yield results accurate within 0.01 %, instead of within 0.1 %, if the $\bar{c}_p$-t-curve

[1]) A. MAGNUS, Ann. d. Physik. **48**, (1915), 998

TABLE II.

The Specific Heats of Platinum in Different Conditions, between 200° and 1600° C.

Temperature in °C.:	c_p JAEGER, ROSENBOHM; WHITE		c_p (stabilized at 1600° C.):	c_p (hammered at 800°—900° C.):
200°	0.03295	0.03303	0.03293	0.03291
300	0.03349	0.03367	0.03355	0.03358
400	0.03413	0.03431	0.03417	0.03435
500	0.03476	0.03496	0.03479	0.03487
600	0.03541	0.03560	0.03540	0.03548
700	0.03605	0.03624	0.03601	0.03608
800	0.03661	0.03689	0.03662	0.03666
900	0.03736	0.03753	0.03722	0.03721
1000	0.03802	0.03818	0.03782	0.03775
1100	0.03869	0.03882	0.03842	0.03827
1200	0.03936	0.03947	0.03901	—
1300	0.04004	0.04011	0.03960	—
1400	0.04072	(0.04076)	0.04019	—
1500	0.04140	(0.04141)	—	—
1600	0.04209	(0.04206)	—	—
(1700)	(0.04279)	(0.04270)	—	—

would really present a perfectly true image of the dependence of c_p upon t. At the moment this is quite impossible, — were it only because of the fact, that the furnace-temperatures cannot be fixed with necessary accuracy. The values of c_p in Table II according to WHITE's measurements are calculated by means of the formula:

$$c_p = 0{,}031753 + 0{,}63964 \,.\, 10^{-5} \,.\, t + 0{,}27 \,.\, 10^{-10} \,.\, t^2,$$

which is valid between 0° and 1300° C. Even by extrapolation up to 1700° C., however, the values calculated prove to be almost identical with those found by us.

The curve for *hammered platinum*, as deduced from the values of $\bar{c}_p$ at 404°.5 C., at 733° C. and at 1061°.1 C., corresponds to the equation:

$$Q'_0 = 0{,}031509 \,.\, t + 0{,}359551 \,.\, 10^{-5} \,.\, t^2 - 0{,}315573 \,.\, 10^{-9} \,.\, t^3.$$

Between 0° and 1100° C. the true specific heat c_p of hammered *platinum*, therefore, can be found from the formula:

$$c_p = 0{,}031509 + 0{,}719102 \,.\, 10^{-5} \,.\, t - 0{,}94672 \,.\, 10^{-9} \,.\, t^2.$$

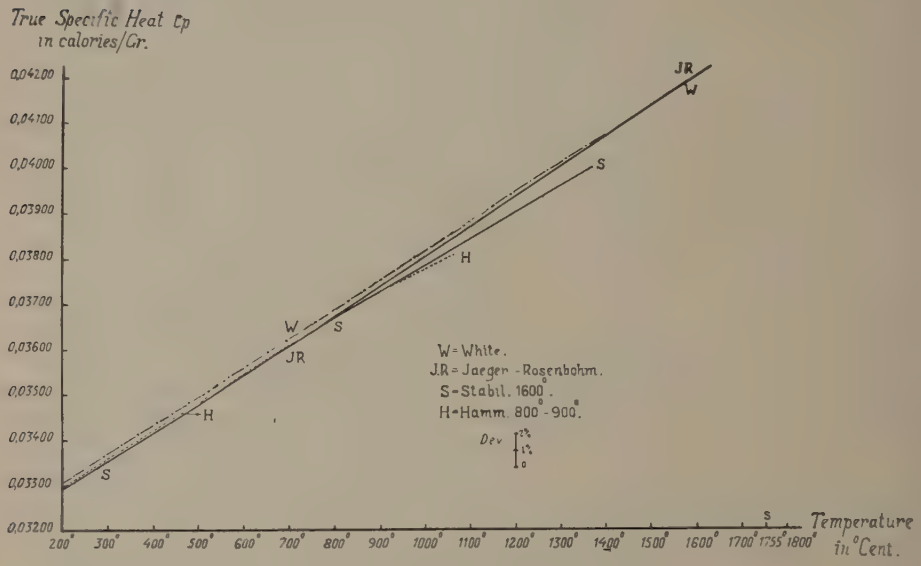

Fig. 2. The True Specific Heats of Platinum in different Conditions.

§ 3. *Silver.* Preliminary experiments had already taught us that *cold-plated silver*[1]) yielded considerably *smaller* values for $\bar{c}_p$ than the metal, if preliminarily fused and then slowly cooled. For this reason purest *silver* was melted and cast into the form of a massive crucible-shaped lump, which exactly fitted into the central bore of the calorimeter. A thin tubular hole was spared in it for the introduction of the hot junction of the thermo-couple, in the same way as occurs in our usual vacuum-crucibles. A small silver hook was fixed at the top, for the purpose of suspending the lump within the electrical furnace; the total weight of *silver* was: 133.339 grammes.

Measurements were made at 100°.87 C., the metal being heated in an airbath by the circulating vapour of conductivity-water, boiling under a known pressure; moreover, such measurements were made between 248°.1 and 804°.4 C. by heating in the electrical furnace.

---

[1]) The *silver*, and also the *gold* in the next paper both contained 100 % of the metal and were obtained through the kindness of Dr. C. HOITSEMA, from the *State's Mint* at *Utrecht*. Between 20° and 0° C., the mean specific heat $\bar{c}_p$ of this *silver*, was somewhat less than *s*: 0.0558. Both metals were obtained as cold-plated sheets.

The total amounts of heat Q_0 delivered between $t°$ and 0° C. were found to be:

Temperature t in °C.:	Amount of Heat Q_0 delivered by 1 Gr. silver, in calories:	Amount of Heat Q'_0 in calories, as calculated from the formula:
100°.87	5.690	—
248.1	14.255	14.266
295.9	17.115	17.116
397.2	23.254	—
640.0	38.306	38.458
804.4	49.096	—

The value of Q_0 at 640° C. is somewhat (about 0.4 %) too low.

Between 0° and 804° C. these quantities of heat are very satisfactorily expressed by the formula:

$$Q'_0 = 0{,}055614 \,.\, t + 0{,}0800383 \,.\, 10^{-4} \,.\, t^2 - 0{,}15741 \,.\, 10^{-8} \,.\, t^3.$$

The true specific heat c_p, therefore, can be calculated from the equation:

$$c_p = 0{,}055614 + 0{,}1600766 \,.\, 10^{-4} \,.\, t - 0{,}47223 \,.\, 10^{-8} \,.\, t^2$$

and the atomic heat C_p by means of the formula:

$$C_p = 5{,}9996 + 0{,}17269 \,.\, 10^{-2} \,.\, t - 0{,}50945 \,.\, 10^{-6} \,.\, t^2. \quad . \quad . \quad (I)$$

The value of C_p at 0° C. exactly coincides with the value obtained by NERNST in measuring c_p itself at that temperature.

From the values of MAGNUS and HODLER [1]), it follows that the atomic heat C_p can be found by means of the equation:

$$C_p = 6{,}047 + 0{,}0749 \,.\, 10^{-2} \,.\, t + 0{,}712 \,.\, 10^{-6} \,.\, t^2 \quad . \quad . \quad . \quad (II)$$

The values of C_p, as calculated from I) and II), and those found by SCHÜBEL [2]), are graphically represented in Fig. 3. Not only are these values in the three cases very strongly deviating, but the real slope of the three curves is even exactly opposite: our curve is *concave* towards the axis of the temperatures, those deduced from MAGNUS' and SCHÜBEL's experiments are *convex*.

---

[1]) A. MAGNUS and A. HODLER, Ann. d. Physik, (4), **80**, (1926), 808; Zeits. f. phys. Chem., **110**, (1924), 188.

[2]) P. SCHÜBEL, Zeits. f. anorg. C., **87**, (1914), 81.

Temperature t in °C.:	Atomic Heat C_p:		
	MAGNUS-HODLER:	SCHÜBEL:	this Laboratory:
0°	6.047	6.02	6.000
100	6.129	6.08	6.167
200	6.225	6.14	6.324
400	6.460	6.43	6.609
600	6.753	7.07	6.852
800	7.102	—	7.061

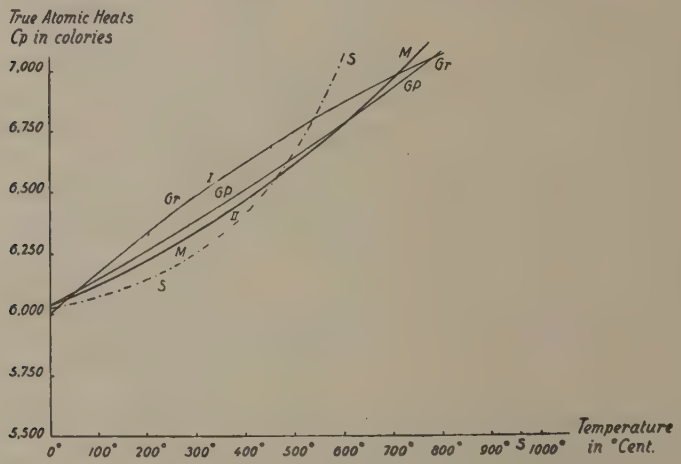

Fig. 3. The Atomic Heats of Silver in various Conditions.

Such discrepancies as these very often occur in literature. They clearly demonstrate how rudimentary our knowledge about the variation of the true specific heat with the temperature still is.

§ 4. Now two vacuum-crucibles were filled with *cold-plated silver*; they contained 23.5861 and 17.8366 grammes of the metal respectively, cut into small pieces. Both crucibles yielded identical results:

Temperature t in °C.:	Total amounts of Heat Q_0 delivered by 1 Gr. silver:
420.4_4°	24.496
628.7	37.360
631.4	37.397
634.9^5	37.802
800.7	48.527
801.2	48.476

The values of Q'_0 are, between 0° and 800° C., very exactly represented by the formula:

$$Q'_0 = 0{,}055936 \,.\, t + 0{,}528033 \,.\, 10^{-5} \,.\, t^2 + 0{,}6055 \,.\, 10^{-9} \,.\, t^3,$$

and, therefore, the true specific heat c_p of this plated *silver* by:

$$c_p = 0{,}055936 + 0{,}105607 \,.\, 10^{-4} \,.\, t + 0{,}18165 \,.\, 10^{-8} \,.\, t^2.$$

The atomic heat C_p can be calculated from:

$$C_p = 6{,}0343 + 0{,}11393 \,.\, 10^{-2} \,.\, t + 0{,}19596 \,.\, 10^{-6} \,.\, t^2.$$

If the values of C_p are now calculated for the same temperatures as above, we find:

Temperature t in °C.:	Atomic Heat C_p:
0°	6.034
100	6.150
200	6.270
400	6.521
600	6.788
800	7.072

With the exception of the (extrapolated) value at 0° C. and that at 800° C., where the metal evidently has already almost reached its stabilized condition, all these values (curve GP in Fig. 3) are not only *appreciably smaller* than those for molten and solidified *silver, but the curve for* $c_p - t$ *appears, moreover, now to show a convex shape towards the temperature-axis,* similarly as was the case with MAGNUS' and SCHÜBEL's curves. This example thus demonstrates most convincingly, that the cause of these divergences often met with in the literature, — as far as they must not be ascribed to experimental errors and methodical inaccuracies, — must doubtlessly be explained by the fact, that probably all those measurements were made with *non*-stabilized samples of the metals studied.

Groningen, Laboratorium for Inorganic and Physical Chemistry of the University.

Chemistry. — *The Exact Measurement of the Specific Heats of solid Substances at High Temperatures:* VII. *Metals in Stabilized and Non-stabilized Condition: Copper and Gold.* By F. M. JAEGER, E. ROSENBOHM and J. A. BOTTEMA.

(Communicated at the meeting of June 25, 1932).

§ 1. In the previous paper [1]) we have drawn attention to the important fact, that metals in the normal and worked states commonly appear to have appreciably different specific heats. Here we shall publish some analogous results obtained in the case of *copper* and of *gold*.

Copper. A series of measurements with electrolytically deposited and then melted and solidified *copper* were made between 300° and 960° C. Of course, it was supposed that the data available in the literature concerning this metal could be considered as reliable. But neither this proved to be true: even with this pure and much applied metal, the data concerning the specific heats at higher temperatures, as measured by different investigators, appeared to be strongly deviating from each other [2]).

A series of measurements (15.7687 Gr. purest *copper* in a platinum vacuum-crucible of 30.0284 Gr.) between 300° and 960° C. [3]) gave the following results:

Temperature t in °C.:	Quantity of heat Q_0 in calor. developed between $t°$ and 0° C. (observed):	Q_0 as calculated from the formula:
313°.14	30.017	—
419.68	40.830 (mean value of 3 determ.)	40.696
630.84	62.593 (mean value of 3 determ.)	62.558
798.67	80.732	80.597
959.3	98.413	—

[1]) F. M. JAEGER, E. ROSENBOHM and J. A. BOTTEMA, these Proceed. (1932), p. 763.

[2]) Conf. e.g.: F. WÜST, A. MEUTHEN and R. DURRER, Zeits. f. Instrum., **39**, (1919), 294; A. NACCARI, Gazz. Chim. Ital., **18**, (1888), 13; F. GLASER, *Metall.* **1**, (1904), 103, 121; A. KLINKHARDT, Ann. d. Phys., (4), **84**, (1927), 182; H. SEEKAMP, Zeits. f. anorg. Chem., **195**, (1931), 356; A. MAGNUS, Ann. d. Phys., (4), **31**, (1910), 597; P. SCHÜBEL, Zeits. f. anorg. Chem., **87**, (1914), 81

[3]) Above 960° *copper* evidently shows an abnormal behaviour: its specific heat then increases more rapidly with the temperature than before. These results will be discussed in a later paper.

Between these limits of temperature the dependence of Q_0 on t is strictly linear; it can be expressed by the formula:

$$Q_0 = 0{,}092597 \,.\, t + 0{,}10416 \,.\, 10^{-4} \,.\, t^2.$$

The mean specific heat of *copper* at t^0, therefore, can be calculated from:

$$\bar{c}_p = 0{,}092597 + 0{,}10416 \,.\, 10^{-4} \,.\, t,$$

and the true specific heat c_p is, therefore, equal to:

$$c_p = 0{,}092597 + 0{,}20832 \,.\, 13^{-4} \,.\, t.$$

The values of $\bar{c}_p$ and of c_p for a series of temperatures between 300° and 900° C., as calculated from these equations, are collected in the following table.

Temperature t in °C.:	Mean Specific Heats $\bar{c}_p$:	True Specific Heats c_p:
300°	0.0957	0.0988
400	0.0968	0.1009
500	0.0978	0.1030
600	0.0988	0.1051
700	0.0999	0.1072
800	0.1009	0.1092
900	0.1020	0.1113

The values of c_p obtained (line *B*) in Fig. 1 prove to be practically identical with those of NACCARI, which in Fig. 1 are indicated by the straight line *N*. The direct measurement of c_p by SEEKAMP by a completely different method gave the values of c_p indicated by the curve *S* in Fig. 4. If we consider that these values, obtained by improving the analogous method of KLINKHARDT, are already 1 % lower than KLINKHARDT's values and that these values still seem to be too high, — their error being greater at higher temperatures [1]), — the agreement of SEEKAMP's directly measured values of c_p with ours is, between the limits of errors, very satisfactory indeed. In Fig. 4 also the straight line *WMD* is drawn; it is the graphical representation of the results obtained by WÜST, MEUTHEN and DURRER and proves once more, how uncertain the data about specific heats in the literature, — even if obtained by an apparently sound method, — may still be.

[1]) H. KLINKHARDT, loco cit., p. 180. This author claims an error of 0.96 % at 200° C. and of 2.1 % at 900° C. Evidently the errors are always positive when using the described experimental method.

The data mentioned are undoubtedly erroneous, although as the method of measurement, that of the ice-calorimeter was used. If there are made no very considerable errors in the evaluation of the temperatures, most probably also here the special state of the metal used was the principal cause of these strange results.

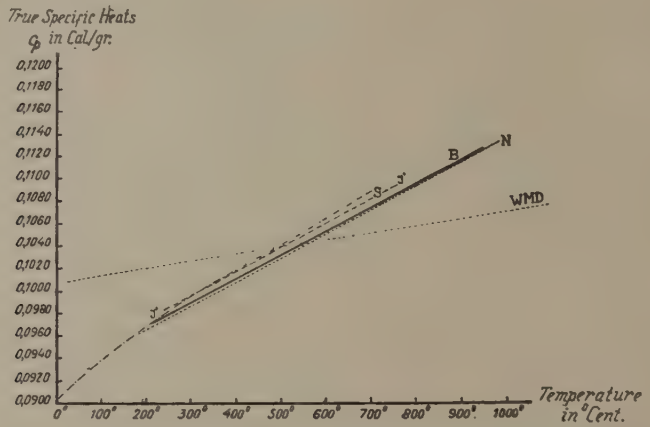

Fig. 1. True specific Heats of Copper in Different Conditions.

§ 2. The measurements with *copper*, within the same interval of temperature, were now repeated with a cylindrical bar of rolled out metal, *no* particular attention being paid to a preliminary stabilisation of the material investigated.

From the mean specific heats at 291° C. (=0.0971), at 474°.1 C. (=0.0989) and at 715°.6 C. (=0.1015), it appears that $\bar{c}_p$ in function of the temperature can fairly well be expressed by the formula:

$$\bar{c}_p = 0{,}093835 + 0{,}10342 \,.\, 10^{-4} \,.\, t,$$

and, therefore, the true specific heat $\bar{c}_p$, in the same interval of temperature, by:

$$c_p = 0{,}093835 + 0{,}20684 \,.\, 10^{-4} \,.\, t \text{ (valid between 300° and 800° C.).}$$

(valid between 300° and 800° C.).

These results are represented in Fig. 4 by the straight line *I'*.

It becomes clear, that the values of c_p of this rolled out *copper* are all *higher* than those of the stabilized metal: they are at lower temperatures than about 340° C. even greater than those determined by SEEKAMP, above 340° C. smaller than those of the same author and at all temperatures higher than those of our line *B*.

The temperature-coefficient of c_p of rolled out *copper* appears to be somewhat smaller than that of normal *copper*, — a fact which points to a gradual approaching of the lines *I'* and *B* to each other, as the temperature increases. This is exactly what one might have expected, because by each

heating at successively higher temperatures, the metal gradually comes nearer to its final, stabilized condition.

The bar of rolled-out *copper* now was heated in a vacuum at 1050° C. during 5 hours and then slowly cooled. Measurements made at 236°, 305° and 468° C. yielded for $\bar{c}_p$ values which, within the limits of the experimental errors (0,1 to 0,3 %) proved to be *identical* with those found for *copper* in its stabilized condition. This fact most convincingly demonstrates, that the deviations described merely depend on the inner structure of the worked metal.

§ 3. **Gold.** As an example of a metal, the specific heats of which in the stabilized and plated states, — although different, — do not very appreciably deviate, we here give the results obtained with molten and solidified *gold* on the one hand, and hard plated *gold* on the other.

The *cold-plated gold*, obtained in a perfectly pure state from the Royal Mint at Utrecht, was in the first place used for preparing a riveted crucible, exactly fitting in the central opening of the calorimeter; this crucible was then filled with strips of *gold* tightly rolled up, and a gold-cover was riveted at the top of it, bearing a hook of the same material for the purpose of suspending it within the furnace. The total weight was about *125* grammes. After the measurements were finished, the crucible was melted by means of a vacuum induction-furnace [1]), the lump thus obtained moulded into the shape of our usual vacuumcrucibles and the measurements then were made in the same way. For the purpose of testing the influence of the presence of a *platinum* crucible upon the results, a platinum vacuum-crucible was filled with pieces of the same molten and solidified material, and the determinations were once more repeated; as we shall see, the results obtained in the latter case appeared to be identical within 0.1 % with those obtained by means of the lump of pure *gold* mentioned.

1. *Lump of pure molten and solidified gold.*

The quantities of heat Q_0 delivered between 1000° and 0° C., for 1 gramm of the metal, were found as follows:

Temperature t in °C.:	Q_0 (observed) in calories:	Q'_0 (calculated) in calories:
418.89	13.3418	—
631.41	20.4354	20.4407
799.72	26.3014	—
958.90	32.0408	32.0791
999.76	33.6045	—

[1]) From C. LORENZ in Berlin: frequency: 80000 Hertz pro second.

These amounts of heat are very well represented by the equation:

$$Q'_0 = 0{,}03123 \,.\, t + 0{,}83176 \,.\, 10^{-6} \,.\, t^2 + 0{,}155194 \,.\, 10^{-8} \,.\, t^3,$$

from which the true specific heat c_p is found to be:

$$c_p = 0{,}03123 + 0{,}16635 \,.\, 10^{-5} \,.\, t + 0{,}46558 \,.\, 10^{-8} \,.\, t^2,$$

while the atomic heat C_p can be calculated by means of the formula:

$$C_p = 6{,}1586 + 0{,}32804 \,.\, 10^{-3} \,.\, t + 0{,}91812 \,.\, 10^{-6} \,.\, t^2.$$

The values of c_p and C_p between 200° C. and the meltingpoint are the following:

t:	c_p:	C_p:
200°	0.03175	6.261
400	0.03264	6.437
600	0.03390	6.685
800	0.03554	7.009
1000	0.03755	7.405
1063	0.03826	7.545

2. *Molten and solidified gold in platinum vacuum-crucible (No. 37).*

Temperature t in °C.:	Final temp. of the calorimeter:	Weight of platinum:	Weight of gold:	Mean specific Heat $\bar{c}_p$ of platinum:	Mean specific Heat $\bar{c}_p$ of gold:	Quantity of Heat Q_0 developed by 1 Gr. of gold:
628°.97	22°.35	28.7888	35.9622	0.03363	0.03239	20.3465
639.0	21.90	28.7888	35.9622	0.03365	0.03237	20.6604
663.36	21.93	28.7888	35.9622	0.03374	0.03257	21.5767

The values of Q'_0 at these same temperatures are calculated from the former equation to be: 20.358 cal., 20.700 cal. and 21.536 cal. respectively, i.e. about 0.13 to 0.3 % too small, — which does not mean any significant deviation from the formula for Q'_0 used.

The curve *A* in Fig. 5 graphically represents the values of C_p for molten and solidified *gold.*

3. *Plated gold in the form of a riveted crucible.*

The results obtained with the hard *plated gold* were the following:

Temperature t in °C.:	Amount of Heat Q'_0 developed by 1 Gr. gold in calories:	Q'_0 as calculated from the formula:
402°.8	12.8079	12.8120
410.6[1])	13.0720	13.0660
412.8	13.1378	—
630.6	20.3847	20.3783
637.9	20.6487	20.6270
800.5	26.2666	—
803.6	26.3871	26.3753
959.6	31.9950	32.0170
997.4[6]	33.4245	—

These quantities of heat can be expressed by the equation:

$$Q'_0 = 0{,}031341 \,.\, t + 0{,}46943 \,.\, 10^{-6} \,.\, t^2 + 0{,}1709 \,.\, 10^{-8} \,.\, t^3.$$

Therefore, the true specific heat c_p by the formula:

$$c_p = 0{,}031341 + 0{,}93886 \,.\, 10^{-6} \,.\, t + 0{,}5127 \,.\, 10^{-8} \,.\, t^2,$$

and the atomic heat C_p of plated *gold* by:

$$C_p = 6{,}1804 + 0{,}18514 \,.\, 10^{-3} \,.\, t + 0{,}1011 \,.\, 10^{-5} \,.\, t^2.$$

Some values of c_p and C_p are calculated for the same temperatures as sub 1:

t:	c_p:	C_p:
200°	0.03173	6.258
400	0.03254	6.416
600	0.03375	6.655
800	0.03537	6.975
1000	0.03741	7.376
1063	0.03813	7.520

[1]) The measurement at 410°.6 C. was executed after all other measurements were finished; then, after the crucible had been heated at 1000° C. for some time, the value of Q_0 mentioned was found. As it exactly fits within the series of the other values for Q_0, this fact proves, that the condition of the *gold* was not appreciably changed by this heating and that the differences between the heated and non-heated plated *gold* are only very small.

On comparing these values with those formerly obtained, it is proved that they are all *somewhat smaller* (0.3 to 0.6 %) than the values for molten and solidified *gold*: the curve *A'* in Fig. 2, over its whole length.

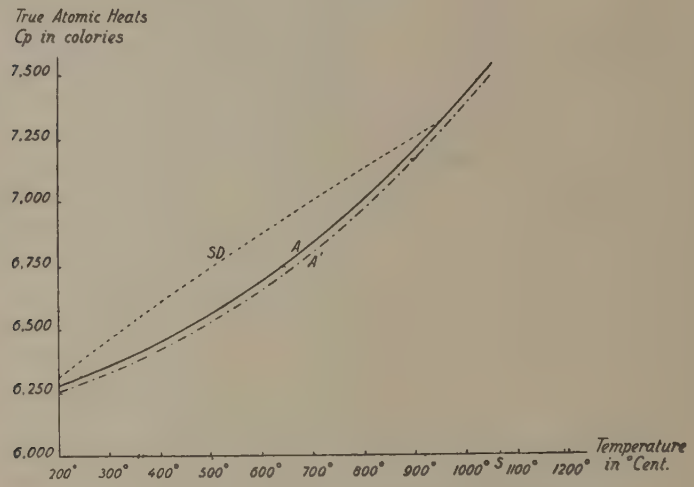

Fig. 2. Atomic Heats of Gold in different Conditions.

is situated somewhat *below* the curve *A*, but the differences are only slight. On melting the plated *gold*, the curve *A* is again obtained.

In this connection it must be remarked, that the values for *gold* obtained at 18° and at 100° C. by JAEGER and DIESSELHORST [1]) exactly coincide with our values at the same temperatures. In Fig. 2 we have, however, also reproduced a curve *SD*, deduced from the measurements of SCHLAEPFER and DEBRUNNER [2]), which evidently strongly deviates from our curve, as well in the absolute values of C_p, as in its slope. The amounts of heat Q_0 published by them, at first sight, do not deviate so very much from ours [3]); but their measurements seem only to be accurate within a limit of about 1.0 or 1.5 %. So for instance, between 381°.5 C. and 0° C., their value for c_p: 0.0319, only differs from ours (0.03177) by + 0.3 to 0.4 %; their value for c_p between 851° and 0° C., however, differs from our value (0.03306 for stabilized, 0.03298 for plated *gold*) already by 1 to 1.6 %.

---

[1]) W. JAEGER and H. DIESSELHORST, Wiss. Abh. d. Phys. techn. Reichsanst., **3.** (1900), 269.

[2]) P. SCHLAEPFER and P. DEBRUNNER, Helv. Chim. Acta, **7**, (1923), 46.

[3]) The amounts of heat Q_0 between $t°$ and 0° C. can, according to the measurements by these authors, be calculated from the formula:

$$Q'_0 = 0{,}03063 \,.\, t + 0{,}3542 \,.\, 10^{-5} \,.\, t^2 - 0{,}104 \,.\, 10^{-9} \,.\, t^3.$$

The atomic heat C_p from: $C_p = 6{,}0397 + 0.1397 \,.\, 10^{-2} \,.\, t - 0{,}6154 \,.\, 10^{-7} \,.\, t^2$. According to these data at 200° C., $C_p = 6{,}317$; at 400° C.: 6.589; at 600° C.: 6,855; at 800° C.: 7,118; at 1000° C.: 7,375.

Notwithstanding these relatively small differences, the *differential* function $\frac{dQ}{dt}$, shows a quite different slope from ours. The fact, that at about 770° C. their value of c_p becomes identical with ours, seems to make it probable, that also in this case an *un*stabilized condition of the *gold* used may, at least partially, have been the cause of the said discrepancies. In this case, however, the latter are situated in the opposite direction, as was the case with the *silver* under analogous circumstances.

From the results here obtained with *platinum, silver, copper* and *gold* under different conditions it becomes, moreover, finally evident, that *no* predictions can be made as to the direction, in which the specific heats of worked and non-worked metals will be changed: the worked metal can show as well *smaller*, as *greater* values of c_p than the normal metal does. With respect to these phenomena, theoretical considerations [1]) still appear untimely, as in the momentaneous state of affairs doubtlessly a considerable number of still unknown factors play a decisive rôle in them.

Groningen, Laboratory for Inorganic and Physical Chemistry of the University.

[1]) J. A. M. VAN LIEMPT and W. GEISS, Zeits. f. anorg. Chem., **171**, (1923), 317; *Die Naturwiss.*, **19**, (1931), 705.

Chemistry. — *The Structure of Cesium-Osmiamate.* By F. M. JAEGER and J. E. ZANSTRA.

(Communicated at the meeting of June 25, 1932).

§ 1. In two previous papers [1]) the structure of *potassium-, ammonium-, rubidium-* and *thallium-osmiamate* have been discussed in detail. In the present paper we wish to publish the results of the analogous investigation of the corresponding *cesium-osmiamate*, which, although equally showing a truly pseudo-tetragonal character, yet in many respects appears to have a different structure.

Crystallographical Data.

From a hot aqueous solution it crystallizes in pale yellow, flat needles, much alike the *rubidium*-salt. From a cold solution, on slow evaporation in the dark, thin flat tables are obtained.

[1]) F. M. JAEGER and J. E. ZANSTRA, these Proceedings, **35**, (1932), 610;

The crystals of the *cesium*-salt are represented in Fig. 1. They are *rhombic-bisphenoidal* and *pseudo-tetragonal*; their orientation with respect

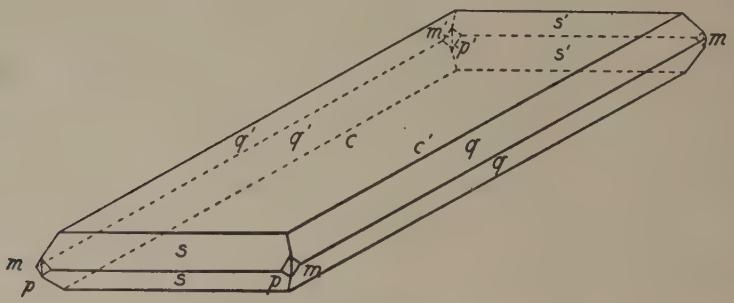

Fig. 1. Cesium-Osmiamate.

to the other pseudo-tetragonal salts is, however, such, that their *a*- and *b*-axis have the direction of the zone-axes [110] and [1$\bar{1}$0] in the crystals of the *potassium*-salt; as we shall see, also their spacings in these directions are completely comparable with those of the other *osmiamates* parallel to [110] and [1$\bar{1}$0]. The axial ratio is:

$$a : b : c = 0{,}9759 : 1 : 1{,}7157.$$

The angular values are not constant, but oscillate within rather wide limits.

As we will see, the ratio $b : c$ must rather be taken: 1 : 0,8577, so that $s = \{101\}$ and $q = \{021\}$.

Forms observed: $c = \{001\}$, predominant, yielding very good reflections; $s = \{102\}$ and $q = \{011\}$, about equally well developed and giving sharp images; $m = \{110\}$ and $p = \{210\}$, subordinate and small, yielding rather dull reflections. The habitus is that of tabular crystals parallel to {001} or of flat needles with their elongation parallel to the *a*-axis.

Angular Values:	*Observed*:	*Calculated*: (from the spectrosc. data):
$c : s = (001) : (102) =$	41° 0′ — 41°56′	40°19′
$c : q = (001) : (011) =$	59 18 — 60 50	59 46
$s : s = (102) : (10\bar{2}) =$	96 18 — 97 56	97 22
$q : q = (011) : (01\bar{1}) =$	59 21	60 28
$m : p = (110) : (210) =$	18 13	18 17
$p : p = (210) : (2\bar{1}0) =$	51 4	52 1½
$m : m = (110) : (1\bar{1}0) =$	87 30	88 36

Perfect cleavability parallel to {001}.

Weakly birefringent; the double refraction is negative. The plane of the optical axes is parallel to {100}; the optical angle is only small, but greater than in the case of the *rubidium*-salt. Also the dispersion, although strong and abnormal, seems to be less than that of the *Rb*-salt. The specific weight at 16° C. is: 5.20.

From some optical particularities, which later-on will be described in a more detailed paper and from the corrosion-figures obtained, it must be deduced that the symmetry of the crystals is *rhombic-bisphenoïdal.*

§ 2. A LAUE-pattern on {001} was prepared by means of *tungsten*-radiation. The image showed rhombic symmetry (Fig. 2) and was analysed

Fig. 2. LAUE-pattern on {001} of Cesium-Osmiamate.

in the usual way, after a gnomonic projection (Fig. 3) had been made. The results are collected in Table I.

The wave-lengths used lie between 0,3082 Å. and 0,75 Å. The fundamental lattice is the simple rhombic one.

From this follows, that (311), (301), (031), (142), (322), (513), (053), (253), (533) and (131) reflect in no lower than the second order, (121), (021) and (032) is no lower than the third order.

§ 3. Rotation-spectrograms were prepared by turning the crystals round the *a*-, *b*- and *c*-axis respectively. From these spectrograms the axial ratio: $a_0 : b_0 : c_0 = 8{,}08 : 8{,}35 : 7{,}22$ was deduced, which furnishes: $a : b : c = 0{,}9676 : 1 : 0{,}8648$; this axial ratio is in sufficient agreement with that found by the direct crystallographical measurements, if to *s* and *q* the symbols: $s = \{101\}$ and $q = \{021\}$ be attributed.

TABLE I.
Analysis of the LAUE-pattern on (001) of the Cesium-Salt.

1st Order Symbols of Spots:	Estimated Intens.:	Glancing Angle θ:	(1st Order):	(2nd Order):	(3d Order):
(231)	2	9° 5½′	0.7146	—	—
(632)	2	9 38½	0.4018	—	—
(311)	10	10 11½	0.8968	0.4484	—
(452)	5	10 11½	0.4484	—	—
(542)	2	10 15	0.4437	—	—
(612)	1	10 36	0.4819	—	—
(301)	1	10 43	0.9984	0.4942	—
(162)	1	10 50	0.5034	—	—
(031)	7	10 59	1.0360	0.5180	—
(432)	2	12 53	0.7126	—	—
(494)	1	13 14	0.3749	—	—
(121)	3	14 29	1.7952	0.8976	0.4488
(854)	2	13 39	0.3964	—	—
(834)	3	14 57	0.4741	—	—
(502)	1	12 56½	0.7010	—	—
(814)	2	15 43½	0.5256	—	—
(474)	1	15 58	0.5433	—	—
(142)	1	15 43½	1.0512	0.5256	—
(585)	1	16 58½	0.4899	—	—
(3.11.6)	1	16 58½	0.4069	—	—
(2.11.6)	1	17 17	0.4224	—	—
(021)	2	16 8½	2.2296	1.1148	0.7432
(274)	1	17 42	0.6600	—	—
(876)	1	17 56	0.4520	—	—
(322)	1	17 35	1.3068	0.6534	—
(513)	2	18 29	0.9578	0.4789	—
(754)	1	14 54	0.4727	—	—
(053)	1	19 12½	1.0346	0.5173	—
(032)	1	21 10	1.8680	0.9340	0.6227
(184)	1	16 5	0.5491	—	—
(294)	1	19 9	0.4270	—	—
(394)	1	13 44	0.4036	—	—
(253)	1	17 52½	0.8998	0.4499	—
(856)	1	19 56	0.5559	—	—
(342)	1	13 0	0.7218	—	—
(533)	1	16 23½	0.7577	0.3789	—
(764)	1	13 57	0.4167	—	—
(131)	4	10 23	0.9492	0.4746	—
(252)	3	12 10	0.6455	—	—

1. The rotationspectrogram round the *a*-axis showed a principal and four accessory spectra. $I_a = 8.08$ Å. The most intensive spots ($\varphi = 30°$) appeared to be: (021); (044); (211); (232); (244) and (421). The even spectra were more intensive than the odd ones.

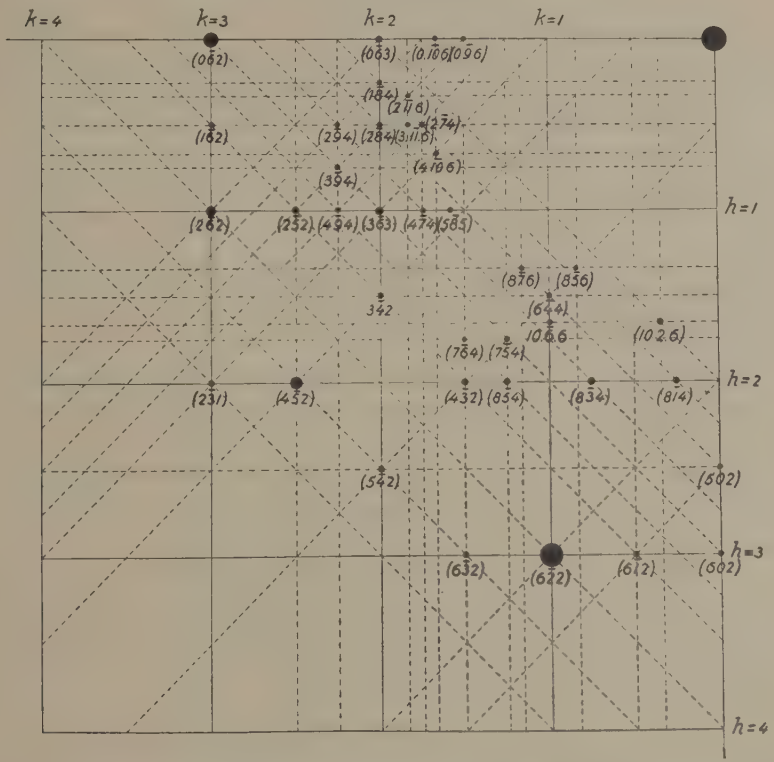

Fig. 3. Gnomonic Projection of the LAUE-pattern on {001} of Cesium-Osmiamate.

2. The spectrum obtained by rotating round the *b*-axis ($\varphi = 60°$) also showed a principal and four accessory spectra. $I_b = 8.35$ Å. The most intensive images were: (002); (004); (105); (206); (602); (113); (214); (215); (216); (310); (410); (413); (513); (021); (023); (225); (126); (423); (623); (233); (234); (235); (330); (531) and (245).

3. The rotationspectrogram round the *c*-axis ($\varphi = 90°$) showed a principal and three accessory spectra. $I_c = 7.22$ Å. The most intensive spots observed were: (040); (460); (640); (021); (251); (351); (461); (421); (621); (042); (252); (212); (402); (412); (602); (642); (023); (233); (253); (353); (213); (413); (423) and (623).

§ 4. Also a powder-spectrogram was obtained which showed a great number of lines. However, this spectrogram was not used for the purpose of comparison of the calculated and observed intensities, for the same

reason as indicated in the case of the *rubidium*-salt. The general results were in agreement with those obtained by the rotation-spectrograms; a full description will be given in the more detailed paper to be published in the *Recueil des Trav. d. Chim. d. Pays-Bas.*

§ 5. *The structure of the Cesium-Salt.*

The discussion of the results obtained led to the conclusion, that the space-group in this case is V^2; the elementary cell contains a mass: $Cs_4Os_4N_4O_{12}$, the crystallographical axes having the direction of the zone-axes [110] and [$1\bar{1}0$] in the *potassium*-salt.

Also in this case it seems advisable to start the determination of the structure by first fixing the positions of the *Os*- and *Cs*-ions, because these ions contribute for the greater part to the intensities observed.

The argumentation leading to the final positions of these atoms will be discussed later-on in detail in our paper in the *Receuil*. Here we will only communicate the results.

1. The parameter in the direction of the *c*-axis is, as well for the *Os*-ions, as for the *Cs*-ions, equal to: $\frac{1}{2}$; layers of the *Os*-ions, and also those of the *Cs*-ions, are in this direction $\frac{1}{2}.c_0$ apart from each other.

2. In the direction of the *b*-axis, as well layers of ions with mutual distances of: $y=0.b_0$ and $y=\frac{1}{2}.b_0$, as layers of other ions with distances of: $y=\frac{1}{4}.b_0$ and $y=\frac{3}{4}.b_0$ must be present.

3. In the direction of the *a*-axis, each time a couple of *Os*-ions is situated on rows having the direction of the *a*-axis, which rows are alternately shifted with respect to each other over $\frac{1}{4}.b_0$. The distances of the *Os*-ions, — and in the same way that of the *Cs*-ions from each other, — must very closely correspond to $\frac{1}{2}.a_0$.

From all data mentioned, the most probable parameters of these ions become:

For the 4 *Os*-ions: [000]; [$\frac{1}{2}$ 00]; [0 $\frac{1}{4}$ $\frac{1}{2}$]; [$\frac{1}{2}$ $\frac{1}{4}$ $\frac{1}{2}$].
For the 4 *Os*-ions: [$\frac{1}{4}$ $\frac{1}{2}$ 0]; [$\frac{3}{4}$ $\frac{1}{2}$ 0]; [$\frac{1}{4}$ $\frac{3}{4}$ $\frac{1}{2}$]; [$\frac{3}{4}$ $\frac{3}{4}$ $\frac{1}{2}$].

Indeed, the intensities of the reflections calculated from these values, in so far as only the action of the *Os*- and *Cs*-ions is taken into account, agree very well with the intensities actually observed, as may be seen from Fig. 4, in which these intensities are compared for the spots of the rotation-spectrogram round [010], plotted against $\sqrt{\frac{h^2}{a_0^2}+\frac{l^2}{c_0^2}}$ as abscissae.

The contribution of the $(3O+N)$-ions, it is true, cannot be neglected; but it is certainly much less than that of the heavy ions mentioned. For fixing their positions, *twelve* parameters must be determined. It is a hopeless task to find out the right combination of their values. The orientation of the $(3O+N)$-complex round an *Os*-ion at [000], must differ somewhat from that round the *Os*-ion at [$\frac{1}{2}$ 00]; otherwise reflections as: (333) and (335), which are really present, could never occur. This different

orientation must be caused by the fact that the N'''-ions with their 10 electrons will be more greatly deformed by the influence of the eight-valent, central *Os*-ion, than the O''-ions will be.

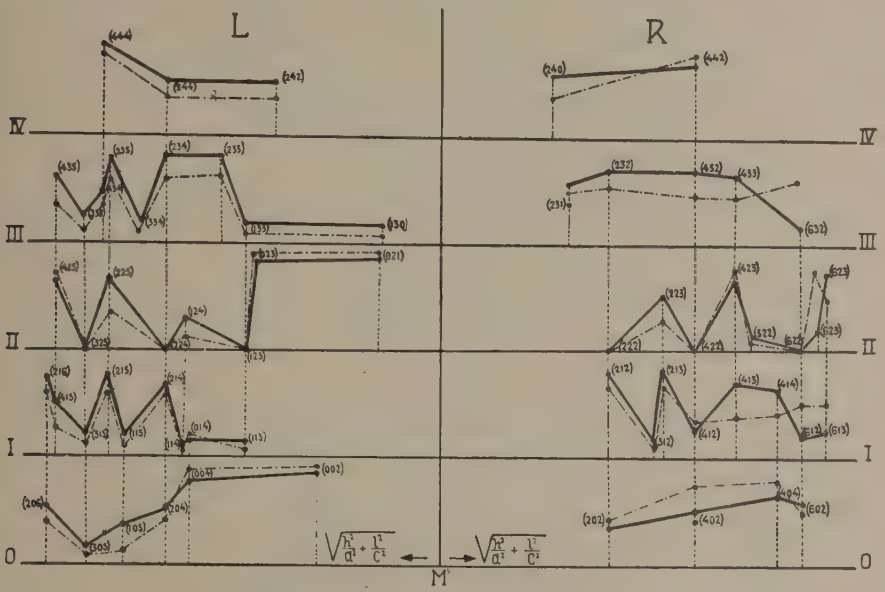

Fig. 4. Rotation-Spectrogram of Cesium-Osmiamate round [010].

The space-group of the *Cesium*-salt is V^2; V^2 must be the right one, as V^4, — the other alternative, — is excluded by the values of the parameters of its fourfold positions in the direction of the *b*-axis. The *Os*-ions in V^2 occupy the two possible twofold positions c) and d) [1], with $u = \frac{1}{8}$; the *Cs*-ions the fourfold position e), with $x = \frac{1}{4}$, $y = \frac{5}{8}$ and $z = \frac{1}{4}$. A comparison of the structures of the *Cs*- and *Rb*-salts with that of the *K*-salt [2]) teaches us, that, while in the latter each ion $\{OsO_3N\}'$ is in the basal plane surrounded by 4 $K^{\bullet}$-ions in such a way, that the distance between a $K^{\bullet}$- and Os-ion is 4.0 Å. In the *Rb*-salt the distances between two $Rb^{\bullet}$-ions already proved to be somewhat different in two directions: 5.57 and 5.84 Å. respectively, the distance between a $Rb^{\bullet}$- and *Os*-ion becoming: 4.07 Å. When the $(3O + N)$-complex is still somewhat more rotated round the direction of the *c*-axis, the original arrangement of the *K*-salt becomes unstable, because it no longer corresponds to a closest packing: now the elementary cell gets expanded in one direction [110] of the original *K*-salt, contracted in the other [1$\bar{1}$0] and the new structure of the *Cs*-salt is produced, in which the distance between a Cs'- and *Os*-ion is 4.6 Å., while the dimensions of the sub-cell (half the original one)

[1]) R. W. G. WYCKOFF, loco cit., p. 57.

[2]) F. M. JAEGER and J. E. ZANSTRA, these Proceedings, 787, (1932),

become: 4.02 and 8.35 Å. Two *Cs*-ions now get each time more distant from each other by two intercalated *O''*-ions. The surface occupied in the

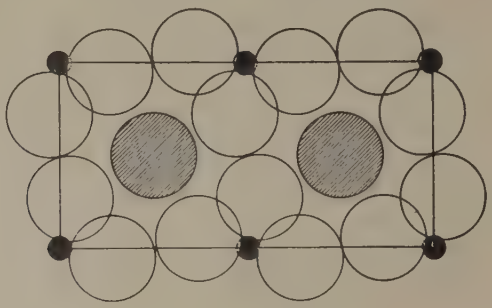

A Potassium-Osmiamate

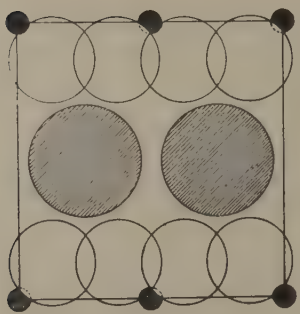

B. Cesium-Osmiamate.

Fig. 5. Comparison of the Structure in (001) of the K- and Cs-salts.

basal plane by 1 molecule $KOsO_3N$ was: 31.9 Å^2, that occupied by 1 molecule $RbOsO_3N$ is: 32.2 Å^2; and that occupied by 1 molecule $CsOsO_3N$ is: 33,1 Å^2. The latter surface is smaller than in the case that the *Cs*-salt had preserved the original structure of the *K*-salt.

The co-ordination-number of the eight-valent *Os*-ion proves to be 6; there are 4 *O''*-ions surrounding it in the basal plane, one above and one below that plane. Also the apparent pseudotrigonal arrangement of the atoms in the plane (100) of the *Cs*-salt, — as it is, for instance, also revealed in the angular values of the crystals in the zône [100], — is clearly visible in this structure. Hence the mutual relations between the tetragonal *K*-salt and the rhombic, but truly pseudo-tetragonal (NH_4)-, *Rb*-, *Tl*- and *Cs*-salts are fully explained by the crystalline structures deduced for all these salts.

Groningen, Laboratory for Inorganic and Physical Chemistry of the University.

Chemistry. — *The Structure of the Ammonium-, Rubidium- and Thallium-Osmiamates.* By F. M. JAEGER and J. E. ZANSTRA.

(Communicated at the meeting of June 25, 1932).

§ 1. In a previous paper [1]) we established the structure of *potassium-osmiamate* and demonstrated that the constitution of this tetragonal-bipyramidal salt is quite analogous to that of *potassium-periodate*, of *potassium-perrhenate* and of the *tungstates* and *molybdates* of the *scheelite-wulfenite*-group; more in particular that this constitution in the case of *potassium-osmiamate* can be expressed by:

$$\{[O]_3''[Os^{VIII}][N]'''\}' \ldots . K^{\bullet},$$

all composing ions having the electronic configurations of inert gases.

In the present paper we wish to communicate the results obtained in the analogous study of some other *alkali*-salts of this series, more particularly of the *ammonium-*, *rubidium-*, and *thallo-osmiamate*. The investigation of the corresponding, but structurally deviating *cesium*-salt will be published in another paper.

§ 2. Although all these salts show a close analogy to the *potassium*-salt in so far, that they prove to possess a truly pseudo-tetragonal character, they deviate from the salt formerly studied by their lower symmetry, as in reality they all are rhombic, and more particularly, rhombic-bisphenoidal.

Crystallographical data.

1. *Ammonium-Osmiamate* crystallizes from its aqueous solutions in apparently tetragonal crystals (Fig. 1), which on closer examination,

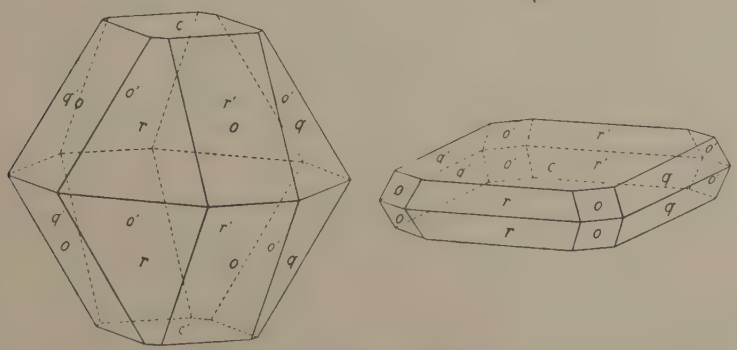

Fig. 1. Ammonium—Osmiamate.

[1]) F. M. JAEGER and J. E. ZANSTRA, these Proceedings, **35**, (1932), 610;

however, prove to be rhombic-pseudotetragonal. In their external appearance they are either analogous to the *potassium*-salt, only differing from them by the occurrence of the basal plane (001), or they are tabular parallel to this face (001), which at the same time is a direction of a not perfect, but good cleavability. The angular values are not quite constant.

Rhombic-bisphenoidal; pseudo-tetragonal.

$a : b : c = 0{,}9437 : 1 : 2{,}3106.$

Forms observed: $o = \{112\}$, narrower than r and q, but yielding good reflections; $r = \{101\}$ and $q = \{011\}$, both lustrous and about equally broad; $c = \{001\}$, either small or predominant, very lustrous.

Angular values:	*Observed:*	*Calculated:* (from the spectrogr. data):
$c : o = (001) : (112) =$	* 58° 13′—59° 44′	59° 17′
$c : q = (001) : (011) =$	* 66 42	66 36
$c : r = (001) : (101) =$	—	67 47
$q : q' = (011) : (01\bar{1}) =$	44 2—45 35	44 26
$r : r' = (101) : (10\bar{1}) =$	—	46 48

Cleavage parallel to {001}, distinct, but not so perfect as in the case of the *rubidium*-salt. The specific weight at 16° C. is: 4.0.

The crystals are biaxial, with a very small optical angle. For red rays, they are almost uniaxial; the plane of the optical axes for the yellow rays is parallel to {100}, for the green and blue rays parallel to {010}. The first bisectrix is parallel to the c-axis; the character of the double refraction is positive.

2. *Rubidium-Osmiamate.* The *rubidium*-salt also is rhombic and shows the closest analogy with the *ammonium*-salt just described. However, the habitus of the crystals here is always tabular parallel to (001), this face being a direction of a perfect cleavability. The crystals are often elongated parallel to the edge (001) : (112); but also regular octagonally or tetragonally limited plates occur (Fig. 2).

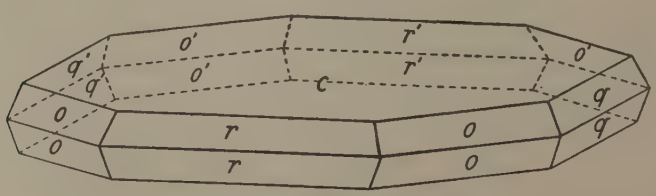

Fig. 2. Rubidium—Osmiamate.

Rhombic-bisphenoidal; pseudo-tetragonal.

$a : b : c = 0{,}9539 : 1 : 2{,}3356.$

Forms observed: $c = \{001\}$, always predominant, very lustrous; $o = \{112\}$, $r = \{101\}$ and $q = \{011\}$, almost equally well developed and yielding excellent reflections.

Angular values:	*Observed:*	*Calculated:* (from the spectrogr. data):
$c : q = (001) : (011) =$*	66° 58′—67° 58′	67° 42′
$c : o = (001) : (112) =$*	59 28	59 25
$c : r = (001) : (101) =$	66 29—67 0	66 49½
$q : q' = (011) : (01\bar{1}) =$	44 4—46 14	44 36
$o : o = (112) : (11\bar{2}) =$	61 4	61 10

The angular values oscillate not unappreciably. The crystals possess a perfect cleavability parallel to {001}. The specific weight at 18° C. is about: 5.0. Optically biaxial; the birefringence is positive. The plane of the optical axes for red and yellow rays is parallel to {100}, that for the green and blue rays parallel to {010}. The first bisectrix is parallel to the *c*-axis; the angle of the optical axes is only small.

Sometimes plates cut parallel to {001} shows a subdivision in four weakly birefringent and biaxial sectors. In this case the angular values oscillate even more than in the ordinary case. Most probably this anomalous optical behaviour is caused by a slight admixture of the potassiumsalt; if a potassiumfree rubidiumsalt is used in the preparation of the osmiamate, no such anomalies manifest themselves any longer.

3. *Thallium-Osmiamate.*

The *thallous* salt, — which is almost insoluble in cold, better soluble in boiling water, — crystallizes, on cooling, in very small, flat crystals, which evidently are quite analogous to the *rubidium*-salt. They are biaxial; their powder spectrogram appeared almost identical with that of the *rubidium*-salt. The axial ratio is: $a : b : c = 0{,}9542 : 1 : 2{,}3679$.

The bisphenoidal symmetry is attributed to all three rhombic salts, in connection with the experiences gained in the case of the *cesium*-salt, the bisphenoidal symmetry of which was proved in several ways, as will be shown in the following paper.

§ 2. For the purpose of controlling the rhombic symmetry of the *ammonium*-, and *rubidium*-salts, LAUE-patterns on {001} we made with *tungsten*-radiation (40—44 K.V.). The image of the *Rb*-salt thus obtained, is reproduced in Fig. 3.

The analysis of this LAUE-pattern in the usual way gave the following results; the gnomonic projection of the image is reproduced in Fig. 4.

Fig. 3. LAUE-Pattern of Rubidium-Osmiamate on {001}.

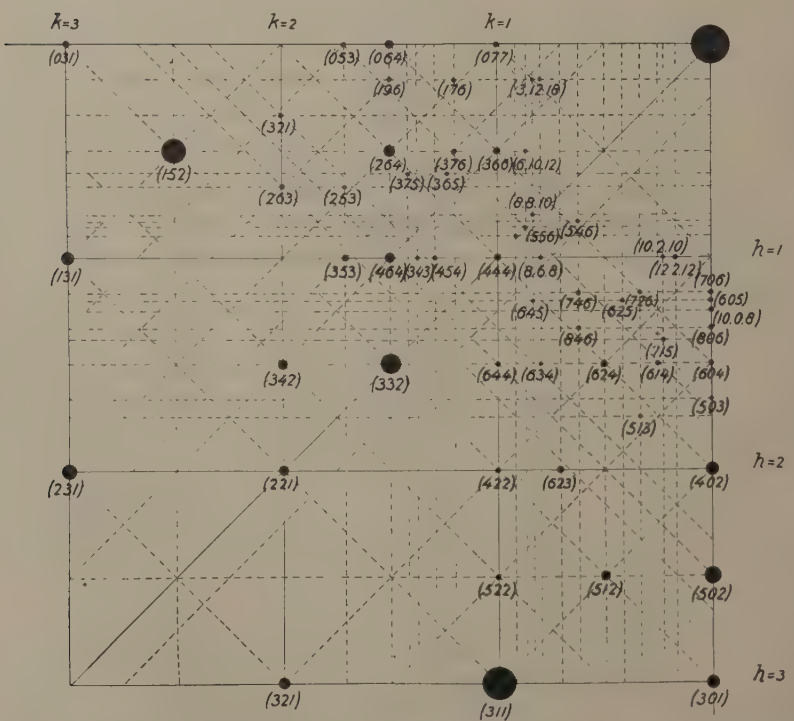

Fig. 4. Gnomonic Projection of the LAUE-Pattern on {001} of Rubidium-Osmiamate.

TABLE I.
Analysis of the LAUE-pattern on (001) of the Rubidium-Salt.

Symbol $\{hkl\}$:	Estim. Int.:	Glancing Angle θ:	(1st order)	(2nd order)	(3d order)	(4th order)	(5th order)	(6th order)	(7th order)
(011)	1	22° 39′	4.1770	2.0885	1.3923	1.0442	0.8354	0.6962	0.5967
(356)	1	23 12	0.7231	0.3616	—	—	—	—	—
(122)	2	20 21	1.7086	0.8543	0.5695	—	—	—	—
(588)	1	19 41	0.3875	—	—	—	—	—	—
(546)	1	21 6	0.6074	—	—	—	—	—	—
(434)	1	18 15	0.6876	0.3438	—	—	—	—	—
(445)	1	20 1	0.6608	0.3304	—	—	—	—	—
(556)	1	19 31	0.5127	—	—	—	—	—	—
(778)	1	18 48	0.3523	—	—	—	—	—	—
(111)	2	16 19	2.2109	1.1055	0.7369	0.5528	—	—	—
(515)	1	21 46	0.7763	0.3882	—	—	—	—	—
(616)	1	21 55	0.6536	0.3268	—	—	—	—	—
(746)	1	16 54	0.4003	—	—	—	—	—	—
(645)	1	15 54	0.4228	—	—	—	—	—	—
(625)	1	17 53	0.5324	—	—	—	—	—	—
(726)	1	18 37	0.4779	—	—	—	—	—	—
(706)	1	19 37	0.5109	—	—	—	—	—	—
(605)	1	19 14	0.5827	—	—	—	—	—	—
(504)	1	18 31	0.6770	0.3385	—	—	—	—	—
(403)	1	16 55	0.8030	0.4015	—	—	—	—	—
(302)	1	15 11	0.9697	0.4848	—	—	—	—	—
(614)	2	14 56	0.4732	—	—	—	—	—	—
(715)	2	16 4	0.4329	—	—	—	—	—	—
(312)	2	14 25	0.8829	0.4415	—	—	—	—	—
(423)	1	15 19	0.6598	0.3299	—	—	—	—	—
(634)	1	13 44	0.3970	—	—	—	—	—	—
(322)	1	12 49	0.6960	0.3480	—	—	—	—	—
(513)	2	8 31	0.5112	—	—	—	—	—	—
(533)	3	11 53	0.4013	—	—	—	—	—	—
(211)	1	10 27	0.9169	0.4585	—	—	—	—	—
(623)	3	10 54	0.3407	—	—	—	—	—	—
(201)	5	11 42	1.1259	0.5630	—	—	—	—	—
(522)	1	8 37	0.3185	—	—	—	—	—	—

TABLE I (*Continued*).
Analysis of the LAUE-pattern on (001) of the Rubidium-Salt.

Symbol $\{hkl\}$:	Estim. Int.:	Glancing Angle θ:	(1st order)	(2nd order)	(3d order)	(4th order)	(5th order)	(6th order)	(7th order)
(512)	4	9° 8′	0.3526	—	—	—	—	—	—
(502)	6	9 14	0.3657	—	—	—	—	—	—
(311)	10	7 17	0.4640	—	—	—	—	—	—
(301)	5	8 46	0.5121	—	—	—	—	—	—
(032)	4	15 39	1.0145	0.5073	—	—	—	—	—
(146)	1	31 45	1.2579	0.6289	0.4169	—	—	—	—
(176)	2	19 30	0.5235	—	—	—	—	—	—
(132)	5	14 51	0.9157	0.4578	—	—	—	—	—
(365)	1	17 18	0.4935	—	—	—	—	—	—
(375)	1	15 16	0.3916	—	—	—	—	—	—
(465)	1	16 7	0.4302	—	—	—	—	—	—
(232)	3	12 55	0.7085	0.3543	—	—	—	—	—
(343)	1	14 1	0.5465	—	—	—	—	—	—
(454)	2	14 27	0.4414	—	—	—	—	—	—
(443)	4	12 38	0.4298	—	—	—	—	—	—
(332)	8	11 0	0.5145	—	—	—	—	—	—
(053)	1	14 5	0.5558	—	—	—	—	—	—
(152)	10	9 17	0.3684	—	—	—	—	—	—
(253)	1	13 3	0.4800	—	—	—	—	—	—
(353)	3	12 1	0.4101	—	—	—	—	—	—
(342)	4	7 17	0.3769	—	—	—	—	—	—
(221)	4	8 23	0.5885	—	—	—	—	—	—
(321)	4	6 29	0.3619	—	—	—	—	—	—
(031)	4	7 59	0.5372	—	—	—	—	—	—
(131)	4	7 34	0.4821	—	—	—	—	—	—
(231)	5	6 42	0.3686	—	—	—	—	—	—
(376)	2	18 15	0.4558	—	—	—	—	—	—
(321)	2	6 36	0.3619	—	—	—	—	—	—
(503)	1	14 6	0.5358	—	—	—	—	—	—
(196)	1	15 29	0.3343	—	—	—	—	—	—
(263)	1	11 23	0.3538	—	—	—	—	—	—
(566)	1	17 37	0.4236	—	—	—	—	—	—

The wave-lengths are calculated from the formula:

$$\lambda = \frac{2.l}{c_0} \left\{ \frac{1}{\left(\frac{h}{a_0}\right)^2 + \left(\frac{k}{b_0}\right)^2 + \left(\frac{l}{c_0}\right)^2} \right\}.$$

In the case of the *rubidium*-salt the wave-lengths produced lie between: 0,2796 Å. and about 0,68 Å. The underlying lattice proves to be *the simple rhombic* one.

The LAUE-pattern on (001) of the *ammonium*-salt was closely analogous to that of the *rubidium*-salt; it possessed rhombic symmetry, with a dyad axis and two symmetry-planes perpendicular to each other. The measurements of DUFET, who thought the *ammonium*-salt to be tetragonal, are, therefore, erroneous.

§ 3. *Rotation-spectrograms of the Rubidium-Salt.*

Rotation-spectrograms of the crystals were made by oscillating them round the principal crystallographical directions through different angles, using *copper*-radiation as the luminous source.

a. The rotationspectrogram round the *a*-axis showed a principal and two accessory spectra. $I_a = 5.55$ Å. The most intensive spots were: (004); (008); (028); (013); (026); (037); (048); (101); (103); (116); (118); (1.1.10); (116); (136); (138); (217); (228); (224) and (244).

b. The rotationspectrogram round the *b*-axis also showed a principal spectrum and two accessory spectra. $I_b = 5.70$ Å. The most intensive images were: (004); (008); (109); (0.0.12); (103); (204); (309); (017); (0.1.11); (112); (315); (316); (129); (121) and (224).

c. The rotationspectrogram round the *c*-axis showed a principal and seven accessory spectra. $I_c = 13.64$ Å. The most intensive spots ($\varphi = 60°$, being double that used in the previous cases) were: (200); (220); (020); (132); (332); (103); (123); (303); (024); (224); (244); (424) and (116). The 2nd, 4th and 6th spectra were more intensive than the 1st, 3d, 5th and 7th spectra.

d. Rotationspectrograms round [110], gave: $I_{(110)} = 8.1$ Å. A principal and three accessory spectra were present. With $\varphi = 60°$, the most intensive images were: (112); (116); (224); (228); (336); (338); (125); (129); (020); (024); (132); (136); (1.3.10); (0.0.12); (211); (200); (204); (310); (316) and (312). In another spectrogram of this kind, also: (2.2.10); (004); (008); (1.1.10); (208) and (3.1.10) were found to be rather intensive besides some of the spots already mentioned. In general, the spots of the highest intensities appear to be those for which $(h + k + l)$ is an *even* number; the triplets $(o\,k\,l)$ also occur only in such cases, where $(k + l)$ is an *even* number. Although the cell is evidently the simple rhombic one, these facts prove that at least the plane (100) is *almost* centred.

§ 4. *Powderspectrograms of the (NH_4)- and Rb-salts* were obtained by means of *iron-*, those of the *Tl*-salt by means of *copper*-radiation. The results obtained will be published later-on in detail in a more extensive paper. The data were not used for the determination of the intensities, as the diffraction-lines were too crowded, so that often several lines were practically coïnciding. For the purpose of comparison of the observed and calculated intensities, therefore, the intensities of the diffraction-spots of the rotationspectrograms were made use of. In general it may be pointed out that the data of the powderspectrograms were in perfect agreement with those obtained in the rotationspectrograms. The following Table II gives a survey of the principal data necessary for the final discussion of the structure of the salts here considered.

§ 5. *Discussion of the Structure of the (NH_4),- Rb- and Tl-Osmiamates.* As the (NH_4)- and *Tl*-salts show, in their behaviour, the closest analogy with the *Rb*-salt, it is sufficient here to limit our discussion to the latter compound.

In the spectrograms of this salt the reflections of (100), (010) and (001) in *odd* orders are absent. In connection with the simple rhombic lattice, its structure, therefore, must belong to the spacegroup V^4. In this group a tetravalent position occurs with the co-ordinates:

$$[x, y, z] \; ; \; [x + \tfrac{1}{2}, \tfrac{1}{2} - y, \bar{z}] \; ; \; [\bar{x}, y + \tfrac{1}{2}, \tfrac{1}{2} - z] \; ; \; [\tfrac{1}{2} - x, \bar{y}, z + \tfrac{1}{2}].$$

For $x = 0$; $y = \frac{1}{4}$; $z = {}^1/_8$ for the *Os*-atoms, the positions of the *Os*-atoms become:

$[0, \frac{1}{4}, {}^1/_8]$; $[\frac{1}{2}, \frac{1}{4}, {}^7/_8]$; $[0, \frac{3}{4}, {}^3/_8]$; $[\frac{1}{2}, \frac{3}{4}, {}^5/_8]$; or, by shifting them over $y = -\frac{1}{4}$ and $z = -{}^1/_8$:

$[0, 0, 0]$; $[\frac{1}{2}, 0, \frac{3}{4}]$; $[0, \frac{1}{2}, \frac{1}{4}]$; $[\frac{1}{2}, \frac{1}{2}, \frac{1}{2}]$, just as in the case of the *potassium*-salt.

In the same way, for $x = 0$; $y = \frac{1}{4}$; $z = {}^5/_8$ for the *Rb*-atoms in the *rubidium*-salt, their positions become:

$[0, \frac{1}{4}, {}^5/_8]$; $[\frac{1}{2}, \frac{1}{4}, {}^3/_8]$; $[0, \frac{3}{4}, {}^7/_8]$; $[\frac{1}{2}, \frac{3}{4}, {}^1/_8]$; or, by the same shift:

$[0, 0, \frac{1}{2}]$; $[\frac{1}{2}, 0, \frac{1}{4}]$; $[0, \frac{1}{2}, \frac{3}{4}]$; $[\frac{1}{2}, \frac{1}{2}, 0]$, also in analogy with those in the *potassium*-salt.

The *Rb*- and *Os*-atoms *are now placed with respect to each other in just the same way* as the *K*- and *Os*-atoms in the *potassium*-salt; the close analogy of this pseudo-tetragonal salt with the really tetragonal *potassium*-salt, beforehand makes it most probable that the deviations from these positions will only be very small.

Now the parameter: $z = {}^1/_8$ in the direction of the *c*-axis is certainly the correct one: for in the rotation-spectrograms, the reflections: (004), (008) and (00.12) are all very strong, while no trace of (002), (006) or (00.10) was ever observed; moreover, the face (001) always occurs as a limiting crystal-face. The value of z must, therefore, be chosen in such a way that the path-difference of z and $\bar{z}$ will be exactly $\frac{1}{4}\,c_0$, and this occurs, if $z = {}^1/_8$.

TABLE II.

Synopsis of the Structures and Properties of the K-, (NH_4)-, Rb- and Tl-Osmiamates.

Salt:	Formula:	Symmetry:	Axial Ratio and Cleavability:	Optical Character:	Dimensions of the Elementary Cell:	Spec. Weight at 0° C.:	Number of Molecules pro Cell:	Character of Lattice:	Space-Group:
Potassium Osmiamate	$K\,Os\,NO_3$	Tetrag.-bipyr.	$a : c = 1 : 2{,}3123$. No distinct cleavability.	Uniaxial; positive.	$a_0 = 5{,}65$ Å.; $a_0 = 5{,}65$ Å.; $c_0 = 13{,}08$ Å.	4.616	4 Mol.	Bodily centred tetrag. cell I'_t	C^6_{4H}
Ammonium-Osmiamate	$(NH_4)\,Os\,NO_3$	Rhomb.-bisphen. (pseudo-tetrag.)	$a : b : c = 0{,}9437 : 1 : 2{,}3106$. Distinct cleavability || (001).	Biaxial: positive. Small opt. angle. 1st Biss. || c-axis.	$a_0 = 5{,}53$ Å.; $b_0 = 5{,}86$ Å.; $c_0 = 13{,}54$ Å.	4.075	4 Mol.	Simple rhomb. cell I_0.	V^4
Rubidium-Osmiamate	$Rb\,Os\,NO_3$	Rhomb.-bisphen. (pseudo-tetrag.)	$a : b : c = 0{,}9539 : 1 : 2{,}3356$. Good cleavability || (001).		$a_0 = 5{,}57$ Å.; $b_0 = 5{,}84$ Å.; $c_0 = 13{,}64$ Å.	5.033	4 Mol.		
Thallium Osmiamate	$Tl\,Os\,NO_3$	Rhomb.-bisphen. (pseudo-tetrag.)	$a : b : c = 0{,}9542 : 1 : 2{,}3679$. Perfect cleavability || (001).		$a_0 = 5{,}42$ Å.; $b_0 = 5{,}68$ Å.; $c_0 = 13{,}45$ Å.	7.281	4 Mol.		

The same reasoning for the equally strongly diffracting *Rb*-atoms, gives $z = 1/8$.

That these values in the direction of the *c*-axis are the right ones, can also be deduced from the intensities of the reflections (011) and (101) in the powder-spectrogram, which in the *Rb*-salt are much weaker than in the case of the (NH_4)-salt; indeed, the strongly diffracting *Rb*-atoms (and in the case of the *thallium*-salt, also the *Tl*-atoms), — almost completely annihilate the diffraction-effect of the *Os*-atoms, if in the direction of the *c*-axis midway between two *Os*-atoms always a *Rb*-atom is placed. Of course, the much more weakly diffracting (NH_4)-groups will not have this annihilating effect.

Because reflections $(o\,k\,l)$ for which $(k + l)$ is *odd*, never occur, it must be clear that the *y*-parameter of the *Os*- and *Rb*-atoms must be $\frac{1}{4}$ and $\frac{3}{4}$ respectively; in that case the sum of the sinus-terms in the structure-factor becomes zero for such planes; and for $(o\,k\,l)$, in which $(k + l)$ is odd, also the sum of the cosinus-terms will always be zero.

Hence the principal difficulty remains the determination of the *x*-parameter. If *x* were really *zero*, we should again have the structure of the *potassium*-salt, in so far as the diffraction of the $(Os + Rb)$-atoms is concerned. But notwithstanding the analogy of the *K*- and *Rb*-salts, the differences between the two structures are evident: the structure of the latter salt certainly is no longer that of a bodily-centred cell and the occurrence of reflections for which $(h + k + l)$ is *odd*, as, for instance, (311), proves that this result cannot be completely explained by the co-operation of the oxygen- and nitrogen-atoms alone, because their intensity is too small, even in the most favourable case. Certainly, therefore, the said phenomenon must also be caused by the position of the *Os*- and *Rb*-atoms. From the intensity of (502), it follows that $0 < x < 0.10$; from that of (746), that $0 < 7x < 180°$, which gives for *x* a maximum value of 0.03.

Indeed, $x = 0.03$ proves to be in excellent agreement with the intensities observed, thus, for instance, for (512) and (152) in the LAUE-pattern.

The final co-ordinates (first set) of the *Os*- and *Rb*-atoms, thus become:

a. 4 *Os*-atoms at: $[0{,}03; \frac{1}{4}; \frac{1}{8}]$; $[0{,}53; \frac{1}{4}; \frac{7}{8}]$; $[0{,}97; \frac{3}{4}; \frac{3}{8}]$; $[0{,}47; \frac{3}{4}; \frac{5}{8}]$.
b. 4 *Rb*-atoms at: $[0{,}03; \frac{1}{4}; \frac{5}{8}]$; $[0.53; \frac{1}{4}; \frac{3}{8}]$; $[0{,}97; \frac{3}{4}; \frac{7}{8}]$; $[0{,}47; \frac{3}{4}; \frac{1}{8}]$.

The second set of co-ordinates can be obtained by a shift over: $y = -\frac{1}{4}$ and $z = -\frac{1}{8}$.

The number of the parameters of the *O*- and *N*-atoms surrounding the *Os*-atoms is very great: 12 parameters must be determined, so that great accuracy cannot be expected.

As in the series of reflections: (004), (008) and (0.0.12), the intensity of the latter is very much weakened in comparison of the others, evidently in the direction of the *c*-axis the total action of the $(O + N)$-atoms is opposite to that of he $(Os + Rb)$-atoms in that direction. This involves for half the height of the $(O + N)$-bisphenoid a value $= 0.04 \,.\, c_0$.

It must be remarked that for a radius of the O''-ion of 1.32 Å., the plane (001) would be a direction of perfect cleavability, if z were $= 0.03$.

The reflections (202) and (402) are only caused by the action of the $(O + N)$-ions; they are more intensive than (118), (114), etc.; also (204) is more intensive than (220). The $(O + N)$-ions, therefore, must be situated nearer to the planes (010) and (100) than to (110); perhaps the line joining the ions O'' and N''' most probably has the direction of the a-axis, as also follows from a model in which these ions are represented by contiguous spheres of the appropriate diameters.

As a proof to what extent the intensities calculated in this way in general agree with those observed, the calculated and observed values for a number of planes are graphically plotted in Fig. 5 against the sixfold glancing angle $6 \cdot \theta$.

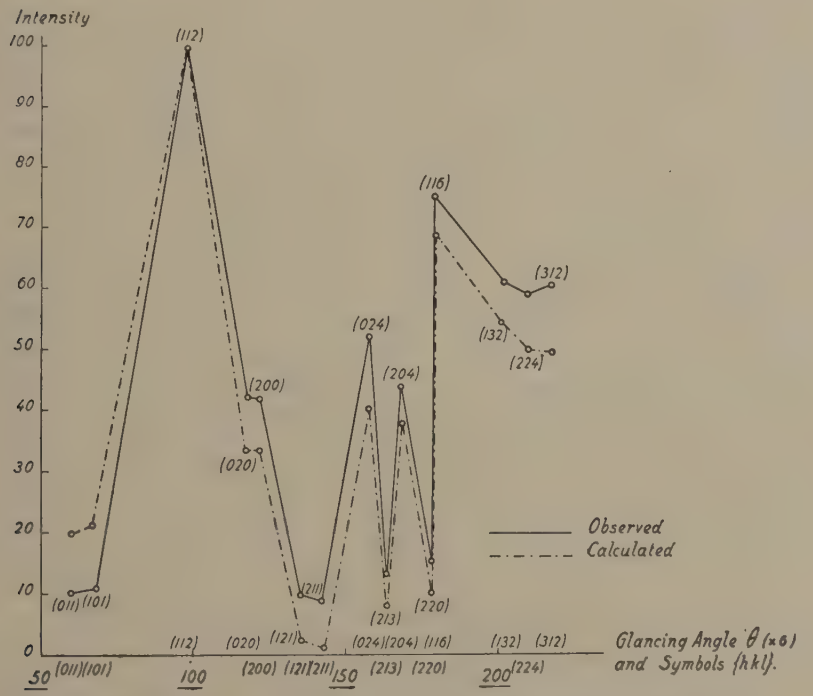

Fig. 5. Observed and calculated Intensities ($h\,k\,l$) of Rubidium—Osmiamate.

The agreement, as expressed by the complete parallelism of the change in intensities of the subsequent planes, is really most satisfactory; so that there can be no doubt about the principal correctness of the structure adopted. That of the (NH_4)-salt and the Tl-salt are only slightly different from the structure mentioned, as is revealed by the very close analogy of their powder spectrograms with that of the Rb-salt.

In the next paper the structure of the more deviating *Cesium-Osmiamate* will be discussed and a comparison of the structures of all the *alkali-osmiamates* finally will be made.

Groningen, Laboratory for Inorganic and Physical Chemistry of the University.

Chemistry. — *Der Einfluss des Dispersitätsgrades auf physikalisch-chemische Konstanten.* (Zweite Mitteilung.) Von ERNST COHEN und C. THÖNNESSEN.

(Communicated at the meeting of June 25, 1932).

1. In einer kürzlich veröffentlichten Mitteilung [1]) konnten wir u.a. zeigen, dass sich Salizylsäure in so feindisperser Form herstellen lässt, dass dieselbe bei 25° C. eine bis zu etwa 15 % höhere Löslichkeit als die normale besitzt. Zu dieser feindispersen Form gelangten wir auf zwei Wegen, nämlich:

a) durch Abschrecken heiss gesättigter Salizylsäurelösungen;

b) durch Schütteln der grobkristallinen Säure mit Goldkugeln in Gegenwart von Wasser.

In dieser ersten Mitteilung hatten wir bereits die Vermutung geäussert, dass für das von uns beobachtete Verhalten der Salizylsäure deren geringe Kristallisationsgeschwindigkeit oder wohl besser, deren geringe „Sammelkristallisationsgeschwindigkeit" [2]) verantwortlich gemacht werden muss. Es handelt sich nämlich darum, dass sehr kleine Kristalle in Lösung gehen und eine in Bezug auf die grossen Kristalle bei der herrschenden Temperatur übersättigte Lösung bilden. Die grossen Kristalle wachsen also infolgedessen auf Kosten der kleinen. Nun ist aber die Geschwindigkeit der Sammelkristallisation eine Funktion der Temperatur. In vorliegender Arbeit konnten wir einen solchen Einfluss der Temperatur dadurch nachweisen, dass wir die Versuche auf verschiedene Temperaturen ausdehnten.

2. Da wir zu Vergleichszwecken die Löslichkeitskurve der Salizylsäure benötigten und die in der Literatur von verschiedenen Autoren angegebenen Löslichkeitsdaten z.T. stark differieren [3]), musste die Löslichkeit der Säure bei verschiedenen Temperaturen sorgfältig neu bestimmt werden. Bei jeder Temperatur wurden stets mehrere Versuche ausgeführt in der Weise, wie sie bereits in der Abhandlung von ERNST COHEN und H. GOEDHART [3]) beschrieben wurde. Die zu sämtlichen Bestimmungen ver-

---

[1]) Proc. Acad. Sci. Amsterdam **35**, 441 (1932).

[2]) Vergl. ERWIN SAUTER, Heterogene Katalyse, Bd. **23** der Wissenschaftlichen Forschungsberichte, STEINKOPF, Dresden und Leipzig 1930, Seite 20.

[3]) Proc. Acad. Sci. Amsterdam, **34**, 1 (1931).

wendete Säure war ein Präparat USINES DU RHÔNE [1]), welches vorher durch 48-stündiges Schütteln mit Wasser bei etwa 50° C. stabilisiert worden war.

Mit grösster Sorgfalt achteten wir besonders darauf, dass unsere Lösungsgleichgewichte stets von *beiden* Seiten her erreicht wurden. Um insbesondere sicher zu sein, dass die untersuchten Gleichgewichte sich, wenn so gewünscht, auch wirklich von der übersättigten Seite her eingestellt hatten, verfuhren wir folgendermassen: Die stabilisierte Säure wurde mit Wasser 24 Stunden bei der betreffenden Temperatur im Thermostaten geschüttelt. Dann brachten wir die Schüttelflaschen in ein Bad, dessen Temperatur etwa 10° C. höher war als diejenige des Thermostaten. Unter häufigem Schütteln blieben die Flaschen darin etwa 40 Minuten. Erst dann brachten wir sie in den Thermostaten zurück und schüttelten bis zur endgültigen Konzentrationsbestimmung stets noch zwei Stunden. Ferner möchten wir noch erwähnen, dass die bei 75° C. ausgeführten Bestimmungen es erforderlich machten, dass bei der Probeentnahme aus der Schüttelflasche die gesamte Entnahmevorrichtung in das Wasser des Thermostaten untergetaucht wurde. Auf diese Weise vermieden wir, dass die Salizylsäure vorzeitig auskristallisierte, wozu sie wegen des grossen Temperaturkoeffizienten ihrer Löslichkeit in diesem Temperaturgebiet sehr neigt. In Tabelle 1 sind die Resultate unserer Bestimmungen zusammengefasst. Die angekreuzten Werte erhielten wir von der übersättigten Seite her.

Die in der letzten Kolumne angegebenen Werte stammen von WALKER und WOOD [2]). Unsere Zahlen weichen z.T. erheblich von denjenigen dieser Autoren ab. Vermutlich sind die Ursachen hierfür einerseits zu suchen in einem Einfluss des Dispersitätsgrades, der sich, wie wir in unserer 1. Abhandlung zeigen konnten, bei Salizylsäure stark bemerkbar machen kann. Andererseits erscheint uns der von WALKER und WOOD eingeschlagene Weg um bei höheren Temperaturen zu gesättigten Lösungen zu gelangen, höchst unsicher. Sie sagen hierüber: "The solutions were usually agitated by means of stirrers driven by a small turbine, but at the higher temperature this was sometimes found to be unnecessary, equilibrium being reached very rapidly with only occasional agitation by hand." Bekanntlich führt dieses Verfahren aber häufig zu falschen Ergebnissen.

3. Man kann sich über den Mechanismus unserer in der ersten Abhandlung beschriebenen Schüttelversuche mit Goldkugeln folgendes Bild machen: Die groben Salizylsäurekristalle werden durch die Goldkugeln zu immer feineren Kristallen zerrieben. Es stellt sich eine, der jeweiligen Kristallgrösse entsprechende, Konzentration ein. Diese höhere Konzentration geht aber wieder auf den normalen Wert zurück, wenn man das Schütteln ohne Goldkugeln fortsetzt; denn die kleinen Kristalle wachsen wieder zu grossen (Sammelkristallisation). So erklären sich unsere früheren

[1]) Proc. Acad. Sci. Amsterdam, **35**, 441 (1932), speziell § 1.
[2]) J. CHEM. Soc. **73** (II), 619 (1898).

TABELLE 1. Schütteldauer 2 Stunden.

Versuchsnummer	Temperatur	Löslichkeit	Löslichkeit n. WALKER u. WOOD
1a	0.0° C.	0.089^{7}	
3a	„	0.089^{9}	
11a	„	0.089^{9} *	
12a	„	0.089^{8} *	
		Mittel 0.089^{8}	0.092
140a	25.0° C.	0.222^{2}	
141a	„	0.221^{9}	
143a	„	0.222^{0} *	
159a	„	0.221^{2} *	
		Mittel 0.221^{7}	0.224
11	40.0° C.	0.392^{8}	
12	„	0.393^{0}	
13	„	0.392^{7} *	
14	„	0.392^{6} *	
		Mittel 0.392^{8}	0.377
15	50.0° C.	0.576^{5}	
16	„	0.577^{5}	
19	„	0.576^{9} *	
20	„	0.577^{7} *	
		Mittel 0.577^{2}	0.540
21	75.0° C.	1.67^{4}	
22	„	1.67^{2}	
25	„	1.67^{0} *	
26	„	1.67^{8} *	
		Mittel 1.67^{3}	1.76

Versuche, bei welchen wir die Salizylsäure durch Schütteln mit Wasser bei 50° C. stabilisieren konnten. Beim Schütteln mit Goldkugeln aber bestimmt die Geschwindigkeit der Sammelkristallisation einerseits und die Intensität des Schüttelns andererseits die durchschnittliche Kristallgrösse und damit die beobachtete Löslichkeit bei konstanter Temperatur. Die normale Löslichkeit bei gegebener Temperatur sei c_1, und die Löslichkeit, die sich beim Schütteln mit Goldkugeln bei derselben Temperatur ergibt, sei c_2. Dann wird die relative Erhöhung der Löslichkeit $\frac{c_2 - c_1}{c_1}$ zunehmen mit der Schüttelintensität und abnehmen mit zunehmender Geschwindigkeit der Sammelkristallisation. Die Schüttelintensität hängt von verschiedenen Faktoren ab, vor allem von der Schüttelgeschwindigkeit, der Anzahl und Grösse der Goldkugeln, der Form des Schüttelgefässes und der Menge der als Bodenkörper vorhandenen Salizylsäure. Alle diese Faktoren lassen sich jedoch angenähert konstant halten, und in diesem Falle ist der Ausdruck $\frac{c_2 - c_1}{c_1}$ nur noch von der Geschwindigkeit der Sammelkristallisation abhängig. Da letztere aber eine Funktion der Temperatur ist und zwar derart, dass sie mit steigender Temperatur zunimmt, kann man erwarten, dass die relative Löslichkeitserhöhung $\frac{c_2 - c_1}{c_1}$ mit steigender Temperatur immer kleiner wird und eventuell ganz verschwindet. M.a.W. wenn man Löslichkeitsbestimmungen der Salizylsäure in Gegenwart von Goldkugeln durch Schütteln bei verschiedenen Temperaturen ausführt und dafür sorgt, dass die Schüttelbedingungen bei allen Temperaturen die gleichen sind, muss der durch den Dispersitätsgrad bedingte Löslichkeitsunterschied gegenüber den normalen Löslichkeiten mit steigender Temperatur abnehmen und eventuell sogar ganz verschwinden. Und dies wäre eine Folge der mit steigender Temperatur zunehmenden Sammelkristallisationsgeschwindigkeit der Salizylsäure.

4. Um die Richtigkeit dieser Ueberlegungen zu prüfen haben wir folgende Versuche angestellt. In zwei dickwandige Schüttelflaschen von etwa 150 ccm Inhalt gaben wir je 320 Goldkugeln. In die erste Flasche füllten wir 4 *g* und in die zweite 6 *g* stabilisierte Salizylsäure ein. Hierauf wurden die Flaschen mit Wasser aufgefüllt und im Thermostaten geschüttelt. Der Motor machte etwa 60 Umdrehungen pro Minute. Nach 48 Stunden entnahmen wir den Flaschen in üblicher Weise eine Probe und bestimmten die Konzentration der Lösung an Salizylsäure in der in unserer ersten Abhandlung beschriebenen Art und Weise. Diese Versuche führten wir stets in gleicher Weise bei verschiedenen Temperaturen aus. Die Resultate sind in Tabelle 2 zusammengefasst. Zum Vergleich sind auch die mittleren Werte der normalen Löslichkeiten bei den betreffenden Temperaturen noch einmal angegeben. Die Zahlen hinter dem Buchstaben *a* beziehen sich auf die

Versuche mit 4*g* Bodenkörper, diejenigen hinter *b* auf solche mit 6 *g* Bodenkörper.

Zunächst zeigt sich deutlich beim Vergleich der *a*- und *b*-Werte, dass die Bodenkörpermenge einen (allerdings geringen) Einfluss übt.

Die Tabelle 2 bestätigt ferner die in § 3 angestellten Ueberlegungen, denn die Unterschiede der Löslichkeit werden mit steigender Temperatur immer kleiner und schliesslich bei etwa 75° C. praktisch gleich Null.

TABELLE 2.

Versuchs-nummer	Temperatur in C°	Löslichkeit nach 48-stünd. Schütteln mit Goldkugeln	Normale Löslichk.	Mittel von $\frac{c_2-c_1}{c_1} \cdot 100$
3	0.0	a) 0.101^5	0.089^8	13.8
4	„	b) 0.103^0		
7	25.0	a) 0.236^2	0.221^7	7.4
8	„	b) 0.240^3		
9	40.0	a) 0.404^7	0.392^8	3.2
10	„	b) 0.407^3		
17	50.0	a) 0.590^3	0.577^2	2.5
18	„	b) 0.593^0		
23	75.0	a) 1.68^3	0.67^8	0.6
24	„	b) 1.69^5		

Zusammenfassung.

Es wurde nachgewiesen, dass die durch den verschiedenen Dispersitätsgrad verursachten Löslichkeitsunterschiede bei der Salizylsäure mit steigender Temperatur abnehmen und schliesslich praktisch ganz verschwinden. Diese Erscheinung liess sich erklären durch die Zunahme der Geschwindigkeit der Sammelkristallisation mit zunehmender Temperatur. Ausserdem stellte sich heraus, dass die von WALKER und WOOD ermittelte Löslichkeitskurve der Salizylsäure mit Fehlern behaftet ist.

VAN 'T HOFF-*Laboratorium.*

Utrecht, im Mai 1932.

Plantkunde. — *Temperatuur en Strekkingsperiode van de Narcis.* (Eerste stuk). Door A. H. Blaauw, Annie M. Hartsema en Ebeline Huisman. (Meded. N°. 35 van het Laboratorium voor Plantenphysiologisch Onderzoek te Wageningen).

(Communicated at the meeting of June 25, 1932).

In vroegere jaren is de periodieke ontwikkeling van Hyacinth en Tulp (naast die van andere gewassen) door ons onderzocht en vervolgens de invloed van de temperatuur in verschillende perioden van die ontwikkeling. Een grondige kennis daarvan is van het meeste belang voor een geheel rationeel doorgevoerde cultuur. Het onderzoek naar de ontwikkeling van de Narcis, waarvoor het materiaal in 1920 en in 1927 reeds verzameld was, is thans bewerkt en zal over eenigen tijd verschijnen.

Op grond van hetgeen ons tijdens dat onderzoek in den zomer van 1931 was bekend geworden, werd een uitgebreide proef over den invloed van de temperatuur in hetzelfde jaar opgezet. Wij publiceeren hieronder een eerste mededeeling over het verband van temperatuur en strekkingsperiode.

Allereerst moeten wij wijzen op een belangrijk verschil met Hyacinth en Tulp. Als het loof van de Narcis op het veld afsterft, zijn alle deelen van de bloem reeds aangelegd; bij Hyacinth en Tulp wordt bijna steeds de bloem pas *na* het rooien gevormd, zoodat men daar den bloemaanleg in zelf-gekozen temperaturen kan doen verloopen. Deze eerste proeven werden uitgevoerd met „niet-geprepareerde" bollen. Onder „prepareeren" verstaan wij hier, dat de *aanleg* van de bloem vervroegd wordt, hetzij dit geschiedt door verwarmen van den bodem (kascultuur of warmwaterbuizen in het veld volgens methode Nyssen); hetzij door de bollen een jaar te planten in een warmer klimaat (Zuid-Fransche cultuur); hetzij door enkele weken vroeger dan normaal te rooien en de bollen bij 30° tot 25° C. te leggen (Hyacinthen volgens methode Dames). Wij kunnen van niet-geprepareerde bollen spreken, als de planten in ons klimaat op het open en niet kunstmatig verwarmde veld op den normalen tijd — d.i. na het afsterven van het loof — zijn gerooid.

Dit is dus het geval met de Narcissen, die wij voor de hier beschreven proeven gebruikten. Terwijl de bloem van de Narcis veel vroeger wordt aangelegd dan van Hyacinth en Tulp, blijft bovendien het loof in het algemeen langer groen, zoodat pas later gerooid wordt. Bij de niet-geprepareerde Narcis kan men dus niet — zooals wij dit voor Hyacinth en Tulp hebben onderzocht — de bloemvorming bij een optimale temperatuur zoo snel mogelijk doen plaats vinden. Daarvoor zou men òf tijdig den grond moeten verwarmen òf zeer vervroegd de bollen moeten rooien.

De Narcis was in de cultuur veel moeilijker dan Hyacinth en Tulp met Kerstmis in bloei te trekken. Dit kan ons te meer verwonderen omdat begin Juli, dus ook als men extra vroeg rooit, de bloemdeelen vrijwel geheel zijn aangelegd, in een stadium dus verkeeren, waarbij men Hyacinth en Tulp reeds naar de koele optimale temperatuur kan brengen. Daar een zoo lage temperatuur als 9° C., die voor de optimale strekking van de Tulp van zooveel belang is, voor den kweeker zonder koelinstallatie meestal niet was te verwezenlijken, zal waarschijnlijk daardoor de vroege trek van de Narcis, die juist de voorlijkste dezer drie gewassen is, zoo lang moeilijkheden hebben opgeleverd.

E. M. STRAIGHT (1928) schrijft over forceeren van Narcissen, echter zonder dat wij hieraan eenige botanische grondslag of vastheid kunnen ontleenen. Deze en ook de volgende onderzoekers spreken in hier genoemde en andere proeven herhaaldelijk van „inkuilen" van de bollen vóór het trekken, zoodat men omtrent de temperatuur, die juist dàn zoo bijzonder belangrijk is, in het duister tast, daar grondtemperaturen niet worden vermeld. Die grond, waar men bollen in kistjes ingraaft, zal afhankelijk zijn van het in dien tijd heerschende weer ; vergelijking met temperatuurproeven is niet mogelijk en de praktijk, die alleen in geval van gebrek aan secure middelen van de koele grondtemperatuur moet gebruik maken, ontvangt daardoor niet meer vastheid. In den herfst kan die grondtemperatuur boven 9° liggen, maar bij vroege koude in een ander jaar evenzeer aanzienlijk onder 9° ; bij de Tulp bijv. geeft dat verlating ; maar in het tweede geval. in een koud najaar dus, zal het bovendien den bloei schaden.

D. GRIFFITH (Oct. 1930) houdt zich eveneens bezig met vervroegen van Narcissen, noemt verschillende temperaturen voor het bewaren en trekken maar erkent, dat men nog ver van eenig vast voorschrift is ".....and practices have not yet crystallized into any formula, that can be authoritatively recommended". Bij onderzoekingen, welke directe vruchten voor de praktijk beoogen, mist men herhaaldelijk een preciesen botanischen grondslag, kennis van de ontwikkeling, het verloop van de strekking der organen, gevolgd door de studie van den invloed eener uitgebreide schaal van temperaturen op die processen, — wat dan ten slotte tot verschillende conclusies voor de toepassing zal leiden.

Reeds vermeldt GRIFFITH : "Recent experiments in this country show that bulbs stored at low temperatures force very much more readily than those held under ordinary unrefrigerated temperatures..... ; "that the preferred temperature would lie somewhere between 50° and 60° F. ....." ; — "Those stored at 45° to 50° were still earlier, but there was a decided dwarfing of both flowers and plants."

J. J. BEYER en E. VAN SLOGTEREN (14 Aug. 1931) beschrijven hun in 1930 genomen proeven over vroegen bloei, waarbij zij uitstekende uitkomsten krijgen (voorloopig nog met door warenhuiscultuur geprepareerde bollen) door toepassing van 9° C., die zij vergelijken met 13° en 17° C. Deze lage temperatuur, die ook voor het doen strekken van de Tulp thans

zooveel wordt toegepast, wordt eerst van 1 Juli tot 17 Sept. gegeven; dan worden de bollen geplant, ten deele bij 9° blijvend, wat het beste en vroegste resultaat geeft. Alle andere proeven worden daarna „buiten opgekuild", zoodat men daaraan geen vergelijking kan vastknoopen (zie hierboven). Ook in een volgend jaar (1931) werden met de lage temperatuur van 9° door de onderzoekers bij verschillende soorten Narcissen goede resultaten voor Kerstmis verkregen.

Ook voor deze vragen over de cultuur van de Narcis was een botanisch onderzoek en beschrijving van de ontwikkeling en van de strekking in verschillende temperaturen zeer gewenscht.

Einde Juli werden voor ons onderzoek de bollen ontvangen van *Narcissus Pseudonarcissus* var. *King Alfred*. De samenstelling van den hoofdknop, die de bloem bevat, is dan op den tijd van het rooien als volgt. Van buiten naar binnen gaande vindt men eerst de *scheedebladen*, meestal 3, dikwijls ook 2 of 4 (bijv.: 64 × 2, — 114 × 3, — 78 × 4) uiterst zelden een 5e. Daarop volgen 3 of 4 *loofbladen* (170 × 3 en 89 × 4). Daarbinnen ligt de bloem omhuld door de spatha, terwijl het basale deel onder de spatha de bloemstengel wordt. De bloem heeft alle deelen gevormd; ook de bijkroon, die in het algemeen laat ontstaat, is in aanleg soms ten deele, maar meestal geheel gereed. De bloemvormende periode is dus na het afsterven van het loof reeds voorbij en alle deelen staan aan het begin van de strekkingsperiode; echter zijn ze nog zoo jong dat niet uitsluitend strekking van voorhanden cellen plaats heeft, maar zeker ook nog celdeelingen plaats vinden.

Op 31 Juli zijn de afmetingen, uit 20 waarnemingen, in mM. gemiddeld aldus:

Scheedebladen				1e Loofblad	Bloem + Stengel	Bloem
1e	2e	3e	4e			
47.8	33.4	22.5	16.6	15.2	9.6	5.3

In dezen jongen toestand zijn de organen van buiten naar binnen gaande afnemend in lengte. Maar de buitenste scheedebladen zijn het eerst uitgegroeid, d.w.z. het 1e bereikt een eindlengte van slechts 6 à 7 cM., het binnenste van 14 à 15 cM. Zoo groeit dus de knop zijn omhullende bladen het een na het ander voorbij, terwijl ook later de bloemstengel de loofbladen in lengte voorbijgroeit. (Zie nader hieronder).

Van 31 Juli af werden bollen in verschillende temperaturen gelegd. Daarvan werden na 4 en na 8 weken telkens 15 bollen gefixeerd om den eersten groei der organen in die verschillende temperaturen te vergelijken.

TABEL 1. Lengte der organen in m.M. na 4 weken (27 Augustus).

In:	5°	9°	11°	13°	15°	17°	20°	25½°
1e Scheedeblad	46.9	48.0	47.4	47.5	46.7	45.2	48.0	50.1
1e Loofblad	19.9	26.1	28.8	28.9	24.8	18.6	17.2	16.3
Bloem + Stengel	11.9	16.5	17.5	19.4	18.4	12.8	11.4	10.0
Bloem	7.5	10.7	11.3	12.4	11.6	8.9	7.5	6.0

Aan het 1e scheedeblad, dat 4 weken tevoren 47.8 mM. was, is geen groei vast te stellen. Het 1e loofblad is in 11° en 13° het meest toegenomen, de bloem in 13°. Opvallend is de traagheid van het proces in 20° en 25½°.

TABEL 2. Lengte der organen in m.M. na 8 weken (24 September).

In:	5°	9°	11°	13°	15°	17°	20°	25½°
1e Scheedeblad	44.0	52.9	51.1	51.6	48.7	45.7	48.3	46.7
1e Loofblad	26.4	40.5	40.1	41.5	37.8	24.3	23.0	16.6
Bloem + Steng l	15.7	26.8	29.5	30.5	29.7	18.7	16.6	10.8
Bloem	10.3	16.7	19.0	19.9	19.9	13.6	11.4	6.3

Het 1e scheedeblad vertoont een geringe toename in 9° tot 13° C. Dat het optimum bij 9° schijnt te liggen heeft weinig waarde, daar het orgaan weldra uitgegroeid is (ruim 6 cM. lengte). Loofbladen en bloem hebben over de geheele 8 weken genomen bij ongeveer 13° C. waarschijnlijk hun optimum, evenals in Tab. 1, het loofblad eer iets naar den lagen kant, de bloem naar den hoogeren kant (13°—15°). Maar het onderscheid is van 9° tot 15° C. over het algemeen zeer gering na 8 weken inwerking.

Dat blijkt vooral, als wij in Tab. 3 de lengtevermeerdering gedurende de laatste 4 weken vergelijken.

TABEL 3. Groei der organen in m.M. in 4 weken (27 Aug.—24 Sept.)

In:	5°	9°	11°	13°	15°	17°	20°	25½°
1e Loofblad	6.5	14.4	11.3	12.4	13.0	5.7	5.8	0.6
Bloem + Stengel	3.8	10.3	12.0	11.1	11.3	5.9	5.2	0.8
Bloem	2.8	6.0	6.8	7.2	8.3	4.7	3.9	0.3

Dat de groei van het loofblad gedurende die 4 weken zoowel in 9° als in 15° een optimum zou vertoonen, de bloem in 15°, het stengelstukje in 11°,

zal waarschijnlijk op toeval berusten van de in 9° tot 15° zoo weinig verschillende cijfers.

De verdere hier te beschrijven proeven betreffen nu alleen de inwerking van 9°, 11°, 13° en 15°, waarin op 18 Sept. elk 20 bollen werden geplant, die dus reeds 7 weken in die temperaturen hadden gelegen. Tab. 2 geeft dus hun toestand 6 dagen na het planten weer.

Bij de nu volgende uitkomsten werden de metingen aan de levende planten verricht; men meet nu verder dus alleen het deel van den knop, dat buiten den bol uitkomt (de „neus"); daarbij kan men rekenen, dat in den bol nog 5 tot 6½ cM. ligt, zoodat dus een dergelijk bedrag bij de nu volgende cijfers geteld moet worden ter vergelijking met Tab. 2 en 1. Bovendien meet men „den knop" en zooals wij beschreven, is aanvankelijk het 1e scheedeblad het langste en geeft dus tevens de knoplengte aan; bij 5 à 6 cM., ongeveer als de knop uit den bol treedt, groeit de knop het 1e scheedeblad voorbij, zoodat dan eenigen tijd het 2e scheedeblad de knoplengte voorstelt. De langste scheedebladen, die ten slotte een eindlengte van gemiddeld 14 à 15 cM. bereiken, worden bij een lengte van 9 à 11 cM. (4 à 5 cM. uit den bol) door de loofbladen gepasseerd, zoodat deze dan de knoplengte aangeven. Treedt de knop te voorschijn dan is het 1e loofblad slechts ± 3 mM. korter dan het langste omsluitende scheedeblad, terwijl dit verschil steeds geringer wordt.

De van 30 Juli af behandelde en op 18 Sept. geplante bollen (20 in elke temperatuur), geven nu verder de volgende uitkomsten:

17 Oct.	9°	11°	13°	15°
	11 zichtbaar (0—5 mM.)	20 zichtbaar 8.5 mM.	19 zichtbaar 6.5 mM.	15 zichtbaar (4.2 mM.)
	9 niet zichtbaar			5 niet zichtbaar

Als optimale temperatuur, over het geheele tijdvak 30 Juli—17 Oct. gerekend, komt hier 11° te voorschijn, vervolgens 13°. Het optimum, dat te voren over het algemeen bij 13° lag, verschuift iets naar beneden. Dit is dus geconstateerd aan bollen, die 18 Sept. geplant zijn. Aan bollen die *niet-geplant* werden en voor verdere fixaties bestemd waren, kwamen de neuzen pas in den loop van November zeer langzaam te voorschijn. Echter precies in dezelfde volgorde als bij de geplante: het voorlijkst 11°, dan 13°, dan 9°. Dit is dus 1°. een bevestiging dat over het geheele tijdvak genomen *gemiddeld* 11° optimaal is, 2°. een bewijs van den invloed van den planttijd, d.w.z. dus van de tijdige beworteling op het uitloopen van den knop, waarop wij in een volgend stuk terugkomen.

	9°		11°		13°		15°	
24 Oct.	4.4	3.4	11.9	5.5	9.7	4.7	8.6	3.8
31 Oct.	7.8	5.3	17.4	5.9	14.4	5.7	12.4	4.8
7 Nov.	13.1	6.3	23.3	6.1	20.1	4.3	17.2	4.4
14 Nov.	19.4		29.4		24.4		21.6	

Een zeer gelijkmatig langzaam voortschrijden in alle vier temperaturen. waarbij 11° steeds de voorste blijft, maar waarbij in 9° de groeisnelheid het meest toeneemt en in de laatste week die van 11° evenaart (vooral relatief ten opzichte van de geheele knoplengte). Bevestigd wordt hier dus, dat het optimum zich iets naar beneden verplaatst.

Thans wordt 11° naar 17° C. overgebracht, daar ± 3 cM. bereikt is.

	9°		11°+17°		13°		15°	
21 Nov.	25.2	5.8	33.3	3.9	30.1	5.7	24.8	3.2

Een week later dan 11° heeft ook 13° de 3 cM. bereikt en gaat naar 17°. De overgang van 11° naar 17° heeft, tegen de verwachting, een kleine groeivertraging gegeven in plaats van een versnelling, althans in de eerste week. De groeisnelheid in 15° blijft iets afnemen.

	9°		11°+17°		13°+17°		15°	
28 Nov.	31.4	6.2	40.8	7.5	31.4	1.3!	27.5	2.7

Met 9° wordt thans ook 15° naar 17° gebracht.

	9°+17°		11°+17°		13°+17°		15°+17°	
5 Dec.	**60.8**	29.4!	49.0	8.2	35.0	3.6	30.3	2.8

In de eerste week na overbrenging in 17° vertoonde 11° een kleine vertraging van den groei, terwijl in de 2e week de groeisnelheid zich weer herstelde; en nu is het opvallend dat 13° in de 1e week in 17° een nog veel sterker groeivertraging vertoont (21 Nov.—28 Nov.), die ook in de 2e week nog zeer merkbaar is.

Maar *totaal anders gedraagt zich 9°*. Hier treedt — na het gedrag van 11° geheel onverwacht — direct na overbrenging in 17° in de eerste week een buitengewoon sterke groei op.

Er ligt dus *tusschen 9° en 11° voor deze soort Narcis een scherpe scheiding*. Want als de neus 3 cM. is (loofblaadjes nog omhuld door een deel der scheedeblaadjes), dan verkeeren toch *die, welke in 9° C. stonden, in een geheel anderen toestand (chemisch-physiologisch) dan die uit 11° en hooger komen*. De bollen uit 9° C. zijn dan in 17° (of hooger) direct tot sterken groei te brengen; d.w.z. bij deze bollen is de *optimale temperatuur voor de strekking bij 3 cM. neuslengte reeds zeer sterk naar boven verschoven*. De bollen uit 11° ondervinden bij dezelfde grootte der organen in de eerste week zelfs vertraging van 17°; die uit 13° zeer sterk, ook nog in de 2e week.

Bij 9° + 17° zijn de loofbladen overal door de scheedebladen gebroken: in 11° + 17° bij de meesten; dit gebeurt meestal als de spruit 4 à 5 cM. uit den bol steekt. Bij 6 cM. gaat nu 9° + 17° naar 20° in licht.

Op 8 Dec. is 11° + 17° ..... 57.2 mM. en op 10 Dec. 64.3 mM. en gaat nu in 20° C. in licht.

	9°+17°+20°		11°+17°+20°		13°+17°		15°+17°	
12 Dec.	134.6 [1])	73.8	67.8	18.8	42.0	7 0	36.0	5.7
19 Dec.	259.4 [2])		104.7 [3])		42.9		38.4	
22 Dec.	**begin bloei**		—		—		—	
28 Dec.	—		—		52.6		43.6	
2 Jan.	—		**begin bloei**		**60.6**		47.1	
	Die uit 13° + 17° gaan thans naar 20° C.							
9 Jan.							51.7	
23 Jan.							59.4	
26 Jan.	Die uit 15° + 17° thans naar 20° C.						**60.0**	
30 Jan.					**begin bloei**			
14 Maart							**begin bloei**	

Hieraan moet nog worden toegevoegd, dat:
in 9° + 17° + 20° de laatste van 20 bollen 4 Jan. bloeide,
in 11° + 17° + 20° de laatste twee op 10 en 26 Febr.,
in 13° + 17° + 20° de laatste pas 21 Maart, terwijl 1 verdroogt,
in 15° + 17° + 20° de laatste van slechts 9 bloeiers op 5 April bloeit, terwijl 11 bloemen verdrogen.

Het in bloei raken gaat dus ook trager na behandeling boven 9°, en van 13° af beginnen bloemen te mislukken.

Samenvatting.

Uit de bovenstaande gegevens ziet men kort samengevat het volgende:

1°. Voor het bereiken van een knoplengte van 3 cM. is bij behandeling sinds 30 Juli met 11°—13°—9° en 15° de verhouding der *groeitijden* ongeveer gelijk 107 : 114 : 120 : 128 (aantal dagen) en dus de verhouding der *gemiddelde groeisnelheden* over dit geheele tijdvak omgekeerd evenredig hiermee.

2°. Worden deze aldus behandelde bollen nu in 17° gebracht, dan blijkt hun chemisch zeer verschillende dispositie, want voor het groeien van 3 cM. tot 6 cM. in 17° is de verhouding der groeitijden, als *nawerking* van 9°—11°—13°—15°, gelijk 8 : 25 : 42 : 66, — de groeisnelheid dus weer omgekeerd evenredig.

3°. Om tenslotte in 20° van 6 cM. in bloei te geraken is de verhouding der groeitijden (in aantal groeidagen) gelijk 17 : 24 : 28 : 48. Daaruit volgt nu, dat de nawerking tot den bloei toe voortduurt, maar tevens dat zij in den eersten tijd het sterkst aan den dag treedt.

---

[1]) Stengel met bloemknop 104 mM.
[2]) „ „ „ 296 mM.
[3]) „ „ „ 76 mM.

4°. Het optimum van de lengtetoename der organen werd aanvankelijk bij ± 13° C. gevonden, tenslotte bij het zichtbaar worden der knoppen is het tot ± 11° C. verschoven, terwijl bij een lengte van 2—3 cM. buiten den bol de groeisnelheid in 11° en 9° nagenoeg dezelfde is. Toch blijkt 9° vergeleken met 11° en hooger, verreweg de optimale temperatuur voor den groei, als men op de *nawerking* let. Wat moet men nu de optimale temperatuur noemen? Het schijnt ons noodig hier een onderscheiding te maken. In het eerste geval stellen wij voor te spreken van het *„directe optimum"*, d.i. dus het gewone optimum in den gebruikelijken zin, n.l. de temperatuur waarin een bepaalde functie gedurende een zeker tijdvak, waarin die temperatuur werkt, het snelst verloopt. Op zichzelf kan dat directe optimum, als men een eenigszins lange periode onderzoekt, bovendien een *verschuivend optimum* blijken te zijn, zooals wij thans bij de Narcis, en evenzeer vroeger bij Hyacinth (1924) en Tulp (1925) hebben gevonden. Wij zien n.l., dat in den eersten tijd, als de organen nog zeer klein zijn, het directe optimum der lengtetoename in de eerste maanden langzaam een weinig naar beneden verschuift, in de laatste weken tijdens de groote strekking zich vrij snel naar boven verplaatst. Waar dit vermoedelijk aan ligt, daarop hebben wij reeds vroeger bij de Hyacinth gewezen (Liter. 1924). Naast dit „directe optimum" willen wij het *indirecte optimum* onderscheiden. Onder een indirect-optimale temperatuur, verstaan wij die temperatuur, welke later door haar nawerking een zeker proces het snelst doet verloopen. Wij moeten ons daarbij wel indenken, dat die z.g. „nawerking" juist aan een of andere vóór-arbeid, voorbereiding te danken is, welke in die temperatuur beter verliep, dan in de eerst geconstateerde direct-optimale temperaturen. Zoo blijkt dus bij de Narcis het directe optimum langen tijd bij 13° tot 11° te liggen, maar het indirecte optimum voor den groei ligt in dien zelfden tijd bij 9° of lager, zooals de nawerking duidelijk doet zien.

Wageningen, Mei 1932.

LITERATUUR.

STRAIGHT. E. M. 1928. Some flowering bulbs. Dep. of Agric. Dom. of Canada Bull. No. 95.

GRIFFITH. D. 1930. Daffodils. U. S. Departm. of Agric. Circular No. 122.

BEYER. J. J. en E. VAN SLOGTEREN 1931. Labor. v. Bloemb. Ond. No. 42. Weekbl. v. Bloemb. cult. 14 Aug. 1931;
zie ook Weekbl. v. Bloemb. cult. 18 Dec. 1931.

BLAAUW. A. H. (1924) The results of the temper. during flower-formation for the whole Hyacinth. Verh. Kon. Ak. v. Wet. 2e Sectie Dl. XXIII, Amst. Bl. 59.

LUYTEN. I., JOUSTRA G. a. BLAAUW. A. H. (1925) De gevolgen v. d. temperatuurbehand. in den zomer voor de Darwin-Tulp (2e stuk). Versl. Kon. Ak. v. Wet. Amst. Dl. XXXIV (= Proceedings Vol. XXIX).

SUMMARY.

Temperature and Stretching-period of the Narcissus (1st part).

The annual development of Hyacinth and Tulip was previously ascertained, next the influence was studied on the flower-forming period

and on the stretching. By means of experiments continued for years together, that treatment was derived from these which is optimal for flower formation and stretching and accordingly brings the bulbs, lifted in July, into bloom in the shortest period. This is a process taking up months, in which the bulbs must be exposed to a series of different temperatures and from which it appears that flower formation and stretching have very different optima. In the stretching-period cell-increase and cell-stretching first act their part side by side, the former in a decreasing, the latter in an increasing measure — two processes with their own requirements. But moreover it appears afterwards in the after effect that a prolonged low temperature (13° and 9°) — probably on account of necessary chemical conversions — is needed in order to enable the great stretching take place rapidly in the last weeks with a much higher optimum.

When the *Narcissus* is lifted, the flower has been, contrary to that of Hyacinth and Tulip, already entirely formed, so that only the influence on the period of stretching can be studied.

The experiments with non-prepared bulbs (i.e. bulbs cultivated in the unheated open field and not lifted extra early either) were commenced on July 31st among others in 5°—9°—11°—13°—15°—17°—20°—25½°. After 4 and 8 weeks 15 individuals were examined; the organs (see Tables 1 and 2) are still growing very slowly, most rapidly at 9° to 15°; as a rule an initial temperature of about 13° is optimal for foliage-leaves and inflorescence; after 8 weeks some shifting of the optimum to 11° seems already perceptible. Next the bulbs are planted in the middle of September and the experiments only continued with 9°—11°—13° and 15°. In the middle of October when the buds ('noses') appear, it is evident that 11° is most forward, then 13°, next 9°; the differences are not great between 9° to 15°, on the other hand the slowness upwards of 20° is striking. When the top of the bud is visible outside the bulb for a few cms. the rate of growth in 9° and 11° is pretty equal. At 3 cms' length each group is transferred to 17° (greenhouse), so first 11°, a week later 13°. In doing so we notice that 11° is slightly retarded by that higher temperature during the first week; next continues growing as in 11°; that 13° undergoes this retardation still in a greater measure (see 7 Nov.—5 Dec.). When, however, 9° 2 weeks later than 11° has reached a length of 3 cms and is transferred to 17°, a very different phenomenon occurs: a *strong growth* sets in directly, so that 9°/17° overtops the other within a week. The growth from 3 to 6 cms in 17° after a treatment with 9°—11°—13°—15° lasts respectively 8—25—42 and 66 days: At a length of 6 cms from the bulb, the plants are transferred to 20° C (greenhouse in full light); in this temperature 9°—17°—20° flowers from Dec. 22nd; 11°—17°—20° from Jan. 2nd; 13° begins on Jan. 30th, one of 20 flowers shrivels up; 15° not until March 14th, only 9 from the 20 bulbs flowering.

What is now the optimum temperature for the stretching? We will distinguish an *'indirect optimum'* contrasted with the *'direct optimum'*: This

latter is the normal optimum in the usual sense, viz. that temperature in which a process during the time that temperature is acting, proceeds most rapidly. Such an optimum, which therefore for the Narcissus lies at about 13° C, may also be a *'shifting optimum'*; this direct optimum falls gradually to 11° and 9° C; in Hyacinth and Tulip we also found this very slow fall for the growth of the still small organs.

But the *'indirect optimum'* appears in the *after effect*, as a result of a preceding action and is after all the best condition for the optimal stretching, because after this indirect optimum the great stretching can proceed rapidly at a certain point of time in a much higher optimum. This indirect optimum lies in Tulip and Narcissus at 9° or lower.

Histology. — *Some remarks on the efferent innervation of the bloodvessels.* By Prof. J. BOEKE.

(Communicated at the meeting of June 25, 1932).

There is still a curious discrepancy between the physiological certainty, that there exists a very elaborate efferent vasomotor influence, dilatator and constrictor, upon the smooth muscle fibers of the wall of the bloodvessels, and the histologists evidence of the morphological basis of this efferent nervous influence. We know, that the innervation of the bloodvessels is effected by the cranial nerves, the spinal nerves and the sympathetic, and that especially the sensory innervation depends largely upon the spinal and cranial nerves. But even concerning the nerves of the adventitia, which are almost certainly of a sensory nature, we are unable to state, which nervous elements are of spinal or cranial origin and which are of sympathetic origin. And it appears, as STOEHR (1932) says, very doubtful whether nerve bundles which course within the vascular adventitia and which have in general received a uniform description, represent in their entirety vasomotor nerves. Not only there are frequently nerves which utilize the adventitia of the bloodvessels, chiefly the smaller arteries, over a certain distance and then re-enter the connective tissue around the vessels and pass out to supply the glands or the smooth muscle fibers of the neighbourhood, but in general we must agree with STOEHR, when he says, that the whole peripheral vascular apparatus, especially at the level of the smaller arteries, forms with the rest of the nervous tissue of an individual organ an indivisible whole.

When we study the pictures of vascular innervation published by the authors, by far the greater part of them give drawings of the apparently

sensory innervation of the adventitia, the nerve fibers simply accompanying the vessels or the capillaries, encircling them and often remaining in a distance of the real vascular wall, without the slightest evidence that they may have an efferent motor function, or any connections with the smooth muscle fibers of the tunica media of the vessel itself.

As a very clear description of what is known about the vasomotor nerves is given by STOEHR (1932), I may perhaps quote this description as a general introduction. As regards (l.c. p. 384) the final disposition of nerves in the wall of medium-sized and larger arteries, we meet first a superficial, mesh-like network in the adventitia. This consists of a number of nerve bundles which travel mostly with the longitudinal axis of the bloodvessel and which are connected with each other. One may here also recognize individual nerve fibers which have branched off from the bundles.

Beneath this external nervous network is to be found a second formation which borders on the media and arises from the branches of the external superficial nerve plexuses. This second network, which lies directly on the media, is characterized by a tremendous number of very fine nervous fibrils, which eventually cross and recross each other in an indiscriminate manner and show numerous loops, bends and small varicose swellings. Occasionally a deeper plexus may appear composed of more regular terminal branches; fine nerve fibrils thus enter into connections at regular distances and in definite directions. In this manner a somewhat more orderly network is produced. Such a finding has been described by DOGIEL and by LEONTOWITSCH as well as by others.

It might be expected that the nerves in the muscular tunic, as the most probable organ of function, should be present in largest numbers and terminate finally in, or be attached to, smooth muscle cells. Curiously enough I (STOEHR) have been unable after studying hundreds of specimens to demonstrate any sign of nerve fibers within the muscular coat itself. This agrees with the results of most authors... Consequently we must say that nerve fibers occur within the media either not at all or very rarely, or, finally, are non-demonstrable by our present methods, an objection which always has to be entertained."

So far the description by STOEHR, which states the difficulties in an admirable way. I could add, that the same difficulties arise everywhere when we study the sympathetic innervation, and that we know still very little about it in every direction. Positive observations in this field are very scarce and have met everywhere with scepticism and doubt; what do we know really about the apparatus of TIMOFIEFF encircling the sensory corpuscles, or about so many nervous apparatus of sympathetic origin? And even this description quoted above leaves us still for a great deal in the dark. For in the first place we must not forget, that one author, who studies the question by means of methylene blue colouring or the Golgi-method, is forming his opinion on thick sections studied under a low power, while another investigator, who uses the silver-

impregnation methods, makes thin sections and studies them with the highest magnification possible. So, what one author calls a very dense network, another author merely regards as a rather coarse network with large meshes. It seems to me, that in such questions, which involve a study of the finest connections of the neurofibrillar strands with the contractile elements, the smooth muscle cells, it is only the investigation of very thin sections under the highest magnifying power available, which enables us to answer the question definitely, and to get a uniformity in the descriptions.

As to the insufficiency of our knowledge of the sympathetic and sympathetic innervation in the second place I could call attention to the descriptions of the socalled "interstitial cells" by LAWRENTJEW and VAN ESVELD. Both these authors found in the intestinal wall besides the usual two types of ganglioncells a much finer plexus, composed of small cells with many processes, which anastomose and thus form a syncytial plexus around the ganglioncells of the plexus of AUERBACH, in the neighbourhood of the bloodvessels, in the mucosa and the submucosa and inside the muscle layers. These syncytial elements, the old "interstitial cells" of CAJAL, LA WILLA, E. MUELLER, etc., form the ends of the terminal sympathetic plexusses; from them, according to LAWRENTJEW, spring the endings on the smooth muscle cells. According to the observations of STOEHR they are of lemmoblastic origin, but we may regard the terminal part of the whole system as a terminal nervous plasmodium, "man kann, physiologisch gedacht, das SCHWANNsche Leitgewebe gemeinsam mit den in seinem Plasma eingebetteten Nervenfäserchen als ein nervöses terminales Plasmodium bezeichnen". (STOEHR, 1930, p. 151). Inside these syncytial elements according to LAWRENTJEW the neurofibrillar strands are running intraprotoplasmatically as finest anastomosing fibrillae, between which are lying the nuclei imbedded in the same protoplasm. Where they are stained in the preparations, these interstitial cells show a much denser distribution than the neurofibrillar strands in the common preparations.

In connection with this it is very important, that LEONTOWITSCH, in a very interesting paper on the ganglion-cells in the arterial wall, which appeared in the year 1930, describes a very dense nervous plexus with intercalated ganglion-cells and nuclei in the wall of the bloodvessels of the mucous membrane of the frogs mouth, stainable with methylene blue after a special method of his own, which is lying "on or in" the muscular tunic, which the author supposes to have a vasoconstrictor and a vasodilatator function (it is divisible into two layers), and which seems to bear a very close resemblance to the network of interstitial elements described by LAWRENTJEW. According to LEONTOWITSCH the plexuses on the arterial wall are connected with each other by an elegant network in the connective tissue of the mucous membrane, which he compares with the diffuse nervous network described years ago by BETHE (1903).

Something akin to this vascular nervous system of LEONTOWITSCH was

described in the year 1926 by WOOLLARD. Here too we see a striking resemblance to the interstitial elements of LAWRENTJEW.

Last not least I would call attention to the almost forgotten perivascular nerve plexus, drawn and described so well by the Italian authors of the beginning of this century, CREVATIN (1899, 1900), CECHERELLI (1904), SALA (1899), SFAMENI (1894, 1900) and RUFFINI (1905). Here we see figured and described an extremely delicate plexus of amyelinitic fibers around the vessels, in the connective tissue, around the sensory corpuscles, so dense and so delicate, that the queston arises in our mind, whether this is always of nervous origin or more of mesenchymatous nature, the more so, because the method used to bring them into view, chloride of gold, is not always entirely elective in its staining, and their observations have not been corroborated by later authors, working with silver methods (here however I have to mention the recent publications by STEFANELLI and O. ROSSI).

So we see from these observations, that there is room for the supposition, that the innervation of the bloodvessels and in general the sympathetic innervation is not so scarce as it is generally assumed.

In the course of the last two years I had the occasion to make a series of observations, which I could confirm later on in the most different preparations made on former occasions for other purposes, observations which showed me that this is really the case, and that there exists a much more elaborate sympathetic innervation than it is described usually.

In the first place I found in a splendidly impregnated series of sections through a human eyeball, presented me by Dr. HALBERTSMA, and very well preserved directly after the enucleation, in the connective tissue of the chorioidea and accompanying the bloodvessels a plexus of very fine amyelinitic nerve fibers, running in small bundles with intercalated nuclei, exactly like the "cable-system" of the terminal interstitial elements of LAWRENTJEW, the nervous plasmodium of STOEHR, through the connective tissue. These bundles, consisting of very delicate varicose nerve fibers, which everywhere anastomose with each other and form a distinct network, spring from the thicker nerve bundles, but they follow an independant course through the connective tissue. Everywhere they follow the blood-vessels, running so close to the endothelium as to seem imbedded in it, the nerve fibrillae often lying in the same plane as the nuclei of the endothelial cells are lying in. Even the capillaries are encircled by them, and besides these vascular bundles we see these bundles running everywhere in the connective tissue. In their general behaviour they look exactly like the pictures CREVATIN and CECHERELLI give of their perivascular plexuses, as will be shown in a more elaborate and better illustrated paper. These structures, after having found them in my recent preparations, I found in exactly the same distribution and abundance in eye-ball preparations, made 20 years ago, only there they were impregnated so faintly, that I had entirely overlooked them at former occasions. They form a most intricate

plexus in the tissue of the chorioidea and in the connective tissue underlying the conjunctiva bulbi.

In the second place I found in the wall of the most different arteries, small arteries, medium-sized and larger arteries (human eye, human glands, parotic and lacrimal, human skin, orbita and tongue of the hedgehog, cat and rabbit) an intricate network of delicate neurofibrillae, which, allthough it is much finer and denser, may be compared with the network, described by STOEHR and LEONTOWITSCH as the second network in the arterial wall. It appears not only as a plexus with neurofibrillar strands crossing and recrossing each other, but as a regular network of extremely delicate neurofibrillae with intercalated nuclei. In the small arteries with only one layer of muscle cells it appears in the form of fig. 1, in the larger arteries with a muscular coat composed of several layers of muscle cells, it is found spread out as a flattened network with broadened meshes, with innumerable neurofibrillae crossing and anastomosing with each other in the most complicated manner, with dispersed nuclei, lying between the neurofibrillae without the faintest trace of a boundary between, exactly as the nervous plasmodium described by LAWRENTJEW in the wal of the intestine, a real syncytial arrangement of the protoplasm of the lemmoblasts with the neurofibrillae imbedded in it, his "interstitial cells", so that here the distinction between the sheaths elements and the conducting protoplasma is lost.

The figure 2 gives only an inadequate picture of the wonderful delicateness and exuberance of this network, which covers the entire muscular coat and extends even between the muscle layers; in cross-sections it is to be followed between the outer muscle cells, but whether it is still present between the deepest muscle cells is difficult to determine, because it becomes so fine that it is more of the nature of the periterminal network extending from the sharply impregnated neurofibrillar structures of the motor endplates or the tactile corpuscles into the protoplasm of the muscle fibers or the tactile cells. This network is to be found everywhere, on and in the media of the smaller arteries, as is shown in the figures 1 and 2, its connection with sympathetic ganglioncells is easily to be proved, for instance in the musculature of the tongue, where the sympathetic ganglia are scattered throughout the interstices of the muscle bundles and are therefore often lying in the neighbourhood of the bloodvessels studied (Fig. 2, gangl.). On the other hand I could see it extending to the muscle cells of the tunica media of the vessel and continuing into an extremely delicate network inside the muscle cells, which is lost in the fine striation of the contractile fibrillae, that is to say in the protoplasmic network, the structure as it appears in the fixated and impregnated tissue-elements. Endrings inside the protoplasm of the muscle cells or endloops of the neurofibrillar structure, as they exist in the musculus ciliaris, I could not find. The connection with the smooth muscle cells seems to be by the structure akin to the periterminal network, described above. So it seems to

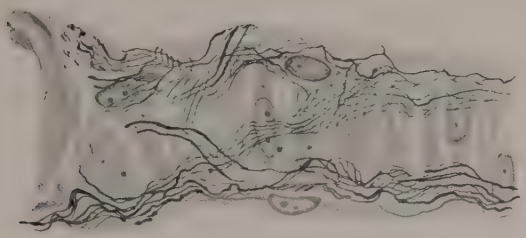

Fig. 1. Nerve plexus in the tunica media of a small artery, human parotic gland, BIELSCHOWSKY-method, highly magnified (1200).

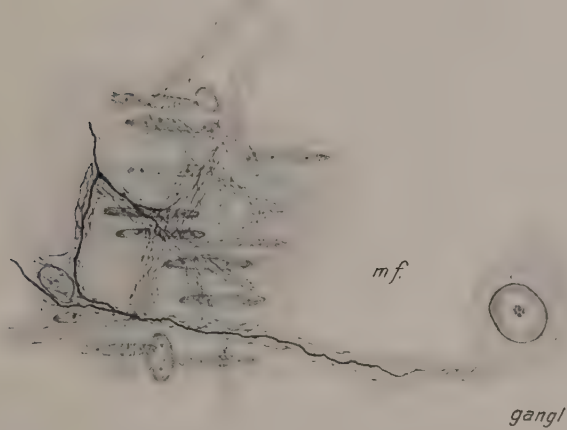

Fig. 2 Thin layer of muscle cells from a middle-sized artery, with nerve plexus, from the tongue of the hedgehog, BIELSCHOWSKY-method, highly magnified. (1200). gangl. a sympathetic ganglioncell, separated from the artial wall by a striated muscle fiber (mf).

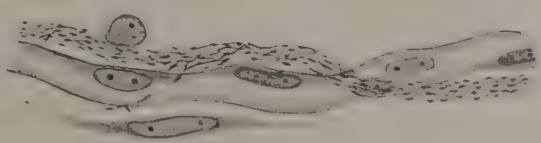

Fig. 3. A capillary with accompanying bundle of neurofibrillae, from the tongue of the hedgehog. BIELSCHOWSKY-method. Highly magnified.

me, that we have here in this network, which may be compared with the dense network described by the above-mentioned authors, the real efferent innervation of the smooth muscle cells of the bloodvessel-wall, and that it covers the entire contractile coat with all its elements. The nuclei dispersed throughout this syncytial nervous plasmodium are of the nature of interstitial nuclei. In the tongue the whole network with the nuclei persists after sectioning of the nervus lingualis; that the nuclei with a little protoplasm remain as seperate stellate cells after periarterial sympathectomy, as is described by WOOLLARD (1926) for the intramuscular plexus, which he describes in the wall of the sciatic artery, seems to me to be due to the method used (methylene blue). In a longer and better illustrated paper I hope to give more arguments for this thesis.

But there is more. In the second place these same plexiform anastomosing bands of extremely delicate neurofibrillar strands are seen running alongside the capillaries, closely adhering to the endothelial wall, just as it was pictured by LAWRENTJEW; they may be traced through the connective tissue, exactly as the perivascular plexus of CREVATIN and CECHERELLI: they are seen encircling and enveloping the striated muscle fibers (in the tongue for instance), being so closely applied to them as to appear nearly imbedded in the sarcolemma, the neurofibrillar strands, when studied with the highest power, often lying exactly in the same plane as the striation of the muscle fiber. They are here however often difficult to find because of the darkly stained muscle fibers themselves. And in the third place, when studied in glands (as for exemple the parotic gland, the lacrimal gland, in man and animals), we see the same dense and extremely delicate nervous network encircling and covering the clumps of gland cells, and from this network spring the fine nerve fibers which run between the gland cells themselves and enter them, (as I described in the Handbook of PENFIELD, 1932). This glandular network is seen in absolute continuity with the nervous network on the bloodvessels, both with that part of it, with accompanies the capillaries as with that extending on the larger vessels. Thus it seems to me, that we may suppose that both are of an efferent nature.

In the fourth place I could follow this network to the smooth muscle cells of the arrectores pilorum, and in some places I could see it even between the elements of the bundles of contractile fibers building up the smooth muscles of the dermal spines (in the hedgehog), but it is extremely difficult to trace it here, for the same reason as in the striated muscles, because of the staining of the muscle fibres themselves. But even here is room for the supposition, that every single muscle cell is getting an innervation from it.

Thus it seems that we are entitled to summon up these observations in the following way: there exists, part of it having been described as "interstitial cells", a system of very delicate interwoven and anastomosing amyelinitic nerve fibers, running in strands or flattened bands of extremely

delicate neurofibrillae with scattered nuclei, forming the ends of the sympathetic plexus. It is found in abundance in the outer layers of the muscular coat of the bloodvessels, both in the smaller and larger vessels and on the wall of the capillaries, and in the tunica media of the bloodvessels it stands in close connection with the muscle fibers. As far as I could see, it is found everywhere in the smooth muscle tissues, in the glands (and from it spring the fine fibers running between and into the gland cells), in the connective tissue (the perivasal plexus of CREVATIN, the connective-tissue-network of LEONTOWITSCH), it runs around and between the striated muscle fibers, and in several instances I could trace the bands of extremely delicate neurofibrillae to a sympathetic ganglion. No trace of cell boundaries or sheaths are to be seen in the strands; only the intercalated nuclei; it represents a true nervous terminal plasmodium. In my opinion this is the real efferent sympathetic terminal system; the neurofibrillar fibers described in the adventitia of the bloodvessels and encircling the capillaries in some distance from the endothelial wall being apparently of an afferent nature. The whole system described here is of an extreme richness and abundance.

LITERATURE CITED:

STOEHR, PH. Jr. 1927. Das periphere Nervensystem, Möllendorff's Handbuch der Mikrosk. Anatomie.

———— 1932. Nerves of the bloodvessels, Penfield's Handbook Nervous System, Vol. I.

LAWRENTJEW, B. 1926. Zeitschr. f. Mikr. Anat. Forschung, **6**. Bd., 1926.

VAN ESVELD, L. W., 1928, Zeitschr. f. Mikr. Anat. Forschung, **15**. Bd., 1928.

LEONTOWITSCH, A. W., 1930, Zeitschr. f. Zellforsch. u. mikr. Anat., **11**. Bd., 1930.

CREVATIN, F., 1900, Mem. d. R. Accad. d. Sc. dell' Inst di Bologna, ser. V., Vol. X.

RUFFINI, A., 1905, Revue Générale d'Histologie, Tome I, Fasc. 3.

WOOLLARD, H. H., 1926, Innervation of bloodvessels, Heart, Vol. **13**, 1926.

STEFANELLI, A., Bolletino di Zoologia, Anno III, 1932.

————, Monitore Zool, Italiano, Anno XLI, 1930.

————, Arch. Zool. Ital. Vol. **13**, 1929.

O. ROSSI, 1929, Arch. Ital. di Anat. e Embr. Vol. XXVI, 1929.

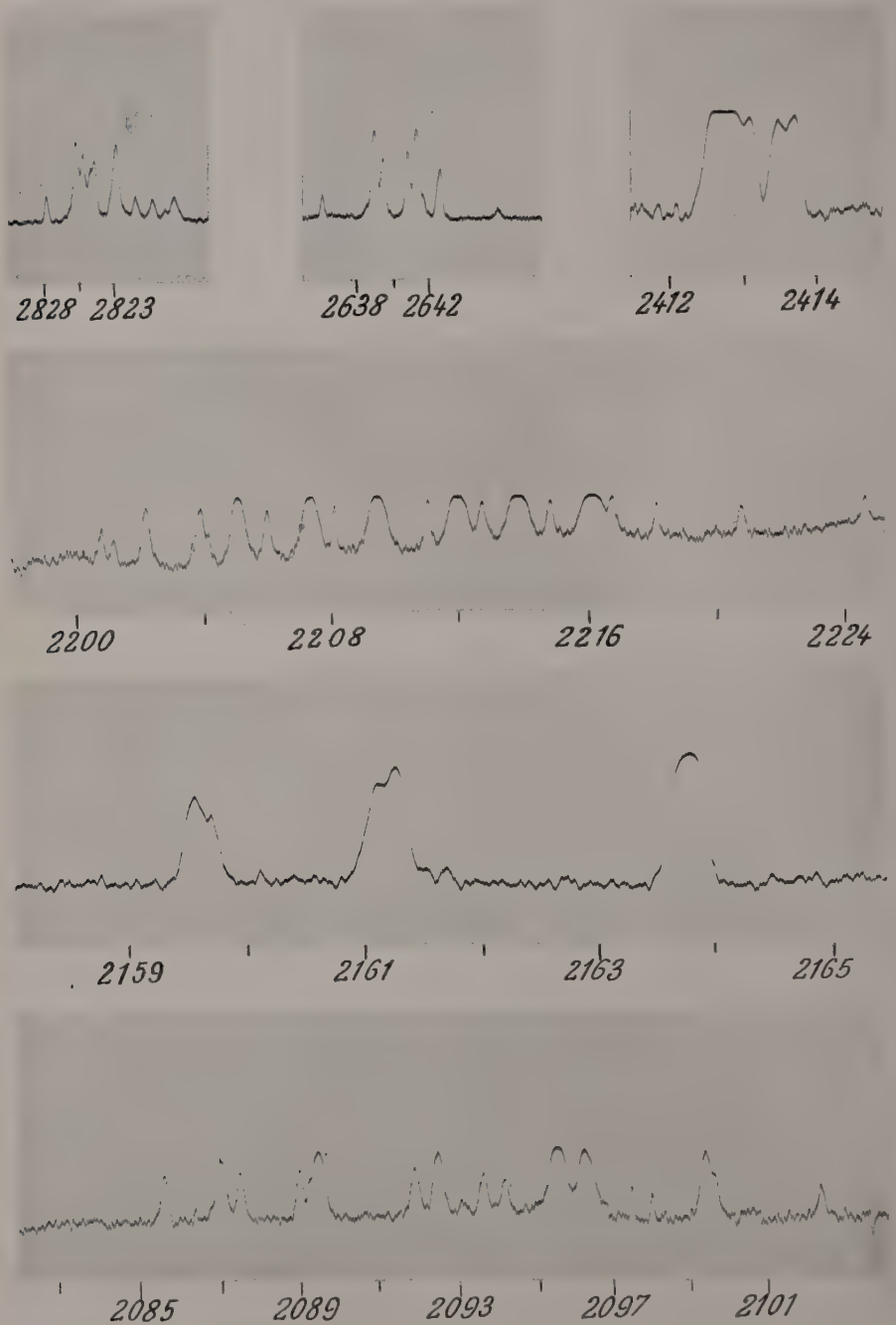

Fig. 2. The spectrum of doubly ionised Neon, Ne III

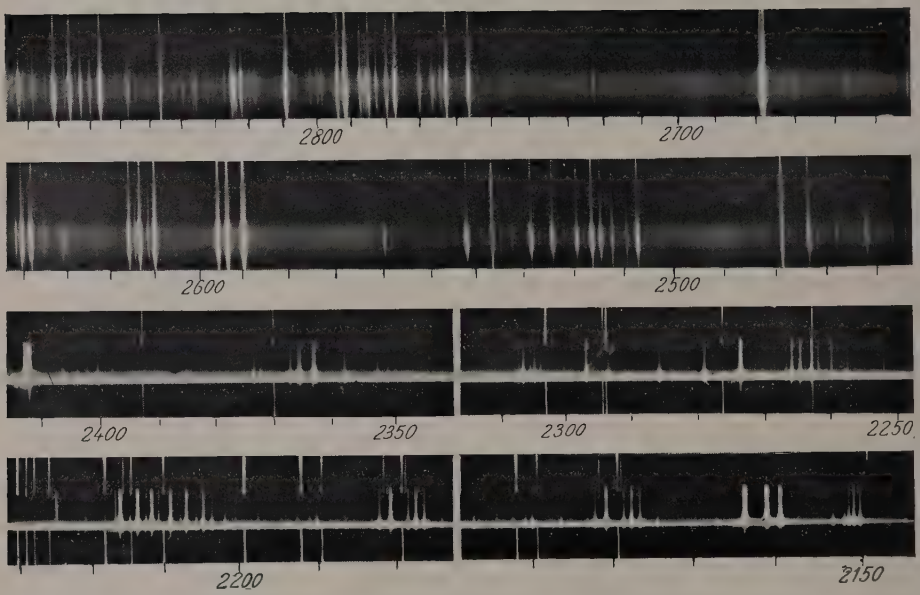

Fig. 1. The spectrum of doubly ionised Neon, Ne III

Physics. — *The spectrum of doubly ionised Neon, Ne III.* By T. L. DE BRUIN. (Communicated by Prof. P. ZEEMAN).

(Communicated at the meeting of June 25, 1932).

Introductory. The spectra and their structure of the neutral Neon atom, *Ne I* [1]) and of the singly ionised atom *Ne II* [2]) are fairly well known. Not much however is known about the spectrum of the doubly ionised atom, *Ne III*. Some years ago during the investigation of the *Ne II* spectrum the author has given some of the most characteristic *Ne III* groups of lines and has shown that *Ne III* and *F II* have an analogous structure. At that time however it was not possible to give the identification of these *Ne III* multiplets. The apparatus used at that time (2 m grating) did not allow to resolve the finer structure and did not record lines farther in the U.V. than 2400 A. The same holds for the investigations by L. and E. BLOCH and DEJARDIN [3]). GANESAN [4]) has investigated the spark spectrum of Neon farther in the U.V. down to λ 1868. He however gives only the strongest lines and his dispersion is to small to detect the finer structure. Now we have repeated our early experiments with a HILGER E_1 quartz spectrograph.

Experimental arrangements. The new HILGER E_1 quartz spectrograph made it possible to photograph the spectrum down to λ 2000 A. In this investigation almost the same light source has been used as in the early experiment only with this difference that now the observations are made "end-on" and still stronger discharges have been used [5]). For details of the experimental arrangements we refer to our earlier paper. With this outfit it was possible to detect a lot of new *Ne III* lines and also to resolve the finer structure of the groups of lines.

Theoretical structure of the spectrum. According to the theory the spectrum of doubly ionised Neon should be similar to that of neutral Oxygen [6]) and that of singly ionised Fluor *F II* [7]) which have already been eluciated with a fairly degree of completeness. The most prominent terms to be expected may be represented in the usual way by the following table 1.

---

[1]) PASCHEN: Ann. d. Phys. **60**. 405. 1919. **63**. 201. 1920.

[2]) T. L. DE BRUIN: ZS. f. Phys. **44**. 157. 1927. **46**. 856. 1928. C. J. BAKKER: Proc. Amsterdam. **32**. 515. 1929. T. L. DE BRUIN u. C. J. BAKKER: ZS. f. Phys. **69**. 19. 1931.

[3]) L. BLOCH, E. BLOCH u. G. DÉJARDIN: Journ. de Phys. **7**. 129. 1926.

[4]) GANESAN: Phys. Rev. **32**. 580. 1928.

[5]) Thanks are due to Mr. J. V. D. ZWAAL for assistance.

[6]) R. FRERICHS: Phys. Rev. **34**. 1239. 1929. **36**. 398. 1930. **36**. 1460. 1930. HOPFIELD: Phys. Rev. **37**. 160. 1931.

[7]) H. DINGLE Proc. R. S. London. 128. 600. 1928.

TABLE I. Neon III.

Electronic configuration						Symbol	Basic term ^4S		Basic term ^2D		Basic term ^2p	
1s	2s	2p	3s	3p	3d		Quintet	Triplet	Triplet	Singulet	Triplet	Singulet
2	2	4				$s^2\,p^4$		P		D		S
2	2	3	1			$s^2\,p^3\,.\,3s$	S	S	D	D	P	P
2	2	3		1		$s^2\,p^3\,.\,3p$	P	P	FDP	FDP	DPS	DPS
2	2	3			1	$s^2\,p^3\,.\,3d$	D	D	GFDPS	GFDPS	FDP	FDP

Analysis of the spectrum. In Neon III only the deepest terms ^3P, ^1D and ^1S and $s\,p^5\,^3P$ are known from the work of BOYCE and COMPTON [1]). These authors have identified these multiplets in the far ultra violet. From our new data it was possible to identify almost all the terms arising from the addition of a $3s$-, $3p$- and $3d$-electron to the core in the ^4S, ^2D and ^2P state. The first step in the analysis was the detection of the finer structure in the 2413 "doublet" and the "triplet" at 2160. The 2413 group is now identified as the $3p^3P\,(^4S)$—$3d^3D\,(^4S)$ combination and the "triplet" at 2160 as the $3p^5P\,(^4S)$—$3d^5D\,(^4S)$ combination. The main multiplets in the *Ne III* spectrum are given in the following table 2.

TABLE 2.

	$3p\ ^5P_3$	$3p\ ^5P_2$	$3p\ ^5P_1$		$3p\ ^3P_{20}$	$3p\ ^3P_1$
	40	30	20		30	25
	2590.04	2593.60	2595.68		2677.90	2678.64
$3s\ ^5S_2$	38597.91	38544.93	38514.05	$3s\ ^3S_1$	37331.62	37321.30
	15				15	
	2163.77				2412.73	
$3d\ ^5D_4$	46201.07			$3d\ ^3D_3$	41434.22	
		10			6	12
		2161.22			2413.54	2412.94
$3d\ ^5D_3$	46202.60	46255.58		$3d\ ^3D_2$	41420.32	41430.62
		6	4		10	8
		2161.04	2159.60		2413.78	2413.18
$3d\ ^5D_2$	46206.45	46259.43	46290.27	$3d\ ^3D_1$	41416.20	41426.49
		2	5			
		2160.88	2159.44			
$3d\ ^5D_1$		46262.85	46293.70			

[1]) J. C. BOYCE a. K. T. COMPTON: Proc. N. A. Sc. **15**. 656. 1929.

The strong group of lines at 2613 A is the $3s\,^3D\,(^2D)$—$3p\,^3F\,(^2D)$ combination.

Termtable and list of classified lines. The identified terms of the *Ne III* spectrum are collected in table 3. Higher series members are to be expected to give lines still farther in the U.V. Therefore it was not possible to determine the absolute termvalues. The termvalues $3s\,^5S_2$, $3s\,^3S_1$, $3s\,^3D_3$ and $3s\,^3P_2$ are rough estimations. On these values all the other terms are based. No intercombinations have been detected. The most of these combinations can be expected in another spectral region. An investigation of the far ultra violet will be necessary to connect the terms with the ground triplet.

One term $a^3D_3 = 155579.32$
$a^3D_2 = 155664.69$
$a^3D_1 = 155743.91$ is not included in the table. It combines with $3p\,^3P\,(^2D)$ and gives an isolated multiplet at 2473—2454 A. However it seems impossible to give a theoretical interpretation of this term and it is also not possible to verify the term by other combinations.

The classified lines in Neon III are collected in table 4.

TABLE 3. Termtable Ne III.

Limit: ^4S					Limit: ^2D					Limit: ^2P				
r.	Term	Termvalue	Term-difference	Theory	Nr.	Term	Termvalue	Term-difference	Theory	Nr.	Term	Termvalue	Term-difference	Theory
1	$^5S_2$	200000.00		3s	15	$^3D_3$	161000.00	29.16	3s	40	$^3P_2$	140000.00	26.75	3s
					16	$^3D_2$	160970.84	20.24		41	$^3P_1$	139973.25	16.91	
2	$^3S_1$	193000.00			17	$^3D_1$	160950.60			42	$^3P_0$	139956.34		
3	$^5P_1$	161485.95	30.88	3p	18	$^3D_1$	125089.76	11.13	3p	43	$^3D_3$	104586.47	2.45	3p
4	$^5P_2$	161455.07	52.98		19	$^3D_2$	125078.63	69.68		44	$^3D_2$	104588.92	9.85	
5	$^5P_3$	161402.09			20	$^3D_3$	125008.95			45	$^3D_1$	104578.77		
6	$^3P_1$	155678.70	10.32		21	$^3F_2$	122733.98	15.92		46	$^3S_1$	104299.28		
7	$^3P_{20}$	155668.38			22	$^3F_3$	122718.06	20.37						
					23	$^3F_4$	122697.69			47	$^3P_2$	102113.79	7.10	
										48	$^3P_1$	102120.89	19.52	
					24	$^3P_2$	115161.36	95.93		49	$^3P_0$	102140.41		
					25	$^3P_1$	115065.43	42.55						
					26	$^3P_0$	115022.88							

TABLE 3. Termtable Ne III. *(Continued).*

Nr.	Term	Termvalue	Term-difference	Theory	Nr.	Term	Termvalue	Term-difference	Theory	Nr.	Term	Termvalue	Term-difference
8	$^5D_4$	115201.02			27	$^3F_2$	78620.10						
			1.53					40.10					
9	$^5D_3$	115199.49			28	$^3F_3$	78580.00						
			3.83					52.80					
10	$^5D_2$	115195.66			29	$^3F_4$	78527.20						
			3.41										
11	$^5D_1$	115192.25		3d	30	$^3G_5$	77586.65						
								26.99					
					31	$^3G_4$	77559.66						
								23.22					
12	$^3D_1$	114252.20			32	$^3G_3$	77536.44						
			4.13										
13	$^3D_2$	114248.07											
			13.91		33	$^3D_3$	77303.37		3d				
14	$^3D_3$	114234.16						69.76					
					34	$^3D_2$	77233.61						
								45.10					
					35	$^3D_1$	77188.51						
					36	$^3P_2$	69775.00						
								27.16					
					37	$^3P_1$	69747.84						
								20.11					
					38	$^3P_0$	69727.73						
					39	$^3S_1$	69519.62	?					

TABLE 4. Classified lines Ne III.

	λ	$v_{vac.}$	Termcombination		λ	$v_{vac.}$	Termcombination
5	2825.82	35377.57	3 s $^3P_0$ (^2P) — 3 p $^3D_1$ (^2P)	30	2677.90	37331.62	3 s $^3S_1$ (^4S) — 3 p $^3P_{20}$ (^4S)
4	2825.28	35384.33	3 s $^3P_1$ (^2P) — 3 p $^3D_2$ (^2P)				
3	2824.47	35394.48	3 s $^3P_1$ (^2P) — 3 p $^3D_1$ (^2P)	3	2642.42	37832.84	3 s $^3P_1$ (^2D) — 3 p $^3P_0$ (^2D)
7	2822.95	35413.95	3 s $^3P_2$ (^2P) — 3 p $^3D_3$ (^2P)	2	2642.25	37835.27	3 s $^3P_0$ (^2D) — 3 p $^3P_1$ (^2D)
				10	2641.07	37852.18	3 s $^3P_1$ (^2D) — 3 p $^3P_1$ (^2D)
2	2802.34	35673.97	3 s $^3P_1$ (^2P) — 3 p $^3S_1$ (^2P)				
3	2800.24	35700.72	3 s $^3P_2$ (^2P) — 3 p $^3S_1$ (^2P)	6	2640.56	37859.50	3 s $^3P_1$ (^2D) — 3 p $^3P_2$ (^2D)
				5	2639.18	37879.28	3 s $^3P_2$ (^2D) — 3 p $^3P_1$ (^2D)
4	2787.73	35860.93	3 s $^3D_1$ (^2D) — 3 p $^3D_1$ (^2D)	10	2638.70	37886.17	3 s $^3P_2$ (^2D) — 3 p $^3P_2$ (^2D)
3	2786.89	35871.73	3 s $^3D_1$ (^2D) — 3 p $^3D_2$ (^2D)				
2	2786.17	35881.00	3 s $^3D_2$ (^2D) — 3 p $^3D_1$ (^2D)	10	2615.87	38216.80	3 s $^3D_1$ (^2D) — 3 p $^3F_2$ (^2D)
5	2785.29	35892.33	3 s $^3D_2$ (^2D) — 3 p $^3D_2$ (^2D)	4	2614.51	38236.68	3 s $^3D_2$ (^2D) — 3 p $^3F_2$ (^2D)
2	2783.03	35921.49	3 s $^3D_3$ (^2D) — 3 p $^3D_2$ (^2D)	12	2613.41	38251.78	3 s $^3D_2$ (^2D) — 3 p $^3F_3$ (^2D)
7	2777.65	35991.05	3 s $^3D_3$ (^2D) — 3 p $^3D_3$ (^2D)	4	2611.42	38281.92	3 s $^3D_3$ (^2D) — 3 p $^3F_3$ (^2D)
25	2678.64	37321.30	3 s $^3S_1$ (^4S) — 3 p $^3P_1$ (^4S)	15	2610.03	38302.31	3 s $^3D_3$ (^2D) — 3 p $^3F_4$ (^2D)

TABLE 4. (*Continued*).

	λ	$\nu_{vac.}$	Termcombination
20	2595.68	38514.05	3 s $^5S_2$ (^4S) — 3 p $^5P_1$ (^4S)
30	2593.60	38544.93	3 s $^5S_2$ (^4S) — 3 p $^5P_2$ (^4S)
40	2590.04	38597.91	3 s $^5S_2$ (^4S) — 3 p $^5P_3$ (^4S)
10	2473.40	40417.96	3 p $^3P_2$ (^2D) — a $^3D_3$
4	2468.20	40503.10	3 p $^3P_2$ (^2D) — a $^3D_2$
2	2463.38	40582.37	3 p $^3P_2$ (^2D) — a $^3D_1$
6	2462.35	40599.32	3 p $^3P_1$ (^2D) — a $^3D_2$
2	2457.55	40678.61	3 p $^3P_1$ (^2D) — a $^3D_1$
5	2454.98	40721.20	3 p $^3P_0$ (^2D) — a $^3D_1$
10	2413.78	41416.20	3 p $^3P_2$ (^4S) — 3 d $^3D_1$ (^4S)
6	2413.54	41420.32	3 p $^3P_2$ (^4S) — 3 d $^3D_2$ (^4S)
8	2413.18	41426.49	3 p $^3P_2$ (^4S) — 3 d $^3D_1$ (^4S)
12	2412.94	41430.62	3 p $^3P_1$ (^4S) — 3 d $^3D_2$ (^4S)
15	2412.73	41434.22	3 p $^3P_2$ (^4S) — 3 d $^3D_3$ (^4S)
5	2266.98	44097.87	3 p $^3F_3$ (^2D) — 3 d $^3F_2$ (^2D)
8	2266.16	44113.83	3 p $^3F_2$ (^2D) — 3 d $^3F_2$ (^2D)
10	2264.91	44138.18	3 p $^3F_3$ (^2D) — 3 d $^3F_3$ (^2D)
3	2264.11	44153.77	3 p $^3F_2$ (^2D) — 3 d $^3F_3$ (^2D)
12	2263.21	44171.33	3 p $^3F_4$ (^2D) — 3 d $^3F_4$ (^2D)
2	2262.16	44191.83	3 p $^3F_3$ (^2D) — 3 d $^3F_4$ (^2D)
15	2216.07	45110.84	3 p $^3F_4$ (^2D) — 3 d $^3G_5$ (^2D)
4	2214.77	45137.31	3 p $^3F_4$ (^2D) — 3 d $_3G_4$ (^2D)
12	2213.76	45157.90	3 p $^3F_3$ (^2D) — 3 d $^3G_4$ (^2D)
5	2212.63	45180.96	3 p $^3F_3$ (^2D) — 3 d $^3G_3$ (^2D)
10	2211.85	45196.89	3 p $^3F_2$ (^2D) — 3 d $^3G_3$ (^2D)
10	2209.35	45248.03	3 p $^3P_2$ (^2D) — 3 d $^3P_2$ (^2D)
4	2208.04	45274.87	3 p $^3P_2$ (^2D) — 3 d $^3P_1$ (^2D)
8	2207.29	45290.25	3 p $^3P_1$ (^2D) — 3 d $^3P_2$ (^2D)
5	2205.95	45317.76	3 p $^3P_1$ (^2D) — 3 d $^3P_1$ (^2D)
7	2204.98	45337.70	3 p $^3P_1$ (^2D) — 3 d $^3P_0$ (^2D)
7	2202.22	45394.51	3 p $^3F_4$ (^2D) — 3 d $^3D_3$ (^2D)
4	2201.23	45414.93	3 p $^3F_3$ (^2D) — 3 d $^3D_3$ (^2D)
7	2197.86	45484.55	3 p $^3F_3$ (^2D) — 3 d $^3D_2$ (^2D)
3	2197.10	45500.28	3 p $^3F_2$ (^2D) — 3 d $^3D_2$ (^2D)
5	2194.92	45545.47	3 p $^3F_2$ (^2D) — 3 d $^3D_1$ (^2D)
7	2190.29	45641.74	3 p $^3P_2$ (^2D) — 3 d $^3S_1$ (^2D)
2	2183.24	45789.10	3 s $^3D_1$ (^2D) — 3 p $^3P_2$ (^2D)
3	2182.28	45809.24	3 s $^3D_2$ (^2D) — 3 p $^3P_2$ (^2D)
10	2180.89	45838.43	3 s $^3D_3$ (^2D) — 3 p $^3P_2$ (^2D)
4	2178.69	45884.72	3 s $^3D_1$ (^2D) — 3 p $^3P_1$ (^2D)
8	2177.73	45904.94	3 s $^3D_2$ (^2D) — 3 p $^3P_1$ (^2D)
5	2176.67	45927.30	3 s $^3D_1$ (^2D) — 3 p $^3P_0$ (^2D)
15	2163.77	46201.07	3 p $^5P_3$ (^4S) — 3 d $^5D_4$ (^4S)
10	2161.22	46255.58	3 p $^5P_2$ (^4S) — 3 d $^5D_3$ (^4S)
6	2161.04	46259.43	3 p $^5P_2$ (^4S) — 3 d $^5D_2$ (^4S)
2	2160.88	46262.85	3 p $^5P_2$ (^4S) — 3 d $^5D_1$ (^4S)
4	2159.60	46290.27	3 p $^5P_1$ (^4S) — 3 d $^5D_2$ (^4S)
5	2159.44	46293.70	3 p $^5P_1$ (^4S) — 3 d $^5D_1$ (^4S)
2	2153.15	46428.92	3 p $^3D_3$ (^2D) — 3 d $^3F_3$ (^2D)
3	2151.78	46458.49	3 p $^3D_2$ (^2D) — 3 d $^3F_2$ (^2D)
5	2151.26	46469.71	3 p $^3D_1$ (^2D) — 3 d $^3F_2$ (^2D)
8	2150.70	46481.81	3 p $^3D_3$ (^2D) — 3 d $^3F_4$ (^2D)
6	2149.92	46498.67	3 p $^3D_2$ (^2D) — 3 d $^3F_3$ (^2D)
20	2095.54	47705.28	3 p $^3D_3$ (^2D) — 3 d $^3D_3$ (^2D)
12	2092.44	47775.84	3 p $^3D_2$ (^2D) — 3 d $^3D_3$ (^2D) 3 p $^3D_3$ (^2D) — 3 d $^3D_2$ (^2D)
15	2089.43	47844.66	3 p $^3D_2$ (^2D) — 3 d $^3D_2$ (^2D)
5	2088.92	47856.34	3 p $^3D_1$ (^2D) — 3 d $^3D_2$ (^2D)
7	2087.44	47890.26	3 p $^3D_2$ (^2D) — 3 d $^3D_1$ (^2D)
10	2086.96	47901.27	3 p $^3D_1$ (^2D) — 3 d $^3D_1$ (^2D

Impurities. Table of unidentified lines. With the stronger discharges the lines of impurities arising from the material of the tube and electrodes are present. Also a few Hg lines have been observed. Si, C, Al and Hg were the chief impurities. It is quite possible that there are still unidentified lines due to impurities in the list of unclassified lines (table 5). Also it is possible that lines of *Ne IV* and *Ne II* are present. A striking group of unidentified lines is at 2365. In this group the difference $\triangle \nu = 6.44$ and $\triangle \nu = 45.23$ occurs.

TABLE 5. Unidentified lines

	λ	$\nu_{vac.}$		λ	$\nu_{vac.}$
4	2905.85	34403.29	2	2204.16	45354.56
6	2866.65	34873.71	6	2203.89	45360.12
			5	2200.82	45423.38
2	2767.02	36129.31	7	2192.74	45590.74
1	2766.07	36141.72	1	2191.45	45617.58
2	2764.70	36159.63	4	2191.16	45623.72
1	2764.38	36163.82	1	2186.62	45718.34
5	2367.02	42234.30 Si?			
5	2365.74	42257.14	6	2129.54	46943.61
6	2365.38	42263.57	7	2124.27	47060.06
8	2363.21	42302.38	2	2102.33	47551.12
5	2362.85	42308.82	4	2099.59	47613.16
5	2357.94	42396.91 Si?	10	2099.34	47618.84
			1	2098.00	47649.24
2	2307.27	43327.91	2	2097.43	47662.19
6	2306.61	43340.31	12	2096.23	47689.47
2	2305.50	43361.17	2	2094.15	47736.83
4	2304.87	43373.02	3	2093.64	47748.46
3	2303.94	43390.52	4	2091.90	47788.17
2	2300.38	43457.67	2	2089.20	47849.92
1	2298.96	43484.51	5	2085.56	47933.43
8	2285.80	43734.83	15	2078.95	48085.81
10	2278.98	43865.70	20	2065.18	48406.39
20	2273.64	43968.72	2	2062.62	48466.46

TABLE 6. Irregular doublet law.

Combination	O I	$\Delta\nu$	F II	$\Delta\nu$	Ne III
	7771.93		3847.09		2590.04
$3s\ ^5S_2\ (^4S) - 3p\ ^5P_3\ (^4S)$	12863.28	13123	25986.36	12610	38597.91
	8446.38		4024.73		2677.90
$3s\ ^3S_1\ (^4S) - 3p\ ^3P_2\ (^4S)$	11836.14	13003	24839.41	12492	37331.62
	7947.57		3898.83		2610.03
$3s\ ^3D_3\ (^2D) - 3p\ ^3F_4\ (^2D)$	12579.00	13062	25641.46	12661	38302.31
			4109.17		2777.65
$3s\ ^3D_3\ (^2D) - 3p\ ^3D_3\ (^2D)$	?		24328.95	11662	35991.05
	8821.83		3541.76		2180.89
$3s\ ^3D_3\ (^2D) - 3p\ ^3P_2\ (^2D)$	12159.34	16067	28226.48	17612	45838.43
	7476.47		3974.79		2822.95
$3s\ ^3P_2\ (^2P) - 3p\ ^3D_3\ (^2P)$	13371.65	11780	25151.47	10262	35413.95
			3603.72		2638.70
$3s\ ^3P_2\ (^2P) - 3p\ ^3P_2\ (^2P)$	?		27741.2	10145	37886.17
			4207.16		2802.34
$3s\ ^3P_2\ (^2P) - 3p\ ^3S_1\ (^2P)$	?		23762.32	11912	35673.97
	9263.88		3505.61		2163.77
$3p\ ^5P_3\ (^4S) - 3d\ ^5D_4\ (^4S)$	10791.7	17726	28517.55	17684	46201.07
	11287.3		4103.52		2412.73
$3p\ ^3P_2\ (^4S) - 3d\ ^3D_3\ (^4S)$	8557.2	15505	24362.45	17072	41434.22
			3602.85		2216.07
$3p\ ^3F_4\ (^2D) - 3d\ ^3G_5\ (^2D)$	?		27747.9	17363	45110.84
			3640.89		2263.21
$3p\ ^3F_4\ (^2D) - 3d\ ^3F_4\ (^2D)$	?		27458.00	16713	44171.33
			3574.92		2202.22
$3p\ ^3F_4\ (^2D) - 3d\ ^3D_3\ (^2D)$	?		27964.7	17430	45394.51
			3414.66		2095.54
$3p\ ^3D_3(^2D) - 3d\ ^3D_3\ (^2D)$	?		29277.09	18528	47705.28

Irregular doublet law. *Ne III* belongs to the isoelectronic configurations: *O I, F II, Ne III, Na IV* .... etc. Several of the terms now detected in *Ne III* are already known in *O I* and *F II*. Now it is possible to check the irregular doublet law for these configurations. As can be seen from table 6 the irregular doublet law holds for these configurations. The $3s$—$3p$ combinations have a displacement of about 12000 units. In all three configurations the $3p\,^3P\,(^2D)$ has an anormal position. The $3p$—$3d$ combinations have a displacement of about 17000 units. With the data in table 6 it is now possible to identify some unknown combinations in *O I* in the far infra red. Further it will not be difficult to identify from the data in table 6 the analogous combinations in *Na IV* in the ultra violet. The $3s$—$3p$ combinations f.i. can be expected around 2000 A.

Photographs and photograms. The photograph gives the most interesting parts of the *Ne III* spectrum. Above 2415 A there is no comparison spectrum. Under 2415 the photograph shows the *Cu* arc lines as comparison spectrum. It should be noticed that in the ultra violet the Neon with this kind of discharge in the narrow part of the tube gives a strong "continuous" spectrum.

The photograms are made with a ZEISS photometer with photoelectric cell.

In conclusion the writer wishes to express his appreciation to Professor P. ZEEMAN for his interest and helpful suggestions during this investigation.

Physics. — *On the Polarisation of Light Originating from Moving and Stationary Particles of Hydrogen Canal Rays.* By Miss W. A. LUB. (Communicated by Prof. P. ZEEMAN.)

(Communicated at the meeting of June 25, 1932).

The phenomenon of the polarisation of the light of canal rays, which was discovered by STARK [1]) in 1906, was examined quantitatively for hydrogen canal rays for the first time by STARK and LUNELUND [2]). They found that in this gas polarisation exclusively occurs with BALMER lines, and that it becomes less with increasing series number, i.s. going from $H\alpha$ to $H\gamma$; probably the polarisation increases with higher voltage. The question whether the polarisation was owing to the light of moving, or to

[1]) J. STARK. Ueber polarisierte Richtemission bewegter Atomionen senkrecht zur Translationsrichtung. Verh. D. Phys. Ges. **8**. 104. 1906.

[2]) J. STARK und LUNELUND. Polarisation der Lichtemission der Kanalstrahlen. Ann. d. Phys. IV, **46**. 68. 1915.

that of particles at rest could not be directly decided in these experiments, because the direction of observation was at right angles to the direction of propagation of the beam, and accordingly the intensities of stationary and moving particles coincided. It was, however, tried to find an answer to this question by an indirect way, and STARK and LUNELUND show that it is probable that the polarisation is due to the light emitted by moving particles.

Since then several investigators, among others E. RUPP [1]), A. WEIGL [2]), R. DÖPEL und R. VON HIRSCH [3]), K. L. HERTEL [4]), have made experiments on the polarisation of the light of canal rays with a twofold purpose.

First in order to examine whether STARK and LUNELUND's supposition about the part played by moving particles was correct. And in the second place in order to examine how great the effect became in the extinguishing beam, in which, if it is possible to speak of a certain direction of preference of the vibrating particle, it is supposed that this preference will manifest itself more clearly, because no disturbing collisions appear then. Further different experiments have been made on the influence of magnetic or electric fields on the polarisation.

For a summary of the results obtained by the different investigators I may refer to RUPP's second paper.

In all these experiments the investigators had, however, not succeeded in observing the polarisation of resting and moving components separately, because the dispersion of the spectrograph used did not allow them to obtain a distinct separation of resting and moving intensity, while the choice of the spectrograph was limited by the small intensity of the beam of canal rays. It seemed, therefore, worth while to try once more if it was not possible to measure to polarisation in the resting and in the moving component at the same time. Besides the course of the polarisation in the BALMER-series could be examined once more.

If one wants to have any chance of success it is necessary to work with a beam of canal rays of such intensity that, with a spectrograph which has a dispersion sufficient to separate resting and moving components, one obtains a spectrum image of great intensity.

The experiments were made with hydrogen, with an arrangement, which as regards the optical part, was the same as used by STARK and LUNELUND. In principle the experiment is very simple. The axis of the spectrograph is placed so as to make an angle of 60° to 70° with the beam of canal rays. By the aid of a calcspar rhombohedron, the light emitted is analysed

---

[1]) E. RUPP. Ueber die Polarisation des abklingenden Kanalstrahllichtes. Ann. d. Phys. IV. **81**. 615. 1926. E. RUPP. Ueber die Polarisation des Kanalstrahllichtes II. Ann. d. Phys. IV. **84**. 94. 1927.

[2]) A. WEIGL. Untersuchungen am Stark Lunelundeffekt. Ann. d. Phys. IV. **82**. 1. 1927.

[3]) R. DÖPEL und R. VON HIRSCH. Ueber die Polarisation des Kanalstrahllichtes. Ann. d. Phys. IV. **82**. 16. 1927.

[4]) K. L. HERTEL. A Study in the Polarisation of Light from Hydrogen Canal Rays. Phys. Rev. II. **29**. 848. 1827.

in vibrations normal to each other. If now, by means of a lens, an image is made of the beam, there are formed two images on the slit of the spectrograph, one of the light that vibrates parallel to the beam, the other of the light vibrating at right angles to the beam. These images are analysed spectrally by the spectrograph, and two spectra are obtained on the photographic plate one above the other. The densities of the two spectral images are measured, and from this the corresponding intensities are calculated. These numerical values must, however, still be corrected. For these values give the polarisation of the light of the beam of canal rays, increased by the polarisation arising from the wall of the tube, lens and spectrograph. The choice of the angle of observation is determined by the following consideration. The polarisation of the light of the canal rays is zero when the observation is made in the direction of the motion, and maximum in a direction normal to the motion, the distance between the spectrum line and its DOPPLER component being maximum in the direction of the motion. Accordingly that angle is chosen that gives a distinct separation between stationary and moving component, and at which the polarisation is as great as possible.

Arrangement.

Canal ray tube.

After preliminary experiments had been made with different forms of canal ray tubes, in which the pierced cathode was always 12 cm., a form of tube was finally found, which gave a very intense beam of canal rays, and which could be comparatively heavily charged during a long time.

The cathode consists of a brass cylinder (5 cm. long, width of the bore 4 mm.) one of the end planes of which is covered with a disk of aluminium. This cathode carries on one side the discharging tube with anode adjusted sideways, and on the other side the observation space. These two tubes of pyrex glass are cemented on the cathode with white sealing wax. The cathode is cooled with water. This, however, makes it necessary for the cathode to be earthed. At the end of the discharging space was placed a quartz plate [1]) which served to receive the cathode rays; moreover the tube was cooled on the outside by a strong current of air. In order to protect the discharging tube, the expedient was applied indicated by DÖPEL and VON HIRSCH [2]), i.e. the cathode was surrounded by a porcelain tube, which projects about one cm. outside the cathode, and which prevents the layer of metal formed by the spraying of the cathode, being deposited on the wall of the discharging tube, in consequence of which sparks might appear, which would cause the tube to burst after a short time.

It has been pointed out above that among other things a correction has to be applied for the polarising action of the wall of the canal ray tube

---

[1]) See Aston. Isotopes. sec. ed. 1924. p. **50**.

[2]) R. DÖPEL und R. VON HIRSCH. loc. cit.

and the lens. To keep the influence of the wall of the tube in the experiments at different angles as much the same as possible, the observa-

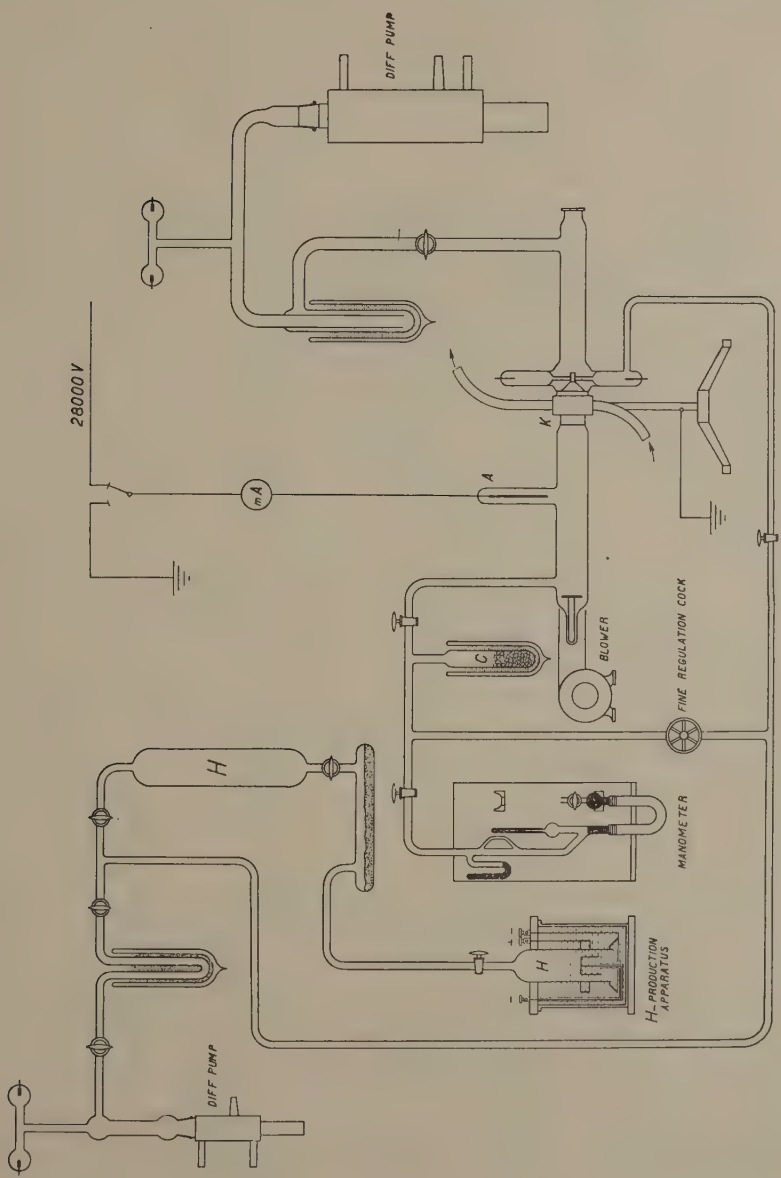

Fig. 1

tion tube was spherically widened on the side of the cathode (see fig. 2) where the cathode is represented magnified. Besides care is taken that the end of the canal is in the middle of this spherical part. In order to

determine the degree of the correction, a GEISSLER tube [1]) was applied as near as possible to the cathode (of which it is known that the light is not polarised), and the light emitted by it is photographed in the same way and on the same plate as the canal rays.

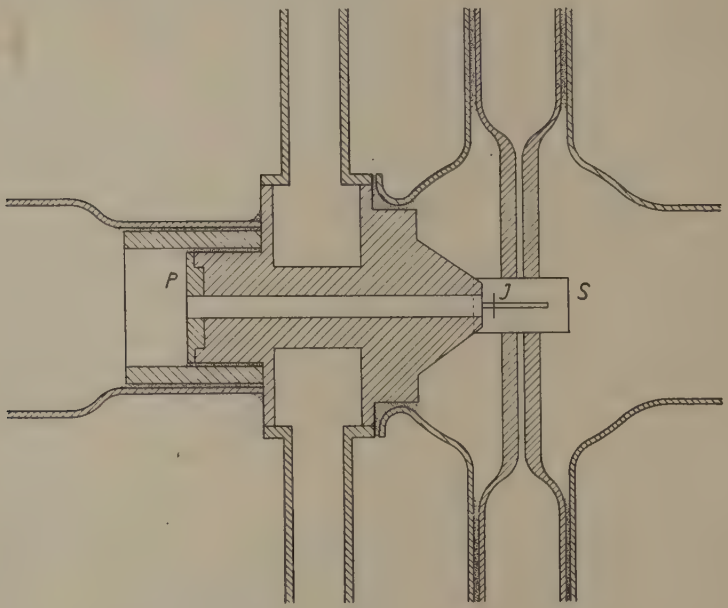

Fig. 2

The difference in intensity between the principal vibrations, as appears from the photographic plate, is therefore, entirely due to polarising influences of tube wall and lens. (The polarisation originating from the spectrograph has been corrected as a whole, see under spectrograph). The correction for the wall and the tube appeared, however, to be so small, that it may be left out of consideration.

With the cathode used the canal ray appeared to be too broad to give two separate images on the slit of the spectrograph, when observed through a calcspar rhombohedron of a thickness of 1.5 cm. Therefore close before the beam a slit was applied of such a breadth that the two images on the photographic plate were just separate. In the definitive experiments a screen with a slit of a length of about 1 cm. and a width of 1 mm. was applied to the cathode, however so, that it was possible to observe the beam close behind the cathode.

The hydrogen was obtained by electrolytic decomposition of potassium hydroxyde in the apparatus, as it has been described by NIESE [2]).

---

[1]) In the schematic figure the Geissler tube has been drawn somewhat too large, so that this spherical part is not sufficiently clearly to be seen.

[2]) G. NIESE. Apparat zur elektrolytischen Reindarstellung von Wasserstoff. Phys. Zs. **24**. 12. 1923.

WIEN's "flowing-through" method was followed [1]). The pressure, which was measured with a MCLEOD, was the same before and behind the cathode. In these experiments we have therefore, to do with the so-called "Umladungsleuchten". A sketch of the arrangement is given in fig. 1.

The direct current under high tension was obtained from a three-phase lamp rectifier installation [2]). For further particulars cf. my Thesis for the doctorate [3]).

Spectrograph. .

As spectrograph the large spectrograph [4]) of C. A. STEINHEIL SÖHNE, Münich was used, with the three glass prisms and the collimator and camera with long focus distance. The polarising action of this apparatus is fairly great. This influence can, however, be obviated by using the method indicated by ZEEMAN [5]) in a communication on the light traversing the slit of a spectroscope. If before the slit of the spectroscope a quartz plate is placed of such a thickness that the direction of vibration of the light under investigation is turned over an angle of 45°, the intensities of the two slit images are diminished in the same degree, and the proportion remains the same.

This method has the drawback that the rotation over 45° only holds good for a definite wavelength. If the experiment was made with another gas than hydrogen, this method would enormously increase the number of expositions. The BALMER-lines differ, however, so greatly in intensity, that in order to obtain densities lying in the favourable area of the density curve, a photo must be taken for every line separately. The thickness of the quartzplates which would give a rotation of 45° for the four BALMER-lines H_α, H_β, H_γ and H_δ may be calculated by the aid of GUMLICH's formula [6]). The quartz plates used here had a thickness of resp. 2.60, 1.37, 1.07, and 0.95 mm.

Measurement of the Intensity.

As was already briefly indicated above the photographic method of measuring intensities was used. For this purpose, besides the real photo,

---

[1]) W. WIEN. Ueber positive Strahlen. Ann. d. Phys. IV. **30**. 349. 1909.

[2]) I wish to thank Mr. J. VAN DER ZWAAL, chief of the technical staff of the laboratory, for his many technical suggestions especially in the high tension work and the care given to the reproductions.

[3]) W. A. LUB. Over de polarisatie van het licht afkomstig van bewegende en stilstaande deeltjes der waterstof kanaalstralen. Thesis. Amsterdam 1932.

[4]) This is the spectograph G.H., which has rendered us excellent services in this experiment, and which excels particularly by the way in which the very high demands of optics are satisfied.

[5]) P. ZEEMAN. On the polarisation impressed upon light by traversing the slit of a spectroscope and some errors resulting therefrom. Proc. R. Academy. Amsterdam 1912.

[6]) GUMLICH. Rotationsdispersion und Temperatur-coefficient des Quarzes. Wied. Ann. **64**. 333. 1898.

a number of intensity marks was printed, according to a somewhat modified method of DORGELO [1]). For this the following arrangement was used, which is given in outline in fig. 3. L_4 is the condenser lens, which projects

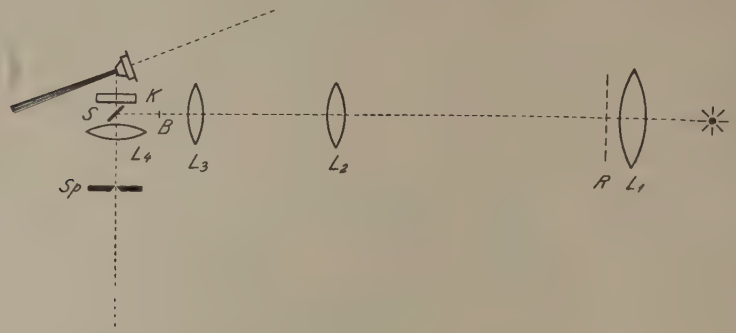

Fig. 3

the canal rays on the slit of the spectrograph. Lens L_1 is illuminated by an OSRAM lamp with a short spiral, and forms an image of the source of light on the lens L_2. Close before L_1 an echelon screen has been adjusted. (Echelon screen from the Firm C. ZEISS, Jena with transmissive power [2]) resp. 40 %, 16 %, 6.3 %, 2.5 %, 1 %). These uniformly illuminated echelon screens are photographed by the lenses L_2 and L_3 in B, at a distance in front of the mirror S equal to the distance from the mirror to beam of canal rays. L_3 forms at the same time an image of L_2 (hence also of the source of light) in the lens L_4. When everything is carefully centred, the illumination of the slit appears to be very uniform.

Procedure of the investigation.

As it was necessary for the investigation of the H_β line to illuminate for a long time, it was desirable to make the arrangement very stable. The whole apparatus was therefore mounted on one of the heavy concrete blocks of the laboratory.

This block weighs 250.000 kg., and rests, detached from the foundation of the building, on a great number of poles driven deep into the ground. During a long exposure the temperature of the room can, besides, be kept constant (down to 0.1°) [3]) by an automatic regulation.

Before the canal rays were photographed, the tube was pumped out for a considerable time with continued rinsing with hydrogen, the discharging going on meanwhile. A new tube had mostly to be treated in this way for a

---

[1]) H. B. DORGELO. Die Intensität der Mehrfachlinien. Zts. f. Phys. **13**. 2066. 1923.

[2]) At our request Prof. L. S. ORNSTEIN was so kind as to induce Dr. VAN WIJK to gauge this echelon screen for us, for which kindness I gladly express my cordial thanks here.

[3]) P. ZEEMAN and T. L. DE BRUIN. Magnetische Zerlegung der Spektrallinien. Handbuch der physikalischen Optik Gehrcke **2**. 605. 1927.

few days, till glass wall and electrodes were sufficiently degassed. As pump the large steel diffusion pump of GAEDE was used. During the time of exposure the greatest care was taken that tension and pressure were accurately constant. If the pressure changed during the exposure, this showed itself directly by a change in the strength of the current. Then the supply of the gas was regulated, till the initial state was restored. For this purpose a hydrogen cock of DESAGA was added to the arrangement. The strength of the current could be kept constant at 1 or 2 mA.

The collimator axis of the spectroscope was directed at a definite angle to the beginning of the beam of canal rays. Mostly this was done so that first the spectroscope was adjusted; with wide slit, without insertion of lens or calcspar it was ascertained whether the light of the beam passed centrically through the collimator tube. When this condition was fulfilled, the condenser lens was inserted, and the canal rays were sharply thrown on the slit. Then it was examined whether the whole collimator lens was filled. This can, however, not be seen until one has passed a long time in the dark, and the eye has thus become exceedingly sensitive to weak light impressions. Then the calcspar rhombohedron was applied.

To find the right adjustment of this an index I was marked on slit I (see fig. 2). In both images a dark line is seen on a light background. If these two lines are exactly above each other, then one can be sure that the position of the calcspar is right.

Every plate is provided with a set of density marks, and with a photo of the GEISSLER tube to ascertain the polarisation of the apparatus. The development took place in metolhydroquinone during three minutes with continued shaking.

The devisity of the negatives was measured by means of a registering microphotometer of MOLL, to which a disk is added for automatic registering of the scalar division [1]).

The image on the photographic plate cannot be much larger than 1 mm. which is a disadvantage in the measurement of the photos. It is, therefore, not possible to measure the density, as is usually done, at different heights of the line. The whole length is measured as much as possible at the same time, and only at the extremities a small part is cut off, just so much as is necessary to preserve the uniformly blackened part of the line. Every line was photo-measured four or five times. For the line at rest and for the DOPPLER component the maximum blacking was always measured.

As photographic plates the following were used: Ilford, Iso Zenith and Special Rapid, and Perutz special Fliegerplatte. Notwithstanding the larger grain of the Iso Zenith, this plate appeared the most suitable for the purpose set on account of the long scale.

---

[1]) W. M. KOK and P. ZEEMAN. The removal of errors caused by irregularities in the registering apparatus in self-registering micro-photometers. Proc. R. Academy 27. 884. 1924.

Results.

Two series of photos were taken, one in which the axis of the spectroscope made an angle of 74° with the direction of propagation of the canal rays, and one in which this angle was 64°. In both series the polarisation was measured for H_β, H_γ, and H_δ, and separately for the stationary and the displaced components.

In the first series it appeared that for H_β the two components were scarcely to be seen separate [1]). No photos of H_α were, therefore, taken at this angle. If observations are made at 64°, the dispersion of the spectrograph in the red appears to be too small, to find even so much as an indication of a separation of stationary and moving intensity. The value for H_α is therefore a superposition of the stationary and moving intensities.

Table I contains the observed intensities with the data of the photos at 74°.

In table II those for the experiments at 64°, while in tables III, IV and V the measured results for the polarisation are combined and the mean results have been computed.

V gives the electric tension used in Volts, i the strength of the current in m.A., p the pressure in mm.

The results summarized in tables III, IV and V show clearly that:

1. the polarisation of the light of canal rays is chiefly due to the moving particles.

2. the particles at rest also emit polarized light, though in a smaller degree [2]).

3. in both kinds of particles the component of the electric vector // the direction of propagation dominates.

4. the polarisation distinctly decreases with increasing serial number, hence decreasing from H_β—H_δ.

Influence of the tension on the polarisation.

After the above results had become known, it appeared worth while examining what changes ensue when a higher tension is applied.

---

[1]) When measuring intensities with these plates it was exceedingly difficult to make the component at rest appear clearly in the photogram. By the aid of the vacuum thermo element and the micro-galvanometer of MOLL and BURGER, and by the choice of the suitable objectives, this has finally succeeded. The accuracy of the measurement is for this reason less in these plates than in the others. I gladly express my indebtedness to Miss E. B. VENEMA, nat. phil. docta, who assisted me in the photometry and measurement of a great many plates.

[2]) I will point out here that STARK in his Axialität der Lichtemission und Atomstruktur already arrived at the conclusion that the resting emission of H_β which is brought about by the collision of the canal rays with resting *He* atoms, is polarised with respect to the direction of movement of the canal rays.

My experiments show that when at the same time the polarisation of the moving and the resting component is separately examined, it appears that both moving and stationary particles of hydrogen emit polarised light.

$H_\gamma \angle 74°$

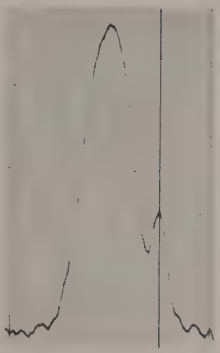

H_γ //

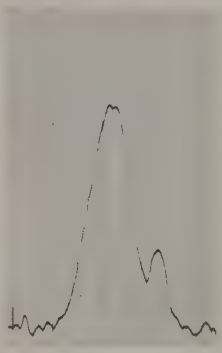

$H_\gamma \perp$

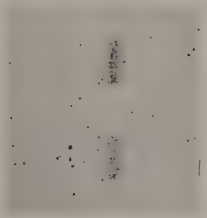

$H_\delta \angle 74°$

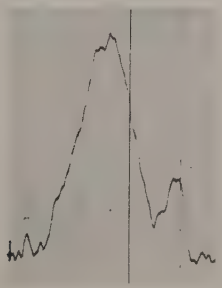

H_δ //

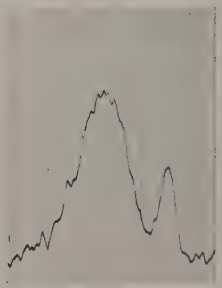

$H_\delta \perp$

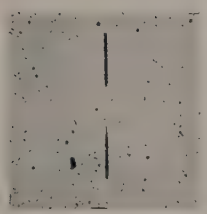

$H\alpha \angle 64°$

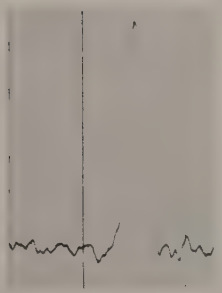

$H\alpha$ //

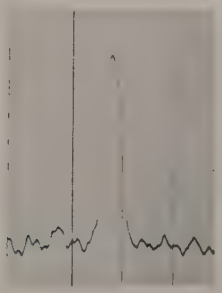

$H\alpha \perp$

PLATE II.

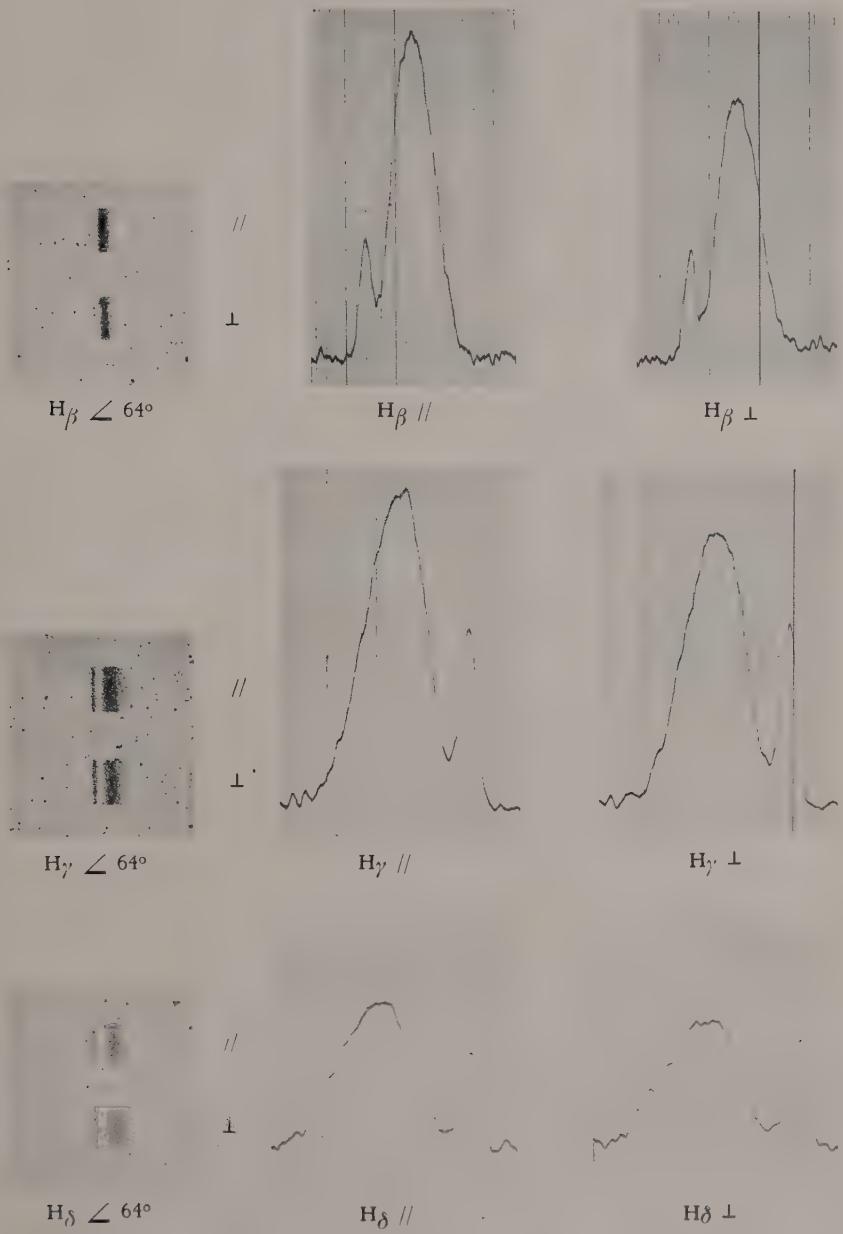
//
⊥
$H_\beta \angle 64°$
H_β //
$H_\beta \perp$
//
⊥
$H_\gamma \angle 64°$
H_γ //
$H_\gamma \perp$
//
⊥
$H_\delta \angle 64°$
H_δ //
$H_\delta \perp$

TABLE I.

Observations under 74°.

Number of plate	Kind of plate	Date	Exposition time	V	i	p	I stat. //	I mov. //	I stat. ⊥	I mov. ⊥
H_β 66	I. Z.	29 Oct. '31	4′	9200	15	0.18	2.72	12.4	1.63	7.03
67	S.R.	29 Oct. '31	8′	9000	20	0.185	1.75	11.7	1 22	6.11
68	I Z.	30 Oct. '31	4′	9150	15	0.18	4.92	19.3	3.86	11.6
68		.	4′	9150	15	0.18	6.17	22.2	4.31	13.3
69	S.R.	30 Oct. '31	7′	9100	18	0.18	2.74	11.7	2.19	7.73
70	Perutz	30 Oct. '31	10′	9200	18	0.18	4.15	16.5	3.57	11.8
70			15′	9200	17	0.18	3.67	13.5	2.28	8.71
H_γ 62	I. Z.	27 Oct. '31	12′	9100	17	0.19	2.43	7.52	1.73	4.88
62			8′	9100	17	0.19	1.23	4.63		2.71
63	Perutz	27 Oct. '31	30′	9100	17—18	0.19	3.06	11.6	2.52	7.48
64	S.R.	27 Oct. '31	30′	9100	17	0.185	1.12	4.24		2.63
64			20′	9100	17	0.185	1.05	4.23		2.48
65	S.R.	28 Oct. '31	30′	9000	18	0.17	2.47	8.71	1.92	5.16
65			20′	9050	17	0.17	1.62	6.00	1.33	3.56
H_δ 71	I. Z.	4 Nov. '31	1 h. 30′	9000	16	0.18	1.12	3.02	1.08	2.00
72	I. Z.	4 Nov. '31	1 h. 45′	9050	17	0.175	1.23	3.51	1.20	2.36
73	I, Z.	5 Nov. '31	1 h. 30′	9000	18	0.18	1.56	3.72	1.31	2.21
75	I. Z.	11 Nov. '31	2 hour	9050	18	0.18	2.48	7.28	2.61	4.71
76	I. Z.	11 Nov. '31	3 hour	9100	18	0.175	4.05	9.12	3.63	6.49

The first researches on the influence of the tension on the polarisation were already made by STARK and LUNELUND [1]).

They were of opinion that the polarisation would increase with increasing tension. This experiment was, however, not exact, because at the same time with the tension the pressure was varied.

In his experiments on the polarisation of light with fading canal rays RUPP [2]) came to the same conclusion: increasing degree of polarisation with increasing tension.

[1]) J. STARK and LUNELUND. Ann. d. Phys. IV **46**. 68. 1915.

[2]) RUPP. Ann. d. Phys. IV. **81**. 615. 1926.

TABLE II.

Observations under 64°.

Number of plate	Kind of plate	Date	Exposition time	V	i	p	I stat. //	I mov. //	I stat. ⊥	I mov. ⊥
H_β 88A.	S. R.	23 Nov. '31	10′	9100	17	0.18	1.76	11.64	1.64	7.60
88B.			10′	9100	17	0.18	1.49	12.22	1.43	7.85
89	I. Z.	23 Nov. '31	5′	8900	17.5	0.19	2.88	18.97	2.30	11.9
89			5′	9100	16	0.188	2.04	14.45	1.70	8.37
90	I. Z.	23 Nov. '31	5′	9100	17	0.18	6.14	24.27	5.09	16.22
90			5′	9100	17	0.18	5.47	21.23	5.30	15.14
H_γ 83A.	I. Z.	20 Nov. '31	15′	9100	17	0.18	5.05	11.91	4.50	8.77
83B.			20′	9100	17	0.18	6.79	14.45	6.37	11.27
84	I. Z.	20 Nov. '20	30′	9100	17	0.18	5.26	12.02	5.24	8.87
84			15′	9100	17	0.18	5.13	11.53	4.95	8.87
85	S. R.	20 Nov. '31	60′	8900	20	0.19	1.97	5.08	1.93	3.68
86	S. R.	20 Nov. '31	50′	9200	15	0.18	3.67	8.71	3.47	6.37
86			30′	9200	15	0.18	3.69	8.53	3.48	6.19
H_δ 92	I, Z.	1 Dec. '31	3 hour	9200	18	0.18	6.22	9.18	6.29	7.36
93	I. Z.	1 Dec. '31	3 h. 30′	9200	18	0.18	4.55	7.67	4.92	6.21
94	I. Z.	2 Dec. '31	6 hour	9200	18	0.18	8.83	12.73	8.83	10.0
H_α 95	Panchr	18 Jan. '32	5′	9100	18	0.183		4.57		3.69
96	Panchr	18 Jan. '32	5′	9200	17	0.18		3.72		2.83
97	Panchr	18 Jan. '32	5′	9100	18	0.18		3.74		3.14
98	Panchr	18 Jan. '32	5′	9400	14	0.17		6.31		4.86

WEIGL [1]) showed that the polarisation diminished with increasing tension and thought that he was justified in ascribing this to the diminution of the moving intensity in proportion to the stationary, when the tension increased.

As my experiments give separately the polarisation of the moving and resting components the influence of tension on the phenomena could be tested again. The results obtained will be given in a future paper.

[1]) WEIGL. Ann. d. Phys. IV, **82**. 1. 1927.

TABLE III.
Polarisation of the light of canalrays under 74°.

H_β	P. Stat.	P. Mov.	H_γ	P. Stat.	P. Mov.	H_δ	P. Stat.	P. Mov.
66	1.67	1.77	62	1.40	1.54	71	1.04	1.51
67	1.43	1.91	62	?	1.71	72	1.02	1.49
68	1.27	1.66	63	1.21	1.55	73	1.19	1.68
68	1.43	1.67	64	?	1.61	75	0.95	1.54
69	1.25	1.51	64	?	1.71	76	1.12	1.40
70		1.40	65	1.29	1.69			
70	1.61	1.50	65	1.22	1.69			
Mean	1.44	1.64	Mean	1.28	1.64	Mean	1.06	1.52

TABLE IV.
Polarisation of the light of canalrays under 64°.

H_β	P. Stat.	P. Mov.	H_γ	P. Stat.	P. Mov.	H_δ	P. Stat.	P. Mov.
88A	1.07	1.53	83A	1.12	1.36	92	0.99	1.25
88B	1.04	1.56	83B	1.07	1.28	93	0.93	1.23
89	1.25	1.59	84	1.00	1.36	94	1.00	1.27
89	1.20	1.73	84	1.04	1.30			
90	1.20	1.50	85	1.02	1.38			
90	1.03	1.40	86	1.06	1.37			
			86	1.06	1.38			
Mean	1.13	1.55	Mean	1.05	1.35	Mean	0.97	1.25

TABLE V.
Polarisation H_α under 64°.

	P	Mean
95	1.24	
96	1.31	
97	1.19	1.26
98	1.30	

I wish to express my gratitude to Prof. P. ZEEMAN, under whose guidance the experiments were made, for his continuous interest in my work.

Laboratorium "Physica" Amsterdam.

Physics. — *The spreading of ovalbumin.* By E. GORTER, J. VAN ORMONDT and F. J. P. DOM. (Communicated by Prof. P. EHRENFEST.)

(Communicated at the meeting of June 25, 1932).

It has been shown previously [1]) by one of us, in collaboration with Dr. F. GRENDEL, that proteins can be made to spread in a mono-layer at the air-water interphase of a Langmuir tray.

For casein the influence of the acidity or alkalinity of the water in the tray has been carefully studied, with the result that at the isoelectric point 4.7 and at a great distance from it, in a distinctly acid and a distinctly alkaline medium, maximal spreading was obtained, whereas at intermediate values of the hydrogen ion concentration at a pH 3 and at pH 8.5 minima were seen. We have concluded that the protein itself and its salts spread beautifully, but that protein-ions occupy a much smaller surface area per molecule.

In the experiments to be related, we have studied the spreading of ovalbumin. We have preferred this protein because it is easily soluble in water without the addition of electrolytes.

Moreover it can easily be prepared in a very pure state. We made use of the HOPKINS—PINKUS method [2]) of preparation as modified by SÖRENSEN.

The ovalbumin was recrystallized 5 to 6 times and then dialyzed against distilled water in the icebox until the sulphate reaction of the water remained negative after 48 hours standing in the dialyzer. Usually several weeks were necessary to reach this state of purity.

The ovalbumin concentration was estimated in two ways:

1. the nitrogen content of the solution was estimated by the TER MEULEN and HESLINGA method [3]). In this method hydrogen gas is passed over a heated mixture of powdered nickel with the sample in which nitrogen is to be estimated and the ammonia formed titrated directly in a receiving tube with 0.01 *n* hydrochloric acid. The nitrogen found, was multiplied by the factor 7.0 to get the ovalbumin.

2. the ovalbumin as such was determined by BANG's method for the estimation of albumin in urine. The albumin is precipitated by boiling with a mixture of dilute acetic acid and sodium acetate, filtered, washed with

---

[1]) E. GORTER and F. GRENDEL. On the Spreading of Proteins. Transactions of the Faraday Society **71**. 1926. p. 477. Biochemische Zeitschrift **201**, 1928, p. 391.

[2]) F. GOWLAND HOPKINS and S. N. PINKUS. Journal of Physiology. **23**. 1898. p. 130.

[3]) TER MEULEN and HESLINGA. Nieuwe methoden voor elementair analyse. Delft 1930. Rec. Trav. Chem. **49** (1930), p. 396.

alcohol and ether and dried to constant weight at 105°. The results of the 2 methods were in good agreement with each other.

These estimations of the ovalbumin content had to be performed fairly often as it appeared to be impossible to keep a solution for an indefinite length of time. Always after some weeks and sometimes even after one week a slight flocculation appeared which made it necessary to filtrate the solution and estimate again. This flocculation had nothing to do with a decay of the protein, but was caused by the instability of the colloidal system when dialysis is prolonged so far that most of the electrolyte is taken away. The stock solutions were always kept in the icebox after adding some preservative, for which thymol was usually taken ; chloroform and toluene seemed less satisfactory, as they rather increased the tendency to flocculate. The concentration of the solution was always about 5 milligram per cc ; e.g. one of the stock solutions had at the outset a concentration of 5.6 mg per cc and after three months when it had been filtered several times, a concentration of 4.6 mg per cc.

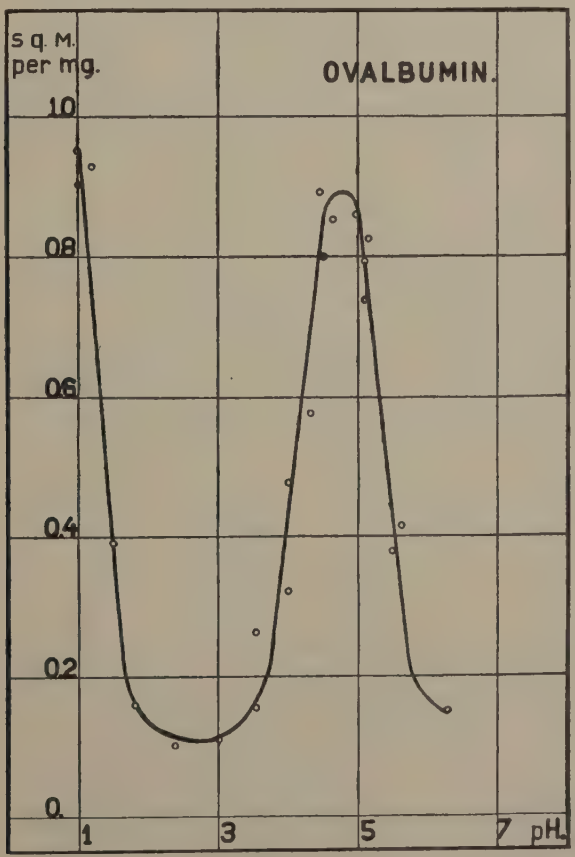

Fig. 1. Influence of *pH*.

The buffer solutions used were in the earlier measurements acetate buffers as described by WALPOLE [1]).

They were diluted to a molarity of $^1/_{300}$ and could be used for pH 3.6 to pH 5.6. The more acid solutions were made with hydrochloric acid. The later experiments were made on veronal-acetate buffersolutions as described by MICHAELIS [2]), also diluted to $^1/_{300}$ mol. This latter buffer has several advantages:

1st. it covers a large pH range, from pH 2 to pH 10;

2nd. it contains only monovalent ions;

3rd. its ionic strength can be kept constant over the whole pH range.

The pH of all buffer solutions was controlled by colorimetric and electrometric measurements.

The influence of changes of the acidity of the water on the spreading of ovalbumin was the same as had been observed with casein. (See fig. 1.)

We have now studied the influence of the addition of different salts to the water in the tray upon the spreading of ovalbumin.

It was easy to show that, at the isoelectric point, salts had no influence on the surface occupied by the protein. But when studying the influence of potassiumchloride on the spreading in acid medium, it was possible to discover a very simple relation between the size of the area and the concentration of Cl ions in the fluid. This relation is to be seen from Fig. 2, where the pCl is plotted against the surface area occupied by the protein.

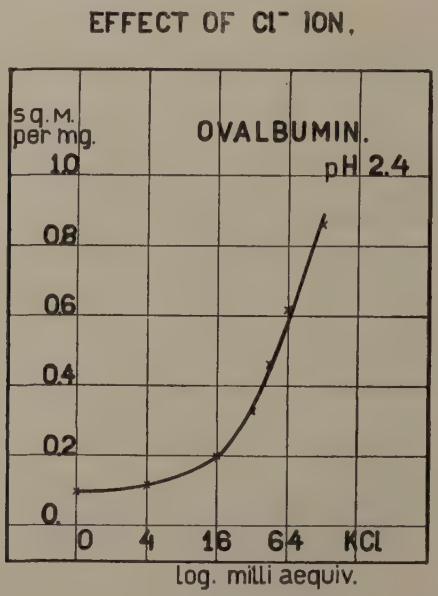

Fig. 2

[1]) G. S. WALPOLE. Journ. Chem. Soc. **105**. (1914). p. 20001.

[2]) L. MICHAELIS. Bioch. Ztschr. **234**. (1931). p. 139.

The part of the curve between pH 1.2 and pH 3, is explained by the presence of Cl ion in the water, because HCl and KCl have exactly the same influence on the spreading (fig. 3). We may conclude from this observation which can be made as well with other salts (e.g. $BaCl_2$ fig. 3*a*) that the addition of

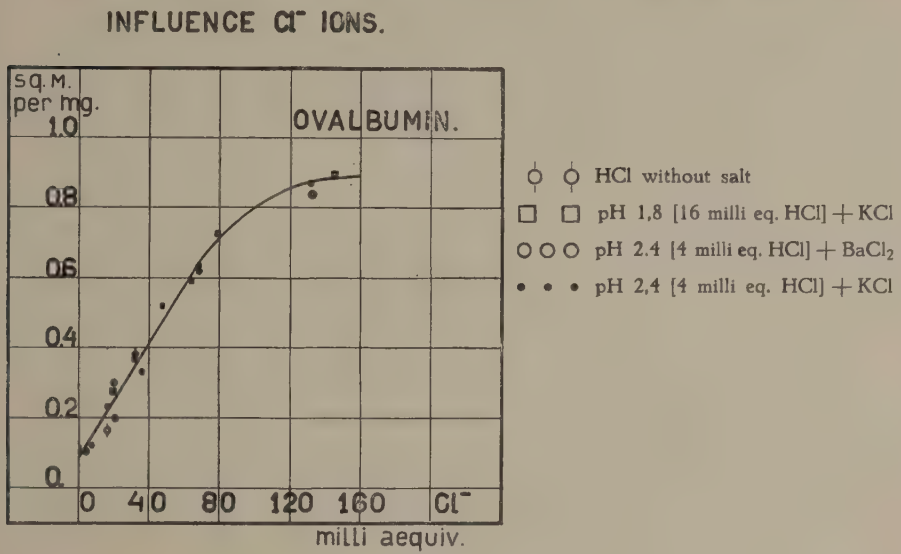

Fig. 3

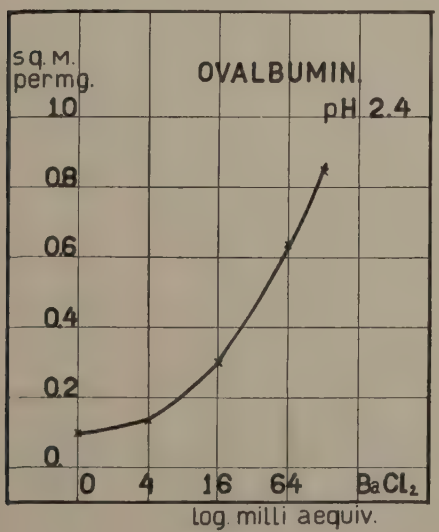

Fig. 3a

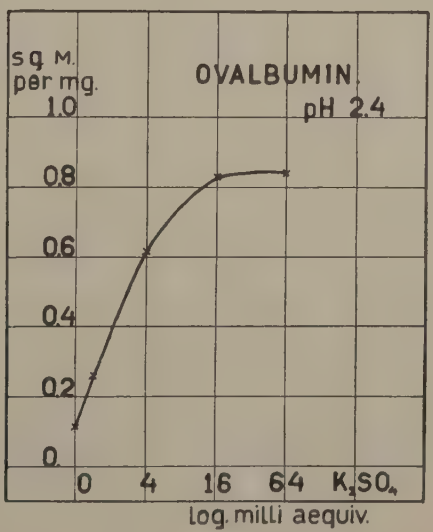

Fig. 4

EFFECT OF MTSK⁻⁻ION.

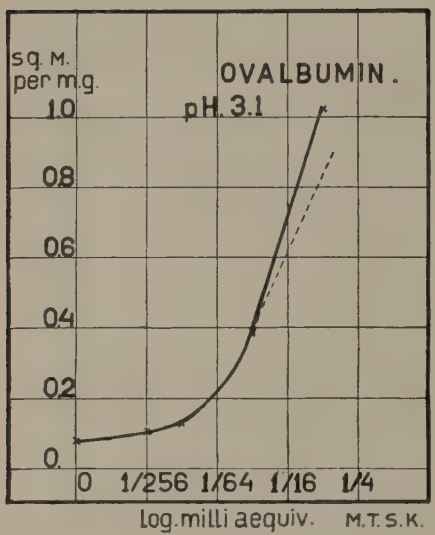

Fig. 5

EFFECT OF K^{+} ION.

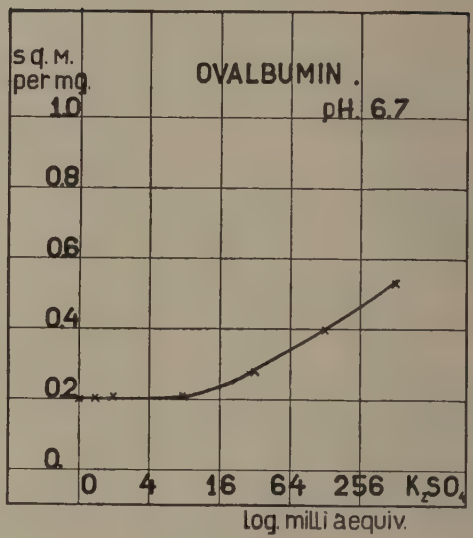

Fig. 6

EFFECT OF Ba^{++} ION.

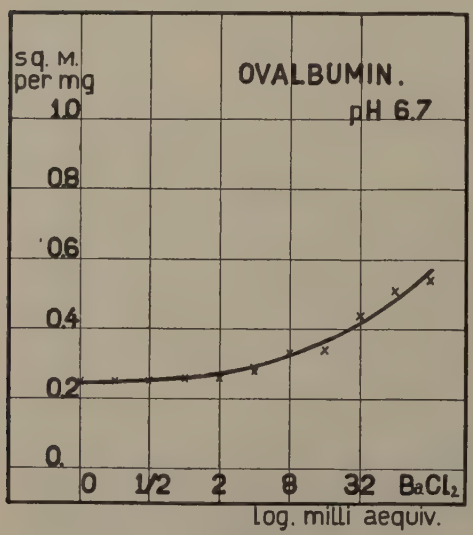

Fig. 7

EFFECT OF LUTEO^{+++} ION.

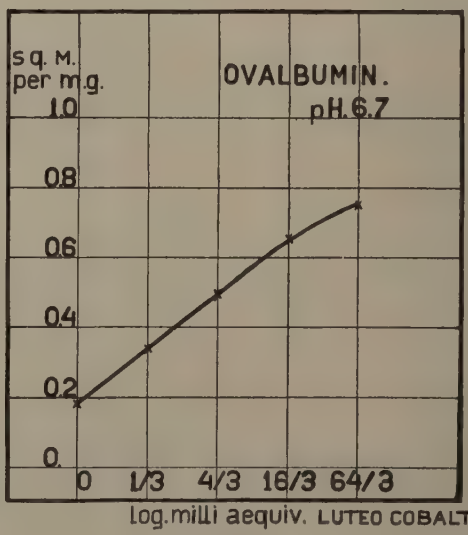

Fig. 8

Cl ions has the tendency to increase the area of spread of a protein salt, that is completely ionized. It has a disionizing effect. The relation between pCl and the area is linear (See already Bioch. Zeitschr. 1. c. p. 404). Now if this interpretation is the right one, bi-valent and tri-valent negative ions should have an identical effect in much lower concentration. This is indeed what had been observed.

We found that SO_4 ions have in much smaller concentration the same discharging effect as the monovalent (See fig. 4). And the tri-valent have an effect, that is identical, but can be observed when making use of still lower concentrations. The tri-valent negative ion was methane tri-

sulphonate 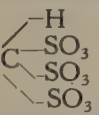 [1]). (See fig. 5.)

It was interesting to see what would happen on the alkaline side of the iso-electric point after addition of positive ions.

It is hardly necessary to say that KCl has also an influence on the minimum spreading at the alkaline side (fig. 6), but that K_2SO_4 and the methane trisulphonate have no effect in the small concentrations used.

On the contrary the bi-valent positive ions Ba^{++} and Ca^{++} have the same effect on the spreading at pH 8 as the SO_4^{--} at pH 3 (fig. 7) and we were also able to observe a very strong influence of luteocobaltchloride $CO(NH_3)_6Cl_3$ on the spreading at pH 8 (see fig. 8). It is obvious, that this adds convincing arguments to the interpretation given before: at the isoelectric point the neutral protein-molecule spreads in a thin layer: the addition of H^+ (and OH^-) ions diminishes the area occupied by the protein, so much so that it occupies only $^1/_9$ of the surface. Further addition of negative ions at the acid side of the isoelectric point (from pH 3 downwards) increases the surface by eliminating the charge of the protein ions. The same holds good for the addition of positive ions in alkaline medium. Valency has a very striking influence: tri-valent ions acting more strongly than bi-valent and mono-valent ions having a much smaller influence than bi-valent.

[1]) We made use of this salt following the advise of Prof. BUNGENBERG DE JONG. It was kindly given to us by Prof. BACKER.

Mathematics. — *Zur generellen Feldtheorie.* DIRAC*sche Gleichungen und* HAMILTON*sche Funktion.* Von J. A. SCHOUTEN und D. VAN DANTZIG. (Communicated by Prof. P. EHRENFEST).

(Communicated at the meeting of May 28, 1932).

In der vorigen Mitteilung [1]) haben wir u. a. gezeigt dass in der

[1]) J. A. SCHOUTEN und D. VAN DANTZIG, Zum Unifizierungsproblem der Physik. Skizze einer generellen Feldtheorie, Proc. Kon. Akad. **35** (1932) 642—655. zitiert mit G. F. I.

projektivisierten Gleichung der Weltlinien statt des nur bis auf einen Gradienten bestimmten elektromagnetischen Potentialvektors der vollständig bestimmte potentielle Impulsenergiepunkt auftritt. Wir zeigen hier dass die projektivisierte DIRACsche Gleichung sich auf eine Form bringen lässt, die ebenfalls nur diesen Impulsenergiepunkt enthält. Gleichzeitig wird dadurch der in der Spingrösse ψ^C auftretende unbestimmte Faktor eindeutig festgelegt. Der Operator $\frac{h}{i}\nabla_\mu$ ist dann quantentheoretisch aequivalent mit dem totalen Impulsenergiepunkt p_μ und der hinter α^μ in der DIRACschen Gleichung auftretende Operator ist aequivalent mit einem *Punkt auf der Fundamentalquadrik*. Aus dieser Form der DIRACschen Gleichung ergibt sich eine HAMILTONsche Funktion, die bis auf einen Faktor $\frac{1}{2m}$ nichts anderes ist als das skalare Produkt dieses Punktes mit dem ebenfalls auf der Quadrik gelegenen komplex konjugierten Punkt. In der Tat liefert diese HAMILTONsche Funktion die richtigen kanonischen Gleichungen für die Weltlinien.

Zum Schluss wird gezeigt, wie man in der Praxis von den nichthomogenen gewöhnlichen Weltkoordinaten zu den homogenen Koordinaten übergehen kann, welche Unbestimmtheit dabei auftritt und was die Bedeutung dieser Unbestimmtheit ist.

§ 1. DIRACsche *Gleichung.*

In G. F. I haben wir die DIRACsche Gleichung auf die Form

$$\frac{h}{i}\,\alpha^{\mu C}_{\cdot\cdot A}\,\nabla_\mu\,\psi^A = 0 \quad . \quad . \quad . \quad . \quad . \quad . \quad . \quad . \quad (1)$$

gebracht, wo ψ^A eine Pseudospinvektordichte vom Gewicht $+\frac{1}{4}$ ist, deren kovariante Differentiation folgendermassen definiert war:

$$\nabla_\mu \psi^C = \partial_\mu \psi^C + \Lambda^C_{A\mu}\,\psi^A - \frac{ei}{ch}\varphi_\mu - \frac{mc}{h\omega}\,x_\mu \quad . \quad . \quad . \quad . \quad . \quad (2)$$

Die $\Lambda^C_{A\mu}$ sind bestimmt durch die Forderung dass die kovariante Ableitung von $\alpha^{\nu C}_{\cdot\cdot A}$ verschwindet; diese lautet in bezug auf das orthogonale anholonome Bezugssystem (c):

$$\nabla_b\,\alpha^{cC}_{\cdot\cdot A} = \partial_b\,\alpha^{cC}_{\cdot\cdot A} + \Pi^c_{ab}\,\alpha^{aC}_{\cdot\cdot A} + \Lambda^C_{Bb}\,\alpha^{cB}_{\cdot\cdot A} - \alpha^{cC}_{\cdot\cdot B}\,\Lambda^B_{Ab} = 0 \quad . \quad . \quad (3)$$

Zur Berechnung der Λ^C_{Ab} wählen wir die Bezugssysteme in den Spinräumen so, dass $\partial_b \alpha^{cC}_{\cdot\cdot A}$ verschwindet. Λ^C_{Ab} lässt sich für jedes b als Sedenion mit der Spur Null jedenfalls linear in den fünf $\alpha^{cC}_{\cdot\cdot A}$ und den zehn $\alpha^{[ac]C}_{\cdot\cdot\cdot A}$ ausdrücken:

$$\Lambda^C_{Ab} = (\tfrac{1}{4}\,\Lambda^D_{Eb}\,\alpha_{c\,\cdot\cdot\,D}^{\cdot\cdot\,E})\,\alpha^{cC}_{\cdot\cdot A} + (\tfrac{1}{8}\,\Lambda^D_{Eb}\,\alpha_{[ca]\,\cdot\cdot\,D}^{\cdot\cdot\,E})\,\alpha^{[ac]C}_{\cdot\cdot\cdot A} \quad . \quad . \quad . \quad (4)$$

Wird dies in (3) eingesetzt, so ergibt sich

$$\Lambda^C_{Ab} = -\tfrac{1}{4}\, \Pi^c_{ab}\, \alpha^{a\,.\,C}_{.\,c\,.\,A} \quad . \quad . \quad . \quad . \quad . \quad . \quad . \quad . \quad (5)$$

Ausgehend von den in dieser Weise berechneten Λ^C_{Ab} lassen sich die $\Lambda^C_{A\mu}$ in bezug auf beliebige Bezugssysteme in der Raumzeitwelt und im Spinraum in der üblichen Weise ableiten. φ_μ ist der Potentialvektor, der sich folgendermassen verändert wenn ψ^C einen Faktor $e^{i\gamma}$ bekommt:

$$'\varphi_\mu = \varphi_\mu + \frac{hc}{e}\,\partial_\mu \gamma \quad . \quad . \quad . \quad . \quad . \quad . \quad . \quad . \quad (6)$$

Die Form (1) hat folgende Nachteile: 1. Die kovariante Differentiation der Spinoren hängt von e und m ab, während die Uebertragung der Projektoren und Affinoren, die in den makrokosmischen Gleichungen auftritt, von e und m unabhängig ist. 2. In der Gleichung der geodätischen Linien ist es gelungen, den unbestimmten Vektor $\frac{e}{c}\varphi_\mu$ durch den bestimmten potentiellen Impulsenergiepunkt $\frac{e}{c\lambda}\, x_\mu$ zu ersetzen; in (2) tritt aber φ_μ noch neben x_μ auf.

Der zweite Uebelstand lässt sich leicht beseitigen. Wir haben in G. F. I bewiesen, dass es bei jeder Wahl von φ_μ einen solchen projektiven Skalar χ vom Exzess (und Grad) 1 gibt, dass

$$\varphi_\mu = \frac{1}{\lambda}(x_\mu + \omega^2\, \partial_\mu \log \chi); \quad \lambda = \frac{\omega k}{c}; \quad k = \sqrt{\frac{\varkappa}{2}}. \quad . \quad . \quad . \quad (7)$$

ist. Für $\varphi = -\omega \frac{e}{kh} \log \chi$ wird wegen (5) und (7) $'\varphi_\mu = \frac{1}{\lambda}\, x_\mu$.

Führen wir also eine Spinvektordichte Ψ^C vom Gewicht $+\,{}^1/_4$ und vom Grad und Exzess $-i\omega \frac{e}{hk}$ ein vermöge der Gleichung

$$\Psi^C = \chi^{-i\omega \frac{e}{hk}} \psi^C, \quad . \quad . \quad . \quad . \quad . \quad . \quad . \quad . \quad (8)$$

so geht die Gleichung (1) über in

$$\alpha^{\mu C}_{\ \ .\,.\,B} \left(\frac{h}{i}\, \partial_\mu \Psi^B + \frac{h}{i}\, \Lambda^B_{A\mu}\, \Psi^A - \frac{e}{\omega k}\, x_\mu\, \Psi^B + i \frac{mc}{\omega}\, x_\mu\, \Psi^B \right) = 0 \quad . \quad (9)$$

Im Gegensatz zu ψ^C ist Ψ^C keine Pseudospinvektordichte sondern eine Spinvektordichte, d.h. (als Funktion der x^ν betrachtet) nicht nur bis auf einen beliebigen unimodularen Faktor sondern bis auf einen (unwesentlichen) *konstanten* Faktor dieser Art bestimmt. Da Ψ^C und ψ^C sich nur um einen unimodularen Faktor unterscheiden, ändert sich physikalisch bei der Ersetzung von ψ^C durch Ψ^C nichts.

Der zweite Uebelstand lässt sich dadurch beseitigen, dass in (9) das Symbol der kovarianten Differentiation von kontravarianten Spinvektordichten vom Exzess $-i\omega \frac{e}{h}\sqrt{\frac{2}{\varkappa}}$ eingeführt wird. Wie einer von uns

früher gezeigt hat[1]), hat die kovariante Ableitung eines Skalars vom Exzess ε die Form

$$\nabla_\mu p = \partial_\mu p + \varepsilon Q_\mu p, \quad . \quad . \quad . \quad . \quad . \quad . \quad . \quad (10)$$

wo Q_μ irgend ein für allemal gegebenes kovariantes Punktfeld vom Exzess Null ist. Daraus folgt, dass die kovariante Differentiation einer kontravarianten Spinvektordichte vom Gewicht $\frac{1}{4}$ und vom Exzess ε folgendermassen lautet:

$$\nabla_\mu \Psi^C = \partial_\mu \Psi^C + \Lambda^C_{A\mu} \Psi^A + \varepsilon Q_\mu \Psi^C, \quad . \quad . \quad . \quad . \quad (11)$$

und dass sich (9) schreiben lässt:

$$\alpha^{\mu C}_{\cdot\cdot A} \left(\frac{h}{i} \nabla_\mu + \frac{e\omega}{k} Q_\mu - \frac{e}{\omega k} x_\mu + i \frac{mc}{\omega} x_\mu \right) \Psi^A = 0. \quad . \quad . \quad (12)$$

Wenn nun die Hyperebene Q_μ nicht mit x_μ koinzident wäre, so würde es eine auch bei Abwesenheit von Ladung und Masse ausgezeichnete Richtung geben, (nämlich diejenige der Gerade durch x^ν und Q^ν), der keine physikalische Bedeutung zukäme. Fordern wir also dass dies nicht der Fall sei, so wird

$$Q_\mu = -\omega^{-2} Q_0 x_\mu, \quad Q_0 = Q_\mu x^\mu . \quad . \quad . \quad . \quad . \quad . \quad (13)$$

Also geht (12) über in

$$\alpha^{\mu C}_{\cdot\cdot A} \left(\frac{h}{i} \nabla_\mu - \frac{e}{k} (Q_0 + 1) \omega^{-1} x_\mu + i \frac{mc}{\omega} x_\mu \right) \Psi^A = 0. \quad . \quad . \quad (14)$$

Vergleichung der Gleichung

$$m i^\nu = p^\nu - \frac{e}{k} \omega^{-1} x^\nu . \quad . \quad . \quad . \quad . \quad . \quad . \quad . \quad (15)$$

mit (14) legt es nahe zu fordern, dass der Operator $\frac{h}{i} \nabla_\mu$[2]) quantentheoretisch aequivalent sei mit dem totalen Impulsenergiepunkt p_μ. Soll nun auch die algebraische Gleichung, die aus (14) entsteht wenn $\frac{h}{i} \nabla_\mu$ durch p_μ ersetzt wird, nämlich

$$\left.\begin{aligned} &\alpha) \quad \alpha^{\mu C}_{\cdot\cdot A} n_\mu \Psi^A = 0, \\ &\beta) \quad n_\mu = p_\mu - \frac{e}{k} (Q_0 + 1) \omega^{-1} x_\mu + i \frac{mc}{\omega} x_\mu, \end{aligned}\right\} \quad . \quad . \quad . \quad . \quad (16)$$

---

[1]) D. VAN DANTZIG, Theorie des projektiven Zusammenhangs n-dimensionaler Räume, Math. Ann. **106**, (1932) 400—454.

[2]) Man kann ohne das Resultat zu ändern auch $\frac{h}{i} \overset{R}{\nabla}_\mu$ wählen, da aus (78) von G. F. I folgt, dass $\alpha^\mu \nabla_\mu \Psi^C = \alpha^\mu \overset{R}{\nabla}_\mu \Psi^C$ ist.

eine Lösung $\Psi^C \neq 0$ haben, so muss der Punkt n^ν auf der Quadrik liegen, wie sich durch Ueberschiebung von (16α) mit $\alpha^{\nu D}_{\cdot\cdot C} n_\lambda$ sofort ergibt. Nun zeigt man aber leicht, dass die beiden Schnittpunkte der Verbindungsgeraden von x^ν und p^ν mit der Quadrik

$$\left.\begin{matrix} n^\nu \\ \bar{n}^\nu \end{matrix}\right\} = p^\nu - \frac{e}{k}\,\omega^{-1}\,x^\nu \pm i\,\frac{mc}{\omega}\,x^\nu \quad . \quad . \quad . \quad . \quad . \quad (17)$$

sind. Vergleich mit (16β) zeigt, dass $Q_0 = 0$ also wegen (13)

$$Q_\mu = 0 \quad . \quad . \quad . \quad . \quad . \quad . \quad . \quad . \quad . \quad (18)$$

sein muss.

Wir wollen die jetzt erhaltene Gleichung

$$\alpha^{\mu C}_{\cdot\cdot A}\left(\frac{h}{i}\,\nabla_\mu - \frac{e}{k}\,\omega^{-1}\,x_\mu + \imath\frac{mc}{\omega}\,x_\mu\right)\Psi^A = 0 \quad . \quad . \quad . \quad (19)$$

zerlegen.

Bekanntlich bestimmt α^0 zwei invariante Ebenen im Spinraum, in Bezug auf welche jeder Spinor zerlegt werden kann. Die Zerlegung von α^0, α^k und α lautet:

$$\left.\begin{aligned} &\alpha^0 = -\,i\,\omega^{-1}\,\underset{0}{\iota}\,\underset{0}{\iota} + i\,\omega^{-1}\,\underset{0}{\bar{\iota}}\,\underset{0}{\bar{\iota}}\,, \\ &\alpha^k = \beta^k + \bar{\beta}^k\,, \\ &\alpha = \underset{0}{\iota}\,\underset{0}{\bar{\iota}}\,. \end{aligned}\right\} \quad \left\{\begin{aligned} &\beta^k = \underset{0}{\iota}\,\alpha^k\,\underset{0}{\bar{\iota}} = \underset{0}{\iota}\,\alpha^k = \alpha^k\,\underset{0}{\bar{\iota}}\,, \\ &\bar{\beta}^k = \underset{0}{\bar{\iota}}\,\alpha^k\,\underset{0}{\iota} = \underset{0}{\iota}\,\alpha^k = \alpha^k\,\underset{0}{\iota}\,, \end{aligned}\right\} \quad . \quad . \quad . \quad . \quad (20)$$

$\underset{0}{\iota}$ und $\underset{0}{\bar{\iota}}$ sind die Einheitsspinoren in den invarianten Ebenen. Je zwei Koordinatenachsen können in jede dieser Ebenen gelegt werden, und die Wahl kann so getroffen werden dass die Komponenten β^k und $\bar{\beta}^k$ sowie $\underset{0}{\iota}$ und $\underset{0}{\bar{\iota}}$ komplex konjugierte Bestimmungszahlen bekommen. Schreiben wir dann $v^{\mathfrak{a}}$, ($\mathfrak{a}, \ldots, \mathfrak{h} = 5, 6$) für einen Vektor in der einen Ebene und $v^{\mathfrak{A}}$, ($\mathfrak{A}, \ldots, \mathfrak{H} = 5, 6$ für den Vektor mit den komplex konjugierten Bestimmungszahlen in der anderen Ebene, so schreiben sich die Bestimmungszahlen von $\underset{0}{\iota}, \underset{0}{\bar{\iota}}, \beta^k, \bar{\beta}^k$:

$$\left.\begin{aligned} &\underset{0}{\iota}{}^{\mathfrak{a}} \quad ; \quad \underset{0}{\iota}{}^{\mathfrak{A}} \\ &\beta^{k\mathfrak{a}}_{\cdot\cdot\mathfrak{A}} \quad ; \quad \bar{\beta}^{k\mathfrak{A}}_{\cdot\cdot\mathfrak{a}} \end{aligned}\right\} \quad . \quad . \quad . \quad . \quad . \quad . \quad . \quad . \quad (21)$$

$\beta^{kc}_{\ldots\mathfrak{A}}$ und $\bar{\beta}^{k\mathfrak{C}}_{\ldots a}$ liegen mit einem Index in der einen, mit dem anderen Index in der anderen Ebene und es ist

$$\left.\begin{aligned} \beta^{(ij)} &= g^{ij}{}_{\underset{0}{\iota}} \quad ; \quad \beta^{ij} = \beta^{i}\ \bar{\beta}^{j} \\ \bar{\beta}^{(ij)} &= g^{ij}{}_{\underset{0}{\bar{\iota}}} \quad ; \quad \bar{\beta}^{ij} = \bar{\beta}^{i}\ \beta^{j}. \end{aligned}\right\} \quad \ldots\ldots \quad (22)$$

Zerlegung von Λ^{C}_{Ab} führt zu

$$\left.\begin{aligned} \Lambda^{c}_{ab} &= -\tfrac{1}{4}\,\Pi^{k}_{ib}\,\beta^{i}_{.k.}{}^{c}_{a} \\ \Lambda^{\mathfrak{C}}_{\mathfrak{A}b} &= -\tfrac{1}{4}\,\Pi^{k}_{ib}\,\bar{\beta}^{i}_{.k.}{}^{\mathfrak{C}}_{\mathfrak{A}} \\ \Lambda^{c}_{\mathfrak{A}b} &= \tfrac{1}{2}\,i\,\omega^{-1}\,\Pi^{k}_{0b}\,\beta^{\ c}_{k.\mathfrak{A}} \\ \Lambda^{\mathfrak{C}}_{ab} &= -\tfrac{1}{2}\,i\,\omega^{-1}\,\Pi^{k}_{0b}\,\bar{\beta}^{\ \mathfrak{C}}_{k.a} \end{aligned}\right\} \quad \ldots\ldots \quad (23)$$

und die Zerlegung von (19) führt zu den Gleichungen

$$\left.\begin{aligned} \frac{h}{i}\,\bar{\beta}^{j}{}_{\ldots\mathfrak{b}}^{\mathfrak{C}}\left(\partial_j\,\Psi^{\mathfrak{b}} + \Lambda^{\mathfrak{b}}_{aj}\,\Psi^{a}\right) + mc\,\Psi^{\mathfrak{C}} &= 0 \\ \frac{h}{i}\,\beta^{j}{}_{\ldots\mathfrak{B}}^{\ c}\left(\partial_j\,\Psi^{\mathfrak{B}} + \Lambda^{\mathfrak{B}}_{\mathfrak{A}j}\,\Psi^{\mathfrak{A}}\right) - mc\,\Psi^{c} &= 0 \end{aligned}\right\} \quad \ldots\ldots \quad (24)$$

wo Ψ^{c}, $\Psi^{\mathfrak{C}}$ die beiden durch Zerlegung von Ψ^{C} entstehenden Spinvektordichten sind. Es ist bemerkenswert, dass e in den Gleichungen (24) nicht mehr explizit auftritt. Implizit kommt e in dem Grad von Ψ^{C} vor.

Elimination von Ψ^{c} bzw. $\Psi^{\mathfrak{C}}$ aus diesen Gleichungen liefert

$$\left.\begin{aligned} -h^2\,\beta^{ij}{}_{\ldots a}^{\ c}\overset{R}{\nabla}_{ij}\Psi^{a} + m^2c^2\,\Psi^{c} &= 0, \text{ [1]} \\ -h^2\,\bar{\beta}^{ij}{}_{\ldots\mathfrak{A}}^{\mathfrak{C}}\overset{R}{\nabla}_{ij}\Psi^{\mathfrak{A}} + m^2c^2\,\Psi^{\mathfrak{C}} &= 0, \end{aligned}\right\} \quad \ldots\ldots \quad (25)$$

welche Gleichungen die zwei (mit $\overset{R}{\nabla}$ anstatt ∇ geschriebenen) Komponenten sind der Gleichung

$$\alpha^{abC}_{\ldots A}\left(\frac{h}{i}\nabla_a - \frac{e}{\omega k}x_a + i\frac{mc}{\omega}x_a\right)\left(\frac{h}{i}\nabla_b - \frac{e}{\omega k}x_b - i\frac{mc}{\omega}x_b\right)\Psi^{A} = 0 \quad (26)$$

[1]) Die Form der Gleichung (25) ist dieselbe wie im feldfreien Fall. Der Spinterm entsteht aus dem ersten Term von (25), dessen alternierter Teil ausser dem Gravitationsterm noch den Term

$$-h^2\,\beta^{ij}{}_{\ldots a}^{\ c}\,\overset{R}{S}{}^{\ldots k}_{ij}\,\overset{R}{\nabla}_k\psi^{a} = \frac{ieh}{2c}\,F_{ij}\,\beta^{ij}{}_{\ldots a}^{\ c}\,\psi^{a} \quad \text{bzw.} \quad \frac{ieh}{2c}\,F_{ij}\,\bar{\beta}^{ij}{}_{\ldots\mathfrak{A}}^{\mathfrak{C}}\,\psi^{\mathfrak{A}}$$

hervorruft.

Aus dieser letzten Gleichung folgt aber bei Ersetzung von $\frac{h}{i}\nabla_\mu$ durch p_μ dass

$$\left.\begin{aligned} H &= \frac{1}{4m}\alpha^{\lambda\mu}(n_\lambda \bar{n}_\mu + \bar{n}_\lambda n_\mu) = \\ &= \frac{1}{2m}\left\{ p_\lambda p_\mu G^{\lambda\mu} - 2\frac{e}{k}\omega^{-1} p_\lambda x^\lambda + \left(\frac{e^2}{k^2\omega^2} + \frac{m^2c^2}{\omega^2}\right) x^\lambda x^\mu G_{\lambda\mu} \right\} \end{aligned}\right\} \quad (27)$$

die HAMILTONsche Funktion ist. Ihr Wert ist $-mc^2$.

In der Tat ergibt diese Funktion unter Benutzung von $\frac{\delta p^\nu}{d\tau} = 0$ gerade die kanonischen Gleichungen der Weltlinien geladener Massenpunkte

$$\left.\begin{aligned} \frac{\partial H}{\partial p_\nu} &= \frac{1}{m}\left(p^\nu - \frac{e}{k}\omega^{-1} x^\nu\right) = \frac{d' x^\nu}{d\tau}; \quad \frac{d'}{d\tau} = i^\mu \partial_\mu \\ \frac{\partial H}{\partial x^\lambda} &= -\Pi^\nu_{\lambda\mu} p_\nu i^\mu = \frac{d' p_\lambda}{d\tau}, \end{aligned}\right\} \quad . \quad . \quad . \quad (28)$$

wo bei der partiellen Ableitung p_ν und x^ν als unabhängig von einander, und $G_{\lambda\mu}$, $G^{\lambda\mu}$ als nur von den x^ν abhängig zu betrachten sind.

§ 2. *Uebergang von den gewöhnlichen zu den homogenen Koordinaten.*

Es ist für die praktische Rechnung wichtig, zu wissen wie sich der Uebergang von den gewöhnlichen zu den homogenen Koordinaten vollzieht. Wir gehen also aus von einer gewöhnlichen V_4 mit Koordinaten ξ^k, $(h, \ldots m = \mathbf{1}, \mathbf{2}, \mathbf{3}, \mathbf{4})$ und Fundamentaltensoren g_{ij}, g^{jk}, und setzen voraus, dass der Potentialvektor φ_i bis auf einen Gradienten gegeben ist. Sodann führen wir 5 Koordinaten x^ν $(\iota, \varkappa, \ldots \omega = 0, 1, 2, 3, 4)$ ein, die der einzigen Bedingung genügen, dass die ξ^k vier unabhängige Funktionen der x^ν vom Grade Null sind. Dann sind die A^k_λ bekannt:

$$A^k_\lambda = \partial_\lambda \xi^k, \quad . \quad . \quad . \quad . \quad . \quad . \quad . \quad . \quad . \quad (29)$$

und damit

$$\left.\begin{aligned} g_{\lambda\mu} &= A^{ij}_{\lambda\mu} g_{ij}, \\ \varphi_\lambda &= A^i_\lambda \varphi_i, \\ x_{\mu\lambda} &= \frac{k\omega}{c}\partial_{[\mu}\varphi_{\lambda]}. \end{aligned}\right\} \quad . \quad . \quad . \quad . \quad . \quad . \quad . \quad (30)$$

Ferner ist bekannt, dass es einen solchen Skalar χ vom Grad und Exzess $+1$ gibt, dass

$$\varphi_\lambda = \frac{c}{k\omega}(x_\lambda + \omega^2 \partial_\lambda \log \chi). \quad . \quad . \quad . \quad . \quad . \quad . \quad (31)$$

ist. Wir können jetzt bei *bestimmter* Wahl von φ_i für χ *eine ganz beliebige Funktion der* x^ν *vom Grade 1* wählen und damit x_λ festlegen. Damit liegen dann auch

$$G_{\lambda\mu} = g_{\lambda\mu} - \omega^{-2} x_\lambda x_\mu \quad . \quad . \quad . \quad . \quad . \quad . \quad . \quad . \quad (32)$$

und $G^{\mu\nu}$ fest, und die A_i^ν lassen sich eindeutig aus dem Gleichungssystem

$$\left.\begin{aligned} A_\mu^k A_i^\mu &= A_i^k, \\ A_i^\mu x_\mu &= 0 \end{aligned}\right\} \quad . \quad . \quad . \quad . \quad . \quad . \quad . \quad . \quad . \quad (33)$$

berechnen. Als Beispiel wählen wir

$$\left.\begin{aligned} \xi^k &= \frac{x^\gamma}{x^0}\,\delta_\gamma^k \qquad (\alpha, \ldots, \theta = 1, 2, 3, 4)\ ^1) \\ \chi &= x^0.\ ^2) \end{aligned}\right\} \quad . \quad . \quad . \quad . \quad (34)$$

Dann ist

$$\left.\begin{aligned} A_\alpha^k &= \frac{1}{x^0}\,\delta_\alpha^k \\ A_0^k &= -\frac{x^\gamma}{x^0\,x^0}\,\delta_\gamma^k \end{aligned}\right\} \quad . \quad . \quad . \quad . \quad . \quad . \quad . \quad . \quad (35)$$

$$\varphi_\alpha = \frac{1}{x^0}\,\delta_\alpha^k \varphi_k \quad ; \quad \varphi_0 = -\frac{x^\gamma}{x^0\,x^0}\,\delta_\gamma^k \varphi_k \quad . \quad . \quad . \quad . \quad . \quad (36)$$

$$\left.\begin{aligned} \frac{1}{\lambda} x_\alpha &= \frac{1}{x^0}\,\delta_\alpha^k \varphi_k - \frac{1}{\lambda}\,\omega^2\,\partial_\alpha \log x^0 = \frac{1}{x^0}\,\delta_\alpha^k \varphi_k = \varphi_\alpha, \\ \frac{1}{\lambda} x_0 &= -\frac{x^\gamma}{x^0\,x^0}\,\delta_\gamma^k \varphi_k - \frac{1}{\lambda}\,\frac{\omega^2}{x^0} = \varphi_0 - \frac{\omega^2}{\lambda x^0}. \end{aligned}\right\} \quad . \quad . \quad (37)$$

Aus obenstehendem folgt, dass der projektive Zusammenhang durch g_{ij} und φ_i *nicht* eindeutig bestimmt ist. Namentlich ist der kovariante Punkt x_λ, dessen Wahl alles festlegt, nur bis auf einen Vektorgradienten bestimmt; der projektive Zusammenhang gestattet also die Transformation

$$'x_\lambda = x_\lambda - \omega^2 \chi_\lambda \, , \quad . \quad . \quad . \quad . \quad . \quad . \quad . \quad . \quad (38)$$

---

[1]) δ_γ^k ist das erweiterte Kroneckes Symbol, dass 0 oder 1 darstellt je nachdem k und γ durch entsprechende oder nicht entsprechende Zeichen aus den Reihen *1, 2, 3, 4* und 1, 2, 3, 4 ersetzt werden. Wir können für $x^\gamma\,\delta_\gamma^k$ natürlich nicht x^k schreiben, weil z.B. $x^1 = |= x^1 (= 0)$ ist.

[2]) In Gleichungen, die *nicht* differenziert werden, kann x^0 durch 1 ersetzt werden, weil die Projektoren doch nur bis auf einen beliebigen Faktor bestimmt sind. Diese spezialisierte Form der Gleichungen ist natürlich nicht mehr bei $\mathfrak{H}$ invariant.

wo χ_λ Vektorgradient eines beliebigen Skalars von Exzess Null ist, d.h. den Bedingungen

$$\left.\begin{aligned} \partial_{[\mu}\,\chi_{\lambda]} &= 0, \\ x^\nu\,\chi_\nu &= 0 \end{aligned}\right\} \quad \ldots\ldots\ldots \quad (39)$$

zu genügen hat. Daraus geht hervor dass sämtliche kontra-bzw. kovariante Vektoren sich bei (38) folgendermassen transformieren:

$$\left.\begin{aligned} {}'v^\nu &= T^\nu_{.\lambda}\,v^\lambda\,; \quad T^\nu_{.\lambda} = \mathcal{A}^\nu_\lambda - \chi_\lambda\,x^\nu\,; \\ {}'w_\lambda &= \overset{-1}{T}{}^\nu_{.\lambda}\,w_\nu\,; \quad \overset{-1}{T}{}^\nu_{.\lambda} = \mathcal{A}^\nu_\lambda + \chi_\lambda\,x^\nu \end{aligned}\right\} \quad \ldots\ldots \quad (40)$$

Es ist also z.B. [1])

$$\left.\begin{aligned} {}'G_{\lambda\mu} &= G_{\lambda\mu} + 2\,x_{(\lambda}\chi_{\mu)} - \omega^2\,\chi_\lambda\,\chi_\mu\,; \\ {}'G^{\mu\nu} &= G^{\mu\nu} - 2\,x^{(\mu}\chi^{\nu)} + \chi_\rho\,\chi^\rho x^\mu x^\nu \end{aligned}\right\} \quad \ldots\ldots \quad (41)$$

$$\left.\begin{aligned} {}'i^\nu &= i^\nu - \chi_\lambda\,i^\lambda\,x^\nu\,; & {}'p^\nu &= p^\nu - m\chi_\lambda\,i^\lambda\,x^\nu \\ {}'i_\lambda &= i_\lambda\,; & {}'p_\lambda &= p_\lambda - \omega\frac{e}{k}\,\chi_\lambda\,. \end{aligned}\right\} \quad \ldots\ldots \quad (42)$$

und

$${}'\nabla_\mu\,T^\nu_{.\lambda}\,v^\lambda = T^\nu_{.\rho}\,(\nabla_\sigma v^\rho)\,\overset{-1}{T}{}^\sigma_{.\mu} \quad \ldots\ldots\ldots \quad (43)$$

wo ${}'\nabla_\mu$ der zu ${}'G_{\lambda\mu}$ und ${}'x_\lambda$ gehörige kovariante Differentialoperator ist. Aus dieser Gleichung folgt leicht

$$\left.\begin{aligned} {}'\Pi^\nu_{\lambda\mu} = \Pi^\nu_{\lambda\mu} &+ (\nabla_\mu\,\chi_\lambda)\,x^\nu - 2\,x^\nu_{.\mu}\,\chi_\lambda - 4\,x^\nu_{.\lambda}\,\chi_\mu + \\ &+ 4\,\chi_\mu\,\chi_\rho\,x^\rho_{.\lambda}\,x^\nu + 2\,\chi_\lambda\,\chi_\rho\,x^\rho_{.\mu}\,x^\nu\,. \end{aligned}\right\} \quad \ldots \quad (44)$$

In jeder E_4^* erleiden also alle Objekte die Punkttransformation T, auch die Quadrik und die „unendlichferne" Hyperebene x_λ. Der Nullkegel, der seine Spitze in x^ν hat und die Quadrik tangiert, bleibt aber invariant. Der projektive Zusammenhang der E_4^* transformiert sich aber ebenfalls mit, und zwar in solcher Weise, dass alle Beziehungen zwischen den transformierten Objekten dieselben sind wie zwischen den ursprünglichen. Bei einer bestimmten Wahl der x_λ wird jede lokale (affine) E_4^* eineindeutig auf die lokale (projektive) E_4^* abgebildet. Der projektive Zusammenhang der E_4^* induziert also einen projektiven Zusammenhang der E_4, der natürlich nicht mit den affinen (RIEMANNschen) Zusammenhang identisch ist. Bei Aenderung der Wahl der x_λ ändert sich nun

[1]) Bei den *gestrichenen* Grössen hat das Herauf- und Herunterziehen der Indizes natürlich mit ${}'G^{\mu\nu}$ bzw. ${}'G_{\lambda\nu}$ zu erfolgen.

zwar der projektive Zusammenhang der E_4^*, aber infolge der Abhänkeit der Abbildung der E_4 auf die E_4^* von dieser Wahl *bleibt der projektive Zusammenhang der E_4 invariant.*

Vom Standpunkte der lokalen E_4 bedeutet Aenderung der Wahl von x_λ nur eine Aenderung der projektiven *Koordinaten*; die x_λ sind ja die Koordinaten der unendlichfernen Hyperebene der E_4. Einführung des Bezugssystems (c) von *G. F.* I § 3 genügt schon um den Einfluss der Wahl von x_λ vollständig aus den Gleichungen zu eliminieren, was darin seine Ursache findet, dass x_λ in bezug auf dieses System stets die Bestimmungszahlen $(-\omega^2, 0, 0, 0, 0)$ hat. Alle Gleichungen in Bezug auf dieses System sind also bei Aenderung der Wahl von x_λ invariant und dasselbe gilt somit ebenfalls für alle physikalische Gleichungen in gewöhnlichen nichthomogenen Koordinaten der V_4.

Mathematics. — *Asymptotische Entwicklungen von* BESSEL*schen,* HANKEL*schen und verwandten Funktionen.* II [1]). Von C. S. MEIJER. (Communicated by Prof. J. G. VAN DER CORPUT).

(Communicated at the meeting of June 25, 1932).

Hilfssatz 4. *Ist*

$$-\frac{\pi}{2} < \Im(s_1) < \frac{\pi}{2}, \quad -\frac{\pi}{2} \leqq \Im(s_2) \leqq \frac{\pi}{2} \quad \text{und} \quad s_1 \neq s_2,$$

so ist $\sinh s_1 \neq \sinh s_2$; *weiter gilt* $\cosh s \neq 0$, *falls* $-\frac{\pi}{2} < \Im(s) < \frac{\pi}{2}$ *ist.*

Beweis. Dieser Satz ist bekannt, siehe z. B. KNOPP, Unendliche Reihen, p. 416 und 417.

Wir definieren nun die Funktion $\zeta = F(z)$ durch die Beziehung

$$\zeta = F(z) = p \sinh qz \quad . \quad . \quad . \quad . \quad . \quad . \quad . \quad (40)$$

Hierin ist $p \neq 0$, $q > 0$ und p und q sind unabhängig von z. Wir betrachten weiter den Rand C des Rechteckes begrenzt durch die Geraden

$$R_1\left(\Im(z) = \frac{\pi}{2q}\right), R_2\left(\Im(z) = -\frac{\pi}{2q}\right), R_3(\Re(z) = b_1) \text{ und } R_4(\Re(z) = -b_2),$$

worin b_1 und b_2 positiv sind. Dann gilt

[1]) Erste Mitteilung: These Proceedings, Vol. 35 (1932), S. 656—667.

Hilfssatz 5. *Ist N ganz rational $\geqq 0$ und liegt z im Innern von C, so ist*

$$\cosh vz\,\frac{dz}{d\zeta}=\frac{1}{2\pi i}\sum_{l=0}^{N-1}\zeta^{2l}\int_C\frac{\cosh vt\,dt}{F(t)^{2l+1}}+\frac{\zeta^{2N}}{2\pi i}\int_C\frac{\cosh vt\,dt}{F(t)^{2N}\,(F(t)-\zeta)}\quad .\quad .\quad . \tag{41}$$

und

$$\sinh vz\,\frac{dz}{d\zeta}=\frac{1}{2\pi i}\sum_{l=0}^{N-1}\zeta^{2l+1}\int_C\frac{\sinh vt\,dt}{F(t)^{2l+2}}+\frac{\zeta^{2N+1}}{2\pi i}\int_C\frac{\sinh vt\,dt}{F(t)^{2N+1}\,(F(t)-\zeta)}\,; \tag{42}$$

hierbei wird der Rand C in positivem Sinne durchlaufen.

Beweis. Aus (40) und Hilfssatz 4 mit $s=qz$ ergibt sich, dass

$$\frac{\cosh vt}{F(t)-F(z)}$$

für jedes z im Innern von C und für alle Punkte $t\neq z$ auf dem Rande und im Innern von C eine analytische Funktion von t ist. Weiter ist $F'(z)\neq 0$ für z im Innern von C. Daher hat man, wegen des Residuensatzes, wenn z innerhalb C liegt,

$$\frac{1}{2\pi i}\int_C\frac{\cosh vt\,dt}{F(t)-\zeta}=\frac{\cosh vz}{F'(z)}=\cosh vz\,\frac{dz}{d\zeta}\,.$$

Nun ist

$$\frac{1}{F(t)-\zeta}=\sum_{k=0}^{n-1}\frac{\zeta^k}{F(t)^{k+1}}+\frac{\zeta^n}{F(t)^n\,(F(t)-\zeta)}\,,$$

also

$$\cosh vz\,\frac{dz}{d\zeta}=\frac{1}{2\pi i}\sum_{k=0}^{n-1}\zeta^k\int_C\frac{\cosh vt\,dt}{F(t)^{k+1}}+\frac{\zeta^n}{2\pi i}\int_C\frac{\cosh vt\,dt}{F(t)^n\,(F(t)-\zeta)}\quad . \tag{43}$$

Ebenso findet man

$$\sinh vz\,\frac{dz}{d\zeta}=\frac{1}{2\pi i}\sum_{k=0}^{n-1}\zeta^k\int_C\frac{\sinh vt\,dt}{F(t)^{k+1}}+\frac{\zeta^n}{2\pi i}\int_C\frac{\sinh vt\,dt}{F(t)^n\,(F(t)-\zeta)}\quad . \tag{44}$$

Da $F(t)$ eine ungerade Funktion von t ist, so enthält die Entwicklung von

$$\frac{\cosh vt}{F(t)^{k+1}}$$

nach steigenden Potenzen von t, falls k ungerade ist, nur gerade Potenzen von t. Hieraus folgt, mit Rücksicht auf den Residuensatz,

$$\int_C\frac{\cosh vt\,dt}{F(t)^{k+1}}=\int_{(0+)}\frac{\cosh vt\,dt}{F(t)^{k+1}}=0.$$

für ungerade k. Auf analoge Weise findet man, falls k gerade ist,

$$\int_C \frac{\sinh \nu t\, dt}{F(t)^{k+1}} = 0.$$

Man bekommt nun (41), wenn man in (43) $n = 2N$ und (42), wenn man in (44) $n = 2N+1$ setzt.

Hilfssatz 6. *Ist N ganz rational $\geqq 0$, $F(t) \neq d$ für alle Punkte t von C und d unabhängig von t, so ist, wenn b_1 und b_2 unbeschränkt wachsen, falls $N > \frac{|\Re(\nu)|}{2q} - \frac{1}{2}$ ist,*

$$\int_C \frac{\cosh \nu t\, dt}{F(t)^{2N}(F(t)-d)} = \frac{2i \cos \frac{\nu\pi}{2q}}{(-1)^N p^{2N-1}} \int_{-\infty}^{\infty} \frac{\cosh \nu x\, dx}{(\cosh qx)^{2N-1}(p^2 \cosh^2 qx + d^2)}. \quad (45)$$

und, falls $N > \frac{|\Re(\nu)|}{2q} - 1$ ist,

$$\int_C \frac{\sinh \nu t\, dt}{F(t)^{2N+1}(F(t)-d)} = \frac{2i \sin \frac{\nu\pi}{2q}}{(-1)^N p^{2N}} \int_{-\infty}^{\infty} \frac{\cosh \nu x\, dx}{(\cosh qx)^{2N}(p^2 \cosh^2 qx + d^2)}. \quad (46)$$

Beweis. Aus den Voraussetzungen folgt, dass im Integral

$$\int_C \frac{\cosh \nu t\, dt}{F(t)^{2N}(F(t)-d)}$$

die Beiträge der vertikalen Seiten von C nach Null streben, falls b_1 und b_2 unbeschränkt zunehmen. Also ist, wenn R_1 und R_2 von links nach rechts durchlaufen werden,

$$\int_C \frac{\cosh \nu t\, dt}{F(t)^{2N}(F(t)-d)} = \left(-\int_{R_1} + \int_{R_2}\right) \frac{\cosh \nu t\, dt}{F(t)^{2N}(F(t)-d)}. \quad (47)$$

Ebenso hat man

$$\int_C \frac{\sinh \nu t\, dt}{F(t)^{2N+1}(F(t)-d)} = \left(-\int_{R_1} + \int_{R_2}\right) \frac{\sinh \nu t\, dt}{F(t)^{2N+1}(F(t)-d)}. \quad (48)$$

Setzt man $t = x \pm i\frac{\pi}{2q}$, je nachdem t auf R_1 oder auf R_2 liegt, so ist wegen

$$\cosh \nu\left(x \pm \frac{i\pi}{2q}\right) = \cosh \nu x \cos \frac{\nu\pi}{2q} \pm i \sinh \nu x \sin \frac{\nu\pi}{2q},$$

$$\sinh q\left(x \pm \frac{i\pi}{2q}\right) = \pm i \cosh qx$$

und (40)

$$\int_{R_1} \frac{\cosh \nu t\, dt}{F(t)^{2N}(F(t)-d)} = \int_{-\infty}^{\infty} \frac{\left(\cosh \nu x \cos\frac{\nu\pi}{2q} + i \sinh \nu x \sin\frac{\nu\pi}{2q}\right) dx}{(ip)^{2N}(\cosh qx)^{2N}(ip\cosh qx - d)} =$$

$$\frac{\cos\frac{\nu\pi}{2q}}{(-1)^N p^{2N}} \int_{-\infty}^{\infty} \frac{\cosh \nu x\, dx}{(\cosh qx)^{2N}(ip\cosh qx - d)}.$$

Ebenso hat man

$$\int_{R_2} \frac{\cosh \nu t\, dt}{F(t)^{2N}(F(t)-d)} = \frac{\cos\frac{\nu\pi}{2q}}{(-1)^N p^{2N}} \int_{-\infty}^{\infty} \frac{\cosh \nu x\, dx}{(\cosh qx)^{2N}(-ip\cosh qx - d)},$$

also

$$\left(-\int_{R_1} + \int_{R_2}\right) \frac{\cosh \nu t\, dt}{F(t)^{2N}(F(t)-d)} =$$

$$\frac{2i\cos\frac{\nu\pi}{2q}}{(-1)^N p^{2N-1}} \int_{-\infty}^{\infty} \frac{\cosh \nu x\, dx}{(\cosh qx)^{2N-1}(p^2\cosh^2 qx + d^2)}.$$

Hieraus und aus (47) folgt (45).
Auf analoge Weise findet man

$$\left(-\int_{R_1} + \int_{R_2}\right) \frac{\sinh \nu t\, dt}{F(t)^{2N+1}(F(t)-d)} =$$

$$-\int_{-\infty}^{\infty} \frac{\left(\sinh \nu x \cos\frac{\nu\pi}{2q} + i\cosh \nu x \sin\frac{\nu\pi}{2q}\right) dx}{(ip)^{2N+1}(\cosh qx)^{2N+1}(ip\cosh qx - d)} +$$

$$\int_{-\infty}^{\infty} \frac{\left(\sinh \nu x \cos\frac{\nu\pi}{2q} - i\cosh \nu x \sin\frac{\nu\pi}{2q}\right) dx}{(-ip)^{2N+1}(\cosh qx)^{2N+1}(-ip\cosh qx - d)} =$$

$$\frac{2i\sin\frac{\nu\pi}{2q}}{(-1)^N p^{2N}} \int_{-\infty}^{\infty} \frac{\cosh \nu x\, dx}{(\cosh qx)^{2N}(p^2\cosh^2 qx + d^2)},$$

woraus, mit Rücksicht auf (48), Beziehung (46) folgt.

Hilfssatz 7. *Ist N ganz rational $> \frac{|\Re(\nu)|}{2q} - \frac{1}{2}$, so ist, falls $\frac{\nu}{2q} + \frac{1}{2}$ keine ganze rationale Zahl ist,*

$$\int_{-\infty}^{\infty} \frac{\cosh \nu x \, dx}{(\cosh qx)^{2N+1}} = \frac{(-1)^N \pi}{q^{2N+1} (2N)! \cos \frac{\nu\pi}{2q}} \prod_{h=0}^{N-1} (\nu^2 - (2h+1)^2 q^2). \quad (49)$$

und, falls $\frac{\nu}{2q} + \frac{1}{2}$ ganz rational ist,

$$\int_{-\infty}^{\infty} \frac{\cosh \nu x \, dx}{(\cosh qx)^{2N+1}} = \frac{(-1)^{N+k+1} (8k+4)}{q^{2N-1} (2N)!} \prod_{\substack{h=0 \\ h \neq k}}^{N-1} (\nu^2 - (2h+1)^2 q^2), \quad (50)$$

worin $k = \frac{|\nu|}{2q} - \frac{1}{2}$ [1]).

Beweis. Setzt man in (45) von Hilfssatz 6 $p=1$ und $d=0$, so findet man

$$\int_C \frac{\cosh \nu t \, dt}{(\sinh qt)^{2N+1}} = \frac{2i}{(-1)^N} \cos \frac{\nu\pi}{2q} \int_{-\infty}^{\infty} \frac{\cosh \nu x \, dx}{(\cosh qx)^{2N+1}}.$$

Da $t=0$ die einzige im Innern von C liegende Nullstelle von $\sinh qt$ ist, hat man also

$$\int_{(0+)} \frac{\cosh \nu t \, dt}{(\sinh qt)^{2N+1}} = \frac{2i}{(-1)^N} \cos \frac{\nu\pi}{2q} \int_{-\infty}^{\infty} \frac{\cosh \nu x \, dx}{(\cosh qx)^{2N+1}}.$$

Hieraus ergibt sich, wegen (38) von Hilfssatz 3 mit $a=q$ und $m=2N$,

$$\cos \frac{\nu\pi}{2q} \int_{-\infty}^{\infty} \frac{\cosh \nu x \, dx}{(\cosh qx)^{2N+1}} = \frac{(-1)^N \pi}{q^{2N+1} (2N)!} \prod_{h=0}^{N-1} (\nu^2 - (2h+1)^2 q^2), \quad (51)$$

womit (49) bewiesen ist.

Ist ν reell und $\frac{|\nu|}{2q} = k + \frac{1}{2}$ (k ganz rational), so sind beide Seiten von (51) gleich Null, die linke Seite wegen des Faktors $\cos \frac{\nu\pi}{2q}$, die rechte Seite wegen des Faktors $\nu^2 - (2k+1)^2 q^2$. Da

$$\int_{-\infty}^{\infty} \frac{\cosh \nu x \, dx}{(\cosh qx)^{2N+1}}$$

[1]) Man hat also k ganz rational $\geqq 0$ und $N > k$.

eine stetige Funktion von ν ist, und

$$\lim_{\substack{|\nu| \neq 2qk+q \\ |\nu| \to 2qk+q}} \frac{\nu^2-(2k+1)^2 q^2}{\cos\frac{\nu\pi}{2q}} = \frac{(-1)^{k+1} 4q^2(2k+1)}{\pi}$$

ist, folgt dann Formel (50) von Hilfssatz 7 aus (51).

Hilfssatz 8. *Ist N ganz rational $> \frac{|\Re(\nu)|}{2q} - 1$, so ist, falls $\frac{\nu}{2q}$ keine ganze rationale Zahl ist,*

$$\int_{-\infty}^{\infty} \frac{\cosh \nu x\, dx}{(\cosh qx)^{2N+2}} = \frac{(-1)^N \pi\nu}{q^{2N+2}(2N+1)!\sin\frac{\nu\pi}{2q}} \prod_{h=0}^{N-1} (\nu^2-(2h+2)^2 q^2) \quad (52)$$

und, falls $\frac{\nu}{2q}$ eine ganze rationale Zahl $\neq 0$ ist,

$$\int_{-\infty}^{\infty} \frac{\cosh \nu x\, dx}{(\cosh qx)^{2N+2}} = \frac{(-1)^{N+k} 16k^2}{q^{2N-1}(2N+1)!} \prod_{\substack{h=0 \\ h \neq k-1}}^{N-1} (\nu^2-(2h+2)^2 q^2), \quad (53)$$

worin $k = \frac{|\nu|}{2q}$ (k ganz rational >0); weiter hat man, falls N ganz rational $\geqq 0$ ist,

$$\int_{-\infty}^{\infty} \frac{dx}{(\cosh qx)^{2N+2}} = \frac{2^{2N+1}(N!)^2}{q(2N+1)!} \quad (54)$$

Beweis. Setzt man in (46) von Hilfssatz 6 $p=1$ und $d=0$ so findet man

$$\int_C \frac{\sinh \nu t\, dt}{(\sinh qt)^{2N+2}} = \frac{2i}{(-1)^N} \sin\frac{\nu\pi}{2q} \int_{-\infty}^{\infty} \frac{\cosh \nu x\, dx}{(\cosh qx)^{2N+2}}.$$

Also hat man, wegen (39) von Hilfssatz 3 mit $a=q$ und $m=2N+1$ angewendet,

$$\sin\frac{\nu\pi}{2q} \int_{-\infty}^{\infty} \frac{\cosh \nu x\, dx}{(\cosh qx)^{2N+2}} = \frac{(-1)^N \pi\nu}{q^{2N+2}(2N+1)!} \prod_{h=0}^{N-1} (\nu^2-(2h+2)^2 q^2), \quad (55)$$

womit (52) bewiesen ist.

Ist $\frac{\nu}{2q}$ ganz rational $\neq 0$ und $\frac{|\nu|}{2q} = k$ (k ganz rational >0), so sind beide Seiten von (55) gleich Null, die linke Seite wegen des Faktors

$\sin \frac{\nu\pi}{2q}$, die rechte Seite wegen des Faktors $\nu^2 - 4k^2q^2$. Da

$$\lim_{\substack{|\nu| \neq 2qk \\ |\nu| \to 2qk}} \frac{\nu(\nu^2 - 4k^2q^2)}{\sin \frac{\nu\pi}{2q}} = (-1)^k \frac{16k^2q^3}{\pi}$$

ist, folgt dann aus (55) Formel (53) von Hilfssatz 8. Werden beide Seiten von (55) durch $\sin \frac{\nu\pi}{2q}$ gekürzt, und strebt ν nach Null, so erhält man (54).

Hilfssatz 9. *Ist α reell, N ganz rational $> |\alpha| - \frac{1}{2}$, so ist, falls $\alpha + \frac{1}{2}$ nicht ganz rational ist,*

$$\int_0^\infty e^{-\zeta^2} \zeta^{2N} d\zeta \int_{-\infty}^{\infty} \frac{\cosh \alpha x \, dx}{\left(\cosh \frac{x}{2}\right)^{2N+1}} = \frac{(-1)^N \pi \sqrt{\pi}}{N!\, 2^{2N} \cos \alpha\pi} \prod_{h=0}^{N-1} (4\alpha^2 - (2h+1)^2) \quad (56)$$

und, falls $|\alpha| = k + \frac{1}{2}$ (k ganz rational) ist,

$$\left.\begin{aligned} &\int_0^\infty e^{-\zeta^2} \zeta^{2N} d\zeta \int_{-\infty}^{\infty} \frac{\cosh \alpha x \, dx}{\left(\cosh \frac{x}{2}\right)^{2N+1}} = \\ &\frac{(-1)^{N+k+1} (8k+4) \sqrt{\pi}}{N!\, 2^{2N}} \prod_{\substack{h=0 \\ h \neq k}}^{N-1} (4\alpha^2 - (2h+1)^2). \end{aligned}\right\} \quad \ldots \quad (57)$$

Beweis. Setzt man in Hilfssatz 7 $\nu = \alpha$ und $q = \frac{1}{2}$, dann findet man, falls $\alpha + \frac{1}{2}$ nicht ganz rational ist,

$$\int_{-\infty}^{\infty} \frac{\cosh \alpha x \, dx}{\left(\cosh \frac{x}{2}\right)^{2N+1}} = \frac{(-1)^N 2\pi}{(2N)! \cos \alpha\pi} \prod_{h=0}^{N-1} (4\alpha^2 - (2h+1)^2)$$

und, falls $|\alpha| = k + \frac{1}{2}$ (k ganz rational) ist,

$$\int_{-\infty}^{\infty} \frac{\cosh \alpha x \, dx}{\left(\cosh \frac{x}{2}\right)^{2N+1}} = \frac{(-1)^{N+k+1} (16k+8)}{(2N)!} \prod_{\substack{h=0 \\ h \neq k}}^{N-1} (4\alpha^2 - (2h+1)^2).$$

Wegen

$$\int_0^\infty e^{-\zeta^2} \zeta^{2N} d\zeta = \tfrac{1}{2} \Gamma(N + \tfrac{1}{2}) = \frac{(2N)! \sqrt{\pi}}{2^{2N+1} N!}$$

folgen hieraus (56) und (57).

Hilfssatz 10. *Ist α reell $\neq 0$, N ganz rational $> |\alpha| - 1$, so ist, falls α nicht ganz rational ist,*

$$\int_0^\infty e^{-\zeta^2}\zeta^{2N+1}d\zeta \int_{-\infty}^{\infty} \frac{\cosh \alpha x\, dx}{\left(\cosh\frac{x}{2}\right)^{2N+2}} = \frac{(-1)^N N!\, 2\pi\alpha}{(2N+1)!\sin\alpha\pi} \prod_{h=0}^{N-1}(4\alpha^2-(2h+2)^2) \quad (58)$$

und, falls $|\alpha| = k$ (k ganz rational > 0) ist,

$$\int_0^\infty e^{-\zeta^2}\zeta^{2N+1}d\zeta \int_{-\infty}^{\infty} \frac{\cosh \alpha x\, dx}{\left(\cosh\frac{x}{2}\right)^{2N+2}} = \frac{(-1)^{N+k} N!\, 16 k^2}{(2N+1)!} \prod_{\substack{h=0 \\ h \neq k-1}}^{N-1}(4\alpha^2-(2h+2)^2). \quad (59)$$

Weiter ist, falls N ganz rational $\geqq 0$ ist,

$$\int_0^\infty e^{-\zeta^2}\zeta^{2N+1}d\zeta \int_{-\infty}^{\infty} \frac{dx}{\left(\cosh\frac{x}{2}\right)^{2N+2}} = \frac{2^{2N+1}(N!)^3}{(2N+1)!}. \quad . \quad . \quad . \quad (60)$$

Beweis. Setzt man in Hilfssatz 8 $\nu = \alpha$ und $q = \frac{1}{2}$ dann findet man, falls α nicht ganz rational ist,

$$\int_{-\infty}^{\infty} \frac{\cosh \alpha x\, dx}{\left(\cosh\frac{x}{2}\right)^{2N+2}} = \frac{(-1)^N 4\pi\alpha}{(2N+1)!\sin\alpha\pi} \prod_{h=0}^{N-1}(4\alpha^2-(2h+2)^2)$$

und, falls $|\alpha| = k$ (k ganz rational > 0) ist,

$$\int_{-\infty}^{\infty} \frac{\cosh \alpha x\, dx}{\left(\cosh\frac{x}{2}\right)^{2N+2}} = \frac{(-1)^{N+k} 32 k^2}{(2N+1)!} \prod_{\substack{h=0 \\ h \neq k-1}}^{N-1}(4\alpha^2-(2h+2)^2).$$

Ist N ganz rational $\geqq 0$. dann hat man

$$\int_{-\infty}^{\infty} \frac{dx}{\left(\cosh\frac{x}{2}\right)^{2N+2}} = \frac{2^{2N+2}(N!)^2}{(2N+1)!}.$$

Wegen

$$\int_0^\infty e^{-\zeta^2}\zeta^{2N+1}d\zeta = \tfrac{1}{2}N!$$

folgen hieraus (58), (59) und (60).

Hilfssatz 11. *Ist α reell, N ganz rational $> \frac{|\alpha|}{2} - \frac{1}{2}$, so ist, falls α keine ungerade ganze Zahl ist,*

$$\int_0^\infty e^{-u}\, u^{2N}\, du \int_{-\infty}^{\infty} \frac{\cosh \alpha x\, dx}{(\cosh x)^{2N+1}} = \frac{(-1)^N \pi}{\cos \frac{\alpha \pi}{2}} \prod_{h=0}^{N-1} (\alpha^2 - (2h+1)^2)\,. \quad (61)$$

und, falls $|\alpha| = 2k+1$ (k ganz rational) ist,

$$\int_0^\infty e^{-u}\, u^{2N}\, du \int_{-\infty}^{\infty} \frac{\cosh \alpha x\, dx}{(\cosh x)^{2N+1}} = (-1)^{N+k+1} (8k+4) \prod_{\substack{h=0 \\ h \neq k}}^{N-1} (\alpha^2 - (2h+1)^2)\,. \quad (62)$$

Beweis. Setzt man in Hilfssatz 7 $\nu = \alpha$ und $q = 1$, dann findet man, falls α keine ungerade ganze Zahl ist,

$$\int_{-\infty}^{\infty} \frac{\cosh \alpha x\, dx}{(\cosh x)^{2N+1}} = \frac{(-1)^N \pi}{(2N)!\, \cos \frac{\alpha \pi}{2}} \prod_{h=0}^{N-1} (\alpha^2 - (2h+1)^2)$$

und, falls $|\alpha| = 2k+1$ (k ganz rational) ist,

$$\int_{-\infty}^{\infty} \frac{\cosh \alpha x\, dx}{(\cosh x)^{2N+1}} = \frac{(-1)^{N+k+1} (8k+4)}{(2N)!} \prod_{\substack{h=0 \\ h \neq k}}^{N-1} (\alpha^2 - (2h+1)^2).$$

Wegen

$$\int_0^\infty e^{-u}\, u^{2N}\, du = (2N)!$$

folgen hieraus (61) und (62).

Hilfssatz 12. *Ist α reell $\neq 0$ und N ganz rational $> \frac{|\alpha|}{2} - 1$, so ist, falls α keine gerade ganze Zahl ist,*

$$\int_0^\infty e^{-u}\, u^{2N+1}\, du \int_{-\infty}^{\infty} \frac{\cosh \alpha x\, dx}{(\cosh x)^{2N+2}} = \frac{(-1)^N \pi \alpha}{\sin \frac{\alpha \pi}{2}} \prod_{h=0}^{N-1} (\alpha^2 - (2h+2)^2) \quad (63)$$

und, falls $|\alpha| = 2k$ (k ganz rational > 0) ist,

$$\int_0^\infty e^{-u}\, u^{2N+1}\, du \int_{-\infty}^{\infty} \frac{\cosh \alpha x\, dx}{(\cosh x)^{2N+2}} = (-1)^{N+k}\, 16k^2 \prod_{\substack{h=0 \\ h \neq k-1}}^{N-1} (\alpha^2 - (2h+2)^2) \quad (64)$$

Weiter ist, falls N ganz rational $\geqq 0$ ist,

$$\int_0^\infty e^{-u}\, u^{2N+1}\, du \int_{-\infty}^{\infty} \frac{dx}{(\cosh x)^{2N+2}} = 2^{2N+1}\,(N!)^2 \quad . \quad . \quad . \quad (65)$$

Beweis. Setzt man in Hilfssatz 8 $\nu = \alpha$ und $q = 1$, dann findet man, falls α keine gerade ganze Zahl ist,

$$\int_{-\infty}^{\infty} \frac{\cosh \alpha x\, dx}{(\cosh x)^{2N+2}} = \frac{(-1)^N \pi \alpha}{(2N+1)!\, \sin \frac{\alpha \pi}{2}} \prod_{h=0}^{N-1} (\alpha^2 - (2h+2)^2)$$

und, falls $|\alpha| = 2k$ (k ganz rational > 0) ist,

$$\int_{-\infty}^{\infty} \frac{\cosh \alpha x\, dx}{(\cosh x)^{2N+2}} = \frac{(-1)^{N+k}\, 16\, k^2}{(2N+1)!} \prod_{\substack{h=0 \\ h \neq k-1}}^{N-1} (\alpha^2 - (2h+2)^2).$$

Ist N ganz rational $\geqq 0$, so hat man

$$\int_{-\infty}^{\infty} \frac{dx}{(\cosh x)^{2N+2}} = \frac{2^{2N+1}\,(N!)^2}{(2N+1)!}.$$

Wegen

$$\int_0^\infty e^{-u}\, u^{2N+1}\, du = (2N+1)!$$

folgen hieraus (63), (64) und (65).

Hilfssatz 13. *Es sei $w \neq 0$, $-\pi < \arg w < 2\pi$, $\arg w^{1/2} = \frac{1}{2} \arg w$,*

$$Max\left(-\frac{\pi}{2}, -\frac{3\pi}{2} + \arg w\right) < \mu < Min\left(\frac{\pi}{2}, \frac{\pi}{2} + \arg w\right), \quad (66)$$

dann kann:

1. *Für jedes ganze $N > |\Re(\nu)| - \frac{1}{2}$ die Funktion $H_\nu^{(1)}(w)$ auf die Gestalt*

$$H_\nu^{(1)}(w) = \sqrt{\frac{2}{\pi}}\, \frac{e^{i\left(w - \frac{1}{2}\nu\pi - \frac{\pi}{4}\right)}}{w^{1/2}} \left\{ \sum_{l=0}^{N-1} \frac{(i)^l \prod_{h=0}^{l-1} (4\nu^2 - (2h+1)^2)}{l!\,(8w)^l} + \right.$$

$$\left. \frac{(-i)^N \cos \nu\pi}{\pi \sqrt{\pi}\, (2w)^N} \int_0^{\infty e^{\frac{i\mu}{2}}} e^{-\zeta^2}\, \zeta^{2N}\, d\zeta \int_{-\infty}^{\infty} \frac{2\, i\, w \cosh^2 \frac{x}{2} \cosh \nu x\, dx}{\left(\cosh \frac{x}{2}\right)^{2N+1} \left(2i w \cosh^2 \frac{x}{2} - \zeta^2\right)} \right\} . \quad (67)$$

gebracht werden.

2. *Für jedes ganze* $N > |\Re(\nu)| - 1$ *die in* (13) *definierte Funktion* $G_\nu(w)$ *auf die Gestalt*

$$G_\nu(w) = e^{iw} 2\nu \sum_{l=0}^{N-1} \frac{(i)^{l+1}\, l!\, \prod_{h=0}^{l-1} (4\nu^2 - (2h+2)^2)}{(2w)^{l+1}\,(2l+1)!} - \frac{e^{iw} \sin \nu\pi}{\pi (i)^{N+1} (2w)^{N+1}} \int_0^{\infty e^{\frac{i\mu}{2}}} e^{-\zeta^2} \zeta^{2N+1}\, d\zeta \int_{-\infty}^{\infty} \frac{2iw \cosh^2 \frac{x}{2} \cosh \nu x\, dx}{\left(\cosh \frac{x}{2}\right)^{2N+2} \left(2iw \cosh^2 \frac{x}{2} - \zeta^2\right)} \tag{68}$$

gebracht werden.

Beweis. 1. Wir gehen von der Integraldarstellung (30) von $H_\nu^{(1)}(w)$ aus und setzen

$$\varphi(z) = iw \cosh z, \quad . \quad . \quad . \quad . \quad . \quad . \quad . \quad . \quad . \quad (69)$$

$z = x + iy$ und benutzen die Methode der Sattelpunkte [1]). Wir betrachten nur den Streifen der z-Ebene zwischen den Geraden R_5 und R_6, worauf $y = \pi$ bez. $y = -\pi$ (einschliesslich R_5 und R_6). Der Punkt $z = 0$ ist ein Sattelpunkt von $\varphi(z)$. Die Gleichung der Kurve $\Im(e^{-i\mu}\varphi(z)) = \Im(e^{-i\mu}\varphi(0))$ ist

$$(\cosh x \cos y - 1) \cos(\arg w - \mu) - \sinh x \sin y \sin(\arg w - \mu) = 0 \ . \tag{70}$$

Diese Kurve hat einen Doppelpunkt in $z = 0$ und ist symmetrisch in Bezug auf diesen Punkt; die zwei Tangenten in $z = 0$ bilden Winkel von $\frac{\pi}{4} - \frac{1}{2}\arg w + \frac{\mu}{2}$ bez. $\frac{3\pi}{4} - \frac{1}{2}\arg w + \frac{\mu}{2}$ mit der positiven x-Achse.

Ist $\arg w - \mu = \frac{\pi}{2}$, dann besteht der im betrachteten Streifen liegende Teil der Kurve (70) aus der reellen und der imaginären Achse und ausserdem aus den Geraden R_5 und R_6.

Ist $\arg w - \mu \neq \frac{\pi}{2}$, dann schneidet die Gerade $x = 0$ die Kurve (70) zwischen R_5 und R_6 nur im Punkte $z = 0$. Die Gerade $x = a$ schneidet, falls $a \neq 0$ und $\arg w - \mu \neq \frac{\pi}{2}$ ist, die Kurve (70) zwischen R_5 und R_6 in zwei Punkte z_1 und z_2, von denen der eine zwischen der reellen Achse und R_5, der andre zwischen der reellen Achse und R_6 liegt. Denn setzt man die linke Seite von (70) gleich $g(x, y)$, dann hat [2]) $g(a, y)$ höchstens zwei Nullstellen im Intervall $-\pi < y < \pi$; $g(a, \pi)$ und $g(a, -\pi)$ haben dasselbe Vorzeichen wie $-\cos(\arg w - \mu)$, und $g(a, 0)$ hat dasselbe Vorzeichen wie $\cos(\arg w - \mu)$, sodass [3]) $g(a, y)$ im Intervall

[1]) Ein Punkt z_0 heisst Sattelpunkt von $f(z)$, falls $f'(z_0) = 0$ ist.

[2]) Die Funktion $\chi(y) = A_1 \cos y + A_2 \sin y + A_3$ hat, falls A_1, A_2 und A_3 reell sind, höchstens zwei Nullstellen im Intervall $-\pi < y < \pi$.

[3]) Wegen (66) ist $\cos(\arg w - \mu) \neq 0$, falls $\arg w - \mu \neq \frac{\pi}{2}$ ist.

$-\pi < y < \pi$ zwei Nullstellen besitzt, von denen die eine im Intervall $-\pi < y < 0$, die andre im Intervall $0 < y < \pi$ liegt. Ist $arg\, w - \mu \neq \frac{\pi}{2}$, dann besteht also der im betrachteten Streifen liegende Teil der Kurve (70) aus zwei Zweigen, die die reelle Achse nur im Punkte $z = 0$ schneiden und die Geraden R_5 und R_6 weder schneiden noch berühren.

Aus (70) geht hervor, dass bei unbeschränkt wachsendem x y nach einem Grenzwert η strebt mit $\cos(\eta + arg\, w - \mu) = 0$. Bezeichnen $\infty + i y_1$ und $\infty + i y_2\, (y_1 > y_2)$ die im Unendlichen liegenden Punkte der obengemeinten Zweige, dann sind also y_1 und y_2 Nullstellen von $\cos(y + arg\, w - \mu) = 0$. Hieraus ergibt sich: Ist $-\frac{\pi}{2} < arg\, w - \mu < \frac{\pi}{2}$, dann ist $y_1 = -arg\, w + \mu + \frac{\pi}{2}$, $y_2 = -arg\, w + \mu - \frac{\pi}{2}$; ist $\frac{\pi}{2} < arg\, w - \mu < \frac{3\pi}{2}$, dann ist $y_1 = -arg\, w + \mu + \frac{3\pi}{2}$, $y_2 = -arg\, w + \mu + \frac{\pi}{2}$. Stets verbindet also einer der Zweige von (70) den Punkt $z = 0$ mit

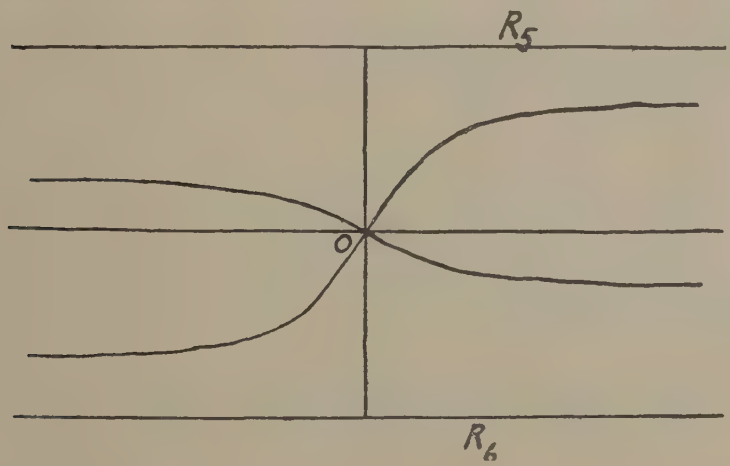

$\infty + i\left(\frac{\pi}{2} - arg\, w + \mu\right)$. Wir werden diesen Zweig L nennen. Ist $arg\, w - \mu = \frac{\pi}{2}$, dann ist L die positive x-Achse. Ist $\frac{\pi}{2} < arg\, w - \mu < \frac{3\pi}{2}$, dann ist $\frac{\pi}{2} - arg\, w + \mu < 0$; da L die reelle Achse nur in $z = 0$ schneidet, liegt also L, falls $x > 0$ ist, zwischen der reellen Achse und R_6, sodass L diejenige Zweige der Kurve (70) ist, welche in $z = 0$ einen Winkel von $\frac{\pi}{4} - \frac{1}{2} arg\, w + \frac{\mu}{2}$ mit der positiven x-Achse bildet. Ist $-\frac{\pi}{2} < arg\, w - \mu < \frac{\pi}{2}$ dann liegt L, falls $x > 0$ ist, zwischen der reellen Achse und R_5, sodass auch dann L diejenige Zweige von (70) ist, die in $z = 0$ einen Winkel von $\frac{\pi}{4} - \frac{1}{2} arg\, w + \frac{\mu}{2}$ mit der positiven x-Achse bildet.

Nehmen wir in (30) L als Integrationsweg, dann erhalten wir wegen (69)

$$H_\nu^{(1)}(w) = \frac{2\, e^{i\,(w-1/2\,\nu\pi)}}{\pi i} \int_L e^{\varphi(z)-\varphi(0)} \cosh \nu z \, dz \quad . \quad . \quad . \quad . \quad (71)$$

Ist $f(z)$ eine analytische Funktion von z, dann ändert sich bekanntlich $\Re f(z)$ monoton auf den Teilen der Kurve $\Im f(z) = 0$, die keinen Sattelpunkt von $f(z)$ enthalten.

Wird jetzt

$$\zeta^2 = \varphi(0) - \varphi(z) = -iw(\cosh z - 1) \quad . \quad . \quad . \quad . \quad . \quad (72)$$

gesetzt, dann ist für jedes z auf L $\Im(e^{-i\mu}(\varphi(0) - \varphi(z))) = 0$; im Punkte $z = 0$ ist $\zeta^2 = 0$, und im Punkte $z = \infty + i\left(\frac{\pi}{2} - \arg w + \mu\right)$ ist $\zeta^2 = \infty\, e^{i\mu}$. Da der Koordinatenursprung der einzige auf L liegende Sattelpunkt von $\varphi(z)$ ist, ändert sich also $\zeta^2 e^{-i\mu}$ monoton von 0 nach ∞, wenn z den Zweig L von 0 nach $\infty + i\left(\frac{\pi}{2} - \arg w + \mu\right)$ durchläuft.

Wenn man (siehe (72))

$$\zeta = \Phi(z) = e^{-\frac{\pi i}{4}} \sqrt{2}\, w^{1/2} \sinh \frac{z}{2} \quad (\arg w^{1/2} = \tfrac{1}{2} \arg w) \quad . \quad . \quad (73)$$

setzt, dann ist, da die Tangente von L in $z = 0$ einen Winkel von $\frac{\pi}{4} - \frac{1}{2}\arg w + \frac{\mu}{2}$ mit der positiven Achse bildet, auch $\zeta e^{-\frac{i\mu}{2}} \geqq 0$ für jedes z auf L. Man findet daher wegen (71) und (72)

$$H_\nu^{(1)}(w) = \frac{2\, e^{i\,(w-1/2\,\nu\pi)}}{\pi i} \int_0^{\infty e^{\frac{i\mu}{2}}} e^{-\zeta^2} \cosh \nu z \frac{dz}{d\zeta} d\zeta \quad . \quad . \quad . \quad . \quad (74)$$

Wir betrachten nun die Kurve C_1, bestehend aus R_5, R_6 und den Geraden $x = d_1$ und $x = -d_2$, worin d_1 und d_2 unbeschränkt wachsen ($x = d_1$ verbindet $\infty - \pi i$ mit $\infty + \pi i$, $x = -d_2$ verbindet $-\infty - \pi i$ mit $-\infty + \pi i$). Wir wenden (41) von Hilfssatz 5 an mit $C = C_1$ und $F(z) = \Phi(z)$, also mit $p = e^{-\frac{\pi i}{4}} \sqrt{2}\, w^{1/2}$ und $q = \frac{1}{2}$. Wir finden dann für jedes z im Innern von C_1

$$\cosh \nu z \frac{dz}{d\zeta} = \frac{1}{2\pi i} \sum_{l=0}^{N-1} \zeta^{2l} \int_{C_1} \frac{\cosh \nu t \, dt}{\Phi(t)^{2l+1}} + \frac{\zeta^{2N}}{2\pi i} \int_{C_1} \frac{\cosh \nu t \, dt}{\Phi(t)^{2N}(\Phi(t) - \zeta)}.$$

Aus Hilfssatz 4 folgt, dass $\Phi(t) \neq \Phi(z)$ ist, falls t auf C_1 und z im Innern von C_1 liegt. Man hat somit wegen (45) von Hilfssatz 6 mit

$p = e^{-\frac{\pi i}{4}}\sqrt{2}\, w^{1/2}$, $q = \frac{1}{2}$ und $d = \Phi(z) = \zeta$ für jedes z innerhalb C_1 und für jedes ganze $N > |\Re(\nu)| - \frac{1}{2}$

$$\int_{C_1} \frac{\cosh \nu t\, dt}{\Phi(t)^{2N}(\Phi(t)-\zeta)} = -\frac{e^{-\frac{\pi i}{4}}(-i)^N \cos \nu\pi}{2^{\frac{2N-1}{2}}\, w^{\frac{2N+1}{2}}} \int_{-\infty}^{\infty} \frac{2\, iw \cosh^2\frac{x}{2} \cosh \nu x\, dx}{\left(\cosh\frac{x}{2}\right)^{2N+1}\left(2\, iw \cosh^2\frac{x}{2} - \zeta^2\right)}.$$

Weiter gilt wegen (38) von Hilfssatz 3, mit $\alpha = \frac{1}{2}$ und $m = 2l$ angewendet,

$$\int_{C_1} \frac{\cosh \nu t\, dt}{\Phi(t)^{2l+1}} = \frac{e^{\frac{\pi i}{4}(2l+1)}}{2^{\frac{2l+1}{2}}\, w^{\frac{2l+1}{2}}} \int_{(0+)} \frac{\cosh \nu t\, dt}{\left(\sinh\frac{t}{2}\right)^{2l+1}} =$$

$$\frac{4\pi i e^{\frac{\pi i}{4}(2l+1)}}{2^{\frac{2l+1}{2}}\, w^{\frac{2l+1}{2}}\, (2l)!} \prod_{h=0}^{l-1} (4\nu^2 - (2h+1)^2);$$

also

$$\cosh \nu z \frac{dz}{d\zeta} = \sum_{l=0}^{N-1} \frac{e^{\frac{\pi i}{4}}(i)^l\, \zeta^{2l}}{2^{\frac{2l-1}{2}}\, w^{\frac{2l+1}{2}}\, (2l)!} \prod_{h=0}^{l-1} (4\nu^2 - (2h+1)^2)$$

$$+ \frac{e^{\frac{\pi i}{4}}(-i)^N \zeta^{2N} \cos \nu\pi}{\pi 2^{\frac{2N+1}{2}}\, w^{\frac{2N+1}{2}}} \int_{-\infty}^{\infty} \frac{2\, iw \cosh^2\frac{x}{2} \cosh \nu x\, dx}{\left(\cosh\frac{x}{2}\right)^{2N+1}(2\, iw \cosh^2\frac{x}{2} - \zeta^2)}.$$

Hieraus und aus (74) folgt, wegen

$$\int_0^{\infty e^{\frac{i\mu}{2}}} e^{-\zeta^2} \zeta^{2l}\, d\zeta = \frac{(2l)!\sqrt{\pi}}{2^{2l+1}\, l!}$$

die erste Behauptung des Satzes.

2. Wir gehen aus von der Definition (13) und nehmen als Integrationsweg die Kurve L. Wir erhalten dann wegen (69)

$$G_\nu(w) = \int_L e^{iw\cosh z} \sinh \nu z\, dz = e^{iw} \int_L e^{\varphi(z)-\varphi(0)} \sinh \nu z\, dz$$

oder, wenn wir (72) benutzen

$$G_\nu(w) = e^{iw} \int_0^{\infty e^{\frac{i\mu}{2}}} e^{-\zeta^2} \sinh \nu z \frac{dz}{d\zeta}\, d\zeta, \quad . \quad . \quad . \quad . \quad . \quad (75)$$

worin $\zeta = \Phi(z)$ durch (73) definiert ist.

Wegen (42) von Hilfssatz 5 mit $C = C_1$ und $F(z) = \Phi(z)$ also $p = e^{-\frac{\pi i}{4}} \sqrt{2}\, w^{1/2}$ und $q = \frac{1}{2}$, hat man, falls z im Innern von C_1 liegt,

$$\sinh \nu z \frac{dz}{d\zeta} = \frac{1}{2\pi i} \sum_{l=0}^{N-1} \zeta^{2l+1} \int_{C_1} \frac{\sinh \nu t\, dt}{\Phi(t)^{2l+2}} + \frac{\zeta^{2N+1}}{2\pi i} \int_{C_1} \frac{\sinh \nu t\, dt}{\Phi(t)^{2N+1}(\Phi(t)-\zeta)}.$$

Wegen (46) von Hilfssatz 6, mit $p = e^{-\frac{\pi i}{4}} \sqrt{2}\, w^{1/2}$, $q = \frac{1}{2}$ und $d = \Phi(z) = \zeta$ angewendet, hat man für jedes z innerhalb C_1 und für jedes ganze $N > |\Re(\nu)| - 1$

$$\int_{C_1} \frac{\sinh \nu t\, dt}{\Phi(t)^{2N+1}(\Phi(t)-\zeta)} = \frac{-2 \sin \nu\pi}{(i)^N (2w)^{N+1}} \int_{-\infty}^{\infty} \frac{2iw \cosh^2 \frac{x}{2} \cosh \nu x\, dx}{\left(\cosh \frac{x}{2}\right)^{2N+2} \left(2iw \cosh^2 \frac{x}{2} - \zeta^2\right)}.$$

Weiter hat man wegen (39) von Hilfssatz 3, mit $a = \frac{1}{2}$ und $m = 2l+1$ angewendet,

$$\int_{C_1} \frac{\sinh \nu t\, dt}{\Phi(t)^{2l+2}} = \frac{(i)^{l+1}}{(2w)^{l+1}} \int_{(0+)} \frac{\sinh \nu t\, dt}{\left(\sinh \frac{t}{2}\right)^{2l+2}} = \frac{8\pi\nu\,(i)^{l+2}}{(2w)^{l+1}(2l+1)!} \prod_{h=0}^{l-1} (4\nu^2 - (2h+2)^2)$$

also

$$\sinh \nu z \frac{dz}{d\zeta} = \sum_{l=0}^{N-1} \frac{4\nu\,(i)^{l+1} \zeta^{2l+1}}{(2w)^{l+1}(2l+1)!} \prod_{h=0}^{l-1} (4\nu^2 - (2h+2)^2)$$

$$- \frac{\zeta^{2N+1} \sin \nu\pi}{\pi (i)^{N+1} (2w)^{N+1}} \int_{-\infty}^{\infty} \frac{2iw \cosh^2 \frac{x}{2} \cosh \nu x\, dx}{\left(\cosh \frac{x}{2}\right)^{2N+2} \left(2iw \cosh^2 \frac{x}{2} - \zeta^2\right)}.$$

Wegen

$$\int_0^{\infty e^{\frac{i\mu}{2}}} e^{-\zeta^2} \zeta^{2l+1}\, d\zeta = \frac{l!}{2}$$

folgt hieraus und aus (75) die zweite Behauptung des Satzes.

Mathematics. — *Sur la représentation conforme.* Par A. VAN HASELEN. (Communicated by Prof. J. G. VAN DER CORPUT).

(Communicated at the meeting of June 25, 1932).

Supposons que la fonction holomorphe $w = u + vi = f(z) = f(x+yi)$ donne une représentation conforme du demi-plan $x > 0$ sur un domaine D, contenu dans le demi-plan $u > 0$ et contenant un demi-plan $u > a > 0$ tel que $w \to \infty$ pour $z \to \infty$.

M. J. WOLFF [1]) a démontré, qu'on a dans ce cas $f(z) = \lambda z - \omega(z)$ où $\lambda \geqslant 0$, $lim \frac{\omega(z)}{z} = 0$, pour $\frac{y}{x}$ borné, et $z \to \infty$, et la partie réelle $R\omega$ de $\omega(z)$ est positive ou nulle.

Nous démontrerons les propositions suivantes:

1. $0 \leqslant R\omega \leqslant a$ dans tout le demi-plan $x > 0$.

2. $\omega = O(log\, z)$ pour $z \to \infty$, $\frac{y}{x}$ borné.

3. Supposons que $\mathfrak{W}(\zeta) = \mathfrak{W}(\xi + i\eta)$ donne une représentation conforme du disque circulaire $C(|\zeta - \frac{1}{2}| \leqslant \frac{1}{2})$ sur un domaine borné Γ de C et que $lim_{\zeta \to 0} \mathfrak{W}(\zeta) = 0$.

M. C. CARATHEODORY [2]) a démontré, que si le domaine Γ contient un cercle, passant par O, on a $lim \frac{d\mathfrak{W}}{d\zeta} = \sigma$, où $0 < \sigma < \infty$ pour $\zeta \to 0$, $\frac{\eta}{\xi}$ borné.

Nous démontrerons qu'on a $\frac{d^2\mathfrak{W}}{d\zeta^2} = O(log\, \zeta)$ pour $\zeta \to 0$, $\frac{\eta}{\xi}$ borné, et donnerons un exemple d'une fonction, pour laquelle $\frac{\frac{d^2 f}{d\zeta^2}}{log\, \zeta}$ tend vers une limite différente de zéro.

Démontrons d'abord le lemme suivant:

Si $\omega(z)$ est une fonction holomorphe dans le demi-plan $x > 0$ et si $0 \leqslant R\omega \leqslant a$, on a

$$\frac{d^2\omega}{dz^2} \leqslant \frac{2a}{x^2} \quad . \quad . \quad . \quad . \quad . \quad . \quad . \quad . \quad . \quad . \quad (I)$$

pour chaque $z = x + yi$ du demi-plan $x > 0$.

Soit γ la droite d'abscisse $\frac{x}{2}$ paralèle à Oy.

---

[1]) C. R. de l'Ac. d. Sc. **38** (1926), p. 500—503.

[2]) Sitzungsberichte des Preuss. Ak. der Wiss. 1929. IV S. 39—54.

On a

$$\omega''(z) = \frac{1}{2\pi i}\int_{\gamma} \frac{\omega'(t)\,dt}{(t-z)^2}$$

car $\omega'(z)$ est bornée à droite de γ en vertu de $|\omega'(z)| \leqslant \frac{u}{\frac{1}{2}x} \leqslant \frac{2a}{x}$.

Donc

$$|\omega''(z)| \leqslant \frac{1}{2\pi} \times \frac{2a}{x} \int_{-\infty}^{+\infty} \frac{ds}{\frac{1}{4}x^2 + (s-y)^2}.$$

Il en résulte que

$$|\omega''(z)| \leqslant \frac{2a}{x^2}$$

1. Pour démontrer la proposition 1 remarquons que les hypothèses faites entraînent que $z = \varphi(w)$ est uniforme et holomorphe dans le demi-plan $u > a$.

Le théorème de M. CARATHEODORY donne, au moyen de la transformation

$$\zeta = \frac{1}{z}, \quad \mathfrak{W} = \frac{1}{w} \quad \text{que} \quad 0 < \lambda < \infty.$$

Or pour $u > a$ on a $\frac{x}{u-a} \geqslant \frac{1}{\lambda}$ et partout la relation $\frac{u}{x} \geqslant \lambda$ est valable, d'ou il résulte que $u \geqslant \lambda \geqslant u - a$ donc $R\,\omega \leqslant a$ pour $u > a$.

Cette dernière inégalité étant manifesté pour $u \leqslant a$ la proposition 1 est démontrée.

2. Pour démontrer la proposition 2, remarquons qu'on a

$$\left|\frac{d\omega}{dz}\right| \leqslant \frac{a}{x}$$

donc

$$\omega = \omega(1) + \int_1^z \frac{d\omega}{dz}\,dz = O(\log z)$$

pour $\frac{y}{x}$ borné.

3. Soit

$$w = \frac{1}{\mathfrak{W}} \quad \text{et} \quad z = \frac{1}{\zeta}$$

On a

$$\frac{d\mathfrak{W}}{d\zeta} = \frac{z^2}{w^2}\frac{dw}{dz}$$

ou

$$\frac{d^2\mathfrak{W}}{d\zeta^2} = -\frac{2z^3}{w^2}\frac{dw}{dz} + \frac{2z^4}{w^3}\left(\frac{dw}{dz}\right)^2 - \frac{z^4}{w^2}\frac{d^2w}{dz^2}.$$

On peut écrire

$$\frac{dw}{dz} = \lambda + \frac{\theta a}{x} \quad \ldots\ldots\ldots\ldots \quad (III)$$

où $|\theta| \leqslant 1$.

De la formule (I) il résulte que

$$\frac{d^2\mathfrak{W}}{d\zeta^2} = -\frac{2z^3}{w^2}\left(\lambda - \theta\frac{a}{x}\right) + \frac{2z^4}{w^3}\left(\lambda^2 + 2\theta\lambda\frac{a}{x} + \theta^2\frac{a^2}{x^2}\right) - \frac{z^4}{w^2} \times \theta \times \frac{2a}{x^2}$$

Ou

$$\frac{d^2\mathfrak{W}}{d\zeta^2} = -\frac{2z^3}{w^2}\lambda + 2\frac{z^4}{w^3}\lambda^2 + O(1)$$

pour $\frac{y}{x}$ borné, ce qui équivaut à $\frac{\eta}{\xi}$ borné.

Donc $\frac{d^2\mathfrak{W}}{d\zeta^2} = O(1) + O(w - \lambda z)$, puisque $\frac{z}{w}$ est borné.

Par conséquent

$$\frac{d^2\mathfrak{W}}{d\zeta^2} = O(1) + O\{\omega(z)\}.$$

En appliquant la proposition 2, nous aboutissons à la proposition 3.

4. Pour donner un exemple d'une fonction, pour laquelle $\frac{d^2\mathfrak{W}}{d\zeta^2}$ a précisément l'ordre de grandeur de $\log \zeta$, il suffira de construire une fonction $w(z)$ satisfaisant aux hypothèses de la proposition 1 et pour laquelle $\omega(z)$ est précisément de l'ordre de $\log z$ pour z infini, $\frac{y}{x}$ borné.

On le voit au moyen de la transformation $\zeta = \frac{1}{z}$, $\mathfrak{W} = \frac{1}{w}$ et de l'application de la relation

$$\frac{d^2\mathfrak{W}}{d\zeta^2} = -\frac{2z^3}{w^2}\lambda + \frac{2z^4}{w^3}\lambda^2 + O(1) = -\frac{2z^3}{w^3}\lambda(w - \lambda z) + O(1).$$

Or, considérons la fonction

$$w = z + i\log(z+1) + C,$$

où $C > \frac{\pi}{2}$. Cette fonction satisfait aux hypothèses de la proposition 1.

De plus $\lambda = 1$ et $\frac{w - \lambda z}{\log z} = \frac{w - z}{\log z} \to i$.

Mathematics. — *On the Rational Commutant of a Square Matrix.* By D. E. RUTHERFORD. (Communicated by Prof. R. WEITZENBÖCK).

(Communicated at the meeting of June 25, 1932.)

If X satisfies the matrix equation

$$AX = XA, \quad . \quad . \quad . \quad . \quad . \quad . \quad . \quad . \quad . \quad (1)$$

then X is said to be a commutant of the matrix A. The solution to this equation in an irrational form has been known for some time [1]), but Prof. TURNBULL pointed out to me that a rational solution must exist if the matrix A is rational, and suggested that I should try to find it. My thanks are due to Prof. TURNBULL for his helpful criticism of this paper.

I. Let I_n be the unit matrix of order n and let $I_{n,m}$ denote the matrix of n rows and m columns which is $[I_n \, .]$ if $m > n$, which is $\begin{bmatrix} I_m \\ . \end{bmatrix}$ if $n > m$, and which is I_n if $n = m$. Let B be the rational canonical form of the matrix A [2]), and let

$$H^{-1}AH = B, \quad . \quad . \quad . \quad . \quad . \quad . \quad . \quad . \quad . \quad (2)$$

where H is nonsingular. Now if Y satisfies the matrix equation

$$BY = YB, \quad . \quad . \quad . \quad . \quad . \quad . \quad . \quad . \quad . \quad (3)$$

then

$$H^{-1}AHY = YH^{-1}AH,$$

or

$$AHYH^{-1} = HYH^{-1}A,$$

and therefore $X = HYH^{-1}$ is a solution to the equation (1). It is sufficient therefore to solve equation (3), where the matrix B is of the rational canonical form.

Let B have diagonal submatrices $B_p, B_q, \ldots, B_t$, where each submatrix B_n is an elementary rational canonical matrix of order n, thus

$$\begin{bmatrix} . & 1 & . & \ldots\ldots & . \\ . & . & 1 & \ldots\ldots & . \\ \multicolumn{5}{c}{\ldots\ldots\ldots\ldots\ldots} \\ . & . & . & \ldots\ldots & 1 \\ a_0 & a_1 & a_2 & \ldots\ldots & a_{n-1} \end{bmatrix}$$

[1]) H. W. TURNBULL and A. C. AITKEN, *Canonical Matrices*. Glasgow, 1932, pp. 143—148.

[2]) *loc. cit.* p. 49.

It is known that when B is in this form, the characteristic function of B_m is a factor of the characteristic function of B_n, if $n > m$. We can now partition the matrix Y into submatrices $Y_{n,m}$ where $Y_{n,m}$ is a matrix of n rows and m colums. To solve the equation (3), it is sufficient to solve the matrix equation

$$B_n\, Y_{n,m} = Y_{n,m}\, B_m \quad . \quad . \quad . \quad . \quad . \quad . \quad . \quad . \quad . \quad (4)$$

We shall first consider the case where n is greater than m.

II. The equation (4) can now be written out in full as follows:

$$\begin{bmatrix} \cdot & 1 & \cdot & \cdots & \cdot \\ \cdot & \cdot & 1 & \cdots & \cdot \\ \cdots & \cdots & \cdots & \cdots & \cdots \\ \cdots & \cdots & \cdots & \cdots & \cdots \\ \cdot & \cdot & \cdot & \cdots & 1 \\ \alpha_0 & \alpha_1 & \alpha_2 & \cdots & \alpha_{n-1} \end{bmatrix} \begin{bmatrix} y_{1,1} & y_{1,2} & \cdots & y_{1,m} \\ y_{2,1} & y_{2,2} & \cdots & y_{2,m} \\ \cdots & \cdots & \cdots & \cdots \\ \cdots & \cdots & \cdots & \cdots \\ \cdots & \cdots & \cdots & \cdots \\ y_{n,1} & y_{n,2} & \cdots & y_{n,m} \end{bmatrix} = \begin{bmatrix} y_{1,1} & y_{1,2} & \cdots & y_{1,m} \\ y_{2,1} & y_{2,2} & \cdots & y_{2,m} \\ \cdots & \cdots & \cdots & \cdots \\ \cdots & \cdots & \cdots & \cdots \\ \cdots & \cdots & \cdots & \cdots \\ y_{n,1} & y_{n,2} & \cdots & y_{n,m} \end{bmatrix} \begin{bmatrix} \cdot & 1 & \cdot & \cdots & \cdot \\ \cdot & \cdot & 1 & \cdots & \cdot \\ \cdots & \cdots & \cdots & \cdots & \cdots \\ \cdots & \cdots & \cdots & \cdots & \cdots \\ \cdot & \cdot & \cdot & \cdots & 1 \\ \beta_0 & \beta_1 & \beta_2 & \cdots & \beta_{m-1} \end{bmatrix} \quad (5)$$

Multiplying out both sides of equation (5) and equating the corresponding elements, we obtain the following equations for the elements $y_{i,j}$:

$$\left.\begin{aligned} y_{i,1} &= \beta_0\, y_{i-1,m} \\ y_{ij} &= \beta_{j-1}\, y_{i-1,m} + y_{i-1,j-1} \end{aligned}\right\} \quad . \quad . \quad . \quad . \quad . \quad . \quad . \quad (6)$$

and

$$\left.\begin{aligned} \alpha_0\, y_{1,1} + \ldots + \alpha_{n-1}\, y_{n,1} &= \beta_0\, y_{n,m} \\ \alpha_0\, y_{ij} + \ldots + \alpha_{n-1}\, y_{n,j} &= \beta_{j-1}\, y_{n,m} + y_{n,j-1} \end{aligned}\right\} \quad . \quad . \quad . \quad . \quad (7)$$

where $m \geqq j > 1$ and $n \geqq i > 1$. For convenience, we have divided the above equations into two sets. If n is greater than or equal to m, then $\varphi(\lambda) = \beta_m \lambda^m + \beta_{m-1} \lambda^{m-1} + \ldots + \beta_0$ is a factor of $\psi(\lambda) = \alpha_n \lambda^n + \alpha_{n-1} \lambda^{n-1} + \ldots + \alpha_0$, where $-1 = \alpha_n = \beta_m$ If $\psi(\lambda)/\varphi(\lambda) = \gamma_{n-m} \lambda^{n-m} + \ldots + \gamma_0$, then

$$\left.\begin{aligned} \alpha_n &= \beta_m\, \gamma_{n-m} \\ \alpha_{n-1} &= \beta_{m-1}\, \gamma_{n-m} + \beta_m\, \gamma_{n-m-1} \\ \alpha_{n-2} &= \beta_{m-2}\, \gamma_{n-m} + \beta_{m-1}\, \gamma_{n-m-1} + \beta_m\, \gamma_{n-m-2} \\ &\cdots\cdots\cdots\cdots\cdots\cdots \\ \alpha_{n-m} &= \beta_0\, \gamma_{n-m} + \beta_1\, \gamma_{n-m-1} + \beta_2\, \gamma_{n-m-2} + \ldots \\ \alpha_{n-m-1} &= \beta_0\, \gamma_{n-m-1} + \beta_1\, \gamma_{n-m-2} + \ldots \\ &\cdots\cdots\cdots\cdots\cdots\cdots \\ \alpha_1 &= \beta_0\, \gamma_1 + \beta_1\, \gamma_0 \\ \alpha_0 &= \beta_0\, \gamma_0 \end{aligned}\right\} \quad . \quad (8)$$

By the repeated use of equations (6), it follows that

$$y_{i,h} = \beta_0\, y_{i-h,m} + \beta_1\, y_{i-h+1,m} + \ldots + \beta_{h-2}\, y_{i-2,m} + \beta_{h-1}\, y_{i-1,m} \quad . \quad (9)$$

Hence

$$\begin{aligned}
&\beta_0\, y_{i-m,h} + \beta_1\, y_{i-m+1,h} + \ldots + \beta_{m-1}\, y_{i-1,h} \\
&= \beta_0\,(\beta_0\, y_{i-m-h,m} + \ldots + \beta_{h-1}\, y_{i-m-1,m}) \\
&+ \beta_1\,(\beta_0\, y_{i-m-h+1,m} + \ldots + \beta_{h-1}\, y_{i-m,m}) \\
&+ \ldots\ldots\ldots\ldots\ldots\ldots \\
&+ \beta_{m-1}\,(\beta_0\, y_{i-h-1,m} + \ldots + \beta_{h-1}\, y_{i-2,m}) \\
&= \beta_0\, y_{i-h,m} + \beta_1\, y_{i-h+1,m} + \ldots + \beta_{h-1}\, y_{i-1,m} = y_{i,h}
\end{aligned}$$

Hence

$$\sum_{k=0}^{m} \beta_k\, y_{i-m+k,h} = 0, \quad (m < i \leqslant n)$$

or more simply

$$\sum_{k=0}^{m} \beta_k\, y_{r+k,h} = 0, \quad (0 < r \leqslant m-n) \quad . \quad . \quad . \quad . \quad . \quad (10)$$

By (8) and (10)

$$\begin{aligned}
\alpha_0\, y_{1,i} + \alpha_1\, y_{2,i} + \ldots + \alpha_{n-1}\, y_{n,i} &= \beta_0\, y_{n-m+1,i} + \ldots + \beta_{m-1}\, y_{n,i} \\
&= \beta_0\,(\beta_0\, y_{n-m+1-i,m} + \ldots + \beta_{i-1}\, y_{n-m,m}) \\
&+ \ldots\ldots\ldots\ldots\ldots\ldots \\
&+ \beta_{m-1}\,(\beta_0\, y_{n-i,m} + \ldots + \beta_{i-1}\, y_{n-i,m}) \\
&= \beta_0\, y_{n-i+1,m} + \ldots + \beta_{i-1}\, y_{n,m}
\end{aligned}$$

Now if $i = 1$, this last is equal to $\beta_0\, y_{n,m}$ and if $i > 1$, then by (9) this last is equal to $y_{n,i-1} + \beta_{i-1}\, y_{n,m}$. Hence equations (7) are satisfied identically in virtue of equations (6), and hence we may neglect equations (7) entirely.

By means of equations (6), every element of $Y_{n,m}$ can be expressed in terms of $y_{1,1}, y_{1,2}, \ldots, y_{1,m}$, to which we may give the arbitrary values $y_1, y_2, \ldots, y_m$. If the h-th row of Y be

$$z_1, z_2, z_3, \ldots, z_m,$$

then by equations (6) the $(h+1)$-th row will be

$$\beta_0\, z_m, \beta_1\, z_m + z_1, \beta_2\, z_m + z_2, \ldots, \beta_{m-1}\, z_m + z_{m-1}.$$

Hence any particular element y_l will appear in $Y_{n,m}$ in the following manner

$$y_l \begin{bmatrix} \cdot & \cdot \ldots\ldots\ldots\ldots \cdot\ 1\ \cdot\ \cdot \ldots\ldots \cdot \\ \cdot & \cdot \ldots\ldots\ldots\ldots \cdot\ \cdot\ 1\ \cdot \ldots\ldots \cdot \\ \cdot & \cdot \ldots\ldots\ldots\ldots \cdot\ \cdot\ \cdot\ 1 \ldots\ldots \cdot \\ \ldots\ldots\ldots\ldots\ldots\ldots\ldots\ldots\ldots\ldots\ldots\ldots\ldots & \ldots\ldots \\ \cdot & \cdot \ldots\ldots\ldots\ldots \cdot\ \cdot\ \cdot\ \cdot\ \cdot \ldots\ldots 1 \\ \beta_0, & \beta_1 \ldots\ldots\ldots\ldots\ldots\ldots\ldots\ldots\ldots\ldots\ldots\ldots & \beta_{m-1} \\ \beta_0\,\beta_{m-1}, & \beta_1\,\beta_{m-1} + \beta_0 \ldots\ldots\ldots\ldots\ldots\ldots & \beta_{m-2} + \beta_{m-1}^2 \\ \ldots\ldots\ldots\ldots\ldots\ldots\ldots\ldots\ldots\ldots\ldots\ldots\ldots & \ldots\ldots \end{bmatrix}$$

or $y_l\, I_{n,m}\, B_m^{l-1}$. Hence if $n \geqslant m$, then the most general solution of equation (4) is

$$Y_{n,m} = I_{n,m}\,(y_1\, I + y_2\, B_m + \ldots + y_m\, B_m^{m-1}), \quad . \quad . \quad . \quad . \quad (11)$$

where the y's are arbitrary parameters. We may write equation (11) as

$$Y_{n,m} = I_{n,m}\,[\varphi\,(B_m)]$$

where $\varphi\,(B_m)$ is an arbitrary rational integral function of the matrix B_m, for any such function can be reduced to one of degree $m-1$ or lower, since B_m must satisfy its own characteristic equation.

III. We now consider the solution of

$$B_n\, Y_{n,m} = Y_{n,m}\, B_m \quad . \quad . \quad . \quad . \quad . \quad . \quad . \quad . \quad . \quad (4)$$

where $n < m$. Let the irrational classical canonical form of B_n be C_n and that of B_m be C_m; thus

$$K_m^{-1}\, B_m\, K_m = C_m; \quad K_n^{-1}\, B_n\, K_n = C_n \quad . \quad . \quad . \quad . \quad . \quad (12)$$

The matrices K_m and K_n are alternants and can readily be found [1]). Further, let

$$L_m^{-1}\, C_m\, L_m = C'_m; \quad L_n^{-1}\, C_n\, L_n = C'_n \quad . \quad . \quad . \quad . \quad . \quad (13)$$

It is also easy to find L_m and L_n; e.g., if

$$C_n = \begin{bmatrix} \alpha & 1 & & \\ & \alpha & 1 & \\ & & \alpha & \\ & & & \beta\ 1 \\ & & & \beta \end{bmatrix}, \text{ then } L_n = \begin{bmatrix} & & 1 & \\ & 1 & & \\ 1 & & & \\ & & & 1 \\ & & 1 & \end{bmatrix}.$$

[1]) *loc. cit.* pp. 58—60.

It will also be found that $L_m = L'_m = L_m^{-1}$ and similarly $L_n = L'_n = L_n^{-1}$. From equations (12) and (13)

$$K'_n B'_n K'^{-1}_n = C'_n = L_n^{-1} C_n L_n = L_n^{-1} K_n^{-1} B_n K_n L_n .$$

Hence

$$B'_n = K'^{-1}_n L_n^{-1} K_n^{-1} B_n K_n L_n K'_n .$$

Let $M_n = K_n L_n K'_n$, then $B'_n = M_n^{-1} B_n M_n$. Also, from equation (4),

$$B'_m Y'_{n,m} = Y'_{n,m} B'_n .$$

Therefore

$$M_m^{-1} B_m M_m Y'_{n,m} = Y'_{n,m} M_n^{-1} B_n M_n ;$$

or

$$B_m T_{m,n} = T_{m,n} B_n , \quad . \quad . \quad . \quad . \quad . \quad . \quad . \quad . \quad (14)$$

where

$$T_{m,n} = M_m Y'_{n,m} M_n^{-1}$$

But we have already shown that the most general solution T_{mn} of equation (14) is $I_{mn}[\varphi(B_n)]$, where $\varphi(B_n)$ is a rational integral function of B_n. Hence the most general solution for Y_{nm} is

$$Y'_{nm} = M_m^{-1} I_{m,n} \varphi(B_n) M_n$$

or

$$Y_{nm} = M'_n \varphi(B'_n) I_{n,m} M_m^{-1'}.$$

Since $L_n = L'_n$, hence $M_n = M'_n$; but $B'_n = M_n^{-1} B_n M_n$, therefore

$$\varphi(B'_n) = M_n^{-1} \varphi(B_n) M_n.$$

Thus

$$\begin{aligned} Y_{nm} &= \varphi(B_n) M_n I_{n,m} M_m^{-1} \\ &= \varphi(B_n) K_n L_n K'_n I_{n,m} K_m^{-1'} L_m^{-1} K_m^{-1}. \end{aligned}$$

We have now solved equation (4) for all cases and so, fitting the submatrices Y_{nm} together, we find a solution Y to equation (3). From this in turn a solution X of equation (1) can be found.

IV. We shall conclude with the solution of a simple example. Suppose that we wish to find the commutant of the matrix A where

$$A = \begin{bmatrix} . & 1 & . & 1 & . \\ . & . & . & 1 & . \\ . & . & . & . & \frac{1}{2} \\ 1 & . & . & -1 & . \\ . & . & 2 & . & . \end{bmatrix}$$

It is easily shown that $H^{-1} A H = B$, where

$$H = \begin{bmatrix} 1 & 1 & . & . & . \\ . & 1 & . & . & . \\ . & . & . & 1 & . \\ . & . & 1 & . & . \\ . & . & . & . & 2 \end{bmatrix} \text{ and } B = \left[\begin{array}{ccc:cc} . & 1 & . & . & . \\ . & . & 1 & . & . \\ 1 & 1 & -1 & . & . \\ \hdashline . & . & . & . & 1 \\ . & . & . & 1 & . \end{array}\right].$$

We have now the following four equations to solve

$$B_3 Y_{33} = Y_{33} B_3, \quad B_3 Y_{32} = Y_{32} B_2, \quad B_2 Y_{23} = Y_{23} B_3 \quad B_2 Y_{22} = Y_{22} B_2;$$

where $B_3 = \begin{bmatrix} . & 1 & . \\ . & . & 1 \\ 1 & 1 & -1 \end{bmatrix}$, and $B_2 = \begin{bmatrix} . & 1 \\ 1 & . \end{bmatrix}$.

By the methods shown in this paper we immediately deduce the following solutions:

$$Y_{33} = a_1 I_3 + a_2 B_3 + a_3 B_3^2,$$
$$Y_{22} = a_4 I_2 + a_5 B_2$$
$$Y_{32} = I_{3,2} (a_6 I_2 + a_7 B_2)$$
$$Y_{23} = (a_8 I_2 + a_9 B_2) K_2 L_2 K'_2 I_{2,3} K'^{-1}_3 L_3^{-1} K_3^{-1},$$

where

$$K_3 = \begin{bmatrix} -1 & 1 & 1 \\ 1 & -2 & 1 \\ -1 & 3 & 1 \end{bmatrix}, \quad L_3 = \begin{bmatrix} . & 1 & . \\ 1 & . & . \\ . & . & 1 \end{bmatrix}, \quad K_2 = \begin{bmatrix} -1 & 1 \\ 1 & 1 \end{bmatrix}, \quad L_2 = I_2;$$

and where $a_1, a_2, \ldots, a_9$ are all arbitrary constants. Fitting the submatrices together as was done before we arrive at a solution of the matrix equation $BY = YB$, and hence we have found a rational commutant of the matrix B. The commutant of A is now given by

$$HYH^{-1}.$$

Chemistry. — *On the Use of a Triode as a Contactfree Relais in the Regulation of the Temperature of a Thermostat.* By E. ROSENBOHM. (Communicated by Prof. F. M. JAEGER.)

(Communicated at the meeting of June 25, 1932).

§ 1. During our measurements of the specific heats of solid substances by means of the large metal-block calorimeter, the necessity was felt of having a reliable method of temperature-regulation by means of a relais which, — also in the case of an extreme prolongation of the experiments, — would safely work without undesirable disturbances. For the purpose of keeping the temperature constant within the thermostat-water surrounding the copper-bloc, a very sensitive contact-thermometer is used, which regulates the action of a HERAEUS' mercury-relais. Although the current in the contact-thermometer proved to be no stronger than about 0.015 Amp. at 2 Volt (0.03 Watt), experience taught us, that even this must be considered as too much for the instrument, if the latter be continually used during a very long interval of time: at the most unexpected moments suddenly the contact appeared to get "sticking", — a rise of temperature of the water in the thermostat of several hundredths of a degree being the inevitable consequence of its bad functioning. As each disturbance of this kind signifies the loss of *1* or *2* days in the work to be done, it became desirable to find out another way of constructing a relais, in which we could *get rid of such unreliable contacts* and in which *no* or only an *unappreciably weak current* was used. This problem can, in a rather simple way, be solved by using a triode *L* in a connection with a very great grid-leak *W* (Fig. 1).

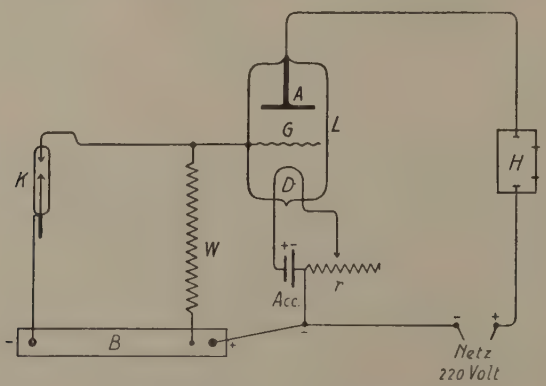

Fig. 1. Triode-Arrangement for a Contactfree Relais to be used for Thermostat-Regulation.

As long as the surrounding water of the thermostat has too low a temperature, no contact in the contact-thermometer *K* is present. Therefore, if *B* is a suitable grid-battery (60 Volt), the voltage applied to the grid *G* is negative and only very small, if the grid-leak *W* be very great, — about

2 to 10 Meg-Ohms. The current necessary to work the mercury-relais *H*, therefore, can pass the valve *L* without any impediment.

If, however, as a consequence of the rise of the temperature of the water after some lapse of time, the contact at *K* is established, the grid *G* will acquire the full negative tension of the battery *B* and the passage of the current in *L* will immediately be stopped. As, with a suitable choice of the resistance *W*, — for instance of 5 Meg-Ohms, — the decrease of the tension in *B* by the partial short-circuiting of *B* will only be extremely small, no practical effect of that decrease will be manifested. The contact-thermometer *K*, it is true, will not be perfectly currentfree; but this current scarcely will have an intensity of a few Mikro-Ampères and is too weak to endanger even the very sensitive contact-thermometer on closing or interrupting the contact in it. Of course, the magnitude of the grid-tension in *G*, as well as the special choice of the valve *L*, depend on the particular circumstances, — in this case on the type of the HERAEUS' relais *H* used. This relais is, at a tension of 220 Volts, worked with about 30 or 40 Milli-Ampères; therefore, a valve *L* of the type *Cossor 4XP* or *Telefunken RE*604 proves to be very well suited for this purpose. Even after a continuous use during 2.5 months, a valve of the first mentioned type showed not the least change of its emission. The current applied to the wire *D* must be not stronger than just necessary; for this reason the storage-cell *Acc* is used in connection with a variable resistance *r* and experience teaches, that ordinarily a tension of about 3.5 Volts is quite sufficient. The connections used in the total equipment are schematically represented in Figure 1 and need no further comment. It proves practically unfeasible to weaken the remaining current in *K* by increasing the resistance of the grid-leak *W* still more, — for instance to more than 10 Meg-Ohms, — because the isolation of the connections to the grid *G* then offers too great difficulties. Special attention and care must be given to the perfect isolation of these wires, as well as of all other connections at *L* and *K*, as the moist atmosphere in the neighbourhood of *K*, for instance, — as a consequence of the watervapour of the surrounding jacket, — is most troublesome in this respect. Therefore, the connections at *K* are suitably made by means of two-wire rubber cables, imbedded in molten and solidified paraffine, which completely surrounds the upper end of the thermometer *K* by means of a cylindrical vessel at all sides adjacent to the glass wall of the instrument.

If in stead of direct current, alternating current be used, the storage-cell *Acc* can readily be replaced by a 4 Volt-transformator, while the relais *H* must then be used in connection with a valve or a metal-rectifier.

The arrangement just described can, by its simplicity and its reliability, strongly be recommanded for the use of thermostatregulation.

Groningen, Laboratory for Inorganic and Physical Chemistry of the University.

Geology. — *Abyssische und hypabyssische Eruptivgesteine der Insel Soemba, Niederländisch Ost-Indien.* Von P. M. ROGGEVEEN. (Communicated by Prof. L. RUTTEN.)

(Communicated at the meeting of May 28, 1932.)

Die hier behandelten Gesteine stammen aus Sammlungen van H. F. C. TEN KATE und H. WITKAMP. TEN KATE besuchte Soemba in 1891 auf einer ethnologischen Forschungsreise [1]). WITKAMP machte in 1910 geologische Untersuchungen in Soemba [2]). Beide Gesteinsammlungen befinden sich im geologischen Institut der Reichsuniversität zu Utrecht. Es werden hier nur die abyssischen und hypabyssischen Eruptivgesteine dieser Sammlungen beschrieben, im Ganzen 39 Stücke. Meistens sind es Gesteine WITKAMP's. Die Gesteine sind zum Teil früher von weiland Prof. A. WICHMANN bestimmt worden. Seine Benennungen sind in den Reiseberichten der beiden Forscher angegeben. Es erschien mir nützlich eine Beschreibung dieses Materials zu geben, besonders weil WICHMANN Manches nicht bestimmt hat und seine Benennungen nicht alle zutreffen.

Über das Alter dieser Eruptivgesteine ist Folgendes zu bemerken. Mehr als die Hälfte dieser Gesteine ist in Mittel-Soemba gesammelt worden, wo WITKAMP an vielen Stellen eine diskordante Bedeckung von Mergeln und Kalksteinen auf den Eruptivgesteinen festgestellt hat. In diesen jüngeren Sedimenten von Mittel-Soemba hat er an verschiedenen Stellen Orbitoiden gefunden [3]), welche von L. RUTTEN als Orthophragmina javana Verbeek und Orthophragmina dispansa Sowerby bestimmt worden sind [4]). Diese Sedimente gehören also zum Eozän. Im südwestlichen Soemba kommt eine Sedimentformation vor, welche wenigstens zum Teil jurassisch ist [5]). In diesen Sedimenten sind intrusive Eruptivgesteine vorhanden, welche also jünger sind. Wenn diese zu derselben Intrusionsperiode gehören wie die Mittel-Soemba-Gesteine, würde dies also auf ein jungmesozoisches Alter dieser Eruptivgesteine hinweisen. Das Vorkommen

---

[1]) H. F. C. TEN KATE: Verslag eener reis in de Timorgroep en Polynesië. Tschr. Kon. Aardr. Gen., 2de serie, deel XI, 1894. S. 541—638.

[2]) H. WITKAMP: Een verkenningstocht over het eiland Soemba. Tschr. Kon. Aardr. Gen., 2de serie, deel XXIX, 1912 (S. 744—775), deel XXX, 1913 (S. 8—27, 484—505, 619—637).

[3]) Vgl. Karte, Fig. 2: W. 165, 166, 167.

[4]) L. RUTTEN: On Orbitoids of Sumba. Proc. Kon. Akad. v. Wet. Amsterdam. 1912. S. 461.

[5]) P. M. ROGGEVEEN: Jurassic in the island of Sumba. Proc. Kon. Acad. v. Wet. Amsterdam. Vol. XXXII, 1929.

Vgl. J. WANNER: Mesozoikum. Leidsche geol. Meded. Deel V, 1931 (Feestbundel Prof. MARTIN). Hfdst. III: De stratigraphie van Ned. Oost-Indië. S. 584. WANNER meint, dass dieses fossilführende Gestein vielleicht zum oberen Lias zu stellen ist.

abyssischer und hypabyssischer Eruptivgesteine in tertiären Schichten ist von Soemba unbekannt. Mit einiger Wahrscheinlichkeit können die hier behandelten Gesteine also zum jüngeren Mesozoikum gestellt werden, obwohl das Vorkommen älterer Eruptivgesteine nicht ganz ausgeschlossen ist. Die Auffassung, dass die Eruptivgesteine von Soemba in alttertiärer Zeit intrudiert sind [1]), ist nicht wahrscheinlich, weil nach der Intrusionsperiode erst noch eine längere Zeit notwendig war für die Denudation, bevor die fossilführenden Eozänsedimente auf den entblössten Eruptivgesteinen zur Ablagerung gelangten.

Die wichtigsten Fundorten sind auf der Übersichtskarte (Fig. 1) angegeben. Die Gesteine werden gruppenweise den Fundorten nach behandelt [2]). Zur genaueren Andeutung sind einige Detailskizzen beigegeben, welche Kopien sind von Teilen der Originalkarten WITKAMP's, worauf gleichfalls seine geologische Beobachtungen eingetragen sind.

Fig. 1

West-Soemba. (Fig. 1.)

W. 109. D. 6835. Südöstlich P. Kawaga.

Diopsiddioritporphyr. (WICHMANN: Augitdiorit).

Quarz: sehr wenig, mit geringen Dimensionen. Orthoklas: sehr wenig, getrübt, nicht idiomorph. Plagioklas [3]): Einsprenglinge bis 4 mm. Die kleinere Generation ca. 0.8 mm. Idiomorph, öfters auch gegenüber angrenzendem Pyroxen. Beide Generationen mit Zonarstruktur. MAW der Zentra etwa 38°: Labradorit. MAW der Ränder ungefähr 0°: Oligoklas. Ziemlich frisch. Antiperthit vorhanden. Bisweilen Pyroxenkörner eingeschlossen.

Diopsid: ziemlich häufig, bis 5 mm. Farblos bis hellgrau. An den Rändern bisweilen faserige Hornblende. Vielleicht etwas sekundärer Serpentin vorhanden. Plagioklas eingeschlossen.

---

[1]) Jaarb. v/h Mijnwezen in Ned. Indië 1924, LIII (1925). Algemeen Gedeelte, S. 37.

[2]) Die Gesteine werden angedeutet mit den Originalnummern WITKAMP's (W-Nummern), die von TEN KATE mit den Nummern der petrographischen Sammlung in Utrecht (P-Nummern). Die Dünnschliffer (D-Nummern) gehören zur Preparatensammlung des Utrechter Instituts.

[3]) Alle Plagioklasbestimmungen sind gemacht mittels Aufsuchung der Maximalauslöschungswinkel in der symmetrischen Zone (= MAW) auf dem Federow'schen Tisch.

Apatit: Säulchen bis 0.6 mm. Eisenerz: bis 0.4 mm, hauptsächlich bei den dunkelen Gemengteilen. Bisweilen etwas Leukoxen an den Rändern.

Als sekundäre Produkte: viel chloritische Substanz und etwas Calcit [1]).

Mittel-Soemba. (Fig. 1 u. 2.)

P. 378, 1891. D. 1874. Lawendé, an der Nordküste. Geröll.

Biotitdiopsidhornblendegranitporphyr. (WICHMANN: Granit).

Quarz: bis 1.7 mm, sehr selten idiomorph bei Orthoklas. Mikropegmatitische Verwachsung mit Orthoklas häufig. Orthoklas: bis 0.8 mm, unregelmässig getrübt, vielfach idiomorph beim Quarz, Zwillinge vorhanden. Mikroperthit selten. Plagioklas: Einsprenglinge bis 2.5 mm, zweite Generation ca. 0.7 mm. Mit Zonarstruktur. MAW des Zentrums 33° (Labradorit), der Ränder 8° (Oligoklas). Pyroxen- und Erzkörner eingeschlossen. Bisweilen zonar mit Sericit.

Biotit: bis 0.2 mm, idiomorph (Basis und Prisma), pleochroitisch von rotbraun bis hellbraungelb. Umwandlung in Chlorit mit Epidotkörnern. Hornblende: mehr als Biotit, bis 1.5 mm, idiomorph, fast gänzlich umgewandelt in Chlorit, mit Epidot und Karbonat. Diopsid: weniger als Hornblende, bis 0.8 mm, stark getrübt, mit Braunfarbung durch limonitische Infiltration.

Apatit: Länge der Kristalle bis 0.4 mm, Breite bis 0.2 mm. Zirkon: selten. Eisenerz: ziemlich häufig, bis 0.5 mm, xenomorph beim Apatit.

Mit sekundärem Chlorit und Epidot. Calcit als Spaltfüllung.

W. 151. D. 6908. Goenoeng Kambong Pehapa.

Hornblendediopsidgranit.

Quarz: bis 1.1 mm, sehr gering undulös. Mikropegmatitische Verwachsungen vorhanden. Orthoklas: bis 1.3 mm, stark getrübt, öfters idiomorph gegenüber angrenzendem Quarz. Mikroperthit selten. Plagioklas: bis 2.2, ausnahmsweise auch idiomorph bei den dunkelen Gemengteilen. Zonar mit Rekurrenzen. MAW im Zentrum ca. 26°: Andesin. MAW der Ränder 7°: Oligoklas. Wenig frisch. Risse mit sauren Plagioklas. Pyroxenkörner eingeschlossen.

Hornblende: bis 1.2 mm, stark chloritisiert, mit Karbonat-Epidot-Körnchen, durch gute Idiomorphie jedoch leicht erkennbar. Mit pleochroitischen Höfen. Diopsid: viel, bis 1.6 mm, selten xenomorph beim Plagioklas. Bisweilen mit zersetzter Hornblende.

Apatit und Zirkon sehr selten. Eisenerz bisweilen mit etwas Leukoxen, bis 0.4 mm.

Sekundärer Epidot nicht selten, bisweilen mit etwas Aktinolith. Sekundärer Chlorit vorhanden.

W. 155. D. 6842. Nordöstlich Goenoeng Tanah Daroe.

Biotithornblendegranit. (WICHMANN: Granit).

Quarz: bis 2.5 mm, bisweilen idiomorph, mit Orthoklas öfters mikropegmatitisch verwachsen. Orthoklas: bis 1.5 mm, im Allgemeinen stark getrübt, selten mit Idiomorphie beim Quarz. Zwillinge selten. Mit sehr spärlichem Mikroperthit. Plagioklas: bis 4 mm, frisch, zonar mit Rekurrenzen. MAW des Zentrums 29°: Labradorit. MAW der Randzonen ungefähr 0°: Oligoklas. Hornblende und Erz eingeschlossen.

Biotit: nicht häufig, bis 0.6 mm, pleochroitisch von hellbraun bis rötlichbraun, idiomorph (Basis und Prisma), pleochroitische Höfe vorhanden. Nur wenig chloritisiert. Hornblende: ungefähr in gleicher Menge wie Biotit, bis 2 mm. Pleochroismus: α-hellbraun, β-grünlichbraun, γ-bräunlichgrün. Diopsid: vielleicht vereinzelte Diopsidkörner im Plagioklas eingeschlossen.

---

[1]) Am Ende jeder Beschreibung werden nur diejenige Sekundärprodukte genannt, welche nicht als Zersetzungsprodukte bestimmter Mineralien entstanden und in diesen abgeschieden sind. Letztere werden nur bei den betreffenden Mineralien genannt.

Apatit und Zirkon sehr selten. Erz: bis 0.2 mm, bisweilen mit etwas Leukoxen.
Turmalin: an einigen Stellen, bis 0.2 mm, wenig idiomorph, Pleochroismus: O-dunkelgraublau, E-braungrau.
Mit etwas sekundärem Chlorit.

W. 155. D. 6841. Nordöstlich Goenoeng Tanah Daroe.
Aplit. (WICHMANN: Hornfels).
Das graue feinkörnige Gestein kommt vor als Gang in dem hieroben beschriebenen Biotithornblendegranit W. 155, im selben Handstück. An der Granitgrenze ist die Randfazies dieses aplitischen Gesteins äusserst feinkörnig und besteht aus Quarz und Orthoklas. Das Zentrum ist etwas grobkörniger:
Quarz: bis 0.2 mm, im allgemeinen intensiv mikropegmatitisch verwachsen mit Orthoklas. Orthoklas: bis 0.3 mm, stark getrübt, die grösseren bisweilen einigermassen idiomorph. Plagioklas fehlt. Biotit: sehr selten, bis 0.6 mm, chloritisiert mit Epidot, nicht idiomorph. Zirkon: sehr selten. Erz: sehr feinkörnig.
Sekundär kommt in geringer Menge Epidot und Chlorit vor.

W. 157. D. 10359. Goenoeng Tanah Daroe.
Biotitdiopsidhornblendegranodiorit. (WICHMANN: Gabbro).
Quarz: nicht viel, bis 2.5 mm, etwas undulös. Orthoklas: nicht sehr viel, unregelmässig getrübt, bis 0.5 mm, selten idiomorph. Plagioklas: bis 2.2 mm, frisch, bisweilen geringe Idiomorphie an Biotit- und Hornblendegrenzen. Zonarstruktur mit Rekurrenzzonen. MAW im Zentrum ungefähr 20°: Andesin. MAW eines Randes um das Zentrum 33°: Labradorit. MAW der Peripherie ca. 7°: Oligoklas. Myrmekit in sehr geringer Menge vorhanden.
Biotit: 1.9 mm, gute Idiomorphie selten, wenig zersetzt, pleochroitisch von hellbraungelb bis dunkelrötlichbraun. Hornblende: mehr als Biotit, bis 2 mm. Pleochroismus: α-fast farblos, β-hellgrün, γ-grün. Mit pleochroitischen Höfen. Öfters Pyroxen eingeschlossen. Diopsid: weniger als Hornblende, bis 0.6 mm.
Apatit vorhanden. Zirkon sehr selten. Erz: bis 0.4 mm.

W. 173*b*. D. 6912. Lakoka Bakoel. Wahrscheinlich ortsfremd.
Biotithornblendequarzdiorit. (WICHMANN: Quarzdiabas).
Quarz: bis 0.4 mm, bisweilen mikropegmatitisch mit Orthoklas verwachsen. Orthoklas: wenig, nicht idiomorph, ungetrübt. Plagioklas: bis 2.8 mm, selten idiomorph bei den dunkeln Gemengteilen. Zonar mit Rekurrenzen. MAW des Zentrums ca. 30°, der Ränder ungefähr 3° (Labradorit und Oligoklas).
Biotit: bis 1.6 mm, wenig idiomorph, gänzlich chloritisiert mit Karbonat und Epidot. Pleochroitische Höfe vorhanden. Hornblende: häufiger als Biotit, bis 1.6 mm, bisweilen xenomorph bei Plagioklas. Pleochroismus: α-farblos, β-braungrün, γ-braungrün. Ziemlich stark zersetzt: Calcit, weiter Epidot und Chlorit.
Apatit und Zirkon sehr wenig. Erz: bis 0.4 mm, bisweilen mit etwas feinem Titanit (bis 0.2 mm).
Chlorit, Calcit und Epidot sekundär vorhanden.

Als eine besondere Gruppe der Mittel-Soemba-Eruptivgesteine sind die metasomatisch-veränderten Gesteine zu betrachten, welche in grosser Anzahl in der Sammlung WITKAMP's vorhanden sind. Sie weisen eine Neubildung auf von Muskovit und Turmalin, während weiter auch Quarz bisweilen neugebildet ist. Einige dieser Gesteine habe ich hier als veränderte Granitporphyre bezeichnet. Es soll jedoch bemerkt werden, dass keines dieser Gesteine Quarz als Einsprengling enthält. Der reiche, ursprüngliche

Quarzgehalt der Grundmassen dieser Gesteine macht es jedoch unmöglich sie zu basischeren Typen zu stellen.

W. 152. D. 10360. Goenoeng Kambong Pehapa.

Metasomatisch veränderter Granit. Graubraunes Gestein mit Quarzschnur (Dicke 0.4 cm).

Quarz bis 2 mm. Ursprünglich wahrscheinlich mikropegmatitisch verwachsen mit Orthoklas, welcher gänzlich von feinschuppigem Muskovit verdrängt worden ist. In

gleicher Weise auch Plagioklas umgewandelt. Die Pseudomorphosen nach Plagioklas (bis 2.5 mm) bestehen aus feinen Aggregaten von feinschuppigem Muskovit und zeigen deutliche Plagioklasidiomorphie.

Leukoxen: ziemlich viel, bisweilen mit Ilmenitform.

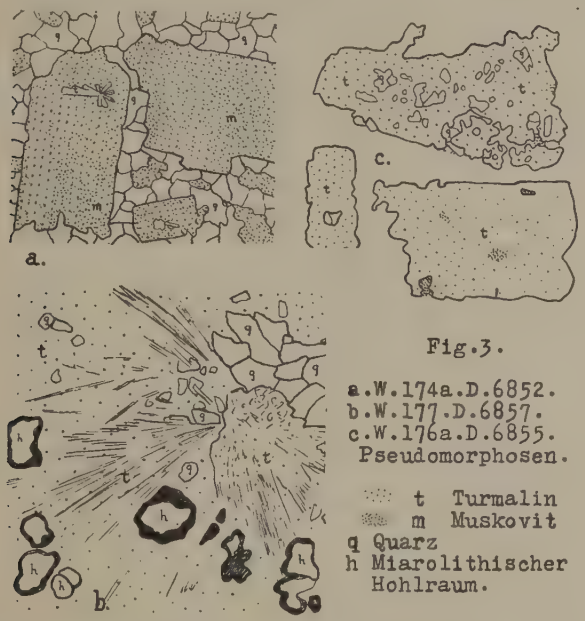

W. 154. D. 10357, 10358. Soengei Memboro, südlich Goenoeng Kambong Pehapa. Geröll.

Metasomatisch veränderter Granit. Rötlichgelbes Gestein mit zahlreichen kleinen (bis 5 mm) Turmalinnestern.

Quarz bis 1 mm, selten mit bipyramidaler Form, mit zerstreutem Muskovit. Mikropegmatitische Verwachsungen mit Orthoklas ursprünglich wahrscheinlich vorhanden. Orthoklas jedoch gänzlich in Muskovit umgewandelt. Plagioklas nur erkennbar an der Form der Muskovitpseudomorphosen (bis 2.2 mm).

Turmalin ziemlich häufig, bis 0.5 mm, öfters mit zonaren Farbenunterschieden. Pleochroismus: O-dunkelbraun oder dunkelblau, E-violettbraun oder violettgrau. Beim Turmalin öfters frischer Quarz, möglich metasomatischer Herkunft. Muskovit im Allgemeinen sehr feine Aggregate bildend, beim Turmalin bisweilen grösser. Brauneisen kommt bisweilen bei den neugebildeten Mineralien vor. Die Muskovitaggregate vielfach mit limonitischer Infiltration. Titanit ziemlich häufig, mit Leukoxenhabitus.

W. 158. D. 6843, 13086. Südlich Goenoeng Kambong Pehapa, bei Soengei Memboro.

Metasomatisch verändertes, granitisches Gestein. (WICHMANN: Syenit?) Bräunlichgraues, etwas poröses Gestein, zum Teil mit vielen kleinen, schwarzen Flecken.

Quarz bis 0.8 mm, mit feinem Muskovit. Mikropegmatitische Verwachsung mit Orthoklas ursprünglich vorhanden; Orthoklas aber gänzlich verdrängt von feinschuppigem Muskovit. Muskovitpseudomorphosen nach Plagioklas im allgemeinen wenig deutlich. Vielleicht auch Muskovitpseudomorphosen nach dunkelen Gemengteilen vorhanden (Biotit?). Turmalin selten. Leukoxen. Brauneisen bekleidet vielfach die miarolithischen Hohlräume. Durchschnitt der letzteren bis 0.5 mm.

W. 161*a*. D. 6844. L. Telatang, südlich Kelokowatoe.

Metasomatisch veränderter Granitporphyr. (WICHMANN: Aplit?). Gelblich graues Gestein.

Quarz bis 0.3 mm, mit undulöser Auslöschung, getrübt von Flüssigkeiteinschlüssen. Plagioklaseinsprenglinge mit guter Idiomorphie, bis 4.2 mm, gänzlich umgewandelt in Muskovit und Turmalin. Muskovit weiter in unregelmässigen Aggregaten und zerstreut. Zum Teil erkennbar als zweite Feldspatgeneration. Turmalin mit Muskovit in den Einsprenglingen, im allgemeinen sphäritisch, in der Grundmasse wenig, zerstreut. Pleochroismus: O hellbläulich, E-farblos. Säulchenlänge bis 0.4 mm. Brauneisen: unregelmässig, in Spalten, als Bekleidung miarolithischer Hohlräume (Durchmesser bis 0.1 mm). Leukoxen im allgemeinen sehr feinkörnig, weiter als Pseudomorphose nach Ilmenit(?).

W. 162*b*. D. 6846, 10368. L. Lendoetana, nördlich Goenoeng Bai.

Metasomatisch veränderter Granitporphyr. Gelbgraues Gestein mit feinem Turmalin auf einer Diaklase. Inhomogen.

D. 6848. Quarz bis 0.1 mm, getrübt von feinem Muskovit. Feldspateinsprenglinge bis 3.5 mm, gänzlich umgewandelt in Muskovit, wenig Turmalin und Quarz (bis 0.2 mm). Der Muskovit bildet sehr feine Aggregate, zum Teil unregelmässig in der Grundmasse. Auch als Füllung feiner Spalten. Turmalin kommt vereinzelt auch in der Grundmasse vor. Bis 0.35 mm. Pleochroismus: O-blau, E-hellviolettbraun. Mit feiner geschlängelten Quarzschnur.

D. 10368. Quarz bisweilen mit bipyramidaler Idiomorphie, wenn auftretend als Zentrum mikropegmatitischer Verwachsungen mit Orthoklas, welche gänzlich in Muskovit umgewandelt ist. Deutliche Pseudomorphosen nach Feldspat fehlen, Umwandlung in feinschuppigen Muskovit. Turmalin kommt sphäritisch vor. Säulchenlänge bis 0.3 mm. Pleochroismus: O-dunkelbräunlichblau, E-hellblaubraun. Brauneisen vorhanden. Sehr feiner Leukoxen ziemlich häufig.

W. 170*b*. D. 6850. Wai Kandilo, östlich Lakoka Bakoel. Geröll.

Metasomatisch veränderter Quarzporphyr (Granitporphyr). (WICHMANN: Quarzporphyr). Grauweisses, porphyrisches Gestein mit veränderten Einsprenglingen.

Feldspateinsprenglinge gänzlich umgewandelt in feinen Muskovit und Kaolin. Die Grundmasse besteht hauptsächlich aus Quartz, im allgemeinen längliche Kristalle (bis 0.25 mm), einigermassen fluidal angeordnet. Muskovit, als feine Aggregate und zerstreut in der Grundmasse. Sekundärer Quarz kommt wenig vor, isometrische Kristalle bis 0.3 mm, nicht getrübt von Muskovit. Feine Leukoxenkörnchen häufig.

W. 173*a*. D. 6911, 10365. Lakoka Bakoel.

Metasomatisch veränderter Granitporphyr. (WICHMANN: Quarzporphyr?). Rötlichgraues Gestein mit dunkeln Flecken.

Quarz bis 0.4 mm, mit Muskovitschüppchen. Frischer, wahrscheinlich sekundärer Quarz selten. Feldspat bis 1.2 mm, gänzlich umgewandelt in Muskovit und etwas Turmalin. Muskovit in der Grundmasse als unregelmässige Aggregate. Turmalin nicht selten, sphäritisch, Säulenlänge bis 0.2 mm. Brauneisen kommt vor als Infiltration und als Füllung einer Spalte.

W. 174*a*. D. 6852, 10371, 10372. Wai Maringoe, nordöstlich Goenoeng Bai. Geröll.

Metasomatisch veränderter Granitporphyr. (WICHMANN: Quarzporphyr (Mikrogranit)). Grauweisses Gestein mit Pyrit. Mit einer blaugrauen Schnur. Fig. 3*a*.

Quarz bis 0.4 mm, körnig. Feldspat bis 1.5 mm, verdrängt von feinschuppigem Muskovit und Turmalin. Muskovit kommt weiter zerstreut vor. Turmalin vielfasch sphäritisch, bis 0.2 mm, Pleochroismus: O-graublau, E-farblos. Pyrit nicht selten, bis 0.2 mm. Leukoxen skelettartig. Sehr kleine braune Körner konnten nicht bestimmt werden (Rutil?).

W. 174*b*. D. 6853. Wai Maringoe, nordöstlich Goenoeng Bai. Geröll.

Metasomatisch veränderter Granitporphyr. (WICHMANN: Quarzporphyr (Mikrogranit)). Porphyrisches Gestein mit veränderten weissen Einsprenglingen und grauer Grundmasse.

Die Grundmasse besteht fast ausschliesslich aus Quarz, bis 0.4 mm, getrübt von feinschuppigem Muskovit, welcher weiter auch als kleine Aggregate in der Grundmasse vorkommt. Die Feldspateinsprenglinge (bis 3.5 mm) sind umgewandelt in Muskovit und Kaolin. Leukoxenartige Körnchen häufig.

Kleine Schnüre bestehen hauptsächlich aus feinem Turmalin, welcher auch im angrenzenden Gestein auftritt. Vielfach sphäritisch, bis 0.2 mm, Pleochroismus: O-graublau, E-hellviolettgrau. Beim Turmalin kommt etwas Brauneisen, bisweilen auch Quarz vor. Mit miarolithischen Hohlräumen.

W. 174*c*. D. 6854, 10369. Wai Maringoe, nordöstlich Goenoeng Bai. Geröll.

Metasomatisch-veränderter Granit. Grauweisses Gestein, zum Teil mit viel Turmalin, welcher mit Quarz in unregelmässigen Schnüren vorkommt.

Quarz bis 0.7 mm, mit wenig sekundärem Muskovit, welcher auch zwischen den Quarzen auftritt. Feldspat, bis 1.5 mm, umgewandelt in Muskovit und etwas Turmalin. Der Turmalin ist sphäritisch; Pleochroismus: O-hellblau, E-farblos, bis 0.1 mm. Leukoxenartige Substanz vorhanden. An einigen Stellen dunkelbraune Körnchen.

Turmalinschnüre mit miarolithischen Hohlräumen. Der Turmalin ist blau oder braun, bis 0.2 mm, sphäritisch. Der hier auftretende Quarz ist xenomorph, bis 1.2 mm.

W. 176*a*. D. 6855. Südlich Goenoeng Bai.

Metasomatisch veränderter Granitporphyr. (WICHMANN: Quarzporphyr). Fig. 3*c*. Grauweisses und blaugraues Gestein mit schwacher Paralleltextur.

Feldspateinsprenglinge gänzlich umgewandelt in Turmalin, Quarz und Muskovit. Bis 3 mm. Die blaugrauen Turmalinaggregate in der Regel sehr fein. Turmalin erkennbar am Pleochroismus der grösseren Individuen und am negativen Hauptzonenkarakter. Bis 0.03 mm. In den Turmalinpseudomorphosen auch Quarz, bis 0.1 mm. Feiner Muskovit bisweilen vorhanden. Die zweite Feldspatgeneration in gleicher Weise verändert wie die Einsprenglinge.

Quarz bis 0.7 mm, getrübt. Frischer Quarz vielleicht sekundär. Muskovit als unregelmässige feine Aggregate beim Quarz. Leukoxen ziemlich häufig, auch skelettartig.

W. 176*b*. D. 6856, 10366, 10367. Südlich Goenoeng Bai.

Metasomatisch veränderter Granitporphyr. Grauweisses Gestein mit blauschwarzen Einsprenglingen. Einige sehr dünne Schnüre mit Turmalin und andere mit Quarz.

Feldspateinsprenglinge (bis 3 mm) gänzlich umgewandelt in Muskovit, Turmalin und Quarz. Muskovit und Turmalin als feine Aggregate, zum Teil beieinander auftretend. Quarz wenig, bis 0.2 mm. Weiter kommt Brauneisen in den Einsprenglingen vor.

Quarz getrübt von feinem Muskovit. Bis 0.5 mm. Zwischen den Quarzen feine Muskovitaggregate, bisweilen erkennbar als Feldspat der zweiten Generation (z.B. 0.2 mm). Feiner Turmalin als kleine Aggregate. Leukoxenpseudomorphosen, bisweilen mit Brauneisen. Zirkon sehr selten.

Mit dünnen Quarzschnüren. In D. 10366 unregelmässige Turmalinschnur mit etwas Quarz, welcher Idiomorphie beim Turmalin zeigen kann. Miarolithische Hohlräume nicht häufig, bis 0.3 mm.

W. 177. D. 6857, 10546. Nordöstlich Goenoeng Lamboe.

Turmalinquarzgestein. Buntes Gestein mit dunkelblaugrauen und ziegelroten Partieen. Die dunkeln Teile bisweilen breccienartig eingeschlossen in der roten Substanz. Mit makroskopischem Turmalin. Das Gestein ist wahrscheinlich eine pneumatolytische Neubildung. Es besteht fast ganz aus Turmalin und Quarz. Fig. 3*b*.

Turmalin bis 1.5 mm, Säule und feine Aggregate. Letztere farblos, graublau oder bräunlichgelb. Die Säulen farblos oder blau. Pleochroismus: O-grünblau, E-hellgrünlichblau. Bisweilen blauer Kern mit farbloser Umhüllung. Säulen sphäritisch angeordnet, im allgemeinen idiomorph bei Quarz. Bei und in den Aggregaten Quarz vielfach idiomorph. Die Turmalinaggregate bisweilen ziemlich scharf begrenzt. In den Turmalinhaltigen Gesteinsteilen miarolithische Hohlräume, bis 1.2 mm, vielfach mit Brauneisen bekleidet.

Quarz bis 1 mm, jedoch auch sehr feinkörnig, bisweilen prismatisch entwickelt. Die makroskopisch wahrnehmbare Rotfarbung der quarzhaltigen Teilen rührt von limonitischen Infiltrationen zwischen den Quarzen her.

W. 189. D. 6865. Goenoeng Kambaoeni Deta.

Metasomatisch veränderter Granit. Bräunlichgraues Gestein.

Quarz bis 1 mm, undulös, auch kataklastisch: in den Kristallen sektorische Auslöschungsunterschiede bis zu 15°. Getrübt von feinschuppigem Muskovit. Feldspat bis 2 mm, idiomorph, umgewandelt in Muskovitaggregate, bisweilen jedoch ursprünglicher Zwillingsbau noch erkennbar. Muskovit weiter unregelmässig vorkommend. Vielleicht auch Muskovitpseudomorphosen nach dunkeln Gemengteilen.

Zirkon sehr selten. Leukoxenpseudomorphosen bis 0.2 mm. Brauneisen in Spalten und in den Pseudomorphosen nach Feldspat, auch beim Leukoxen.

W. 191. D. 6866. L. Kandjoenga Bakoel, südlich Goenoeng Kambaoeni Deta.

Granophyrischer Granitporphyr mit metasomatischen Veränderungen. Rosagraues, granitisches Gestein.

Quarz ca. bis 1 mm, sehr intensiv mikropegmatitisch mit Orthoklas verwachsen. Orthoklas stark getrübt von feinschuppigem Muskovit, sehr selten idiomorph. Plagioklaseinsprenglinge bis 1.5 mm, die zweite Generation ca. 0.3 mm. MAW ungefähr 20°: Andesin. In der Regel stark verdrängt von feinem Muskovit. Andere Muskovitpseudomorphosen vielleicht nach dunkelen Gemengteilen (Hornblende, Biotit).

Apatit vorhanden. Eisenerz bis 0.3 mm, bisweilen mit Leukoxen.

Sekundär vorhanden: Calcit und Chlorit. Der Calcit bildet unregelmässige Flecken (bis 0.4 mm). Beim Calcit vielleicht auch etwas sekundärer Quarz. In feinen Spalten: Calcit und Quarz. Letzterer mit gleicher Orientierung als im angrenzenden Gestein.

W. 195. D. 6868. Prai Kela. Geröll.

Metasomatisch verändertes Gestein. Graurosagefärbtes Gestein mit häufigem feinen schwarzen Turmalin.

Muskovit häufig, unregelmässige Aggregate. Hierbei vielfach sehr feine Kaolinaggregate, mit unregelmässigen Begrenzungen. Turmalin häufig, bis 1.3 mm, Idiomorphie kann von Quarz gehindert werden. Blaugefarbt mit zonaren Intensitätsunterschieden. Pleochroismus: O-dunkelblau, E-hellgraublau. Quarz ziemlich häufig beim Turmalin, wahrscheinlich auch Neubildung. Leukoxenartige Substanz vorhanden.

Ost-Soemba. (Fig. 1 und 4.)

W. 291. D. 6924. Südlich Nggoehar.

Hornblendediorit.

Quarz: wenig, bis 1 mm, schwach undulös. Orthoklas: wenig, xenomorph. Plagioklas bis 3.3 mm, idiomorph, bisweilen auch gegenüber angrenzender Hornblende, mit Zonarstruktur. MAW des Zentrums 31°: Labradorit. MAW der Ränder 9°: Oligoklas. Unfrisch mit Sericit und etwas Epidot.

Hornblende: bis 2.5 mm. Pleochroismus: α-farblos, β-grün, γ-grün. Umwandlung in Chlorit mit Epidot-Karbonat-Körnern.

Apatit: sehr wenig. Eisenerz: bis 0.8 mm, bisweilen mit Leukoxenkörnern. Pyrit ziemlich häufig, bis 0.5 mm. Titanit: selten, untypisch.

W. 292. D. 13089. L. Taring, südlich Nggoehar.

Biotitdiopsidhornblendegranodiorit.

Quarz: nicht sehr viel, bis 1.7 mm, öfters stark mikropegmatitisch verwachsen mit Orthoklas. Orthoklas: nicht sehr viel, bis 1.3 mm, selten idiomorph, getrübt. Sehr wenig Mikroperthit. Plagioklas: bis 3 mm, im allgemeinen xenomorph bei den dunkelen Gemengteilen. Zonar mit Rekurrenzen. MAW des Zentrums ca. 28°: Labradorit. An der Peripherie ungefähr 10°: Oligoklas. Mit Sericitisierung.

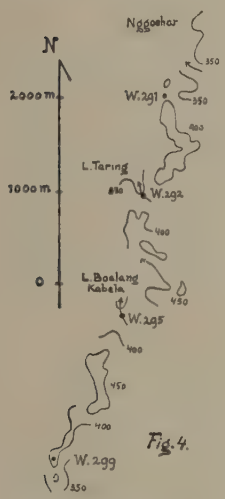

Biotit: wenig, idiomorph (Basis und Prisma), fast gänzlich umgewandelt in Chlorit mit Epidot und Karbonat. Hornblende: häufig, bis 2.2 mm. Pleochroismus: α-hellbraungelb, β-braungrün, γ-grün. Pleochroitische Höfe vorhanden. Diopsid: weniger als Hornblende, farblos, idiomorph.

Erz: bis 0.8 mm. Apatit: wenig.

Sekundärer Epidot und Chlorit vorhanden.

W. 295*b*. D. 6940. L. Boelang Kabela, südlich Nggoehar. Geröll.

Pegmatit. (WICHMANN: Pegmatit).

Quarz im Dünnschliff bis 1 cm, gänzlich pegmatitisch mit Orthoklas verwachsen. Orthoklas bis 0.8 cm, getrübt, ? idiomorph. Plagioklas: sehr wenig, im Orthoklas ein idiomorphes Albitkristall (1 mm) eingeschlossen. Biotit: sehr wenig, bis 6 mm, dünnplattig, chloritisiert. Apatit und Zirkon: sehr wenig. Erz fehlt.

Mit sekundärem Epidot. Sehr feine Spalten mit Muskovit. Kleine Schnur mit Epidot und Quarz.

W. 299. D. 6927. Südlich Nggoehar, zwischen L. Boelang Kabela und Melanggoe.

Biotithornblendegranodiorit. (WICHMANN: Gabbro).

Quarz: nicht häufig, bis 1.5 mm, mikropegmatitische Verwachsungen mit Orthoklas vorhanden. Orthoklas: nicht idiomorph, schwach perthitisch. Plagioklas: bis 0.4 mm, sehr selten idiomorph gegenüber Hornblende. Zonar mit Rekurrenzen. MAW des Zentrums 33°: Labradorit. MAW der Peripherie 4°: Oligoklas. Sericitisation kommt vor, bisweilen zonar.

Biotit: nicht häufig, bis 0.9 mm, idiomorph, bisweilen xenomorph bei Hornblende. Stark zersetzt: Chlorit mit linsenkörnigen Karbonat-Epidot-Fleckchen. Pleochroitische Höfe um Zirkon vorhanden. Hornblende: häufig, bis 2.2 mm, Pleochroismus: α-farblos, β-bräunlichgrün, γ-hellgrün. Pleochroitische Höfe selten.

Apatit und Zirkon sehr selten. Eisenerz: bis 0.9 mm, bisweilen mit Leukoxen.

An einer Stelle im Orthoklas vielleicht Turmalin.

Mit etwas sekundärem Chlorit.

W. 313. D. 13090. Südlich Goenoeng Kambahika.

Hornblendebiotitgranit. (WICHMANN: Granit).

Quarz: bis 2.5 mm, schwach undulös, bisweilen geringe Idiomorphie beim Orthoklas. Mikropegmatit selten. Orthoklas: bis 2.7 mm, Zwillinge selten, xenomorph. Wenig Mikroperthit. Plagioklas: bis 3.3 mm, fast nie idiomorph bei den dunkelen Gemengteilen. Zonar mit Rekurrenzen. MAW des Zentrums 31°: Labradorit. Zum Teil ziemlich stark zersetzt, besonders in der Umgebung kleiner sekundären Schnüren. Umwandlung in Sericit und Epidot.

Biotit: bis 0.6 mm, idiomorph (Basis und Prisma), selten frisch, chloritisiert mit Epidot-Karbonat-Flecken, pleochroitische Höfe vorhanden. Hornblende: in ungefähr gleicher Menge wie Biotit. Pleochroismus: α-lichtbräunlich, β-grünbraun, γ-bräunlichgrün. Mit pleochroitischen Höfen.

Apatit: selten, bisweilen blassviolett. Zirkon: u. A. in den dunkelen Gemengteilen, hofbildend. Eisenerz: bis 0.6 mm. Titanit: mehrere Kristalle.

Kleine Schnüre mit Epidot, wenig Chlorit und Quarz.

W. 320. D. 10375. 10376. An der Südküste bei L. Longi. Geröll.

Aplitischer Granitporphyr mit Turmalinnestern.

Quarz: bis 0.3 mm, körnig. Orthoklas: leicht getrübt, bis 0.3 mm. Plagioklas: Einsprenglinge bis 2.3 mm, stark getrübt von sekundärem Sericit und Epidot. Quarz kann die Idiomorphie der Plagioklasaussenränder stören. Apatit und Titanit in geringer Menge vorhanden.

Mit zerstreutem, feinschuppigem Muskovit. Sekundärer Epidot kommt vor.

Die unregelmässige Turmalinnester, welche mehrere cm gross sein können, bestehen aus grossem Turmalin (im Dünnschliff bis 5 mm), welcher von Quarz (bis 0.4 mm) durchsiebt ist. Pleochroismus: O-blaubraun, E-hellbraun. An den Rändern feinstrahliger Turmalin (sehr lichtblau), wobei feiner Muskovit vorkommt. An verschiedenen Stellen braune Körner mit hoher Lichtbrechung (Rutil?).

W. 348*b*. D. 13091. L. Lakaheri bei Watoebara. Geröll.

Hornblendediopsiddiorit.

Quarz: sehr wenig, bis 1 mm. Orthoklas: sehr wenig, stark getrübt. Plagioklas: bis 3.7 mm, mit Zonarstruktur. MAW des Zentrums ca. 34°: Labradorit. Erz und Diopsid eingeschlossen. Zum Teil mit viel Sericit, Epidot und etwas Chlorit.

Hornblende: bis 2.7 mm, stark zersetzt, an einer Stelle jedoch frische braune Hornblende (α-hellbraun, β-tabackbraun). Umwandlung in Chlorit, Epidot und Karbonat. Diopsid: in fast gleicher Menge wie Hornblende, bis 1.5 mm, in Rissen Umwandlung in Calcit, weiter mit sekundärem Epidot und peripher bisweilen faseriger Hornblende auftretend. Erz und Apatit eingeschlossen in den dunkelen Gemengteilen. Apatit: ziemlich häufig, Länge bis 0.9 mm, Dicke bis 0.3 mm, idiomorph gegenüber Erz. Eisenerz: bis 1.2 mm, bisweilen mit geringer Leukoxenbildung. Pyrit: vereinzelte Körner, wahrscheinlich sekundär.

Sekundär treten auf: Chlorit, Epidot und wenig Calcit.

P. 404, 1891. D. 1846. An der Südküste, zwischen Tg. Moa und Lailungi.

Hornblende(grano)dioritporphyr. (WICHMANN: Syenit?).

Quarz und Orthoklas: wenig, intensiv mikropegmatitisch verwachsen. Plagioklas: Einsprenglinge bis 2 mm. Zonar, MAW des Zentrums ca. 28°: Labradorit. Teilweise getrübt von starker Sericitisation, sekundärer Epidot vorhanden.

Hornblende: bis 4.5 mm, idiomorph, bisweilen feinen Plagioklas einschliessend. Pleochroismus: α-hellbräunlich, β-grünbraun, γ-braungrün. Mit schwacher Chloritisation. Weiter sind einsprenglingartige Epidotpseudomorphosen vorhanden.

Apatit und Zirkon in geringer Menge. Magnetit: bis 0.4 mm. bisweilen mit guter Idiomorphie.

Mit sekundärem Epidot und Chlorit.

P. 389. 1891. D. 1866. Laiwora, gegenüber Noesa Saloera.

Biotithornblendegranit mit dunkelm Einschluss.

Quarz: bis 2 mm, bisweilen idiomorph gegenüber Orthoklas. Orthoklas: ungleichmässig getrübt, xenomorph. Plagioklas: bis 2.2 mm, mit zonarem Bau. MAW des Zentrums ca. 24°: Andesin. MAW der Ränder ca. 0°: Oligoklas. Zum Teil getrübt von Sericitisation. Myrmekit in kleiner Menge vorhanden. Biotit: bis 1.8 mm, idiomorph (Basis und Prisma), stark zersetzt: chloritisiert mit karbonatischen Linsen.

Hornblende: weniger als Biotit, bis 0.4 mm, Pleochroismus: α-hellbräunlich, β-braungrün, γ-grün. Apatit und Zirkon vorhanden. Eisenerz: bis 0.6 mm. Titanit: ein Kristall von 0.6 mm, pleochroitisch von grünlichgrau bis bräunlichgrün.

Einschluss. Quarz: sehr spärlich, mit geringen Dimensionen. Orthoklas: nur an den Rändern des Einschlusses als Fortsetzung granitischer Orthoklaskristalle. Plagioklas: bis 0.5 mm, fast alle stark sericitisiert, vielfach mit Idiomorphie gegenüber angrenzenden dunkeln Gemengteilen. Biotit: bis 0.7, mit Umwandlung in Chlorit, xenomorph beim Plagioklas. Hornblende: mehr als Biotit, bis 1 mm, meistens idiomorph. Pleochroismus: α-hellbräunlich, β-grünbraun, γ-dunkelgrün. Apatit und Zirkon vorhanden. Eisenerz: bis 0.4 mm, oktaedrisch. Titanit: nicht selten, bis 0.6 mm. Sekundär: Chlorit und Epidot.

P. 394. 1891. D. 1867. Tg. Ngiloanarara bei Waidjeloe.

Biotithornblendegranit. (WICHMANN: Hornblendegranit).

Quarz: bis 3 mm, selten einigermassen idiomorph bei Orthoklas. Orthoklas: bis 2.2 mm, unregelmässig getrübt, fast nie idiomorph, Zwillinge selten. Plagioklas: bis 4.5 mm, möglich eine zweite Generation vorhanden mit Abmessungen von ca. 1 mm. Zonar mit Rekurrenzen, MAW des Zentrums ca. 28° (Labradorit), der Ränder ca. 10° (Oligoklas). Myrmekit vorhanden.

Biotit: bis 2.2 mm, idiomorph (Basis und Prisma), nur wenig Chloritisation. Hornblende kann eingeschlossen vorkommen. Pleochroismus von gelbbraun bis schwarzbraun. Hornblende: mehr als Biotit, bis 0.9 mm, selten xenomorph beim Biotit. Pleochroismus: α-grünlichbraun, bräunlich, β-dunkelgrünbraun, γ-dunkelgrün, dunkelbraungrün. Pleochroitische Höfe selten. Das Zentrum der Hornblendekristalle bisweilen gebleicht.

Apatit und Zirkon vorhanden. Eisenerz: bis 0.5 mm.

Mit wenig sekundärem Epidot.

W. 245. D. 10543. Östlich Lairondja.

Metasomatisch-verändertes, wahrscheinlich porphyrisches Gestein. Rosaweisses Gestein mit gelber Verwitterungsrinde, mit zerstreuten, bis 3 mm grossen Turmalinsphärolithen.

Einsprenglingartige Pseudomorphosen, wahrscheinlich nach Feldspat, bis 2.5 mm, Formen undeutlich. Umgewandelt in Turmalin, spharitisch, Säulenlänge bis 0.7 mm, Pleochroismus: O-dunkelblau, E-hellblau. Feinfaseriger Turmalin fast farblos. Im Zentrum der Pseudomorphosen Quarz, bis 0.1 mm, peripher feinerer und feinschuppiger Muskovit.

Quarz: zahlreich in der Grundmasse, bis 0.2 mm. Muskovit: häufig, feinschuppig, unregelmässige Aggregate. Gelbbraunfärbung von limonitischer Infiltration. Feiner Turmalin ziemlich häufig. Leukoxen: feinkörnig, auch als Pseudomorphosen.

Umgebung von Waingapoe. (Fig. 1.)

W. 7. D. 6811. Westlich Waingapoe, zwischen Wai Rinde und Makaminggit. Aus Tertiärkonglomerat?

Hornblendegranit. (WICHMANN: Quarzdiorit?).

Quarz: bis 1.6 mm, selten einigermassen idiomorph, mikropegmatitisch verwachsen mit Orthoklas. Orthoklas: bis 0.8 mm, fast immer xenomorph, Zwillinge vorhanden. Mikroperthit selten. Plagioklas: bis 2.8 mm, mit Andeutung einer zweiten Generation, bisweilen idiomorph gegenüber angrenzender Hornblende. Zonar. MAW des Zentrums ca. 31°: Labradorit. MAW der Ränder ca. 4° (Albit).

Biotit: sehr wenig, idiomorph (Basis und Prisma), gänzlich chloritisiert. Hornblende: mehr als Biotit, bis 3 mm, Pleochroismus: α-hellbräunlichgrün, β-braungrün, γ-grün.

Apatit und Zirkon selten. Eisenerz: bis 0.9 mm.

P. 370. 1891. D. 1849. 13092. Ungefähr 1500 m. südlich Waingapoe, Oberfläche einer Kalksteintafel. Aus Tertiärkonglomerat.

Hornblendediopsiddiorit. (WICHMANN: Diabas?).

Quarz: sehr wenig, meistens feinmikropegmatitisch mit Orthoklas verwachsen.

Orthoklas: wenig, getrübt, xenomorph. Plagioklas: bis 4.4 mm, bisweilen idiomorph gegenüber angrenzenden dunkeln Gemengteilen. Mit zonarem Bau. MAW des Zentrums 36°: Labradorit. MAW der Ränder vielleicht 14° (Oligoklas-Andesin). Zum Teil sericitisiert.

Hornblende: bis 2.5 mm, Pleochroismus: α-hellbräunlich, β-grün, γ-blaugrün. Diopsid: unfrisch, farblos, mit feinen streifenförmigen schwarzen Interpositionen, vielfach von Hornblende umhüllt, mit sekundärem Calcit.

Apatit ziemlich häufig. Eisenerz: oktaedrisch, bis 1 mm. Pyrit: bei den dunkeln Gemengteilen, bis 0.4 mm, mit sekundärem Chlorit.

P. 371. 1891. D. 1852. Tafelland hinter Waingapoe. Aus Tertiärkonglomerat.

Hornblendebiotitgranitporphyr. (WICHMANN: Hornblendegranit).

Quarz kommt vor in zwei Generationen. Die erstere mit annäherend bipyramidaler Idiomorphie, bis 1 cm, an den Rändern Biotit, Orthoklas, usw. einschliessend. Die zweite Generation ungefähr 1 mm. Orthoklas: nicht sehr viel, bis 1 mm, xenomorph, stark getrübt. Plagioklas: Einsprenglinge bis 4.5 mm, die zweite Generation ca. 1 mm. Zonar mit zahlreichen Rekurrenzen. Bisweilen zonar getrübt. Spalten mit saurem Plagioklas gefüllt.

Biotit: wenig, bis 2.1 mm, gänzlich umgewandelt in Chlorit mit Epidot. Hornblende: ungefähr in gleicher Menge wie Biotit, bis 1.5 mm. Pleochroismus: α-hellbräunlich, β-grünlichbraun, braun, γ-grün, grünlichbraun.

Apatit und Zirkon sehr selten. Eisenerz: bis 0.9 mm, bisweilen mit etwas Leukoxen. Calcit in schmalen Spalten.

W. 208*a*. D. 13087. Wai Hili, südlich Kiritana (südlich Waingapoe). Aus Korallenkalkstein?

Diopsidbiotithornblendegranit.

Quarz: bis 1.7 mm, mikropegmatitische Verwachsung mit Orthoklas vorhanden. Orthoklas: bis 1.3 mm, getrübt, öfters idiomorph beim Quarz, Zwillinge vorhanden, schwach perthitisch. Plagioklas: bis 4 mm, zonar. MAW des Zentrums ca. 29°: Labradorit. Bisweilen mit zonarer Zersetzung.

Biotit: bis 0.5 mm, idiomorph (Basis und Prisma), gegenüber angrenzender Hornblende bisweilen xenomorph, pleochroitisch von rotbraun bis hellgelblich. Mit Umwandlung in Chlorit mit Epidot-Karbonat. Hornblende: in gleicher Menge wie Biotit, bis 1.3 mm, bisweilen Pyroxen umhüllend. Pleochroismus: α-bräunlich, β-bräunlichgrün, γ-grün. Mit pleochroitischen Höfen um Zirkon. Umwandlung in Chlorit vorhanden. Diopsid: weniger als Biotit, bis 0.7 mm.

Apatit und Zirkon vorhanden. Eisenerz: bis 0.6 mm, bisweilen mit etwas Leukoxen. Titanit: kleine Kristalle, leukoxenartig.

Mit etwas sekundärer Chlorit und Epidot.

W. 209*b*. D. 13088. Meradamoendi, südlich Waingapoe. Geröll.

Biotithornblendegranitporphyr.

Quarz: 1.2 mm, selten einigermassen bipyramidal-idiomorph gegenüber angrenzendem Orthoklas, mikropegmatitische Verwachsungen vorhanden. Orthoklas: bis 1 mm, stark getrübt, nicht idiomorph. Mikroperthit vorhanden. Plagioklas: Einsprenglinge bis 2.2 mm, die zweite Generation im Mittel 1 mm. Zonar mit Rekurrenzen. MAW des Zentrums ca. 23°: Andesin. MAW der Ränder ca. -5°: Oligoklas. Antiperthit kommt vor. Mit Sericitisierung.

Biotit: bis 0.6 mm, in der Regel mit Umwandlung in Chlorit. Hornblende: mehr als Biotit, bis 1 mm. Pleochroismus: α-hellgrünbraun, β-grünbraun, γ-bräunlichgrün.

Apatit und Zirkon: sehr wenig. Erz: bis 0.5 mm. Titanit: an verschiedenen Stellen, mit unregelmässiger Form.

Utrecht, 20. Mai 1932.

Geology. — *The joint systems in the vicinity of the Salida Mine (West Coast of Sumatra).* By H. TERPSTRA. Communicated by Prof. H. A. BROUWER.

(Communicated at the meeting of June 25, 1932).

Between the rivers A. Tambang and A. Doeri in the vicinity of the Salida mine reddish brown silicious slates occur in two places, with an inclination varying from 40° to 60°. Further, S.W. of the Bukit Karang, in a conspicuously low and flat stretch of ground, we see clay- and coal slates, with from ½ to 2 meters thick coal- and sandstone banks and from 5 to 10 centimeters thick layers of pyrite.

The inclination of these rocks is of 5° to 10°, rising sometimes in the vicinity of the eruptive dykes to 50°. The sandstone banks we saw at various altitudes, both flat and with northerly and westerly inclinations of 30°, in the rivers A. Galagah, A. Serassa, and A. Sarik.

On the Bukit Tambang we found only loose blocks of these sediments. Fossils were not found here. They are well known in such sediments in the more northerly situated Loempo. According to Professor GERTH, however, the Gastropods and Lamellibranchiates found here do not permit an exact determination of age. ZWIERZYCKI (3) [1]) considers these as Tertiary rocks.

The eruptive rocks occur as andesite bodies, and dacite and basalt dykes. The following dykes, among others, were found:

In the Sungei Beramas Simpangkiri, 2 basalt dykes in dacite, 3 and 5 meters wide, strike N. 320° E., inclination 70° W., and Str. N. 40° E., incl. 40° W.;

Numerous dacite dykes in andesite or bordering upon andesite with sediments (Bukit Karang), as a rule having a strike approximately from East to West. (Only a dyke near the Bukit Kapas Katjik seems to have a more northerly strike);

Further another andesite vein was found in coal slate, Str. N. 80° E., incl. 50° N., in the A. Kajoe Menang.

Propylitization, kaolinization (which sometimes turned out to be a product of weathering), and silicification, which are

[1]) WING EASTON (1), AERNOUT (2), and ZWIERZYCKI (3) have already given some particulars concerning this region, where in 1929 I was engaged for six weeks in geological investigations into the nature of ore deposits on behalf of the BARISAN Mining Company. The management of this company was so kind as to grant its permission for this publication.

not always connected with visible quartz veins, have altered the rocks considerably.

In consequence of the first of the above-mentioned processes, the eruptive rocks have been transformed into a blue clayey mass, with much pyrites, which sometimes turned out to contain gold.

Further the silicification is often so considerable that it is no longer macroscopically ascertainable whether we are concerned with an original vein or with silicified country rocks.

The Tertiary quartz veins, whether mineralized or not, always occur along the west coast of Sumatra in "vein regions", which may be arranged in a definite way ; (I hope to deal with this subject again in a publication on the geology of Mocco-Mocco (N. Benkoelen)).

In such a vein region the veins are again accumulated in groups, lying in certain zones or lines.

The main vein of a group (i.e., the thickest) will as a rule have the same strike as the zone or line, while the strikes of the offshoot veins will be in accordance with those of the other zones.

As the veins are markedly lenticular and sometimes have no outcrop, because they are covered with detritus or do not break through to the surface, the arrangement often becomes a difficult matter to carry out.

We divided up the Salida vein group as follows :

I.	5 zones	with an approx. strike of N. 30° E.,	with	16	groups	&	veins.
II.	2 zones	,, ,, ,, ,, of N. 40° W.,	,,	3	,,	,,	
III.	2 zones	,, ,, ,, ,, of N. 10° E.,	,,	4	,,	,,	
IV.	1 zone	,, ,, ,, ,, of N. 90° E.,	,,	2	,,	,,	

I. Zones with an approx. strike of N. 30° E.

*a*1.	Sarik vein with the continuation in the A. Pinang.	Up to some meters wide.	Str. N. 27° E.	Incl. 80° E.
*a*2.	Serassa vein.	Up to some meters wide.	Str. N. 27° E.	Incl. 70° E.
*a*3.	Ilalang Roentjing vein.	Up to some meters wide.	Str. N. 40° E.	Incl. 70° E.
*b*4.	Doeri vein.	Up to some meters wide.	Str. N. 20° E.	Incl. 80°—90° E.
*b*5.	School vein.	veinlet, up to 40 cM.	Str. N. 40° E.	Incl. 80°—90° E.
*b*6.	Olo, Teleng, Katjai veins.	Up to 4 M. wide.	Str. N. 35° E.	Incl. 80° E.
*b*7.	Djambak vein.	?	?	
*b*8.	Kambang vein.	2 M. wide.	Str. N. 20° E.	Incl. 75° W.
*c*9.	Perakvein.	Some meters.	Str. N. 27° E.	

*c*10. A. Doeri vein. 140 M. above sea level.	Up to 1 M. wide.	Str. N. 50° E.	Incl. 50° NW.
*d*11. A. Goedang Arang vein, 140 M. above sea level.	1 sq. meter.	Str. N. 40° E.	Incl. ?
*d*12. A. Doeri vein.	Wider than 3 M.	Str. N. 30° E.	Incl. 70° W.
*d*13. Main vein of the Salida mine.	Up to 20 M. wide.	Str. N. 30° E.	Incl. 75° E.
*d*14. A. Pisang vein.	0.15 M. wide.	Str. N. 45° E.	Incl. 90°
*d*15. *a*. Bukit Beramas veins	Some meters.	Str. N. 30° E.	?
b. Beramas Kanan vein.	1 M. wide.	Str. N. 40° E.	Incl. 60° E.
e16. A. Solokketjil vein.	Approx. 0.15 M.	Str. N. 27° E.	Incl. 85° W.

II. Zones with an approximate strike of N. 40° W.

*a*17. Painan vein.	Some meters	Str. N. 30°—40° W.	
*a*18. Beramas Kiri vein.	veinlet.	Str. N. 40° W.	?
*b*19. Kambang vein.	?	?	

III. Zones with an approximate strike of N. 10° E.

*a*20. A. Solokketjil vein.	0.05 M. wide.	Str. N. 0—10° E.	Incl. 85° E.
*b*21. Leader vein in the Salida mine, N. and S. offshoot.	Some meters. wide.	Str. N. 12° E.	Incl. 80°—90° E.
*b*22. S. Bank A. Doeri vein, 160 M. above sea level	Up to 4 M. wide.	Str. N. 0° E.	Incl. 80°—90° E.
*b*23. veinlets in dacite near A. Goedang Arang.	Some centimeters wide.	Str. N. 10° E.	Incl. 40° W.

IV. Zones with an approximate strike of N. 90° E.

*a*24. A. Goedang Arang vein, 110 M. above sea level.	2 M. wide.	Str. N. 70° E.	Incl. 40° N.
*a*25. veinlet in the A. Sarik (near vein a1).	Some centimeters wide.	Str. N. 90° E.	Incl. 82° N.

The quartz veins, which cut both the sediments and the eruptive rocks, are very variously mineralized.

Some contain only gold or gold-bearing pyrites, while the Main and Leader veins of the Salida mine, and also the Sarik, Perak, Serassa, and Doeri veins, also contain, besides the above, silver-, lead-, sinc- and iron minerals.

The great differences in the mineralization of veins in the same place, as for instance the Leader vein with hessite and the Main vein without this mineral, in the Salida mine, indicate that mineralization has taken place in various ways and at different times.

That the quartz veins of various strikes originated at different times is quite certainly not always to be assumed (see fig. 1).

The displacement of a vein by another, even the bending of a vein towards another, can also be explained in various ways.

For we can assume that vein *a* (see fig. 2) is younger than vein *b*, and only follows it for some distance (called by HÖVIG (4) "pairing"), or that vein *a* is older than vein *b*, and that the latter was first a fault fissure which was later filled up.

Fig. 1.

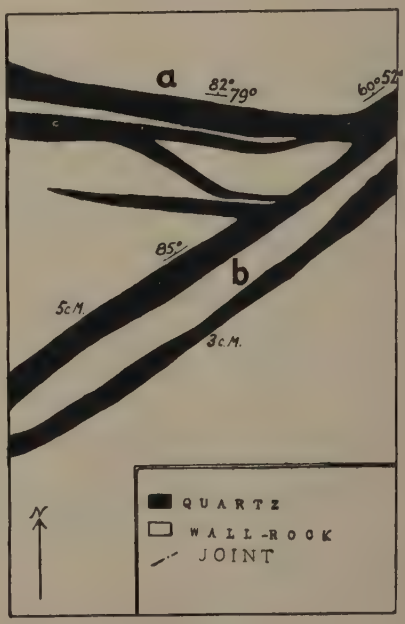

Fig. 2.

QUARTZ VEINS in the A. SARIK, Scale: 1 : 10.

Surface Exposure, vertical seen to N. 65° E.

Surface Exposure, horizontal

Only precise examination of the country rock on typical joints parallel to the fault, and of the ore at the point where the veins meet, would throw light on the subject.

AERNOUT (2), for instance, is of opinion that, in the Salida mine, the Leader is older than the Main vein, on the grounds of the observations that:

1. The wedges of the then-known Leader bend towards the Main vein.
2. Leader ore occurs in the Main vein between N. and S. Leader.

It has appeared however from the surface investigation that the N. Leader vein could be followed as far as 600 M. N. 10° E. from the junction. So the offshoot which at a point 150 M. distant from this junction bends towards the Main vein (which like the S. Leader has not been found on the surface), is only a diagonal bifurcation of the N. leader.

Nor does the mere fact that Leader ore occurs between the two junctions prove that this ore is younger, since we do not know which ore envelops the other.

In this region the best ore columns have been formed at the point where the country rock is andesite, the quartz veins are the widest, and two veins, differing in strike only to the extent of 20°, meet each another.

Moreover it is striking that the courses of the rivers are approximately identical to those of the veins, and that often parts of the various rivers lie on the same line.

It is a familar occurrence along the west coast of Sumatra (see: HÖVIG (5), p. 138, AERNOUT (6), p. 165, HARTING (8), p. 248, PHILIPPI and VAN TUYN (9), p. 28).

In our region, the courses of the rivers are controlled by:

1. Varying resistance to the river erosion of the various rocks, on account of which the rivers will flow parallel to the eruptive dykes.
2. If there are only one sort of rocks the rivers will follow by preference the strikes and dips of the joint-planes of the rocks (see: CLOOS (11) p. 137), and in sedimentary rocks also the strikes and dips of the bedding planes.

Thus the plan of drainage has been regulated in conformity with the structure of the underlying rock basement, and the repeating rectangles of the master-joints appeared in the lines of drainage. Such a type of relief has been described as "checkerboard topography" (see: HOBBS (7), p. 226).

It was noticeable that we found no faults here. But also in the vicinity of the Mangani mine, where we could follow a lot of faults, we saw that the courses of the rivers were determined by them only in a few cases.

The origin of the joint systems can be explained (as ZWIERZYCKI (10), p. 53, has already done for larger regions) according to the method of CLOOS, and thus by assuming a pressure perpendicular to the Sumatra direction, which would give rise to two pairs of joint systems, viz.:

a. One more or less perpendicular to the pressure (N. 40° W.).
b. Two diagonal to it (N. 10° E. and N. 90° E.).
c. One in the direction of the pressure (N. 30° E.).

But we must emphasize the fact that these joints have been opened not once, but several times.

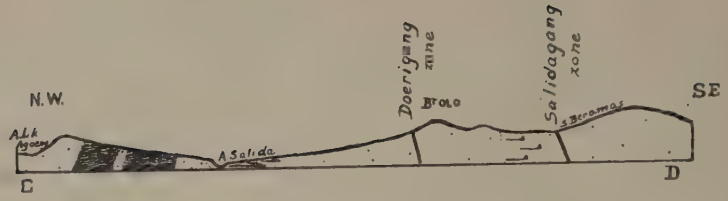

Section: N. 310° E.: A. L. AGOENG — Sei BERAMAS.

Scale: 1 : 40.000.

Section: N. 310° E.: G. KAJOE MENANG — Bt. PETAI.

Scale: 1 : 40.000.

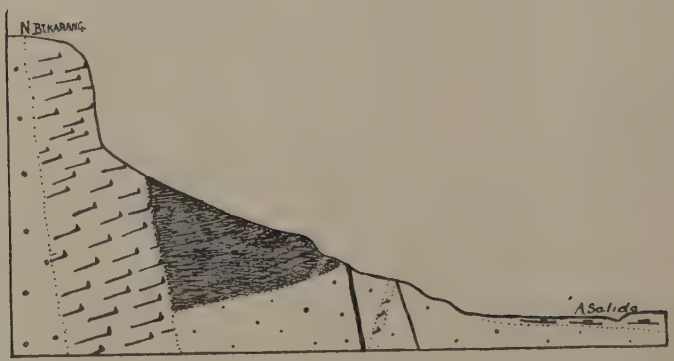

N—S Section along the A. SARIK.

Approx. vertical Scale : 1 : 6.600.

Approx. horizontal Scale : 1 : 10.000.

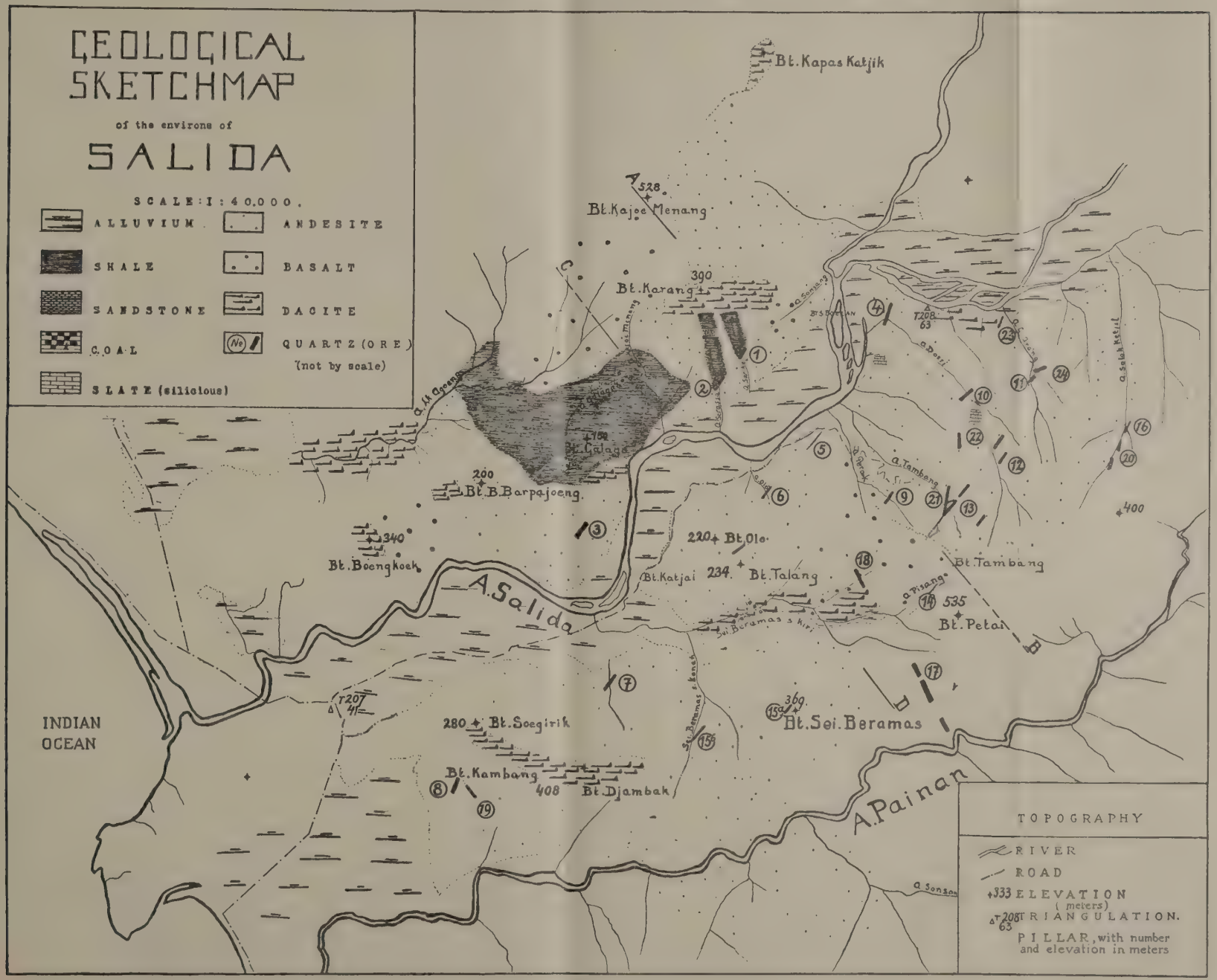
GEOLOGICAL SKETCHMAP
of the environs of
SALIDA
SCALE: I: 40.000.
ALLUVIUM
ANDESITE
SHALE
BASALT
SANDSTONE
DACITE
COAL
QUARTZ (ORE)
(not by scale)
SLATE (silicious)
Bt. Kapas Katjik
Bt. Kajoe Menang
528
Bt. Karang
390
Bt. Talaga
200
Bt. B. Barpajoeng
340
Bt. Boengkoek
220
Bt. Olo
Bt. Katjai
234
Bt. Talang
Bt. Tambang
400
535
Bt. Petai
A. Salida
A. Painan
INDIAN OCEAN
280
Bt. Soegirik
Bt. Kambang
408
Bt. Djambak
369
Bt. Sei. Beramas
TOPOGRAPHY
RIVER
ROAD
+333 ELEVATION (meters)
TRIANGULATION.
PILLAR, with number and elevation in meters

LITERATURE.

In the Geological Mining Bibliography of the Dutch East Indies, closed in February, 1932, the following numbers mention something about Salida: 1040—1173—1186—1213—1238—1318—1332—1344—1415—1417—1449—1450—1982—2792—3008—3011—4369.

In the text reference has been made to:

1. Dr. N. WING EASTON. Die wichtigsten Edelmetall-Lagerstätten Sumatras. Archiv für Lagerstättenforschung Heft. 35. Berlin, 1926. pp. 42—44.
2. Ir. W. A. J. AERNOUT. Enkele nieuwere gegevens over de ertsafzettingen van Salida „De Mijningenieur", 8e Jaargang, 1927. pp. 73—76.
3. Dr. J. ZWIERZYCKI. Toelichting bij blad VII van de geol. overzichtskaart (Schaal 1 : 1.000.000) van den N.O. Indischen Archipel. Weltevreden 1922. pp. 21—34—50.
4. Ir. P. HÖVIG. Afzettingen van nuttige Delfstoffen (Vademecum voor het personeel van het mijnwezen). 2de verb. druk Batavia 1925. pp. 49—56.
5. Ir. P. HÖVIG. De goudertsen van de Lebongstreek. Jaarboek Mijnwezen, 41 Jg. 1912. Verhand. Batavia 1914. pp. 138—143.
6. Ir. W. A. J. AERNOUT. De ertsmijn Lebong Donok. „De Mijningenieur", 8e Jg., 1927. pp. 165—167.
7. Prof. W. H. HOBBS. Earth features and their meaning. N. York 1926.
8. Ir. A. HARTING. Verslag van een Mijnb. geol. onderzoek in de omstreken van Tampang Sawah. J. b. M. w. 1929. Verh. 1930.
9. Dr. H. PHILIPPI en Dr. J. VAN TIJN. De Westkust van Kroei (Benkoelen). „De Mijningenieur", 13de Jg., No. 2. 1932.
10. Dr. J. ZWIERZYCKI. Toelichting bij Bl. VIII van de geol. Overzichtskaart van den Ned. O.I. Archipel. Weltevreden, 1930.
11. H. CLOOS. Tektonische Behandlung magmatischer Erscheinungen. Teil I. Berlin 1925.

An interesting survey of the history of the mine is given by:

J. E. DE MEYIER. De Goud- en Zilvermijn Salida, in „De Indische Gids", XXXII, 1911. pp. 28—67.

The following book has just appeared:

ELIAS HESSE. Goldbergwerke in Sumatra, 1680—1683, 1931, p. 195. N°. X, of „Reisebeschreibungen von Deutschen Beamten im Dienst der W.I. und O.I. Kompagnie 1602—1797", herausgegeben v. S. P. L'HONORÉ NABER (Den Haag).

Botany. — *Spiralwachstum, Wandbau und Plasmaströmung bei Phycomyces.* Von A. J. P. OORT und P. A. ROELOFSEN. (Communicated by Prof. F. A. F. C. WENT.)

(Communicated at the meeting of June 25, 1932).

Einleitung. Da in den letzten Jahren die Kenntnis über die Feinstruktur der Zellwand so sehr zugenommen hat, lag es auf der Hand auch die Wand des Sporangienträgers von *Phycomyces* näher zu untersuchen und dies um so mehr als *Phycomyces* Spiralwachstum zeigt (OORT 1931) und eines der wenigen Objekte ist, von welchen wir die Richtung des Streckungswachstums der einzelnen Zelle genau ermitteln können. Spiralwachstum nennen wir die Erscheinung, wobei die Zellwand in eine Spiralrichtung anwächst, sodass der oberhalb der wachsenden Zone liegende Teil der Zelle um seine Achse dreht. Dabei ist zu erwähnen, dass die Wachstumszone sich von ½ mm bis 2—3 mm unter dem Sporangium befindet und dass also ausser dieser Zone kein Wachstum und also auch keine Drehung stattfindet. Die Richtung der Spirale ist der botanischen Nomenklatur zufolge meistens rechts, d.h. dass man, wenn man die Spirale als eine Wendeltreppe betrachtet, beim Hinaufsteigen die rechte Hand an der Innenseite hat. Es gab keine feste Beziehung zwischen der Grösse des Längenwachstums und der Drehung, sodass der Winkel, den die Spirale mit der Längsachse macht, bei demselben Träger zu verschiedenen Zeitpunkten und bei verschiedenen Trägern in der Grösse wechselt. Dieser Winkel kann selbst null oder die Spirale links sein, aber das bleiben Ausnahmen. Im Mittel wurde für die Rechtsspirale ein Winkel von 6° gefunden

In der obengenannten Mitteilung über Spiralwachstum bei *Phycomyces* wurde schon auf eine mögliche Beziehung zwischen Spiralwachstum, Wandstruktur und Protoplasmaströmung hingewiesen. Es ist das Ziel dieser Arbeit eine Einsicht in den Wandbau und die Protoplasmaströmung zu bekommen, um damit zu versuchen der Erscheinung des Spiralwachstums und des Wachstums im allgemeinen näher zu kommen.

Ueber die Ursache des Spiralwachstums sind verschiedene Hypothesen, welche ganz mit den Hypothesen über die Entstehung einer Spiralstruktur vergleichbar sind, aufzustellen. Da es wahrscheinlich ist, dass Spiralwachstum und Spiralstruktur zwei Erscheinungen mit derselben Ursache sind, werden wir die Hypothesen, welche über die Entstehung einer Spiralstruktur handeln, hier kurz mitteilen. Mutatis mutandis kann dies dann auch auf das Spiralwachstum Anwendung finden.

A. Die Spiralstruktur wird durch die Zellwand selbst bestimmt. Strömt auch das Protoplasma spiralig, so wäre die Ursache in einer Induktion aus

der Zellwand zu suchen. Dabei gibt es dann verschiedene Möglichkeiten, wovon man einige bei NAEGELI und SCHWENDENER (1877, S. 415), HERZOG (1924) und FREY (1927, S. 628) angeführt findet.

B. Die Spiralstruktur soll von einer spiraligen Protoplasmaströmung bestimmt werden. Diese richtet die Teilchen der Wand und setzt sie in Spiralketten gerichtet ab. Wie man sich solches sehr verständlich machen kann, hat VAN ITERSON (1927, S. 186), der die alte Theorie von DIPPEL (1868) wieder aufnimmt, dargelegt. Später (1931, S. 27) führt VAN ITERSON eine Arbeit von SINGER (1930) an, worin dies für Stärke bewiesen wird. Zugleich wird darauf hingewiesen, dass dies auch für *Phycomyces* wahrscheinlich ist. Auch FREY (1930) neigt sich in neuester Zeit mehr der Protoplasmatheorie zu.

Wir werden nun erst untersuchen, wie es sich mit der Wandstruktur und Protoplasmaströmung bei Phycomyces verhält und kommen dann später auf diese Hypothesen zurück.

Gearbeitet wurde hauptsächlich mit einer + Kultur von *Phycomyces Blakesleeanus* Burgeff. Soweit die — Kultur untersucht wurde, konnte kein Unterschied mit der + Kultur festgestellt werden. Die *Varietät piloboloïdes* ist auch untersucht; dabei wurde aber hinsichtlich der Zellwand kein wesentlicher Unterschied gefunden, weiterhin wird darum nur von *Phyc. Blakesl.* die Rede sein. Erwähnenswert ist hier nur, dass während der für die Varietät charakteristischen Anschwellung des Sporangienträgers, keine Drehung des Sporangiums statt findet und also auch keine Torsion des Trägers auftritt, wie BURGEFF (1914, S. 279) erwähnt hat.

Methode. Der Pilz wurde in Töpfchen mit feuchtem Brot kultiviert. Die Plasmaströmung kann man am besten studieren, wenn man die Träger vorsichtig aus dem Substrat loszieht und sie auf einem Objektträger in Luft, Wasser oder Paraffinöl betrachtet. Die Strömung kann so noch Stunden ungestört weitergehen, wie sich auch in Versuchen, worin die Träger nicht losgelöst wurden, zeigte.

Zum Studium des Feinbaus der Zellwand muss die einfache Wand untersucht werden. Zudem ist es notwendig die Achse der Zelle zu behalten um die Richtung der Teilchen hinsichtlich dieser bestimmen zu können. Der Zartheit wegen kann man nicht wie bei Fasern verfahren und es müssen also die verwendeten Präparationsmethoden — zur Raumersparung kurz — beschrieben werden.

1. Eine turgeszente Hyphe wird auf einen Objektträger gelegt, die Basis wird festgeklebt und unter dem Mikroskop wird die Zelle nahe an der Befestigungsstelle angeschnitten. Durch das Loch schiebt man einen dünn ausgezogenen Glasfaden in die Hyphe und kratzt nun vorsichtig mit einem Messerchen über den Faden, sodass die Wand der Länge nach durchgeschnitten wird. Der Faden wird dann fortgenommen und die Wand so gut wie möglich flach gelegt. Die Achsenrichtung bleibt nahezu behalten, aber von der zarten Wachstumszone bekommt man niemals gute

Präparate. Um Torsionen vorzubeugen darf man den Glasfaden nicht so weit durchschieben, bis die Hyphe von selbst aufspaltet.

2. Die Wachstumszone kann man dadurch studieren, dass man turgeszente Träger auf ein *nasses* Objektglas legt und sie durch Druck sprengt. Dies veranlasst eine Spaltlinie, die bis 3 cm lang sein kann. Diese Spaltlinie zeigt eine steile Rechtsspirale, sodass die Längsrichtung nicht beibehalten bleibt.

3. Zur genauen Bestimmung der Auslöschungsrichtungen kann man auch einen Träger unter einem scharfen Winkel durchschneiden, dann das Stück 90° um seine Achse drehen und platt drücken. Man bekommt so ein rautenförmiges Stück der einfachen Wand nebst einem Stück der doppelten Wand, wovon die Längsrichtung ganz genau behalten bleibt. Für die Wachstumszone ist diese Methode nur in Kombination mit 1 brauchbar. Man schneidet unter scharfem Winkel durch und schiebt anderswoher einen Glasfaden ein, bis dieser der Zellwand eng anliegt. Nun kann man das Präparat ohne Mühe in die gewünschte Lage drehen, was ohne Glasfaden in der schlaffen Wachstumszone nicht möglich wäre.

4. Zum Studium der verschiedenen Schichten der Wand, kann man von einer nach Methode 1 präparierten einfachen Wand Streifen abziehen. Dafür ist es erwünscht, die Wand vorher durch Eintrocknen auf den Objektträger entweder mit der Innen-, oder mit der Aussenseite festkleben zu lassen. Den Bau in tangentialer und axialer Richtung kann man an Schnitten untersuchen. Diese sind aber schwierig herzustellen. Die Doppelbrechung in tangentialer Richtung studiert man am Einfachsten am Rand von Zylinderpräparaten (d.h. von Präparaten, bei denen man durch Einschieben von Glasfäden die Zylinderform behalten hat). Zudem kann man sich leicht über die Doppelbrechung orientieren, indem man die Ränder von in die Wand gestochenen Löchern — wo die Wand also mehr oder weniger hervorsteht, — betrachtet.

Chemische Eigenschaften der Zellwand. Van Wisselingh (1925, S. 187) führt *Phycomyces* als einen Fall an, wobei er das Vorkommen einer Substanz, die von ihm Chitin genannt wurde, bewiesen hat. Tatsächlich fällt die Chitosanreaktion positiv aus ; zudem konnten wir auch Chitosansulfatsphaeriten bekommen. Wenn man die entgegengesetzten Meinungen über das eventuelle Vorkommen von meistens nicht scharf definierten Stoffen, wie Kallose, Pilzzellulose, Pektinen in Betracht zieht, so darf man vielleicht diese Chitinbestimmung nicht als ganz beweisend ansehen ; man vergleiche aber auch Kühnelt (1928). Zellulosereaktionen fallen negativ aus, aber aus den Untersuchungen von Thomas (1928, 1930) ergibt sich, dass die Wand Stoffe enthalten kann, welche durch andere derart verdeckt werden, dass sie erst nach langer Behandlung zum Reagieren imstande sind.

Kongorot und Rutheniumrot werden, wenn die Wand durch Aufkochen in Lauge permeabel gemacht ist, stark aufgenommen ; aber das sagt nichts

aus, weil auch Chitosan sich damit färbt. Da die optischen Eigenschaften, wie näher erörtert werden soll, von Zellulose-fasern stark abweichen, ist es wohl sehr wahrscheinlich, dass die Wände grösstenteils aus Chitin bestehen und dass Zellulose nicht oder nur in geringer Menge vorkommt.

Es muss noch erörtert werden, dass die Wand an der Aussenseite für Farbstoffe, Wasser und Plasmolytika völlig impermeabel ist. Dabei ist zu erwähnen, dass diese Stoffe von innen direkt eindringen. Das äusserste Schichtchen hat also kutikulare Eigenschaften, die es aber erst unter der Wachstumszone bekommt.

Protoplasmaströmung. Unter der Wachstumszone ist das wandständige Plasma dünn und besteht, dem Anschein nach, aus vielen dünnen Fädchen, die alle in einer Richtung laufen. In diesen Fädchen werden Körnchen und Fetttropfen gleichende Teilchen mitgeführt. Hauptsächlich bewegen sie sich der Spitze hin, aber fast immer findet man auch wenige Fädchen, die basalwärts gehen. Diese Plasmaströmchen laufen meistens in einer steilen Spirale rechts um die Achse herum. Der Neigungswinkel, den die Spirale mit der Achse bildet, kann bei demselben Träger von $\pm 15°$ rechts bis $\pm 15°$ links wechseln, doch sind Umkehrungen von rechts nach links oder umgekehrt ziemlich selten. Ein ausschliesslich links strömender Träger wurde nur einmal beobachtet. Neigungswinkel von fast null oder null wurden ziemlich oft gefunden.

In der Wachstumszone hat es den Anschein, als ob das ganze Zellvolumen mit Plasma gefüllt ist. Lässt man die Zelle leer laufen, dann sieht man einen deutlichen Unterschied zwischen einem in Dicke variierenden wandständigen Plasma und einem flüssigeren zentralen Plasma. Die Strömung ist gering und ohne bevorzugte Richtung. Die Teilchen wirbeln durcheinander, ohne dass man aussagen kann, welcher Teil durch die BROWNsche Bewegung und welcher Teil durch eine eigene Bewegung verursacht wird.

Der Bau der Zellwand. Untersucht man eine einfache oder doppelte Zellwand zwischen gekreuzten Nikols, so findet man nur eine schwache Doppelbrechung. Das rührt daher, dass die natürliche schwach dichroïtische blau-schwarze Farbe der Wand, die schon wenige cm unter dem Sporangium aufzutreten anfängt, die Untersuchung stört. Durch vorsichtiges Erwärmen in Lauge, Bleichen in Chlor oder Behandlung mit Diaphanol verschwindet diese. Die Doppelbrechung tritt nun deutlich hervor, ist aber noch schwach, sodass wir nur orientierend beobachten können, dass es eine dünne äussere Schicht gibt, die in radialer Richtung gesehen (also in Flächenaufsicht) isotrop ist, und eine dicke innere, die hinsichtlich der Achse positiv doppelbrechend ist. Eine schiefe Auslöschung ist nur in günstigen Fällen und in starkem Licht zu finden. Die Wachstumszone ist in radialer Richtung isotrop, hier ist also nur die äussere Schicht anwesend. In tangentialer und axialer Richtung gibt es eine schwache Doppelbrechung.

Für eine nähere Untersuchung haben wir die wenig bekannte Tatsache, *die Doppelbrechung mittels Färbungen zu verstärken* (siehe u.a. SCHMIDT 1931), benutzt. Es zeigte sich, dass Jod in Chlorzinkjodlösung ein sehr geeigneter Farbstoff war. Ausser Verstärkung der Doppelbrechung trat dazu ein starker Dichroismus auf. Die Jodfärbung hat zudem noch den Vorteil, dass damit die Streifung viel deutlicher hervortritt.

Es stellte sich nun heraus, dass es in ausgewachsenen Wänden mindestens drei Schichten gibt, die zusammen ungefähr 3 μ dick sind. Die Dicke der einzelnen Schichten ist nicht genau feststellbar, Schicht 1 und 3 sind sehr dünn (0.5 μ oder dünner), während die mittlere also mindestens 2 μ dick ist.

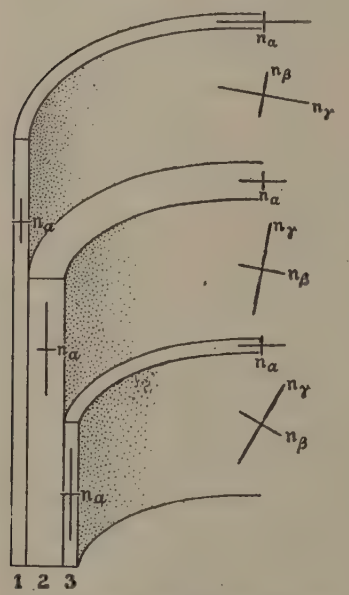

Fig. 1. Schematische Darstellung der Wandschichtung mit eingetragenen Brechungsindices.

Wir werden nun die Schichten gesondert besprechen (Fig. 1).

Schicht 1 (primäre Wand) stimmt mit der oben genannten äusseren Schicht überein. In der Wachstumszone tritt sie gesondert auf, ist aber über die ganze Länge als eine leicht von der folgenden zu spaltende Schicht vorhanden. Die längste Achse des dreiachsigen Indexellipsoids, n_γ, läuft nahezu tangential, n_β nahezu axial und n_α radial. Die Hyphe ist also bezüglich der Längsrichtung negativ. Der Dichroismus ist positiv in Hinsicht auf n_γ, also negativ hinsichtlich der Längsachse (Tafel 1, Fig. 1 und 2 : *a*). Die Auslöschung zwischen gekreuzten Nikols ist schief, der Neigungswinkel ist nur gering. Die Spirale verläuft meistens rechts, bisweilen auch links. Genaue Winkelmessungen waren nicht möglich, doch ist es deutlich, dass n_β mit der Wachstumsrichtung, wenigstens ungefähr, übereinstimmt. In Zylinderpräparaten (siehe Methode) findet man zu beiden Seiten der Mitte zwei nicht aufleuchtende Zonen dort, wo die negative Doppelbrechung in radialer Richtung in die positive in tangentialer Richtung übergeht (Tafel 1, Fig. 4 : *a*).

Bei Druckerhöhung mit Tusche in und unter der Wachstumszone markierter und in Wasser gelegter Träger, können wir beobachten, dass die Zelle sich ausschliesslich in der Wachstumszone dehnt und sich während der Dehnung so dreht, dass die Richtung der grössten Dehnbarkeit meistens in einer steilen Rechtsspirale verläuft. Die Dehnung ist elastisch, sie geht also bei Druckabnahme wieder zurück. Auch in normalen turgeszenten Zellen sieht man bei Turgorverminderung die Dehnung unter Drehung zurückgehen. Wird der Druck zu gross, so platzt die Zelle in und

TAFEL I

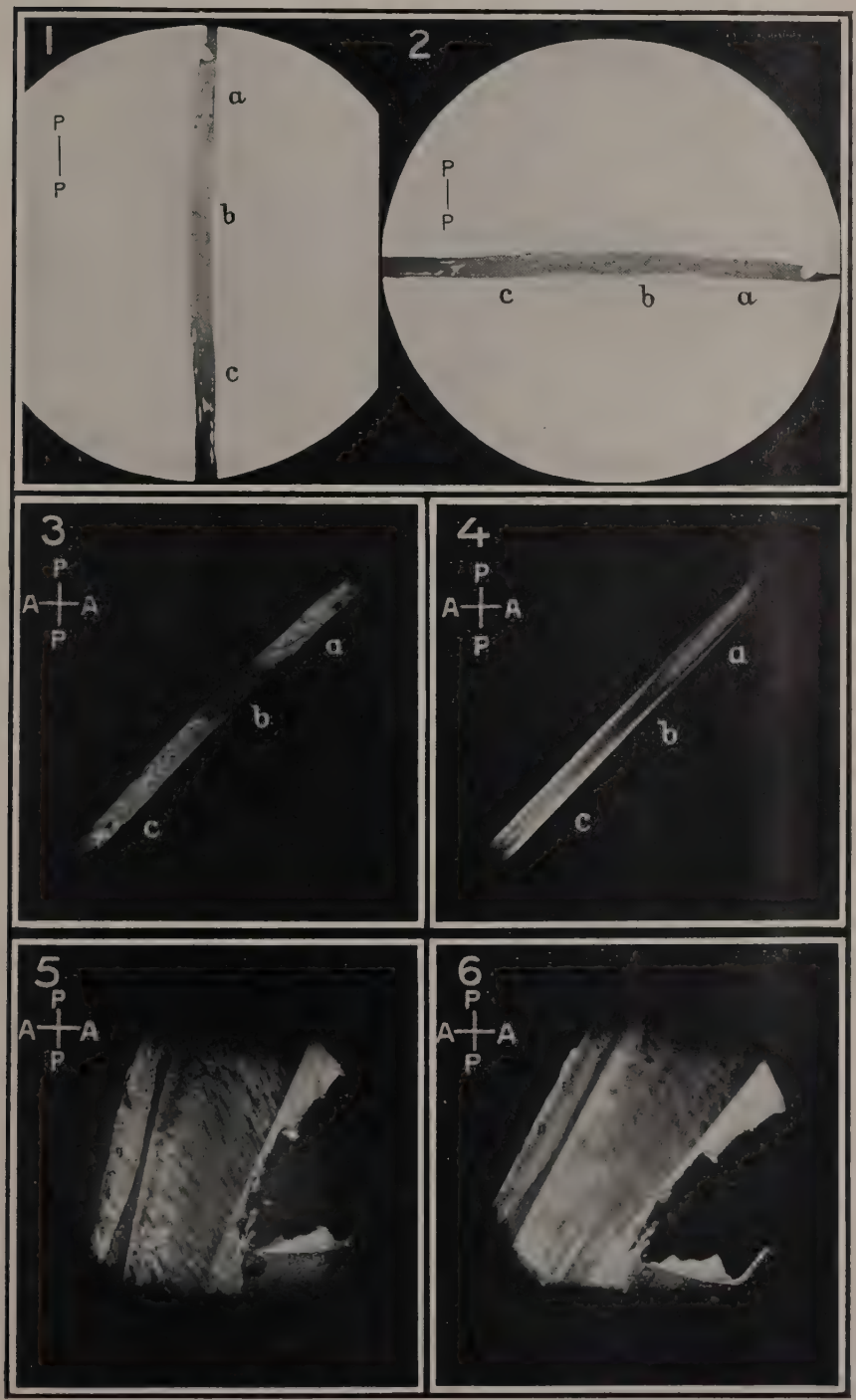

unter der Wachstumszone auf. Die Spaltlinie verläuft in einer steilen, meist Rechtsspirale. Die Richtung, worin die Elastizitätsgrenze zuerst überschritten wird, steht also senkrecht zur Richtung der grössten Dehnbarkeit und stimmt also mit n_γ überein.

Zusammenfassend finden wir also, dass die Wachstumsrichtung, die Richtung einer der Achsen des Indexellipsoids (n_β), die Richting der Dehnbarkeit und der Spaltbarkeit zusammenfallen ; n_γ steht senkrecht dazu und läuft tangential.

Bisweilen beobachtet man eine sehr feine Streifung, ungefähr parallel zu der Spaltlinie. Zudem gibt es bei Quellung ein System in Längs- und Querrichtung verlaufender Aederchen, die den Eindruck von kleinen Rissen machen.

Bisweilen gibt es dem Anschein nach, noch andere Streifungssysteme, aber wir haben hiervon kein deutliches Bild bekommen. So ist es eine Frage, ob diese primäre Wand noch aus mehr Schichtchen gebildet ist. Die Wand lässt sich aber nicht in mehr Schichtchen spalten. Sie ist schlaff und biegsam und zerreisst in allen Richtungen, zeigt auch keine Fibrillarstruktur. Das äusserste Schichtchen der primären Wand ist unter der Wachstumszone für Farbstoffe usw. impermeabel und hat also kutikulare Eigenschaften. Das schliessen wir daraus, dass die primäre Wand von innen her ganz gut, von aussen her nicht gefärbt wird, und polare Permeabilität ziemlich unwarscheinlich ist. Jod wird stark aufgenommen, vermutlich noch relativ stärker als durch Schicht 2.

Schicht 2 (sekundäre Wand) tritt unter der Wachstumszone auf und bekommt eine grössere Dicke als 1. n_γ verläuft parallel zu der Protoplasmaströmung, wie in vielen Fällen festgestellt wurde. Von markierten Trägern wurde erst die Protoplasmaströmung bestimmt und danach die Auslöschungsrichtung. Besonders bei Umkehrung in einer Linksspirale, war die Parallelität sehr auffällig. Im Gegensatz mit 1 ist die Doppelbrechung positiv hinsichtlich der Achse (Fig. 1), ebenso der Dichroismus (Taf. 1, Fig. 1 und 2 : *c*). n_β verläuft tangential, n_α wie bei 1 radial. Weil Schicht 1 negativ, Schicht 2 positiv hinsichtlich der Achse ist, findet man beim Dickerwerden von Schicht 2 unter der Wachstumszone eine Stelle, wo beide Schichten einander kompensieren und die also in Diagonalstellung unter gekreuzten Nikols nicht aufleuchtet (Tafel 1, Fig. 3 : *b*). Auch Zylinderpräparate zeigen dasselbe, aber nur in der Mitte (Tafel 1, Fig. 4 : *b*). Diese Kompensationsstelle liegt bei gut wachsenden Trägern 3 bis 4 mm unter dem Sporangium, also 1 bis 2 mm unter der Wachstumszone. Wir haben dies u.a. bestimmt, indem wir zuerst die Länge der Wachstumszone und danach von derselben Zelle die Kompensationsstelle massen. Es ist wohl sehr wahrscheinlich, dass Schicht 2 also ungefähr am Ende der Wachstumszone aufzutreten anfängt.

In gequollenen Präparaten findet man eine sehr deutliche Längsstreifung, parallel zu n_γ und der Plasmaströmung, meistens also in einer steilen

Rechtsspirale. Schneidet man die Zelle unter scharfem Winkel durch, so bekommt man am Rand sehr schöne Fibrillen. Diese laufen parallel zur Streifung. Die Dehnbarkeit ist sehr gering, die Spaltung parallel der Streifung geht leicht.

Schicht 3 ist sehr dünn. Sie tritt unter der Wachstumszone auf, aber es lässt sich schwer sagen wo, weil das gesonderte Auftreten dieser Schicht in den Präparaten mehr oder weniger zufällig ist. Sie ist nur nach Jodfärbung zu finden und nur wenn diese genügend stark ist, während Schicht 1 und 2 sich schon in schwachen Chlorzinkjodlösungen färben. Meistens sieht man Schicht 3 (präpariert nach Methode 4) mit einem dickeren oder dünneren Schichtchen von 2 überdeckt. Ist Schicht 2 völlig oder mit Schicht 1 anwesend, so ist Schicht 3 durch die stärkere Färbbarkeit von Schicht 1 und 2 meistens nicht zu beobachten. Das Indexellipsoid ist vermutlich dreiachsig, n_γ verläuft unter einem Winkel von 20°—40°, immer in einer Rechtsspirale. Keine Beziehung mit der Protoplasmaströmung. Die Schicht zeigt eine ziemlich grobe netzförmige oder schachbrettartige Zeichnung, keine Streifung wie bei Schicht 2. Das auf Tafel 1, Fig. 5 und 6, abgebildete Präparat löscht unter einem Winkel von 20° mit der Längsrichtung aus. Dreht man das Präparat aus dieser Lage 10° nach links (Taf. 1, Fig. 5), so sieht man eine Zeichnung von abwechselnd lichten und dunkeln Feldchen. Dreht man das Präparat aus dem Dunkelstande nach rechts (Taf. 1, Fig. 6), so sind die dunkeln Feldchen licht und die lichten dunkel geworden. In der ersten Lage ist die Zeichnung am besten zu sehen, die lichten Fleckchen sind lichtgelb, die dunkeln dunkelgrau. In der zweiten Lage tritt Schicht 2 störend auf (sieh Streifung), die lichten Feldchen sind gelborange, die dunkeln orangerot und der Farbenunterschied ist damit weniger intensiv. Auch bei dieser Schicht ist der Dichroismus hinsichtlich n_γ positiv.

Die wechselnden Neigungswinkel, sowohl von Schicht 1, wie von 2 und 3 machen es wahrscheinlich, dass nicht die Wand, sondern die Protoplasmaströmung die Teilchen richtet (siehe Einleitung).

Micellarstruktur und Formdoppelbrechung. Die gefundene Verstärkung der Doppelbrechung und der Dichroismus deuten auf eine Micellarstruktur hin. Dabei sind doppelbrechende oder nicht doppelbrechende Teilchen, die sog. Micellen, in eine intermicellare Substanz eingebettet. Gibt es einen Unterschied im Brechungsindex zwischen Micellen und intermicellarer Substanz, so tritt der Theorie von WIENER (1912) zufolge Doppelbrechung auf (Formdoppelbrechung). Sind die Teilchen selbst doppelbrechend, so ist die Wand auch doppelbrechend (Eigendoppelbrechung). Meistens sind beide Formen der Doppelbrechung zugleich da, sind also doppelbrechende Teilchen in eine Substanz von anderem Brechungsindex eingebettet. Bei *Phycomyces* ist die Eigendoppelbrechung den Resultaten mit ungefärbten Zellen gemäss, gering (wenn nicht Eigen-

und Formdoppelbrechung einander ganz oder teilweise kompensieren). Dies weist also auf einen Unterschied mit Zellulose, die eine starke Eigendoppelbrechung hat, hin. Wegen der schwachen Doppelbrechung in ungefärbtem Zustand ist es beschwerlich die Doppelbrechung in verschiedenen Imbibitionsflüssigkeiten zu untersuchen, um daraus auf die *Form* der Teilchen zu schliessen. Doch wollen wir die Möglichkeiten betrachten. Zufolge WIENER ist die Formdoppelbrechung in idealen Fällen mit einem optisch einachsigen Kristall zu vergleichen. Indem wir nun ein dreiachsiges Indexellipsoid fanden, das praktisch nur auf die Formdoppelbrechung zurückzuführen ist, weil die Färbung ausschliesslich die Formdoppelbrechung verstärkt, können wir nun z.B. annehmen, dass die Micellen wohl in einer Richtung orientiert sind, aber in radialer Richtung hinsichtlich der Längsrichtung schief stehen. Im Querschnitt wird dann keine Isotropie gefunden. Oder wir können annehmen, wie auch FREY (1930) es tut, dass die Micellen hauptsächlich in einer Richtung orientiert sind, aber in einer bestimmten Ebene Abweichungen zeigen. Schicht 1 würde dann zum Typus „Röhrenstruktur" gehören, wobei die Teilchen tangential mit Abweichungen in axialer Richtung gerichtet sind. Schicht 2 würde zum „Faser"-typus gehören, wobei die Teilchen axial mit Abweichungen in tangentialer Richtung gerichtet sind. Wiewohl FREY diese Fälle nur für Stäbchendoppelbrechung behandelt, gilt diese Betrachtung auch für Plättchendoppelbrechung nur mit Umkehrung des Vorzeichens der Doppelbrechung. Bei *Phycomyces* würden beide Fälle möglich sein, weil, wie schon gesagt, ein Schluss auf die Form noch nicht möglich ist. Obendrein kann man ein dreiachsiges Indexellipsoid auch durch eine vollkommen parallele Orientierung rhombischer (also dreiachsiger) Micellen erklären.

Dichroismus. Auf einige Besonderheiten des schon früher erwähnten Dichroismus wollen wir näher eingehen. Im Gegensatz zu Rameh-fasern oder Cobaea-fäden, welche den Dichroismus schwarz-farblos aufweisen, ist der Dichroismus in mit Chlorzinkjod gefärbten Zellwänden von *Phycomyces* nur relativ. Bei schwacher Färbung tritt der Farbenunterschied gelb-orange, bei starker Färbung rotbraun-schwarz auf. Auch diese Tatsache weist auf einen Unterschied mit Zellulose hin. Die Adsorptionskräfte sind bei Chitin offenbar viel weniger stark, wodurch die Jodteilchen weniger gerichtet werden. Auch der Umstand, dass das Jod wiederum ziemlich rasch aus der Wand verschwindet, spricht dafür. Es würde selbst möglich sein, dass bei *Phycomyces* das Jod nur *ab*sorbiert wird, welche Möglichkeit von FREY für Zellulose angeführt, aber verworfen wird.

Bestimmen wir die Auslöschungsrichtungen von dichroitisch gefärbten Fasern unter gekreuzten Nikols (z.B. Rameh, Vinca, Flachs mit *Ag, Au, J* oder *Te* gefärbt), so finden wir, dass diese niemals einen Winkel von 90° miteinander bilden, wie bei ungefärbten Fasern. Unter Berücksichtigung der Tatsache, dass in Chlorzinkjod gefärbte Fasern als Nikol wirken und aus verschieden orientierten Schichten bestehen, kann man dies sehr leicht

erklären. In Fig. 2 sind die verschiedenen Möglichkeiten abgebildet. Bei Cobaea-fäden und Kunstseide bilden die Auslöschungsrichtungen einen geraden Winkel miteinander. Diese fallen zugleich mit den Schwingungsebenen zusammen (Fig. 2 : *a*, links). Hier haben wir es also mit einer ein-

Fig. 2. Schema der Auslöschungsrichtungen in Chlorzinkjod gefärbter Fasern und Zellen unter gekreuzten Nikols. $P - P$, bzw. $A - A$ Schwingungsebene des Polarisators bzw. Analysators. Links: Cobaea-fäden und Kunstseide (*a*). Mitte: Rameh-faser und doppelte Wand von Phycomyces (*b*), Baumwolle (*c*), alle mit Rechtsspiralstruktur. Rechts: Flachs- und Vinca-fasern (*d*), Baumwolle (*e*), alle mit Linksspiralstruktur.

fachen, in der Längsrichtung verlaufenden Struktur zu tun. Bei Ramehfasern fallen die Auslöschungsrichtungen in den Quadranten I und III (Fig. 2 : *b*, Mitte). Dies deutet auf eine Struktur, die hauptsächlich [1]) in einer Rechtsspirale verläuft, hin. Bei Vinca- und Flachs-fasern liegen die Auslöschungsrichtungen in den Quadranten II und IV (Fig. 2 : *d*, rechts). Hier haben wir es also mit einer Struktur, die hauptsächlich [1]) in einer Linksspirale verläuft, zu tun. Bei Baumwolle fallen die Auslöschungsrichtungen je zwei und zwei ungefähr zusammen. Die Strukturrichtung bildet hier dann auch einen grossen Winkel ($\pm 29°$, siehe Balls 1923) mit der Längsrichtung. Wir finden nun abwechselnd Auslöschung in den Quadranten I und III (*c*, Mitte) und in II und IV (*e*, rechts); dies weist auf eine bald Rechts- bald Links-spiralstruktur, wie sie tatsächlich da ist, hin.

Ohne weiter hierauf eingehen zu können, haben wir zu erwähnen, dass die Untersuchung speziell mit Chlorzinkjod gefärbter Zellwände uns instand setzt zu bestimmen, ob eine Wand aus verschieden orientierten Schichten besteht. Finden wir, dass die Auslöschungsrichtungen keinen Winkel von 90° miteinander bilden, so sind wir sicher, es mit mindestens zwei verschieden orientierten Schichten zu tun zu haben. Finden wir einen geraden Winkel, so dürfen wir auf eine oder mehrere gleich gerichtete Schichten schliessen.

Bei *Phycomyces* und bei schwächer dichroitischen Färbungen haben wir

[1]) Wir legen den Nachdruck auf das Wort: hauptsächlich. Flachs hat z. B. eine dünne primäre Wand, die rechtsgewunden ist und eine dicke sekundäre Wand, die linksgewunden ist. Offenbar bestimmt hier die dicke Schicht die Auslöschungsrichtung in der gefärbten Wand.

es nur mit einer partiellen Nikolwirkung oder mit Nikolwirkung für eine bestimmte Farbe zu tun. Doch ist nach der oben angegebenen Methode bei *Phycomyces* schon direkt auf Spiralbau zu schliessen. Auf das Zusammenwirken von verschieden orientierten Schichten, die hinsichtlich der Farbe verschiedenes Absorptionsvermögen und einen verschiedenen Dichroismus besitzen können, sind die bisweilen komplizierten Erscheinungen (z.B. der eigenartige Farbenwechsel, der bei Schicht 2 und 3 auftritt) zurückzuführen.

Zusammenfassung.

1. Die Zellwand von *Phycomyces* besteht wahrscheinlich hauptsächlich aus Chitin und enthält kein oder wenig Zellulose. Auf das Fehlen der Zellulose weisen auch die schwache Eigendoppelbrechung und die dichroïtischen Erscheinungen hin.

2. In der primären Wand (Schicht 1 ist in der Wachstumszone allein vorhanden) stimmt die Richtung der grössten Dehnbarkeit, der Spaltbarkeit, einer feinen Streifung und von n_z mit der Wachstumsrichtung überein. Diese verläuft meistens in einer steilen Rechts-, bisweilen auch Linksspirale. n_γ steht senkrecht auf dieser Richtung und verläuft ungefähr tangential. Die Plasmaströmung hat keine bevorzugte Richtung.

In der sekundären Wand (Schicht 2) steht n_γ axial, parallel zur Streifung und zur Plasmaströmung, die hier deutlich gerichtet ist. Diese Schicht tritt unterhalb der Wachstumszone auf und erreicht eine ziemliche Dicke. Die Richtung der Streifung verläuft meistens in einer steilen Rechtsspirale, bisweilen (anscheinend öfters als bei Schicht 1) ist sie auch gerade oder verläuft sie in einer steilen Linksspirale.

Eine dritte, dünne Schicht hat eine schachbrettartige Struktur und verläuft unter einem Winkel von 20°—40° immer in einer Rechtsspirale.

3. Die Eigendoppelbrechung ist schwach, ebenso wie die Formdoppelbrechung. Diese letzte kann aber durch Färbung mit Chlorzinkjod sehr verstärkt werden.

Die Erscheinungen der Färbung (Dichroïsmus und Verstärkung der Doppelbrechung) deuten auf eine Micellarstruktur hin. Die Form der Teilchen konnte nicht bestimmt werden. Es ist möglich, dass die Farbe nur absorbiert wird und nicht adsorbiert, wie für Zellulose wahrscheinlich ist.

4. Es wird hingewiesen auf die Möglichkeit dichroïtisch gefärbte Zellwände zwischen gekreuzten Nikols auf die eventuelle Anwesenheit verschieden orientierter Schichten zu untersuchen.

Wageningen } Juni 1932.
Utrecht }

LITERATUR.

AMBRONN, H. und FREY, A. Das Polarisationsmikroskop. 1926.

BALLS, W. L. The determiners of cellulosestructure, as seen in the cellwall of cotton hairs. Proc. Roy. Soc. London. 95 B: 72. 1923.

BURGEFF, H. Untersuchungen über Variabilität, Sexualität und Erblichkeit bei Phycomyces nitens Kunze. Flora **107**: 259. 1914.

DIPPEL, L. Die wandständigen Protoplasmaströmchen in den Pflanzenzellen usw. Abh. Naturf. Ges. Halle **10**: 55. 1868.

FREY, A. Die Technik der dichroitischen Metallfärbungen. Zeitschr. f. wiss. Mikrosk. **42**: 421. 1925.

——— Das Wesen der Chlorzinkjodreaktion und das Problem des Faserdichroismus. Jahrb. wiss. Bot. **67**: 597. 1927.

——— WYSSLING. Mikroskopische Technik der Micellaruntersuchung von Zellmembranen. Zeitschr. f. wiss. Bot. **47**: 1. 1930.

HERZOG, R. O. Ueber den Feinbau der Faserstoffe. Naturw. **12**: 955. 1924.

ITERSON, G. VAN. De wording van den plantaardigen celwand. Chem. Weekblad **24**: 166. 1927.

——— Links en rechts in de levende natuur. Handelingen 23e Ned. Nat. en Geneesk. Congres. S. 4. 1931.

KÜHNELT, W. Studien über den mikrochemischen Nachweis des Chitins. Biol. Zentralbl. **48**: 374. 1928.

NAEGELI, C. und SCHWENDENER, S. Das Mikroskop. 1887.

OORT, A. J. P. The Spiral-growth of Phycomyces. Proc. Roy. Acad. Sc. Amsterdam. **34**: 564. 1931.

SCHMIDT, W. J. Dichroitische Färbung tierischer und pflanzlicher Gewebe. Abderh. Handb. Abt. V, Teil 2, Heft 16. S. 1835. 1931.

SINGER, R. Ueber die Strömungsdoppelbrechung der Molekülkolloide. Ztschr. physik. Chem. **A, 150**: 257. 1933.

THOMAS, R. C. Composition of fungus hyphae. Amer. Journ. Bot. **15**: 537. 1928 und **17**: 779. 1930.

WIENER, O. Die Theorie des Mischkörpers für das Feld der stationären Strömung. Abh. Sächs. Ges. d. Wiss., math. phys. Kl. **32**: 507. 1912.

ERKLÄRUNG DER TAFEL I.

Fig. 1 und 2. Einfache Wand in der Wachstumszone (*a*) und darunter (*c*). *P* — *P*, Schwingungsebene des Polarisators. Bei *a* ist der Dichroismus negativ, bei *c* positiv hinsichtlich der Längsrichtung, *b* ist die Kompensationsstelle.

Fig. 3. Dasselbe Präparat wie bei 1 und 2 in Diagonalstellung zwischen gekreuzten Nikols. Buchstaben wie bei 1 und 2.

Fig. 4. Ein Zylinderpräparat in Diagonalstellung zwischen gekreuzten Nikols, Buchstaben wie bei 1 und 2. In *a* wird die aufleuchtende Mitte zu beiden Seiten von nicht aufleuchtenden Zonen begrenzt, dort, wo die negative Doppelbrechung in radialer Richtung in die positive in tangentialer Richtung übergeht. Äusserster Rand des Präparats in *a* wiederum aufleuchtend.

Fig. 5 und 6. Schicht 3 mit einem dünnen Schichtchen von 2 bedeckt in verschiedenen Lagen unter gekreuzten Nikols (siehe Text). Sämtliche Präparate in Chlorzinkjod gefärbt. Aufnahme auf panchromatischen Platten. Vergrösserung von 1—3 $\pm$ 8 $\times$, von 4 $\pm$ 25 $\times$, von 5 und 6 $\pm$ 160 $\times$.

Medicine. — *The transport of the Javanese "endemic Dengue" to Amsterdam.* By J. M. HOFFMANN †, W. K. MERTENS and E. P. SNIJDERS. (Communicated by W. SCHÜFFNER).

(Communicated at the meeting of June 25, 1932).

After we had succeeded in transporting to Amsterdam the virus of the dengue, occurring in Sumatra, by way of Aëdes aegypti and Aëdes albopictus, which had been infected at Medan [1]), we also tried to procure the virus of cases of dengue occurring in Java for our experiments at Amsterdam.

At the first attempt in June 1931, one of us took some tubes with dried serum from the patients (volunteers) J. and v. D. at Tjimahi, to Amsterdam. These sera were taken on November 21, 1930 (J. 1st day of illness) and on January 20, 1931 (v. D. 1st day of illness) by the second of us, during his experiments at Tjimahi, and were dried in vacuo by Prof. OTTEN at the Pasteur Institute at Bandoeng. These two patients had both an attack of the typical "VAN DER SCHEER's fever" (5 days fever). The dried sera were dissolved on July 7 and 8, 1931 at Amsterdam, filtered through a Seitz-filter and then injected into 3 volunteers, viz. B., S., and G. B. received 1½ cc. serum of v. D., S. and G. received each 1 cc. serum of J. Only one showed a reaction, namely G., who had been injected with 1 cc. serum of J., which was then 229 days old. Eight days after this injection (July 16, 1931) G. felt out of sorts, he had a rise of temperature to 38.2°. The number of his leucocytes dropped from 6000—8000 to 4400, subsequently regaining its original value. The next day he was subjected to the bites of 10 Aëdes aegypti. The temperature was then normal again (even low: 36.5 at 5 p.m.; so was the pulse-rate: 60 per minute) and the patient felt better again. Rashes were not observed. The mosquitoes had died, before we had the opportunity to allow them to bite new volunteers. So this first attempt could not be carried on further. But as we thought it very probable that the fever of G. was a slight attack of dengue, we resolved to repeat the experiments.

As these first samples of sera containing virus were not brought from Java to Holland in a refrigator, we now decided to have the other samples transported at 4° C., in order to increase the chance of success.

On February 25, 1932 the samples arrived at Amsterdam. For the first experiment we used the serum which had been stored for the shortest

[1]) Proceedings Kon. Acad. v. Wetensch. 1930. afd. Nat. Vol. XXXIX, no. 9; Geneesk. Tijdschr. v. N.I. 1931. Vol. **71** p. 241 en 345; Amer. Jrl. of Trop. Med. 1931. Vol. XI p. 171.

period: M. This serum had been taken on May 17, 1931 at Weltevreden on the 2nd day of the illness. It had been preserved in a refrigator for 20 days, and had been dried above P_2O_5 at a pressure of 1 mM mercury. The tube was sealed on June 12, 1931.

This serum M. was dissolved on February 26, 1932 to about its original volume, and was then injected subcutaneously, without having been filtered, into the left forearm of the volunteers Dr., P. and L, respectively ¼, ½ and ¾ cc. Only one of these persons got a typical attack, after an incubation of 4 days. (Dr. injected with ¼ cc.). His fever lasted 4 days (running as high as 39.2° C. during the first two days), accompanied by a decrease in the number of leucocytes. He showed the two types of rashes peculiar to dengue: a diffusely spread eruption of large, rather faint spots on the first day, and a slightly papular, brightly red second exanthema of small spots from the 4th to the 7th day. The subjective complaints were very characteristic also: headache, pain in the muscles of the eyeball and transient pains in the joints. With the serum of Dr., we have been able to transmit the disease to a further series of volunteers, as indicated in the following diagram

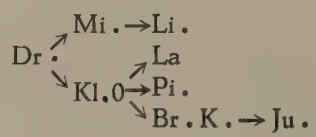

In all cases in which the inoculation was successful, the patients showed a clinical picture, which was much the same as that of Dr.

So we succeeded in bringing to Holland the virus of the Javanese endemic dengue, in a serum taken on the 2nd day of the disease, which serum was 285 days old (and had been kept during 260 days in a dried state) and to transmit the infection in a series of cases. The disease of the experimental subjects shows much resemblance with that of the volunteers infected with the Sumatran strain. Now that we have both kinds of dengue-virus at our disposal at Amsterdam, we will further be able to investigate whether there are slight differences between the two (in any case closely related) strains, or that we must look upon them as quite identical.

Medicine. — *Plasmoquine prophylaxis in benign tertian malaria*[1]). By N. H. SWELLENGREBEL and A. DE BUCK. (Communicated by Prof. W. SCHÜFFNER).

(Communicated at the meeting of June 25, 1932).

In a previous note we described our attempts to prevent the outbreak of fever and the appearance of parasites (benign tertian malaria) in the circulating blood in persons subjected to the bite of infected anopheles, but protected by a six days' course of prophylactic treatment with plasmoquine pure (3 c.g. daily supplemented, in one instance, by 0.9 gr. of quinine) commenced on the evening preceding the infecting bite. These attempts were unsuccessful except in one instance (case N°. 15). This subject showed neither fever nor parasites for the next 2 months. Still we remarked: "We will have to watch him till next summer in order to make sure he is not suffering from malaria with much protracted incubation". The first object of the present note (which is to be considered as an appendix of our previous one) is to report on the subsequent history of this case:

After being bitten by infected mosquitoes on Sept. 4 and 5, 1931, he remained in good health till April 23, 1932. On that day, 7 months 18 days after the infecting bite, he had fever and parasites of benign tertian malaria were found in his blood.

The question arises whether this is simply a case of protracted incubation, as described by JAMES and by SCHÜFFNER, KORTEWEG and SWELLENGREBEL, or whether the long period of incubation is the effect of the prophylactic treatment at the time of the infecting bite. If the latter supposition is correct, we must assume that the period of incubation would have been of normal duration if no prophylactic treatment had been given. Now all 7 control-cases, infected in the beginning of September, had their attack of malaria after the usual lapse of time and the same applies to the other cases, subjected to some kind of prophylaxis. Consequently the infections, caused by the bites of our infected mosquitoes, did not exhibit any tendency to run a course with long incubation and it seems not unreasonable to assume that the one exception to this rule is to be explained by the harmful effect of plasmoquine on the malaria parasites. Still, we prefer to leave this point undecided.

A second question, suggested by the perusal of the accompanying graph, concerns the nature of a malarial attack occurring at the end of a period of protracted incubation. N°. 15's attack occurred at a time when relapses[2]) of malaria among our other subjects became more numerous, following upon a period in which they had been rare. Does not this coincidence prove that N°. 15's malaria is a relapse, like all others supervening at or about the same time, and is not every case of malaria occurring after prolonged

[1]) The investigations on which this paper is based have been carried out with the support and under the auspices of the International Health Division of the Rockefeller Foundation.

[2]) We use this word in its general sense and not in the limited sense of JAMES' terminology.

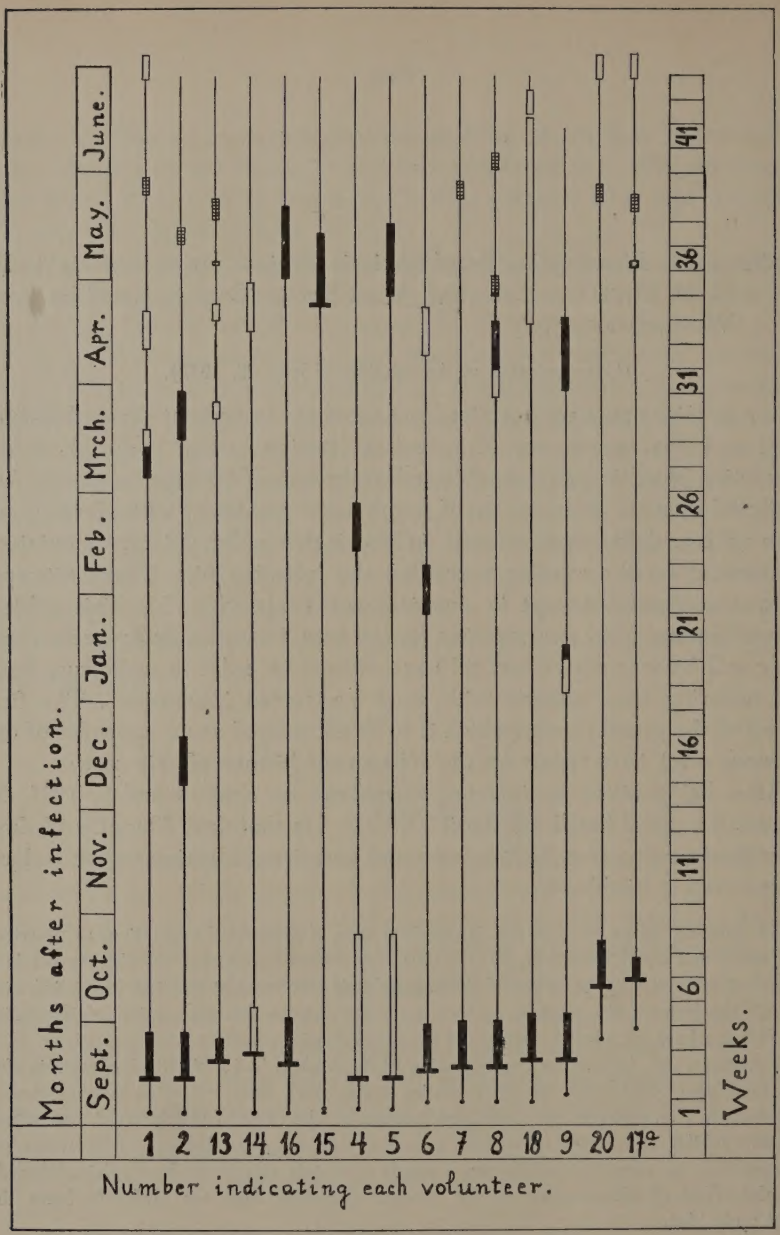

EXPLANATION OF THE GRAPH.

Each subject is represented by a vertical line. The dot (or dots: N°. 15) at the bottom of each line indicates the date (or dates: N°. 15) on which the subject was infected with malaria by the bite of mosquitoes. The beginning of the first attack of malaria consequent upon this infection is marked by a short horizontal line. The vertical column on this line indicates the course of treatment of this first attack:

black. Quinine 1 gr. + Plasmoquine 0.03 gr. daily.
white. Quinine 1 gr. daily.

The length of this column shows the time during which treatment was continued (see time-scale on the right).

The columns higher up the vertical lines mark duration and kind of treatment in the successive relapses. The colour of these columns has the same meaning as that of the bottom ones. But near the top relapses are treated with atebrine 3 × 0.1 gr. daily for 5 days; this is indicated by chequered columns.

incubation to be considered as a relapse, following upon a primary attack so slight as to be overlooked even under experimental conditions? The type of fever in case 15 proves that it was different from the relapses occurring at or about the same time. In the latter ones the fever proved immediately amenable to quinine and was freely intermittent (in so far as a fever showing only on one day can be called by that name). In case 15 it lasted for 4 days as a remittent fever (quinine treatment was commenced on the third day). In other words, it was KORTEWEG's initial fever as we encounter only in subjects suffering from malaria for the first time in their lives. Consequently, case 15's malaria was not a relapse in disguise but a true primary one.

The second object of this note is to draw attention to the fate of our other experimental subjects figuring in the accompanying graph. Although their subsequent histories might seem to be in no way related to the subject matter of this paper (i.e. the effect of prophylaxis by plasmoquine), these histories enable us, we believe, to arrive at a more correct understanding of the result of our experiment. Nine of our volunteers, after having developed the malaria we unsuccessfully endeavoured to prevent, were treated by a fortnightly course of quinine 1 gr. + plasmoquine 3 cg. All of them had relapses. In three (N°. 2, 6, 9) they occurred within 8—24 weeks after infection ("relapse" according to JAMES' terminology); the other six (N°. 1, 16, 8, 18, 7, 20) developed relapses after 6—8 months, termed "recurrences" by JAMES. In three instances (N°. 2, 6, 8) the renewed attacks, treated in the same way, were followed by a third attack after 3 (N°. 2, 6) and 1 (N°. 8) months and by a fourth after 1 month and 27 days (N°. 2). This is a heavy relapse-rate and it becomes the more significant when comparing it with PIEBENGA's experience in Franeker, since the middle of 1930. He successfully prevented relapses of any description in a series of 67 patients, treated by the same dosage and during the same time as our series of subjects. There are, however, two differences between the series:

1. PIEBENGA's were natural infections, our home-strain of benign tertian parasites acting as the virus; ours were artificial infections, the mosquitoes carrying a foreign (JAMES' Madagascar) strain. We know there are several points of difference between the two. Dr. P. C. KORTEWEG [1]) found the period of incubation longer in the home strain (three weeks on an average) than in the foreign (12 days). He also found the home-strain less reliable in causing human malaria after infection by means of mosquitoes: 38 % of failures (due, perhaps, to much prolonged incubation) in 66 cases, against 4 % in 52 cases after infection with the foreign strain.

These observations seem to suggest a lesser vitality of our home strain as compared with the foreign one. This decrease of vitality, although not necessarily involving a diminished resistance against all drugs, may be expected to do so in respect of some at least. This would afford some measure of explanation of PIEBENGA's successful prevention of relapses by

[1]) Dr. KORTEWEG has kindly permitted us to make use of his report prior to its publication.

plasmoquine treatment, contrasting so strikingly with our own complete failure.

2. The second difference is the number of infected mosquitoes biting the subjects. In PIEBENGA's cases this number is unknown but we may safely assume that it rarely, if ever, was more than one and, at any rate, far inferior to the number of infecting bites inflicted on our volunteers (4—10). It is possible that the vitality of the parasites or the susceptibility of the victims is raised by inoculation of very high doses of sporozoites. to the extent of neutralising the prophylactic effect of plasmoquine and diminishing its curative action in the subsequent primary attacks and relapses.

The same considerations apply to a comparison of our experience with results obtained in North-Holland (Zaan-region) by treating malaria for one week with plasmoquine 3 cg. + quinine 1 gr. a day. These results, although less satisfactory than PIEBENGA's, were far better than ours: 53 % of the cases did not relapse. Finally we should point out that the usual relapse rate of malaria in Holland, after ordinary quinine treatment, hardly exceeds 50 %. In our 15 volunteers it is 100 %.

So we are forced to the conclusion that the malaria our volunteers suffered from was exceptionally refractory to treatment with plasmoquine. Without being able to decide which factors (quantitative or qualitative) caused this state of things, we may assume that they were influencing the experiment from the very beginning. Once this is admitted, it follows that our failure to prevent the primary attack, as well as the relapses, can no longer be regarded as contradictory to statements announcing satisfactory results obtained elsewhere. It only shows that a system of prophylaxis and treatment, which has definitely proved its great practical value, may occasionally break down under the stress of an unusually great number of infected mosquitoes or the prevalence of some strain of parasites of particular vitality.

ERRATUM

Proceedings Royal Acad. Amsterdam, Vol. 35, N°. 5, 1932.

[1]) The title of the Dutch paper is: C. P. J. PENNING, *Onderzoek der Bevolking van de Over-Veluwe* 1932.

The footnote printed here as [1]), refers to the name of BERNSTEIN on page 708.